5-2018

# Plant cell wall modification during tomato processing and its effects on the physical and rheological properties of end products

Xing Fei
*Purdue University*

# PLANT CELL WALL MODIFICATION DURING TOMATO PROCESSING AND ITS EFFECTS ON THE PHYSICAL AND RHEOLOGICAL PROPERTIES OF END PRODUCTS

by

**Xing Fei**

**A Dissertation**

*Submitted to the Faculty of Purdue University*

*In Partial Fulfillment of the Requirements for the degree of*

**Doctor of Philosophy**


School of Agricultural & Biological Engineering

West Lafayette, Indiana

May 2018

# THE PURDUE UNIVERSITY GRADUATE SCHOOL
# STATEMENT OF COMMITTEE APPROVAL

Dr. Osvaldo H. Campanella, Co-Chair
Department of Agricultural and Biological Engineering
Dr. Bradley L. Reuhs, Co-Chair
Department of Food Science
Dr. Carlos M. Corvalan
Department of Food Science
Dr. Owen G. Jones
Department of Food Science
Dr. Ganesan Narsimhan
Department of Agricultural and Biological Engineering

**Approved by:**

Dr. Bernard Engel
Head of the Graduate Program

*Dedicated to my beloved ones. My Son, Wife, Parents, Family and Friends*

# ACKNOWLEDGMENTS

I would like to express my deepest appreciation to my major advisors Dr. Osvaldo Campanella and Dr. Bradley Reuhs, for their invaluable guidance and continued support. Dr. Campanella is one of the finest persons I have ever met. He gave me the freedom to explore my research area, and was always ready to help when I faced a problem. His dedication to work, enthusiasm for research, caring for students, and kindness to every people around him always inspired me in every aspect of my life. He set an excellent example that will guide me through my future career and life. I am so grateful to have Dr. Reuhs being my co-advisor. Without his mentorship and help, some parts of this work would not have been possible. I learned a lot from doing polysaccharide analysis with him, as well as the stories he shared with me about history and music that were full of value and fun.

I would like to thank Dr. Owen Jones for his endless advice and support. Thank you for always being the research meetings with us, and always giving me encouragement and good suggestions during my research. I would also like to thank Dr. Carlos Corvalan and Dr. Ganesan Narsimhan for their valuable advice, discussions, and assistance as my advisory committee members. I also wish to thank the USDA NIFA and the Bilsland Dissertation Fellowship for providing financial support.

My sincere thanks also goes to Dr. Bhavesh Patel, who helped me a lot in experiments and shared with me good experiences both in research and life. I also wish to thank Anton Terekhov and Dr. Yunus Tuncil for their training and assistance with NMR and GC. I would like to extend my appreciation to the visiting students and scholars who involved and assisted me in this project: Nathalia Medeiros, Cintya Syozi, Dr. Danshi Zhu, Dr. He Liu, and Raquel Lopez-Lozano. Thank you all for your contributions! A big thank you goes to my fellow graduate

colleagues in the Rheology Lab, and the staffs of Department of Agricultural and Biological Engineering for helping me whenever I have questions.

I wish to give special thanks to my wife and my parents for their solid support these years. Thanks to my cute guy, my little boy Lucas, you bring me so much joy every day!

# TABLE OF CONTENTS

# LIST OF TABLES

# LIST OF FIGURES

# ABSTRACT

Author: Fei, Xing. PhD
Institution: Purdue University
Degree Received: May 2018
Title: Plant Cell Wall Modification during Tomato Processing and Its Effects on the Physical and Rheological Properties of End Products
Major Professors: Osvaldo H. Campanella; Bradley L. Reuhs

Understanding the relationship between structure and functional properties in plant-cell-wall-derived foods has become a growing interest to both academia and industry. Tomato is one of the most cultivated vegetable crops and mostly is consumed as processed products in the form of suspensions. Rheological properties of tomato product, a key functional attribute, depends on both the serum and particle phases of these products. Although recent studies have suggested that the particle phase is the dominant factor, the relationship between fundamental particle properties and the bulk rheology of the suspension is still unclear. This research systematically evaluated the contributions of soluble pectin and particle phase on the rheology of tomato suspensions, and identified that the particle structure and its physical properties are crucial in determining the rheology of such systems. Alteration of these properties either by processing conditions or by internal enzymatic activity could cause a significant change in the rheology of tomato products.

The serum phase of the suspensions displayed a Newtonian behavior with a low viscosity (~0.1 mPa.s). The contribution of soluble pectin to the overall viscosity of the suspensions was found to have a little influence despite that reconstituted suspensions were prepared either with large pectin concentrations or with pectin having a high degree of methylation. However, the presence of pectin was important because its role on stabilization of the suspension systems by increasing the interaction between particles. When pectin concentration was low, wall slippage

during measurements was observed due to phase separation by using cone-plate geometry. A vane geometry was able to alleviate the slippage artifact and a good correlation ($R^2$=0.91) was found between the empirical Bostwick consistometer method and fundamental measurements performed employing the vane geometry. Hence, the vane geometry was recommended in the viscosity measurements of cell-wall-derived suspensions.

The particle structure and its physical properties, and the associated particle interaction controlled the rheological properties of the cell-wall-derived suspensions. Changes in the particle phase were achieved in this study by two means: external processing with various conditions and molecular biological modification by reduced pectin methylesterase (PME) activity. The effects of thermal breaking, and physical treatments such as ultrasound and high shear were employed at the laboratory scale. The concentration process to produce tomato paste from tomato juice at an industrial scale was also investigated. The focus was on effects that this process has on the properties of the particles and the rheology of the suspensions when they are reconstituted from the paste to juices. These diverse processing and modification conditions produced particles with various structures and strengths, and as a result caused significantly changes on the rheological properties of suspensions.

Although both the ultrasound and high shear treatments reduced significantly the particle size of the treated tomato suspensions, the former led to an increase in their rheological properties whereas the latter caused a significant decrease. It could be explained by formation of particles with structural differences provoked by these two treatments. Ultrasound treated suspensions contained more intact particles, and with large strength, which was evaluated by a compression test on a limited number of particles. Conversely, high shear treated suspensions resulted in mostly ruptured particles that lost mechanical strength. The water-soluble pectin

(WSP) fraction increased after ultrasound and shear treatments. However, soluble pectin is not the direct cause for the changes in the suspension rheology; it is an indicator or consequence of the changes in particle properties.

This research also explained the viscosity loss during the industrial tomato juice concentration process from the perspective of particle alterations. The particle phase was extensively modified as the concentration process reduced the particle volume and concentrated its mass into a smaller size. The original tomato juice had a relatively higher volume fraction and viscoelasticity than those of reconstituted juices from dilution of pastes to achieve the same soluble solids ($^{o}$Brix). This resulted in original juices with higher consistency and viscosity. During dilution, paste particles cannot re-expand to the original shape and volume than those present in the original juice. Due to the fact that the concentrated solute present in pastes cannot be fully solubilized, more paste is necessary to achieve the viscosity of the original juice.

In addition, tissue structure modification using molecular biology and via suppression of pectin methylesterase (PME) activity resulted in a closely packed cellular structure with smaller pore size when compared to the tissue of the original wild type tomato (OWT). An 85-90% reduction in PME activity significantly strengthened the microstructures of cell wall particles, and reduced serum separation, which improved tomato suspension rheological properties.

The last part of this research investigated the flow behaviors of industrially processed hot-break (HB) and cold-break (CB) tomato suspensions under steady-state and dynamic oscillatory shear conditions. The HB suspensions exhibited considerably higher viscosity and viscoelastic properties than CB suspensions because their particles had a structure that was able to retain better water and higher mechanical strength. Both industrially processed samples exhibited temperature-dependent and time-dependent rheological behaviors. The consistency

coefficient (*k*) as a function of temperature could be modeled by an Arrhenius-like equation. The activation energy of the HB sample was higher than that of the CB sample, indicating a more integral structure resisting changes in temperatures. The thixotropic behavior of HB and CB suspensions was described by the Stretch Exponential equation. A characteristic time ($\lambda_s$) used in the Stretch Exponential equation increased with temperature for the HB sample whereas it showed the opposite trend for the CB sample. These differences could be explained by differences in the particle structure and initial viscosity. Particle interactions showed great impact on the rheological properties. When particle concentration was low (solid % < 1.0%), both HB and CB samples almost had the same apparent viscosity due to a limited contact between particles. However, when the particle phase was high, the particle-particle contact significantly increased, and the HB sample demonstrated a considerably higher viscosity and viscoelasticity. Results indicated that the HB system has larger particle elasticity and stronger particle interaction than the CB system. Furthermore, the local Young's modulus distributions of individual HB and CB particles investigated by Atomic Force Microscopy (AFM) were in good agreement with the bulk rheology data. It can be concluded that the differences in rheological properties of tomato products are originated from differences in their particle phases.

# CHAPTER 1. INTRODUCTION

## 1.1 Motivation and Objectives

As one of the most cultivated vegetable crops worldwide, tomatoes had a global production of 170.8 million tons in 2014 and 80% of them were consumed as processed products such as tomato sauce, juice and ketchup (FAO, 2014; Rickman, Barrett, & Bruhn, 2007). Rheology is a key functional property for these widely sold products, which are mainly a suspension of plant cell wall particles dispersed in a continuous serum phase (Moelants et al., 2014; Rao, 1987). Pectin is one of the major components of cell wall and after processing is distributed in both the serum and the particle phases. It has been assumed for years that the undesirable low viscosity of many products is caused by the activity of pectolytic enzymes that catalyze the breakdown of pectin in the cell wall (Moelants et al., 2014; Moelants et al., 2013; Yoo & Rao, 1994). Currently, to alleviate that problem the industry uses the hot-break process with a range of temperatures of 77-95 ℃ to inactivate the enzyme pectin methylesterase (PME) and have products with a higher viscosity. However, this process sacrifices flavor and color attributes, and increases energy expenditures as well. Furthermore, a high energy consuming concentration process is performed after the “break” step, where most tomatoes are processed into tomato paste before any further manufacturing (Abu-Jdayil, Banat, Jumah, Al-Asheh, & Hammad, 2004). Although the concentration of tomato juice to paste facilitates transportation and improves preservation, the subsequent dilution for the production of final tomato products results in products with lower consistency (Tanglertpaibul & Rao, 1987). This problem has a major economic impact since more tomato concentrate must be added in order to achieve the same viscosity as the original product before concentration (Thakur, Singh, & Nelson, 1996).

These two big issues are a serious concern within the food industry and need urgent solutions of alternative processing systems.

Recent studies have suggested that the contribution of solubilized pectin to the overall texture of tomato products is not significant. Instead the particle concentration and particle properties including size, deformability and morphology are the dominant factors affecting the rheology of tomato suspensions (Appelqvist, Cochet-Broch, Poelman, & Day, 2015; Moelants et al., 2014). However, the relationship between the particle properties and the bulk rheology of the tomato suspension is still unclear due to the structurally complex cell wall material. Pectin is susceptible to processing and could be degraded and solubilize into the serum phase. Although this pectin conversion has been identified (Anthon, Diaz, & Barrett, 2008), the resulting changes of structural and rheological attributes have not been fully characterized. In addition, many studies were conducted via bulk rheological characterization and results are still inconclusive concerning the effects of the particle properties on the suspension rheology. Studies at the individual particle level are needed for better understanding such systems. Thus, systematically studying the contributions of soluble pectin, particle size and its properties, and associated particle interactions on the rheological properties of the suspension system will contribute greatly to our understanding of the rheological profile of the cell wall suspension system. It will also open doors to the development of new approaches to produce tomato and potentially other vegetable and fruit products with enhanced quality.

The central hypothesis of this study is that the rheological properties of cell wall suspension systems are determined by the overall particle interactions, which are influence by the combined effect of the particle concentration and the particle physical properties. These

effects must be identified individually and tailored by processing simultaneously. In order to test this hypothesis, four specific objectives are pursued in this research:

1. Determine the effects of soluble pectin on the viscosity of serum and suspension;

2. Determine the effects of particle properties;

3. Determine the effects of processing conditions on the rheological properties of tomato suspensions; and

4. Determine the rheological behavior of industrially processed tomato suspensions under different conditions.

## 1.2 Organization of the Dissertation

The motivation and objectives of this research are summarized in Chapter 1. A literature review is presented in Chapter 2.

Chapters 3 to Chapter 7 describe the main research activities and are presented in a manuscript format.

The effects of soluble pectin on the viscosity of serum and reconstituted tomato suspensions are presented in Chapter 3. This chapter also builds a sound correlation between fundamental measurements of viscosity and the widely used empirical Bostwick consistometer method.

Chapter 4 presents the effects of thermal, high shear and ultrasound processing on the rheological properties of tomato suspensions, from a point of view that considers the particle microstructure and its properties. Pectin alteration and color changes during processing are also studied in this chapter.

In Chapter 5, viscosity losses after dilution of concentrated tomato paste is characterized and explained by a particle “shrink and condense” model.

Chapter 6 includes two parts focusing on the particle properties. In the first part, the effects of reduced PME activity of tomatoes genetically modified on the particle microstructure and pulp viscoelasticity are presented. In the second part, the mechanical strength of individual particles is investigated by an atomic force microscopy (AFM) method.

In Chapter 7, the flow behavior of hot-break and cold-break samples processed industrially are investigated, with a focus on particle interaction.

Chapter 8 presents a summary of key findings in this research and recommendations for future work.

## 1.3 References

Abu-Jdayil, B., Banat, F., Jumah, R., Al-Asheh, S., & Hammad, S. (2004). A comparative study of rheological characteristics of tomato paste and tomato powder solutions. *International Journal of Food Properties, 7*(3), 483-497. doi: 10.1081/Jfp-120040203

Anthon, G. E., Diaz, J. V., & Barrett, D. M. (2008). Changes in pectins and product consistency during the concentration of tomato juice to paste. *Journal of Agricultural and Food Chemistry, 56*(16), 7100-7105. doi: 10.1021/jf8008525

Appelqvist, I. A. M., Cochet-Broch, M., Poelman, A. A. M., & Day, L. (2015). Morphologies, volume fraction and viscosity of cell wall particle dispersions particle related to sensory perception. *Food Hydrocolloids, 44*, 198-207. doi: 10.1016/j.foodhyd.2014.09.012

FAO. (2014). Food and Agriculture Organization of United Nations Statistics. Retrieved Aug, 2017, from http://www.fao.org/faostat/en/#data/QC/visualize

Moelants, K. R. N., Cardinaels, R., Jolie, R. P., Verrijssen, T. A. J., Van Buggenhout, S., Van Loey, A. M., . . . Hendrickx, M. E. (2014). Rheology of Concentrated Tomato-Derived Suspensions: Effects of Particle Characteristics. *Food and Bioprocess Technology, 7*(1), 248-264. doi: DOI 10.1007/s11947-013-1070-3

Moelants, K. R. N., Jolie, R. P., Palmers, S. K. J., Cardinaels, R., Christiaens, S., Van Buggenhout, S., . . . Hendrickx, M. E. (2013). The Effects of Process-Induced Pectin Changes on the Viscosity of Carrot and Tomato Sera. *Food and Bioprocess Technology, 6*(10), 2870-2883. doi: 10.1007/s11947-012-1004-5

Rao, M. A. (1987). Predicting the Flow Properties of Food Suspensions of Plant-Origin. *Food Technology, 41*(3), 85-88.

Rickman, J. C., Barrett, D. M., & Bruhn, C. M. (2007). Nutritional comparison of fresh, frozen and canned fruits and vegetables. Part 1. Vitamins C and B and phenolic compounds. *Journal of the Science of Food and Agriculture, 87*(6), 930-944. doi: 10.1002/jsfa.2825

Tanglertpaibul, T., & Rao, M. A. (1987). Rheological Properties of Tomato Concentrates as Affected by Particle-Size and Methods of Concentration. *Journal of Food Science, 52*(1), 141-145. doi: DOI 10.1111/j.1365-2621.1987.tb13991.x

Thakur, B. R., Singh, R. K., & Nelson, P. E. (1996). Quality attributes of processed tomato products: A review. *Food Reviews International, 12*(3), 375-401.

Yoo, B., & Rao, M. A. (1994). Effect of Unimodal Particle-Size and Pulp Content on Rheological Properties of Tomato Puree. *Journal of Texture Studies, 25*(4), 421-436. doi: DOI 10.1111/j.1745-4603.1994.tb00772.x

# CHAPTER 2. LITERATURE REVIEW

## 2.1 Plant Cell Wall Tissue and Derived Suspension

Both the food industry and consumers are showing a growing interest in plant tissue based fruit and vegetable products for a healthy diet (Lopez-Sanchez et al., 2011). Most of these foods can be considered as suspensions in a commonly aqueous medium in which the solid particles are derived from cell wall tissues (Moelants, Cardinaels, Jolie, et al., 2014; M. A. Rao, 1987). Edible plant tissues are usually rich in individual parenchyma cells glued together by the middle lamella which is the outermost layer of the cell wall (Brett & Waldron, 1990) (Figure 2.1). The structural integrity and the texture of cell wall material play a central role in the sensorial quality of such foods and are mainly determined by the mechanical properties of the cell wall, cell adhesion and the internal turgor generated by osmotic pressure (Jackman & Stanley, 1995; Waldron, Parker, & Smith, 2003). The cell wall is primarily composed of polymeric components and is the main structural element in fruits and vegetables. Each component adds its functions to the individual cells or jointed tissues in terms of structural strength, rigidity, flexibility and porosity (Carpita & Gibeaut, 1993).

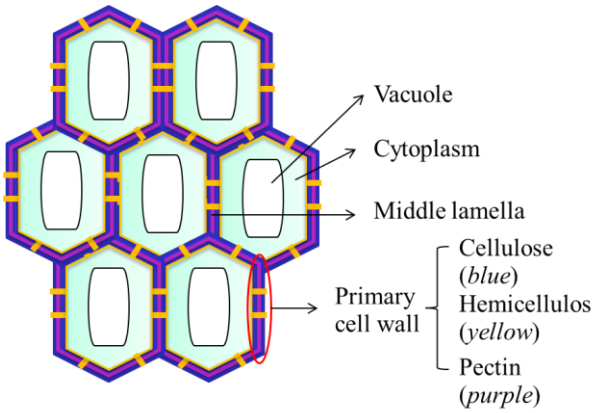


Figure 2.1 Schematic plot of parenchyma tissue. The parenchyma cells are glued together by the pectin that is rich in the middle lamella.

### 2.1.1 Cell Wall Polysaccharides

The primary plant cell wall is a complex composite material that consists of three main polysaccharides: pectin, cellulose microfibril and hemicellulose (Figures 2.1 and 2.2) (Palin & Geitmann, 2012; Sankaran et al., 2015). This classification is based on the chemical structure as well as ways of extraction (Selvendran, 1985), and in fact these three polysaccharides can form cross-links with varying levels of proteins and phenolics (Carpita & Gibeaut, 1993). The cell wall structure is so complex that the interactions between the three main polysaccharides are still not fully understood (Carpita & Gibeaut, 1993). For decades, most of cell-wall-related research has focused on the functions of cell wall from a plant physiological perspective (Waldron et al., 2003). However, these studies have provided general methods and vision on the role of the cell wall on textural qualities of derived foods. The contribution of cell wall on the viscosity of tomato puree has been noticed as early as 1950s by Whittenberger and Nutting (1958). In order to understand the structure of the cell wall, solvents such as ethanol, sodium dodecyl sulphate and water have been used to extract cell wall material. Cellulose microfibrils, hemicellulos and pectin are also the main components of alcohol insoluble residue (AIR). AIR is often referred to as cell wall material and has been shown to have a high correlation to the viscosity of tomato juice (Janoria & Rhodes, 1974).

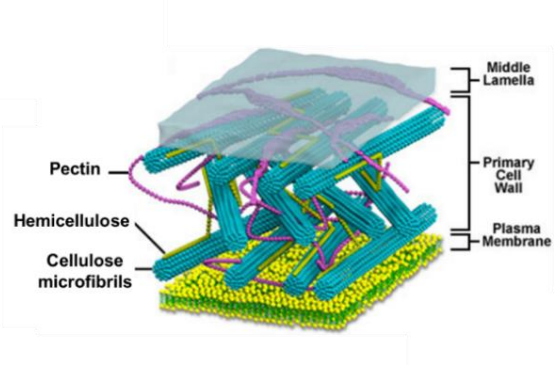


Figure 2.2 Schematic plot of primary cell wall, adapted from Davidson (2015). It consists of three main polysaccharides: pectin, cellulose microfibril and hemicellulose.

Cellulose consists of linear β-(1, 4)-linked glucose (Glc) chains with a degree of polymerization (DP) of 2000 to 6000 and aggregated together by hydrogen bonding, in primary cell walls (Delmer, 1987). These glucose polymers are usually built up into long microfibrils of a few nanometers in the primary cell walls. Due to the restricted orientation around these β-(1, 4)-linkages between each molecule, cellulose microfibrils are relatively rigid and able to control cell expansion. As the main loading bearing, cellulose microfibrils, associated with hemicellulos, form the skeletal scaffolding of the cell wall matrix (Knoerzer, Juliano, & Smithers, 2016). It has been demonstrated that the mechanical properties of cell wall are determined by the stiffness of the cellulose itself as well as the physical entanglements and the orientation of the microfibers (Whitney, Gothard, Mitchell, & Gidley, 1999). Cellulose present in natural plants is insoluble in water and most organic solvents because of the semi-crystalline structure and its high molecular weight (Deguchi, Tsujii, & Horikoshi, 2006). It is also the most stable polysaccharide component during food processing; however, it could be partially degraded by exogenous enzymes. Sankaran et al. (2015) studied the effect of cellulase on the rheological and particle properties of carrot cell wall suspensions. Decrease in their elastic properties measured by the storage modulus and particle size were observed after cellulase treatment for 8 h, but the microfibril architecture still remained the same which indicates that the enzyme could not penetrate the microfibril matrix and only has activity on the exterior part of the cell-wall-derived particles.

Hemicellulose is so-called by its solubility. Unlike cellulose which is strongly resistant to hydrolysis and insoluble, hemicellulose is usually solubilized by weak and strong alkali treatments that break the hydrogen bonds to cellulose microfibrils. Structurally, hemicelluloses are branched heterogeneous polymers of pentoses (xylose, arabinose), hexoses (mannose, glucose, galactose), and sugar acids (Saha, 2003). In general, these hemicelluloses all share a

cellulosic backbone and differ in the side chains. Hemicelluloses are the second most common polysaccharides in nature, and account for 20 to 30% of the AIR. Xyloglucans are the main hemicellulose form found in primary cell walls of edible vegetables and fruits such as tomatoes (Seymour, Colquhoun, Dupont, Parsley, & Selvendran, 1990; Waldron et al., 2003). They have a cellulose backbone of β-(1, 4)-linked Glc, to which side chains are substituted with (1, 6) linked xylose groups. Hemicelluloses are mainly imbedded in the interior of the cell walls (Cosgrove, 2005), so the structure breakdown would only have little influence on the particle interactions or particle properties. Thus, some studies suggested that the contribution of hemicelluloses to the bulk rheology is negligible (Sankaran et al., 2015).

Pectin is rich in galacturonic acid (GalA), and also contains significant amounts of rhamnose (Rha), arabinose (Ara), and galactose (Gal) (Brett & Waldron, 1990). It can form a gel matrix interspersing the cellulose-hemicellulose network, making the cell wall form structures consisting of two distinct networks. The pectin matrix, which is abundant in the middle lamella (Steele, McCann, & Roberts, 1997), determines cell to cell adhesion that contributes to the firmness and elasticity of the tissue (Fuchigami, 1987). There are three domains thought to be present in all pectic polysaccharide structures: homogalacturonan (HG), rhamnogalacturonan-I (RGI), and rhamnogalacturonan-II (RG II) (Willats, McCartney, Mackie, & Knox, 2001) (Figure 2.3).

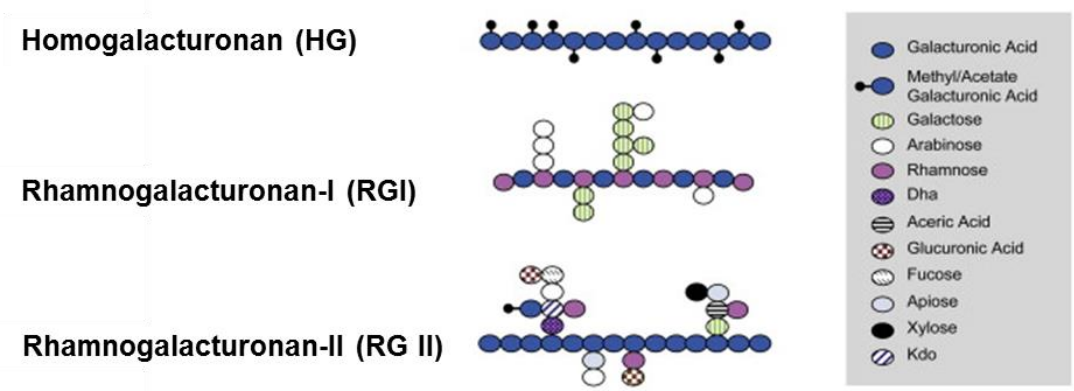


Figure 2.3 Schematic structure of pectin displaying the three main pectic polysaccharides: homogalacturonan (HG), rhamnogalacturonan I (RG-I), and rhamnogalacturonan II (RG-II). Use with permission from the authors (Palin & Geitmann, 2012).

HG is a linear homopolymer of 100 to 200 (1, 4) α-linked D-GalA units (Thibault, Renard, Axelos, Roger, & Crepeau, 1993), which can be methoxylated at C-6 and may also be acetylated on O-2 and O-3 (Ishii, 1997; Vincken et al., 2003). Demethoxylation of HG results in the capability of HG molecules to be cross-linked by calcium ions to form so-called "egg-box" gelling structures. Degree of methoxylation (DM), pattern of methyl esterification (PM) and the molecular size determine the gelling properties of pectin (Thakur, Singh, & Handa, 1997). RGI is an acidic pectin domain that comprises up to 100 units of the disaccharide (1, 2) α-L-rhamnose-(1, 4) α-D-GalA, with the backbone residues potentially O-acetylated at C-2 or C-3(Albersheim, Darvill, ONeill, Schols, & Voragen, 1996). RGII, on the other hand, is a branched pectic domain containing a HG backbone of (1, 4) α-linked-D-GalA with complex side chains linked to the galacturonic residues.

Compared to cellulose and hemicellulose, pectin is the component most affected by various processing conditions, thus influencing the structure and texture of derived foods (Moelants, Cardinaels, Van Buggenhout, et al., 2014). Although pectin varies with the source, as

well as maturity and location found within the plant (Seymour, Harding, Taylor, Hobson, & Tucker, 1987; Stein & Brown, 1975), it is believed that both of pectin concentration and chemical structure (in particular, HG) can affect the structural and textural properties of plant-tissue-based foods (Moelants, Cardinaels, Van Buggenhout, et al., 2014). To further study pectin chemical properties, water-soluble pectin (WSP), chelator-soluble pectin (CSP) and sodium-carbonate-soluble pectin (NSP) are usually extracted from AIR sequentially due to the differences in solubility in these solvents and the bonding to the cell wall (Christiaens, Van Buggenhout, Houben, et al., 2012). WSP is loosely bound to the cell wall through non-covalent and non-ionic bonds (Selvendran & Oneill, 1987), whereas CSP mainly contains ionically cross-linked pectin usually bonding with $Ca^{2+}$ in the middle lamella (Sila, Smout, Elliot, Van Loey, & Hendrickx, 2006) and NSP is predominantly linked to cell wall polysaccharides through covalent ester bonds (Chin, Ali, & Lazan, 1999; Christiaens, Van Buggenhout, Houben, et al., 2012). Christiaens et al. (2012) observed pectin fraction changes in tomato cell walls by applying various treatments (not pretreated, high temperature blanched or high pressure pretreated). Nuclear magnetic resonance (NMR), gas chromatography (GC), and high performance size exclusion chromatography (HPSEC) are the common techniques used to characterize pectin structure. However, only average values in the sample can be obtained (e.g. DM) by these traditional methods. Recently, immunolabelling assays with anti-pectin antibodies have been used to analyze pectin patterns based on that antibodies have different affinities to pectin with different DM (Christiaens, Van Buggenhout, Chaula, et al., 2012; Christiaens, Van Buggenhout, Houben, et al., 2012; Moelants et al., 2013). Monoclonal antibodies such as JIM5, JIM7, LM18, LM19, PAM1 and 2F4 can locate specific pectin structure, which are further visualized by fluorescence microscopy (Christiaens, Van Buggenhout, Chaula, et al., 2012; Christiaens, Van

Buggenhout, Houben, et al., 2012). *In situ* visualization of the cell wall components changes (e.g. pectin) is very helpful because it gives us the insight of the alteration of cell-wall-derived particle structure due to processing.

### 2.1.2 Tomato and Derived Foods

Tomatoes (*Lycopersicon esculentum*), a botanically berry-type fruit, originated in Central and South America, belongs to the Solanaceae family (Frusciante et al., 2007). As one of the most cultivated vegetable crops worldwide, tomato had a global production of about 170.8 million tons in 2014 (FAO, 2014), with China contributing for about 30% of the total, followed by India, the United States (U.S.) and Turkey as the major production countries. In the U.S., tomato is the most popular garden vegetable widely produced in 20 states (Leon Garcia, 2013). California is the leading producer accounting for 96% of the U.S. processing tomato output and 30% of the fresh ones (USDA, 2012).

Anatomically speaking, most tomato fruits have four or five locules surrounded by the pericarp tissue (UCLA, 1996). A typical structure of a tomato fruit contains outer cuticle (skin), seeds, pericarp (the fleshy part of the fruit), and gelatinous parenchyma around the seeds. In an individual cell, a single, large vacuole is found and usually comprises 30-80% cell volume. Vacuole stores salts, sugars, and sometimes proteins, which maintains turgor pressure on the cell as these solutes cause an osmotic pressure gradient across the plasma membrane. It should be noted that turgor pressure is one of the most important factors that control the texture of the tomato tissue and derived products.

Overall, fresh tomato fruit contains about 94% water and 6% dry material including both soluble and insoluble components. Free glucose (Glc) and fructose (Fru) are the major soluble carbohydrate components, along with organic acids. The insoluble components include cellulose,

hemicellulos and some pectin (partial, ~70%), which are also defined as AIS and have shown a high correlation to the viscosity of tomato products in previous studies (Janoria & Rhodes, 1974; M. A. Rao, Bourne, & Cooley, 1981; Tanglertpaibul & Rao, 1987a). Tomato is also the main dietary source of lycopene and some β-carotene (Frusciante et al., 2007), which have been demonstrated to have many potential health benefits such as reduction of some cancer types and cataract formation (Ambrosini, De Klerk, Fritschi, Mackerras, & Musk, 2008).

In general, most tomatoes are processed into tomato paste (i.e. concentrate) before any further manufacturing (Abu-Jdayil, Banat, Jumah, Al-Asheh, & Hammad, 2004). About 80% of tomatoes in the U.S. are consumed as processed products including tomato preserves (tomato juice, pulp, puree, and paste), dried tomatoes (tomato powder, flakes, and dried fruits) and tomato based foods (tomato soup, sauces, and ketchup) (Heuvelink, 2005). The most commonly consumed processed tomato form is originated from tomato concentrate that can be considered as suspensions, such as tomato sauce, juice or ketchup (Rickman, Barrett, & Bruhn, 2007). According to FDA, the labeling of final products depends on the soluble solid content in the products. For example, tomato soluble solids should be between 8-24% in “tomato puree”, whereas in “tomato paste” it should be greater than 24% (FDA, 2017). Tomato is used so extensively in the food industry, and therefore it was chose as a model plant in this research to investigate its rheology in relation to cell wall materials.

## 2.2 Serum Pectin

Most tomato products are suspensions in which cell wall particles are dispersed in a continuous serum phase (Moelants, Cardinaels, Jolie, et al., 2014; M. A. Rao, 1987). The serum phase contains solubilized cell contents and cell wall material such as sugars (Glc, Fru and minor sucrose (Suc)), organic acids, and in particular solubilized pectin (Lopez-Sanchez et al., 2011)

which is thought to be the constituent of serum phase that more influence its rheology, more specifically its viscosity (Moelants, Cardinaels, Van Buggenhout, et al., 2014).

Tomato serum exhibits the properties of a Newtonian fluid as stated in many previous reports (Tanglertpaibul & Rao, 1987a; B. Wu, 2011). Tanglerpaibul and Rao (1987a) reported a linear relationship between serum viscosity and pectin concentration. It has been suggested that both the content and the properties of pectin influence the viscosity of the serum phase. Many studies have shown that an increase in serum viscosity can be achieved by increasing pectin content (Moelants, Cardinaels, Van Buggenhout, et al., 2014; Moelants et al., 2013; Tanglertpaibul & Rao, 1987a). However, a few studies demonstrated the effects of pectin properties such as DM, MW distribution, composition and conformation on serum viscosity, (Diaz, Anthon, & Barrett, 2009; Moelants et al., 2013). Moelants et al. (2013) investigated the influence of the GalA content and properties (DM and size) of pectin on the viscosity of the serum phase of thermal treated and high pressure homogenization treated samples. They concluded that the chemical characteristics of serum pectin only had a limited effect on the rheological properties of tomato suspension. In previous study performed at Purdue University, hot- and cold-break tomato sera from industrial processing were collected and analyzed by NMR, GC, SEC, and HPAEC. $H^1$-NMR analysis showed that the sera consisted almost entirely of simple sugars, whereas baseline noise obscured the pectin resonances, indicating a relatively low abundance of pectin in the sera. HPAEC and GC results confirmed that free glucose and fructose are the major components of tomato sera. Although SEC results did show reduction in the overall MW of the cold-break serum pectin, the role of soluble pectin in product viscosity is probably limited due to the extremely low concentration (B. Wu, 2011).

### 2.2.1 Pectin Degradation

As discussed before, pectin is naturally found in the intercellular layer and middle lamella of cell walls and may function as a hydrating agent and also as a cementing material for the cellulose-hemicellulose networks (McCann & Roberts, 1996). Therefore, changes of pectic structure would greatly affect the structure and texture of derived foods (Moelants, Cardinaels, Van Buggenhout, et al., 2014). Approximately 30% of tomato cell walls are formed by pectin and only a proportion of them is water soluble (Carpita & Gibeaut, 1993). Cell wall pectin could become soluble in the serum phase (in products) via demethoxylation and depolymerization by thermal processing and the enzymatic activity (Tiback, Langton, Oliveira, & Ahrne, 2014). Pectin (particularly, HG) is conventionally categorized into high methoxylated (HM) pectin (DM > 50%) and low methoxylated (LM) pectin (DM < 50%), and its structure can be degraded by both enzymatic and chemical conversion reactions shown in Figure 2.4 (Vanburen, 1979).

Enzymatic pectin conversions involve either esterases or depolymerases. Pectin methylesterase (PME) catalyzes the specific hydrolysis of the C-6 methyl ester bond of GalA residues, releasing methanol and creating negatively charged carboxyl groups (Sila et al., 2009). Polygalacturonase (PG) hydrolyses α-(1, 4)-linked D-GalA and causes pectin depolymerization and solubilization, and consequent reduction in firmness (Moelants et al., 2013). Demethoxylation by PME could have either a positive or negative effect on the texture of plant cell walls and derived foods depending on the presence of PG and also on the processing conditions (Knoerzer et al., 2016). The demethoxylated pectin can cross-link with divalent ions (e.g. $Ca^{2+}$, $Mg^{2+}$) leading to the formation of supramolecular assemblies and/or gels, with a better texture retention. In addition, β-elimination depolymerization during processing is resisted by low DM (demethoxylated) pectin, which will ease the process-induced structural degradation. However, PME also provides a preferred low DM substrate for PG depolymerization causing

texture or viscosity loss, although it could control the cloud stability during juice production (Sila et al., 2009). As two most important enzymes, PME and PG are always targeted in order to control to a certain point of pectin changes during processing, by inactivating the undesired one and boosting the desired one (Van Buggenhout, Sila, Duvetter, Van Loey, & Hendrickx, 2009). It would finally lead to precisely controlling the texture or rheology changes of many processed cell-wall-based products (Duvetter et al., 2009).

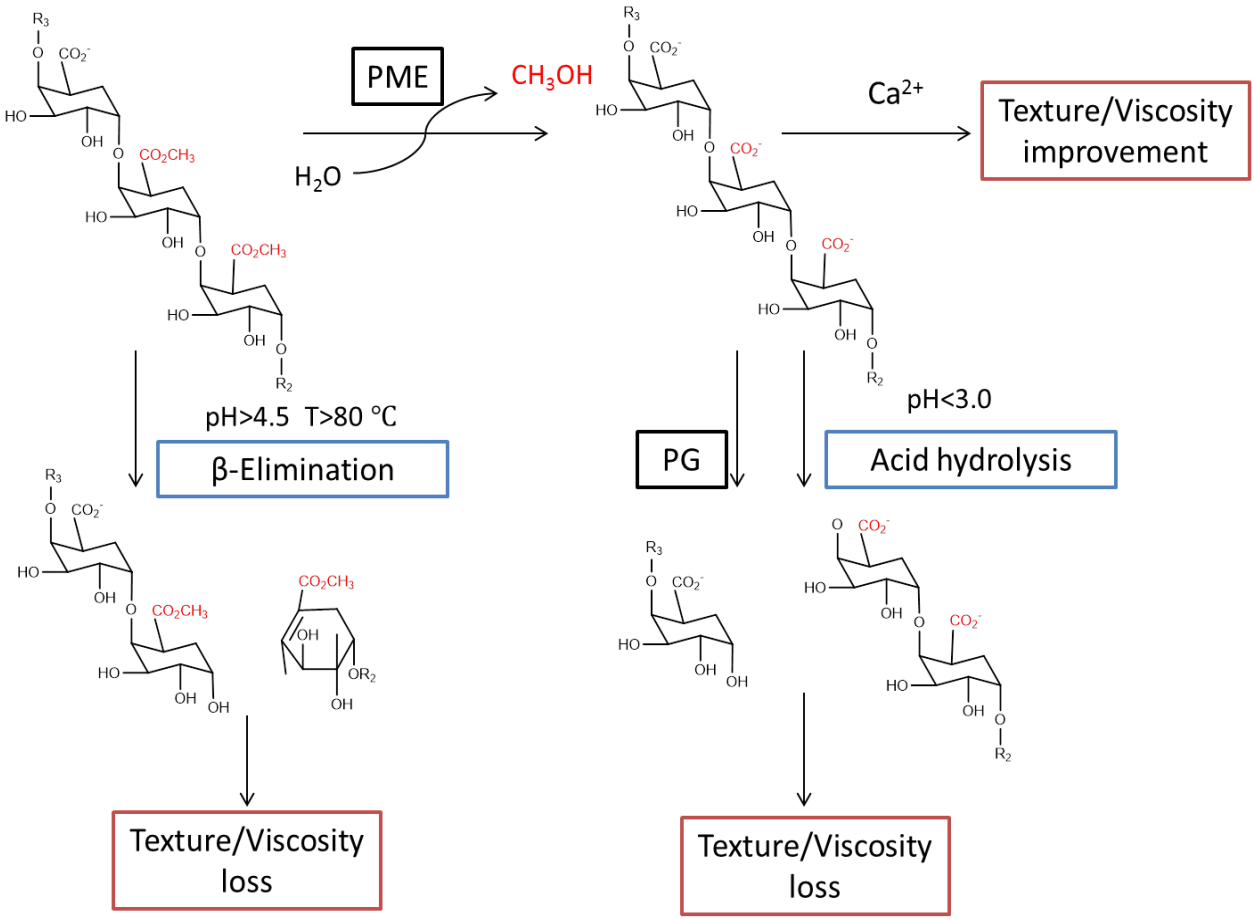


Figure 2.4 Schematic overview of major chemical and enzymatic conversion reactions on pectin (only homogalacturonan). PME = pectinmethylesterase, PG = polygalacturonase, R1 = initial fragment of the pectin polymer, R2 = terminal fragment of the pectin polymer.

Chemical conversion reactions including β-elimination and acid hydrolysis also occur during thermal processing. β-elimination depolymerization usually happens at high temperature (>80 ℃) and weakly acidic or neutral pH (>4.5) (De Roeck et al., 2009). It is reported that β-elimination reaction is promoted by increasing temperature, pH and DM of pectin (Krall & McFeeters, 1998; Sila et al., 2006). Because most cell wall material have a pH above 4.5 and are treated with a high temperature (>80 ℃) during processing, they are very susceptible to the β-elimination reactions (Sila, Smout, Vu, Van Loey, & Hendrickx, 2005). On the other hand, acid hydrolysis happens at a low pH (<3.0), with low DM pectin hydrolyzed faster. The rate of hydrolysis increases with decreasing pH, and rising temperature which is opposite to β-elimination. However, it was reported that acid hydrolysis is negligible in plant cell wall suspension since the pH of the system is generally between 4 to 6 (Brett & Waldron, 1990). Sila et al. (2006) showed the thermal texture degradation had a strong correlation with the rate constant of the β-eliminative reaction, which suggests that the β-elimination reaction is the main chemical conversion during thermal processing.

### 2.2.2 Genetically Modified Tomato Pectin

Pectin degradation associated enzymes PME and PG, present in most fruits and vegetables, are also the most important enzymes to modify the cell wall structure during the ripening process (Errington, Tucker, & Mitchell, 1998). Genetic engineering of crops using recombinant technology has provided promising means to alter in vivo levels of these enzymes for creating “designer” pectin and desired texture of derived foods (Thakur, Singh, & Handa, 1996; Thakur, Singh, Tieman, & Handa, 1996; Tieman, Harriman, Ramamohan, & Handa, 1992). Since the present study uses PME genetically modified tomato fruits, this section only describes genetically engineered PME and its effects on pectin and rheological properties.

Gaffe, Tieman, and Handa (1994) demonstrated the presence of multiple isoforms of PME in tomato fruit. Harriman, Tieman, and Handa (1991) showed the transcript of PME became detectable in 15 days old tomato fruit and reached maximum levels in mature fruit before declining in ripening fruit. However, the maximum PME activity was present in the turning stage of fruit ripening. Tieman et al. (1992) genetically altered the levels of PME in ripening fruits and developed a series of genetically modified tomato genotypes with reduced PME activity (ranged from 7% to 40% of the wild type). In addition, the ripening process of genetic lines was not interfered by the reduction of PME activity, showing almost identical to the wild type without a loss of crop production (Tieman & Handa, 1994).

This research group's following results have shown that reduction in PME activity exhibited remarkable improvements in various qualities of processed tomato products over wild type (Thakur, Singh, & Handa, 1996; Thakur, Singh, Tieman, et al., 1996; Tieman et al., 1992). As expected, both DM and MW of pectin in transgenic fruits have shown significant increases. The transgenic fruit juice also contained higher total (over 5% higher) and soluble solids (3 to 6% higher) contents compared to parental wild type fruits, which was partly due to the highly methoxylated pectin produced by transgenic lines only loosely bonded to the cell wall (Handa, Tieman, Mishra, Thakur, & Singh, 1996). It has been reported that 85-90% reduction in PME activity in transgenic fruits displayed a maximum increase in juice and serum viscosity, and precipitate weight ratio (Takada & Nelson, 1983; Thakur, Singh, Tieman, et al., 1996). The tomato product (ketchup) made from the low PME also exhibited significant improvements in quality attributes, with much higher viscosity and consistency and lowed serum separation compared to products having high PME (Thakur, Singh, Tieman, et al., 1996). However, those studies only focused on the changes of pectin; and few have demonstrated the plant tissue

structural changes by genetic modified PME pectins in relation to the product textural properties. Thus, the effects of reduced PME activity on the cell wall tissue as well as the particles in the derived products need to be further investigated.

## 2.3 Particle Phase

The particle phase of plant-cell-wall-derived foods has become of interest recently. As food suspensions, their rheologies are greatly controlled by particle phase volume, particle properties and associated interactions (Mueller, Llewellin, & Mader, 2010). However, many models used to investigate the structure and rheology are based on particles that are hard spheres, non-deformable and non-interacting, and diluted systems (Fuchs & Ballauff, 2005; Vanderwerff & Dekruif, 1989). Opposing to these ideal assumptions, real plant cell wall particles are soft, highly deformable and non-spherical, and often forming concentrated suspensions. These soft particles can deform and adjust themselves in the available space in the suspension, therefore the actual volume fraction of the suspension may change with increasing concentration (Tan, Tam, Lam, & Tan, 2004). Although the currently used models assuming hard spheres particles is far from reality, it has provided fundamental and semi-empirical information to understand rheological properties of dense suspensions from plant-cell-wall-derived materials (van der Vaart, Rahmani, et al., 2013). On the other hand, only few models have been developed to study suspensions consisting of soft particles, and they have not been applied to fruit and vegetable suspensions.

### 2.3.1 Particle Volume Fraction

Particle volume fraction is one of the most important factors influencing the rheology of suspension (Mueller et al., 2010). Particle phase volume fraction ($\phi$) is defined as the ratio

between the volume of particles in the suspension and the total volume of the suspension. The classical model theoretically derived by Einstein for hard spherical shows that the viscosity of the suspension is a linear function of the volume fraction, according to Equation 2.1 (Einstein, 1906):

$$\eta = \eta_s(1 + 2.5\phi) \tag{2.1}$$

where $\eta$ is the viscosity of the suspension whereas $\eta_s$ is the viscosity of the medium. In addition to the assumption of hard spheres Einstein's equation applies to diluted ($\phi$<0.05) and semi-dilute ($\phi$<0.15) suspension. To account the effects of particle interactions that occur at increasing volume fractions, the Batchelor's equation was an extension to Einstein's equation by including second order term involving the volume fraction (Batchelor, 1977):

$$\eta = \eta_s(1 + 2.5\phi + C\phi^2) \tag{2.2}$$

The coefficient *C* have a range of values from 4.2 to 6.2, which depends on the hydrodynamic interaction between two particles and the suspension microstructure (Batchelor, 1977).

Ball and Richmond (1980) found that for non-colloidal spheres *C*=5.2 was most accurate. Vaart et al. (2013) used C=5.9 to directly link viscosity and volume fraction for a suspension of hard spheres (i.e. poly-methylmethacrylate (PMMA)). However, this model is only valid up to $\phi$ of 15-10%. When $\phi$ >20%, multi-particle interactions take place, which makes it difficult to describe the rheology of the suspension theoretically (Brady & Bossis, 1985). Therefore, many phenomenological equations such as MPQ (Maron & Pierce, 1956; Quemada, 1977), Krieger and Dougherty (1959), and Mendoza and Santamaria-Holek (2009) models have been proposed to describe the viscosity of concentrated suspensions to the volume fraction $\phi$ at high particle concentrations. The Krieger and Dougherty model is a widely used semi-empirical equation to describe the effect of particle concentration on the suspension viscosity:

$$\eta_r = \frac{\eta}{\eta_s} = (1 - \frac{\phi}{\phi_m})^{-[\eta]\phi_m} \tag{2.3}$$

$\eta_r$ is the suspension relative viscosity, $[\eta]$ is the intrinsic viscosity, and $\phi_m$ is the maximum packing fraction. For dilute suspensions of hard spheres, $[\eta]$ is taken as 2.5 and the Krieger-Dougherty model may reduce to the Einstein's equation. For dilute suspensions containing soft spheres, $[\eta]$ is determined by using well-known methodologies from specific viscosity versus concentration plots (Beresovsky, Kopelman, & Mizrahi, 1995; Moelants et al., 2013). $\phi_m$ is often taken as 0.64 for monodisperse hard spheres which is the random close packed limit (Sierou & Brady, 2001).

At very low particle concentration, soft spherical particles exhibit a similar behavior to that of hard spheres (Mason & Weitz, 1995), and the above described models may well apply. However at high concentration, these models are no longer valid because the permanent contact between particles, which significantly affect the rheological behavior of the suspensions (van der Vaart, Rahmani, et al., 2013). It should be noted that the determination of $\phi$ and the influence of the particle softness and its associated deformation during flow is critical to define the rheological behavior of suspension containing soft particles, because they can be prone to measurement artifacts. For concentrated suspensions of soft particles, some semi-empirical models have been proposed to link the mechanical properties of single particles to the bulk rheology of the suspensions (Evans & Lips, 1990; Seth, Cloitre, & Bonnecaze, 2006; van der Vaart, Rahmani, et al., 2013). For example, Evans and Lips (1990) developed the model expressed by Equation 2.4 to estimate the elastic modulus G of a suspension containing Sephadex microgel particles, in which the interparticle forces were assumed to be dominated by the elastic deformation of the contacting particles:

$$G = \left[ \left( \phi_r^{2/3} - \phi_r^{1/3} \right)^{1/2} - \frac{8}{3} \left( \phi_r - \phi_r^{1/3} \right)^{3/2} \right] \left( \frac{\phi_m n G_P}{5\pi(1-v)} \right) \tag{2.4}$$

$\phi_r$ is the relative phase volume related to the packing volume $\phi_m$ and defined by $\phi_r = \phi / \phi_m$; $n$ is the number of particles of the nearest neighbors; $G_P$ is particle shear elastic modulus which is a function of Young's modulus ($E$) and the Poisson ratio ($v$) of the particle described as $G_P = E / \left[ 2(1+v) \right]$. To characterize the modulus $G_P$ of a single particle, measurements such as micromanipulation (Yan et al., 2009) and atomic force microscopy (AFM) (Liu, Sun, & Simmons, 2013) have been reported. These techniques yield more information about concentrated suspension behavior governed by inter-particle interactions and microstructure. Micromanipulation can be used to measure the deformation or break response to compression of single suspension cell between two parallel flat surfaces (Thomas, Zhang, & Cowen, 2000). Blewett et al. (2000) reported a compression study of single tomato cells using this technique and concluded that the peak force was associated to the cell wall elasticity and the turgor pressure, which are essential to maintaining cell strength. AFM has been extensively used for studying the mechanical properties of single particles in colloidal system even biological cells (Mahaffy, Park, Gerde, Kas, & Shih, 2004; Radmacher, Fritz, Kacher, Cleveland, & Hansma, 1996). Usually Hertz model (Equation 2.5) is applied to fit the force-indentation curve, which yields the Young's modulus of the particles.

$$F = \begin{cases} \dfrac{4ER^{0.5}}{3(1-v^2)} \delta^{1.5} & \text{For spherical tip of radius } R \\ \dfrac{2E \tan\theta}{\pi(1-v^2)} \delta^2 & \text{For sharp cone tip of opening angle } 2\theta \end{cases} \tag{2.5}$$

$F$ is contact force determined by the AFM tip; $E$ is Young's modulus of the particles; and $\delta$ is the sample deformation (i.e., indentation).

Unlike hard spheres, it is more difficult to determine the actual volume fraction for soft plant cell wall particles. The simplest way is to relate the weight of particles to their specific volume. However, this conversion should be treated with caution since the actual phase volume may change at high concentration due to particle deformation. Particle volume fraction is sometimes expressed as particle concentration, water-insoluble solids (WIS), or pulp content, all based on the sample preparation. Regardless, the concentration of the dispersed phase is considered to have a major influence in the flow behavior of suspensions containing cell wall material (Moelants, Cardinaels, Jolie, et al., 2014; Moelants et al., 2013). In general, rheological parameters such as viscosity, yield stress and storage modulus increase with increasing particle concentration (Appelqvist, Cochet-Broch, Poelman, & Day, 2015; Moelants, Cardinaels, Jolie, et al., 2014; Yoo & Rao, 1994). To characterize its effect, the power law model is usually used and it has been found a positive correlation between the consistency index ($k$) and the particle concentration (Moelants, Cardinaels, Jolie, et al., 2014; Tanglertpaibul & Rao, 1987a; Yoo & Rao, 1994). According to Lopez-Sanchez et al. (2011), the volume fraction ($\phi$) is a result of the way that particles pack together and is closely related to the particle size, morphology, and deformability, and has similar importance than particle concentration in affecting the rheological properties of suspensions containing plant cell wall material. The critical volume fraction $\phi_c$ is a key parameter that can be obtained from dynamic oscillatory measurements (Day, Xu, Oiseth, Lundin, & Hemar, 2010). Day et al. (2010) reported that when $\phi$ is lower than $\phi_c$, the complex modulus $G^*$ follows a power law function with the volume fraction $\phi$. However when $\phi$ is larger than $\phi_c$, the particles are highly packed, the material behaves more like a viscoelastic solid so more elaborated and advanced models as those described by Mason et al. (1995) and Adam et al. (2004) seem to be more suitable.

### 2.3.2 Particle Properties

Particle properties including particle size distribution, particle morphology, and particle deformability also influence the rheology of suspension (Moelants, Cardinaels, Jolie, et al., 2014; Moelants et al., 2013; Yoo & Rao, 1994). It has been reported that particle size distribution has a strong impact on the rheology of highly concentrated suspensions (Willenbacher & Georgieva, 2013). Suspensions with broad size distribution exhibit smaller viscosities compared to those with narrow size distribution for the same particle volume fraction. This can be explained by the more efficient particle packing when the size ratio is large, since smaller particles could fit voids between large particles. However, the effect of the particle size and distribution on the rheology of plant-cell-wall-based suspensions is still not clear and different conclusions have been reported in previous studies (Redgwell, Curti, & Gehin-Delval, 2008; Schuvens, van Vliet, & van Dijk, 1998; Tanglertpaibul & Rao, 1987b; Yoo & Rao, 1994). DenOuden and VanVliet (1997) sorted tomato suspensions by wet sieving them and found suspensions with larger particle fractions had a significantly lower apparent viscosity and lower yield stress for both homogenized and non-homogenized samples. However, a lower viscosity was found in tomato concentrate produced using smaller screen size compared to those produced with intermediate screen size (Tanglertpaibul & Rao, 1987b). On one hand, smaller particles have a larger surface area than that of larger particles at the same volume fraction. Therefore, the interaction between particles can increase in suspensions having smaller particle size thus leading to suspension with larger viscosity and yield stress (Yoo & Rao, 1994). On the other hand, larger particles can occupy more space at the same pulp content and therefore be more likely to collide and prevent them from moving past each other resulting in larger viscosity (Quemada, 1998). Generally, after mechanical treatments, the average particle sizes of plant cell wall materials range between 40 to 500 μm (Moelants, Cardinaels, Van Buggenhout, et al., 2014). These soft particles are much

larger than particles in colloidal systems for which most models have been developed. Application of models for suspensions containing cell wall material needs to be further investigated to elucidate the effect of these particles on the bulk rheology on these suspension systems.

Generally, plant cell wall particles are not spherical which introduces additional effects on the rheology of suspensions. The contribution of non-spherical particles to the bulk rheology depends on their orientation with respect to the flow. In addition, the particle interactions are strongly influenced by the particle morphology (Mueller et al., 2010). Food processes generate different type of particles that are associated with the particle size (Day, Xu, Oiseth, Hemar, & Lundin, 2010; Moelants, Cardinaels, Jolie, et al., 2014). Appelqvist et al. (2015) studied the viscosity profiles of carrot-derived suspensions having a wide solid content range and different cell types, which include cluster cells, single cells and cell fragments. Suspensions containing these three different types of cells showed distinct rheological patterns and indicated the particle interactions varied with the types of cells and different particle phase volumes. The influence of particle morphology and cell type on the suspension rheology has been shown by several authors (Appelqvist et al., 2015; Day, Xu, Oiseth, Lundin, et al., 2010; Moelants, Cardinaels, Jolie, et al., 2014). Dynamic yield stress is obtained by extrapolation of the flow curve to zero shear rate (i.e. stress at zero shear rate) whereas the static yield stress is measured by probing with shear stress as minimum required to initial flow (Cheng, 1986). Moelants et al. (2014) reported that the ratio of the static to dynamic yield stress could be a measure to characterize the particle morphology and the ratio turned out to be larger for particles with more irregular surfaces, i.e. with a tendency to create structures in the solid phase of the suspensions. In addition, plant cell wall particles are highly deformable due to the nature of parenchyma cells and their deformability,

which can affect the value of maximum packing fraction $\phi_m$ and thereby influence the rheological properties of suspensions containing them (Snabre & Mills, 1996). It has been reported that PME treated apple suspensions have shown a high elastic modulus due to cross-linking of pectin (Bengtsson, Wikberg, & Tornberg, 2011). The influence of particle properties is complex because as particle size changes, other properties such as morphology, deformability and associated critical volume fraction $\phi_c$, and particle interaction will change simultaneously (Moelants, Cardinaels, Van Buggenhout, et al., 2014).

## 2.4 Processing Conditions

As discussed before, the rheology of plant-cell-wall-derived foods is influenced by the structure and function of particles as well as serum pectin, which is related to pectin degradation and is greatly affected by the food processing techniques applied and the intensity of that process (Van Buggenhout et al., 2009). For example in the tomato industry, most tomatoes are processed into tomato pastes (i.e. concentrate) before any further food production (Abu-Jdayil et al., 2004). They are considered as concentrated suspensions and have a minimum concentration of natural soluble solids of 24% (w/w) (Agriculture, 1977). These products are stored in bulk, and can be reconstituted up to 18 months later for various products, such as soups and sauces. The basic sequence of unit operations in a typical, medium-sized plant is shown in Figure 2.5. Except for the preparation steps (sorting and trimming) which aim to minimize contaminants, the flowing steps mainly fall into two categories: thermal and mechanical procedures. Thermal processing includes breaking, concentration, and sterilization, while mechanical processing contains crushing or chopping, extraction, and homogenization. These processing conditions have great effects on the major quality attributes of tomato products including color, flavor, and consistency

(i.e., viscosity). Process-induced changes in chemical and physical properties of both particle and serum phases are reviewed in this section.

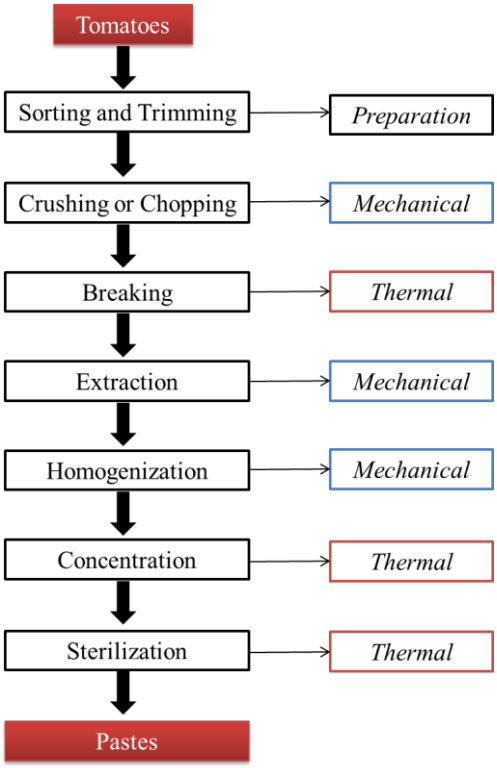


Figure 2.5 Flow chart for tomato paste production, reproduced from Moresi and Livarotti (1982).

### 2.4.1 Thermal Processing

Thermal processing is a commonly used treatment before intense mechanical destruction of plant cell wall tissue. Blanching, breaking, and sterilization are known to result in softening of plant cell wall tissue, because it can cause a loss of cell firmness through disruption of cell membrane as well as pectin thermal degradation (Greve, Mcardle, Gohlke, & Labavitch, 1994). The initial loss of firmness is caused by turgor loss due to cell membrane disruption (Greve, Shackel, et al., 1994). In addition, solubilization and depolymerization of pectin in the middle

lamella that controls cell-cell adhesion further accelerate this process (Greve, Mcardle, et al., 1994; Van Buren, 1979; Waldron et al., 2003).

In tomato processing industry hot break (HB) and cold break (CB) are two processes commonly used in the "break" stage, which play vital role in determining the quality of final product (Nelson & Hoff, 1969). In the HB system, the crushed material is pumped into a heat exchanger and heated rapidly in a temperature range of 82.2 to 104.4 ℃. By contrast, for the CB procedure, crushed tomatoes are further processed at a temperature in the range of 66 to 77 ℃, and then transferred to a holding-tank, where they are held for a period of time ranging from seconds to several minutes (Gould, 1983). The two main objectives of the break steps are the partial or full inactivation of degradative enzymes, and the softening of tissues to facilitate further processing (G. L. Marsh, Buhlert, & Leonard, 1980). Due to less thermal abuse, CB products exhibit better retention of color and flavor, but with a reduced viscosity. The overall viscosity of products increases with the temperature regime used in the break process (Gould, 1974, 1992; Hand, Moyer, Ransford, Hening, & Whittenberger, 1955; Hsu, 2008; Luh & Daoud, 1971; Thakur, Singh, & Nelson, 1996), and for years many researches attributed it to the inactivation s of pectolytic enzymes such as PME and PG. In the HB treatment, they can be efficiently inactivated due to a sufficiently high temperature; therefore the enzymatic pectin degradation and its associated cell-wall weakening effects are prevented (Moelants, Cardinaels, Van Buggenhout, et al., 2014). However, in the CB treatment, the remaining activity of pectolytic enzymes can continue to break down pectin and release water-soluble pectic oligomers.

Several studies also showed that break temperatures affected the particle properties. Redgwell et al. (2008) reported that CB can produce intact tomato single cells. Lopez-Sanchez et al. (2011) noticed that CB and low temperature HB led to the formation of a microstructure that

was similar to that of a non-heated material, whereas high temperatures used in the HB treatment generated a highly disrupted mixture of cell content and cell wall materials. It also should be noticed that during prolonged thermal processing, the thermal degradable pectin present in the cell wall and middle lamella is leached out, which not only weakens the binding between cells but also influences the viscosity of the serum phase. Moelants et al. (2013) found an increase in the amount of serum pectin and a decrease in average molar mass when the thermal treatment shifted from mild to intense could be explained by β-elimination of pectin in the cell wall, which promotes pectin thermo-solubilization and depolymerization. Hurtado et al. (2002) and Anthon et al. (2008) also observed a similar increase of water-soluble pectin in tomato paste during thermal processing. Thermal processing alters both particle and serum phase and consequently changes the rheological properties of the suspension. Xu et al. (1986) measured the apparent viscosity of tomato juices and pastes treated at different break temperatures, and found that the highest temperature (107 ℃) produced the highest viscosity. It was suggested that was caused by enzymatic inactivation and a higher release of soluble pectin at the highest temperature. However, Lopez-Sanchez et al. (2011) hypothesized that changes in particle properties caused by thermal treatments were responsible for the changes of rheological characteristics of tomato suspensions.

Concentration of tomato juice to paste is another step using intense heating during the paste production. The purposes of this process are for long-term storage and easy transportation (Anthon et al., 2008). Typically, this process takes more than 2 h of heating under reduced pressure in either batch-type or continuous evaporation systems. However, subsequent dilution for production of tomato products exhibits a loss of consistency (Anthon et al., 2008). The cause for this problem has not yet been completely determined, although some hypotheses have been proposed, such as pectin hydrolysis during the high temperature heating (Hurtado et al., 2002),

irreversible deleterious changes in the particles due to high osmotic and ionic strength (George L. Marsh, Buhlert, & Leonard, 1977), and mechanical shear on the juice during pumping (Beresovsky et al., 1995; Mizrahi, 1997). According to Anthon et al. (2008), there was little or no change in the total pectin content during the concentration of both HB and CB juices. However, insoluble pectin was decreased resulting in a higher Bostwick value, but these two measurements weren't directly connected due to different pattern changes, i.e. insoluble pectin decrease was observed at the late stage of concentration, whereas the product consistency was lost at the initial stage. Beresovsky et al. (1995) found that the loss of consistency still happened without applying heat or vacuum. It indicated that mechanical effect other than thermal effect could be responsible for the consistency loss. Furthermore, Anthon et al. (2008) suggested that the reduction in the particle size and precipitate ratio could be the main causes for the loss in consistency.

### 2.4.2 Mechanical Processing

In industrial processing, the material (juices and pastes) is subjected to high shear forces during the "finisher" stage which generally involves a extraction step, sometimes combined with a homogenization step. The main purpose of the extraction step is to remove skin and seeds and to squeeze the juice out of the remaining residue (Goose & Binsted, 1973). Both screw type and paddle type finishers are commonly used in industry, and screen size and blade speed are usually selected to control the gross viscosity of tomato products. The screen size affects the product viscosity by generating particles with different sizes. As discussed in the previous section, the effects of particle size on the suspension rheology can be explained by two different manners: (1) increases of viscosity due to the large surface area of small particles and (2) decreases of the viscosity due to volume exclusion of large particles (Tanglertpaibul & Rao, 1987b).

Tanglertpaibul and Rao (1987b) found that a finisher screen size of 0.686 mm yielded products with a higher apparent viscosity than that of products processed with either smaller (0.508 mm) or larger (0.838 and 1.143 mm) screen sizes. Noomhorm and Tansakul (1992) also reported similar results. Based on these results, it was suggested that to obtain a maximum apparent viscosity, an intermediate screen size was recommended (Tanglertpaibul & Rao, 1987b). Changing speed of the blade in the finisher also caused a variation in the viscosity of the product. At any given screen size, higher speed yielded tomato juice and puree with higher viscosity (Noomhorm & Tansakul, 1992).

Homogenization, another way to refine texture, is a standard procedure in industrial ketchup production. This procedure can significantly prevent serum separation as increases the volume of particles and enhances their effective dispersion due to the rupture of the plant cells (Thakur, Singh, & Nelson, 1996). Both reduced particle size and notably changes in microstructure have been reported after homogenization. The former was believed to contribute to a better consistency (Redgwell et al., 2008), while the latter was more important in preventing serum separation (Robinson, Kimball, Ransford, Moyer, & Hand, 1956). After homogenization, microfibrils and cell fragments were released, which could prevent efficient packing into a precipitate of low volume associated with a low medium viscosity (Shomer, Lindner, & Vasiliver, 1984). Homogenization has been reported to modify not only the particle size but also the particle properties such as the aspect ratio, shape, and the orientation of particles, thus improving the rheological properties (e.g. the viscosity) of the suspensions compared to non-homogenized samples (Bayod, Mansson, Innings, Bergenstahl, & Tornberg, 2007). Recently high pressure homogenization (HPH) was reported to produce small particles such as single cells and cell fragments (Lopez-Sanchez et al., 2011; Moelants, Cardinaels, Jolie, et al., 2014;

Sankaran et al., 2015). The serum phase was also affected by HPH processing as decreased the chain length of serum pectin (Moelants et al., 2013). Such reduction in serum viscosity was observed by Augusto et al. (2012), but not by Moelants et al. (2013). The effect of HPH on rheological properties is also related to the plant source. Lopez-Sanchez et al. (2011) reported that HPH reduced the viscosity of carrot and broccoli suspensions however increased the viscosity of tomato suspensions. The swelling of tomato cells upon treatment was noticed which was in agreement with Thakur et al. (1995). It indicated the network structure in the tomato suspensions was enhanced by HPH.

In recent studies, thermal treatments combined with mechanical treatments were applied to yield suspensions with different particle sizes and morphologies. Day et al. (2010) reported a blanching (80 ℃ for 10 min) or cooking (100 ℃ for 30 min) process followed by a blending process (8 min) can generate carrot suspensions predominantly with cluster cells or single cells respectively. A further high shear homogenization using microfluidization even produced “cell fragment” suspensions (Appelqvist et al., 2015). The viscoelastic properties of these suspensions were different for the different treatments. During processing, plant cell wall composition, particle structure, as well as serum pectin change simultaneously, which poses difficulties for rheological measurement and analysis (Moelants, Cardinaels, Van Buggenhout, et al., 2014). A reconstitution principle has been applied by some authors to generate model suspensions because well-characterized systems have to be established for proper studies (Moelants, Cardinaels, Jolie, et al., 2014; Yoo & Rao, 1994).

### 2.4.3 Ultrasound Processing

Ultrasound has been used as an alternative processing option to conventional thermal approaches (Chandrapala, Oliver, Kentish, & Ashokkumar, 2012). When ultrasound passes

through a liquid medium, it generates an effect known as acoustic cavitation (AC) which locally results in a very high local temperature (5500 ℃), high pressure (500 MPa), and enormous shear forces at the point of collapsing cavitation bubbles (Chandrapala, Oliyer, Kentish, & Ashokkumar, 2012; Sehgal, Sutherland, & Verrall, 1980). Multiple physical and biochemical effects caused by cavitation can lead to changes in the structure of cell wall materials through the breakdown of weak intermolecular interaction forces and disruption of particles and cellular compartments(Farkade, Harrison, & Pandit, 2006). The effect of ultrasound on the structure of plant cell tissue depends on the source of tissue as well as the processing conditions. Both high and low intensity ultrasound treatments have been used extensively in applications. However, high-intensity power output may cause significant mechanical tissue disruption, resulting in loss of turgor pressure and softer tissue, which makes this setting inappropriate for processing whole and sliced fruit and vegetable products (Knoerzer et al., 2016). Thus, low-intensity ultrasound pretreatment is the choice to improve the structure and texture of many plant-cell-wall-based foods (Day, Xu, Oiseth, & Mawson, 2012).

Studies reported to date were mainly focused on the effect of ultrasound on PME and PG inactivation (J. Wu, Gamage, Vilkhu, Simons, & Mawson, 2008), for which protein denaturation is assumed to be the main reason (O'Donnell, Tiwari, Bourke, & Cullen, 2010; J. Wu et al., 2008). Controlling the viscosity by ultrasound has been successfully applied to many food systems, most of which are starchy based such as corn, potato, tapioca, and sweet potato (Chandrapala, Oliyer, et al., 2012). Recently, ultrasound treatment has been reported to improve the structural and textural properties of non-starchy cell wall materials including carrot and peas (Day et al., 2012; Knoerzer et al., 2016). Day et al. (2012) compared the effects of ultrasound pre-processing treatment to low temperature blanching pretreatments (60 ℃ for 10 and 40 min)

on the mechanical properties of carrot cell wall tissue, and found the application of ultrasound could shorten the blanching time (from 40 to 10 min) to achieve the same result. However, in terms of the structure and properties of the particles, there are only a few reports on the application of ultrasound to improve the rheological properties of non-starchy plant cell wall materials.

## 2.5 Rheological Properties and Measurements

Food rheology as a powerful analytical tool focuses on the physical characterization of individual food components, including raw material prior to processing, intermediate products during manufacturing, and finished foods (Tabilo-Munizaga & Barbosa-Canovas, 2005). From a chemical standpoint, foods are very impure (Bourne, 1977) and structurally extremely complex with a range of hierarchical nanostructures and microstructures (Donaldis, 2004; Mezzenga, Schurtenberger, Burbidge, & Michel, 2005; Trappe & Sandkuhler, 2004). Therefore, the rheological properties of food materials are determined by the main components and their interactions on a wide variety of length scales (Fischer & Windhab, 2011). In a plant cell wall suspension system, three different components are found: low MW materials such as glucose and fructose, high MW water soluble polymers such as pectins, both in the serum phase; and insoluble particles including cell fragments, single cells, and cell clusters. This dynamic composition and associated interactions among components make suspensions to exhibit a rheological behavior that depends on material sources and processing conditions, and therefore represent a serious challenge for their characterization.

### 2.5.1 Viscosity of Plant-Cell-Wall-Derived Suspension

Most “pure” dilute liquid foods are considered as Newtonian fluids, such as milk, tea, coffee, beer, wines, and soda drinks (M. A. Rao, 1977b). The major characteristic of these fluids is that the viscosity is influenced only by temperature and the food composition and independent of the applied shear rate and previous shear history (M. A. Rao, 1977a, 1977b).

However, most food materials including plant cell wall suspensions are non-Newtonian in nature. Many models have been employed to describe the rheology of various food materials successfully, such as power law (V. N. M. Rao, Harrington, Hamann, & Humphries, 1975), Casson (Servais, Ranc, & Roberts, 2003; Taylor, Van Damme, Johns, Routh, & Wilson, 2009), Bingham (Fraiha, Biagi, & Ferraz, 2011; Oliveira, de Souza, & Monteiro, 2008), and Herschel-Bulkley (Sherman, 1970). All these models can be considered as a developed or modified form from the generalized Newtonian fluid (GNF) constitutive equation (Equation 2.6), an equation of a tensor order that describes properly the rheological behavior of simple liquids.

$$\underline{\underline{\tau}} = -\eta(\dot{\gamma})\,\underline{\underline{\dot{\gamma}}} \tag{2.6}$$

where $\underline{\underline{\tau}}$ is shear stress tensor, $\underline{\underline{\dot{\gamma}}}$ is shear rate tensor, and $\eta(\dot{\gamma})$ is the apparent viscosity.

Ofoli et al. (1987) used a four-parameter model (Equation 2.7) to characterize the rheology of fluid foods, which has accurately described flow curves expressed as shear stress versus shear rate, and apparent viscosity versus shear rate. The general model given by Equation 1.7 can result in other well-recognized models if the parameters are defined as illustrated in Table 2.1.

$$\tau^{n_1} = \tau_0^{\,n_1} + \mu_\infty \dot{\gamma}^{n_2} \tag{2.7}$$

$\mu_\infty$ is the high-shear limiting viscosity and $n_1$ and $n_2$ are rheological parameters.

Table 2.1 GNF rheological models and their ability to characterize specific fluid food behavior, adapted from Ofoli et al. (1987)

| Fluid type | Shear stress | Finite Yield Stress | Variable Shear Behavior | Finite High Shear $\eta$ | Rheological Parameters | | | |
|---|---|---|---|---|---|---|---|---|
| | | | | | $\tau_0$ | $\mu_\infty$ | $n_1$ | $n_2$ |
| Power law | $\tau = k\ \dot{\gamma}^{\ n}$ | No | Yes | No | 0 | $k$ | 1 | n |
| Bingham | $\tau = \tau_0 + \mu_0\ \dot{\gamma}$ | Yes | No | Yes | $\tau_0$ | $\mu_0$ | 1 | 1 |
| Herschel Bulkley | $\tau = \tau_0 + k\ \dot{\gamma}^{\ n}$ | Yes | Yes | No | $\tau_0$ | $k$ | 1 | n |
| Casson | $\tau^{0.5} = {\tau_0}^{0.5} + (\mu_\infty\ \dot{\gamma}\ )^{0.5}$ | Yes | No | Yes | $\tau_0$ | $\mu_\infty$ | 0.5 | 0.5 |

The power law model is the one of the most widely used models to describe the rheological behavior of plant cell wall suspensions, where *k* is the consistency coefficient and *n* is a flow index. The *n* value measures the departure of the fluid from pure Newtonian behavior. The apparent viscosity decreases with increasing shear rate for *n* value less than 1, indicating a shear thinning behavior. For *n* greater than 1, the fluid is showing shear-thickening behavior. Many studies have reported that plant-cell-wall-derived suspensions exhibited shear thinning behavior (Moelants, Cardinaels, Jolie, et al., 2014; Tanglertpaibul & Rao, 1987a), which indicate that there are particle structural changes upon application of a shear flow (Morrison, 2001). Tomato products such as tomato concentrate and ketchup all showed shear thinning with *n* values in a range from 0.22 to 0.42 (Autio & Houska, 1991; Rani & Bains, 1987; M. A. Rao & Qiu, 1989). However, serum and concentrated serum only exhibited slight shear thinning behavior with *n* values in the range 0.9 to 1.0 (Tanglertpaibul & Rao, 1987a; B. Wu, 2011). These results demonstrate that the shear thinning behavior of plant cell suspensions, notably

tomato products, was mainly caused by the characteristics of the suspension solid phase and also depended on the insoluble solid content.

The flow behavior of cell wall derived suspensions has also shown time-dependent effects, known as thixotropy and rheopexy. At fixed temperature and shear rate, the viscosity of a thixotropic fluid decreases with time whereas the viscosity of a rheopectic fluid increases with time (H. A. Barnes, 1997). Although characterization of time-dependent behavior is important for understanding the structure changes during processing, there are only few reports for tomato products in which they were characterized as thixotropic fluids (Augusto, Falguera, Cristianini, & Ibarz, 2012). Weltman model(1943) and Figoni and Figoni model(1983) are widely used to describe thixotropic behavior in foods. In addition, suspensions containing plant-cell-wall-based particles also showed temperature-dependent behavior, which could be described by an Arrhenius-like equation (Equation 2.8).

$$\eta(\dot{\gamma}) = A \cdot \exp(\frac{B}{T}) \tag{2.8}$$

where A and B are empirical parameters, and T is the absolute temperature.

### 2.5.2 Rheological Measurements

Steady-state shear is the most widely used measurement to characterize the viscosity of suspensions. All GNF models discussed in previous section are applicable to describe the rheology of suspensions containing cell-wall-derived particles. In particular, the power law and Herschel-Bulkley models are the most commonly used. However, these tests characterize a material's response to an applied shear rate or shear stress range, and only give us information about the material's viscous properties (i.e. resistance to flow). It has also been noted that GNF

models fail to predict shear normal stresses $N_1$ and $N_2$, which are related to elastic effects. It can be inferred from the GNF tensor form of the model.

Shear flow:
$$\underline{\underline{\dot{\gamma}}} = \begin{pmatrix} 0 & \dot{\gamma}_{21}(t) & 0 \\ \dot{\gamma}_{21}(t) & 0 & 0 \\ 0 & 0 & 0 \end{pmatrix}$$

GNF:
$$\underline{\underline{\tau}} = -\eta \underline{\underline{\dot{\gamma}}} = \begin{pmatrix} 0 & -\eta\dot{\gamma}_{21}(t) & 0 \\ -\eta\dot{\gamma}_{21}(t) & 0 & 0 \\ 0 & 0 & 0 \end{pmatrix} \tag{2.9}$$

Therefore, based on the steady-shear tests the response is assumed to be independent of the previous shear history and is only a function of the instantaneous rate-of-deformation tensor, so it is not possible to describe viscoelastic effects (material with memory) as done using transient tests such as creep and recovery, small strain oscillatory shear (SAOS) (Matsumoto & Sherman, 1981). To describe these behaviors, viscoelastic models transient tests should be applied.

The SAOS test is performed by subjecting a material to a sinusoidal deformation strain (or stress) and measuring the resulting stress (or strain) as a function of time. The SAOS test has become a well-established method for measuring the linear viscoelastic properties of various viscoelastic materials (Hyun et al., 2011; Tschoegl, 1989). The response of stress in the linear range is proportional to the applied strain given by the following equation:

Applied strain:
$$\gamma(t) = \gamma_0 \sin(\omega t) \tag{2.10}$$

Resulting stress:
$$\tau(t) = \tau_0 \sin(\omega t + \delta) = \gamma_0 G'(\omega)\sin(\omega t) + \gamma_0 G''(\omega)\cos(\omega t) \tag{2.11}$$

where $G'(\omega)$ is storage modulus defined as $G'(\omega)=\frac{\sigma_o}{\gamma_o}\cos\delta$ and $G''(\omega)$ is loss modulus defined as $G''(\omega)=\frac{\sigma_o}{\gamma_o}\sin\delta$; $\gamma_0$ is applied strain amplitude and $\tau_0$ is measured stress amplitude; $\omega$ is frequency and $\delta$ is measured phase angle. One of the main advantages of the SAOS test is that the deformation that applies to the sample is very small and practically has negligible effects on the structure of the tested samples, i.e. it is considered as a non-destructive test. Normally, a strain sweep at a low frequency (e.g., 1 Hz) should be performed first to determine the linear viscoelastic range (LVR) where G' and G" should be independent of the applied strain. From studies on fruit and vegetable suspensions such as apple (Espinosa-Munoz, Renard, Symoneaux, Biau, & Cuvelier, 2013), peach (Massa, Gonzalez, Maestro, Labanda, & Ibarz, 2010), tomato (Valencia et al., 2002) and carrot (Day, Xu, Oiseth, Hemar, et al., 2010; Day, Xu, Oiseth, Lundin, et al., 2010), it has been concluded that these systems exhibit weak gel behavior with storage modulus G' greater than loss modulus G", regardless of the frequency.

However, during most food processing the deformations applied to the material can be very fast and of large intensity (Hyun et al., 2011). Therefore, the stress response is no longer a sinusoidal wave proportional to the strain input. Furthermore, linear viscoelasticity theory no longer hold the definition of the G' and G" moduli defined in LVR, so those viscoelastic parameters lose their physical meaning (Sim, Ahn, & Lee, 2003). In recent 20 years, with the benefit of novel analog-to-digital converter (AD converter), large amplitude oscillatory shear (LASO) test coupled with Fourier transformation (FT) analysis became a powerful tool to study the properties in non-linear range (Hyun et al., 2011). Before that, Lissajous–Bowditch loop, plot of stress versus strain or plot of stress versus strain rate, was the major tool of LAOS analysis (Kwang Soo Cho, 2016).

Nowadays, LAOS measurements can be conducted easily on most commercial rheometers, which gives first-harmonic moduli (i.e., G' and G") before any data transformation (see Equation 2.12). Interpretation of the first-harmonic moduli is the simplest way to characterize materials even when the transformed data is unavailable (Hyun et al., 2011). Hyun et al. (2002) summarized at least four types of complex fluids based on the G' and G" values: type I, strain thinning (both G' and G" decreasing); type II, strain hardening (both G' and G" increasing); type III, weak strain overshoot (G' decreasing, and G" increasing followed by decreasing); type IV, strong strain overshoot (both G' and G" increasing followed by decreasing). Further FT analysis could be done after the stress decomposition (SD), in which the shear stress of LAOS is decomposed into elastic and viscous parts (K. S. Cho, Hyun, Ahn, & Lee, 2005). SD is mathematically the equivalent to FT-rheology (Kim, Hyun, Kim, & Cho, 2006) and recently Ewoldt et al. (2008) proposed Chebyshev polynomial to connect SD with FT-rheology. Although FT becomes an effective method for quantitative analysis of LAOS, the mechanics are still in developing in many materials (Hyun et al., 2011). LAOS methodology becomes popular in various polymer material characterizations. However, only limited studies with not very conclusive results have been performed using the LAOS technique to test food products (Duvarci, Yazar, & Kokini, 2017; Joyner & Meldrum, 2016; van der Vaart, Depypere, et al., 2013).

$$\tau(t) = \gamma_0 \sum_{n,odd} \left[ G_n'(\omega, \gamma_0) \sin(\omega t) + G_n''(\omega, \gamma_0) \cos(\omega t) \right] \tag{2.12}$$

### 2.5.3 Wall Slip in Measurements

In a flow of two-phase system, wall slip describes the displacement of the dispersed phase away from solid boundaries, resulting a low-viscosity, depleted layer of liquid (Howard A. Barnes, 1995). In a concentrated suspension, wall slip occurs where the local concentration of

suspended particles at the wall is lower than in the bulk, which creates a large velocity gradient in this low viscosity layer (Buscall, 2010). This phenomenon is called apparent wall slip to distinguish true slip for polymer melts (H. A. Barnes, 1999). Wall slip generally occurs in many rheological measurements even without notice and it has been considered as a serious source of artifacts during testing of multiphase systems (Cloitre & Bonnecaze, 2017). When wall slip is present in the measurement, it causes erroneous interpretation of rheological parameters (e.g. yield stress) and flow curve.

Suspensions of soft and deformable particles are sensitive to wall slip due to the deformable nature that enables them to contact and bypass the roughness modified to the smooth surface to suppress wall slip. Meeker, Bonnecaze, and Cloitre (2004) studied the wall slip in microgel pastes and identified three regimes of slip depending on the stress value. They also concluded that the slip depended on solvent viscosity, bulk shear modulus, and particle size. To eliminate slip from rheological measurements, rough shearing surfaces are commonly used. The idea is turning the smooth surface responsible for slip to a rough one. It could be done either by physical modification of the geometry surface such as creating a grooved of serrated surface (Meeker et al., 2004), or by sticking sandpaper (Khan, Schnepper, & Armstrong, 1988). Although some of these techniques are useful for suppressing wall slip, they are still empirical and sometimes it is impossible to decide the proper level of surface roughness. According to some studies, the optimum roughness value is that of the particle size when the particles are well dispersed. Buscall (2010) reported the roughness had to be much larger than or equal to the order of the particle size in the system in order to eliminate wall slip. In the study of food materials, plates with sandpaper attached to their surface are usually used to suppress wall slip (Sankaran et

al., 2015). Sharma et al. (2015) used a serrated plate to study the steady shear viscosity of Mozzarella-type cheeses; however, apparent slip still occurred at higher shear rates.

A specific geometry, the "vane geometry", can be used to avoid the wall slip phenomenon. The vane geometry was originally developed by Boger and others (1983) for measuring yield stress at a low rotation speed. The geometry confines the material between the vane blades, which forms a virtual inner cylinder. Therefore, the yielding occurs at the outer perimeter of the cylindrical volume defined by the blades which significantly suppresses the slip. The shear stress ( $\tau$ ) and shear rate ( $\dot{\gamma}$ ) based on a vane geometry with four blades are given by Equation 2.13 and 2.14, respectively.

$$\tau = M \frac{1}{2\pi r^3} \left(\frac{h}{r} + \frac{2}{3}\right)^{-1} \tag{2.13}$$

$$\dot{\gamma} = \omega \frac{2R^2}{R^2 - r^2} \tag{2.14}$$

$M$ is the torque exerted on the sample; $r$ and h are the radius and height of the vane geometry (virtual inner cylinder); $R$ is the radius of cup (or cell); and $\omega$ is rotational velocity. These equations assume that the material is entrapped between the blades and the inner part of the cylinder. However, the vane does not form a "perfect" cylinder. In addition, the flow in the vane geometry is complex and at high rotation speeds secondary flows could occur. Therefore, the calculated conversion factors have to be slightly correct when using this geometry to study low viscosity Newtonian fluids (Krulis & Rohm, 2004). The vane geometry now is widely used in concentrated suspension system for the steady-shear as well as dynamic oscillatory shear (SAOS and LAOS) measurements. For fruit and vegetable suspensions, some researchers employed the vane geometry to characterize rheological properties of suspensions produced from tomato,

carrot and broccoli (Lopez-Sanchez et al., 2011; Moelants, Cardinaels, Jolie, et al., 2014; Tiback et al., 2014). These studies all obtained reliable rheological data without evidenced wall slip.

## 2.6 References

Abu-Jdayil, B., Banat, F., Jumah, R., Al-Asheh, S., & Hammad, S. (2004). A comparative study of rheological characteristics of tomato paste and tomato powder solutions. *International Journal of Food Properties, 7*(3), 483-497. doi: 10.1081/Jfp-120040203

Adams, S., Frith, W. J., & Stokes, J. R. (2004). Influence of particle modulus on the rheological properties of agar microgel suspensions. *Journal of Rheology, 48*(6), 1195-1213. doi: 10.1122/1.1773782

Agriculture, U.S. Department of. (1977). United States Standards for Grades of Canned Tomato Paste.

Albersheim, P., Darvill, A. G., ONeill, M. A., Schols, H. A., & Voragen, A. G. J. (1996). An hypothesis: The same six polysaccharides are components of the primary cell walls of all higher plants. *Pectins and Pectinases, 14*, 47-55. doi: Doi 10.1016/S0921-0423(96)80245-0

Ambrosini, G. L., De Klerk, N. H., Fritschi, L., Mackerras, D., & Musk, B. (2008). Fruit, vegetable, vitamin A intakes, and prostate cancer risk. *Prostate Cancer and Prostatic Diseases, 11*(1), 61-66. doi: 10.1038/sj.pcan.4500979

Anthon, G. E., Diaz, J. V., & Barrett, D. M. (2008). Changes in pectins and product consistency during the concentration of tomato juice to paste. *Journal of Agricultural and Food Chemistry, 56*(16), 7100-7105. doi: 10.1021/jf8008525

Appelqvist, I. A. M., Cochet-Broch, M., Poelman, A. A. M., & Day, L. (2015). Morphologies, volume fraction and viscosity of cell wall particle dispersions particle related to sensory perception. *Food Hydrocolloids, 44*, 198-207. doi: 10.1016/j.foodhyd.2014.09.012

Augusto, P. E. D., Falguera, V., Cristianini, M., & Ibarz, A. (2012). Rheological Behavior of Tomato Juice: Steady-State Shear and Time-Dependent Modeling. *Food and Bioprocess Technology, 5*(5), 1715-1723. doi: 10.1007/s11947-010-0472-8

Augusto, P. E. D., Ibarz, A., & Cristianini, M. (2012). Effect of high pressure homogenization (HPH) on the rheological properties of tomato juice: Time-dependent and steady-state shear. *Journal of Food Engineering, 111*(4), 570-579. doi: 10.1016/j.jfoodeng.2012.03.015

Autio, K., & Houska, M. (1991). Measurement of flow curves for model liquids and real food systems with two commercial viscometers. *Journal of Food Engineering, 13*(1), 57-66. doi: https://doi.org/10.1016/0260-8774(91)90037-S

Ball, R. C., & Richmond, P. (1980). Dynamics of Colloidal Dispersions. *Physics and Chemistry of Liquids, 9*(2), 99-116. doi: Doi 10.1080/00319108008084770

Barnes, H. A. (1997). Thixotropy - A review. *Journal of Non-Newtonian Fluid Mechanics, 70*(1-2), 1-33. doi: Doi 10.1016/S0377-0257(97)00004-9

Barnes, H. A. (1999). The yield stress - a review or 'pi alpha nu tau alpha rho epsilon iota' - everything flows? *Journal of Non-Newtonian Fluid Mechanics, 81*(1-2), 133-178. doi: Doi 10.1016/S0377-0257(98)00094-9

Barnes, Howard A. (1995). A review of the slip (wall depletion) of polymer solutions, emulsions and particle suspensions in viscometers: its cause, character, and cure. *Journal of Non-Newtonian Fluid Mechanics, 56*(3), 221-251. doi: https://doi.org/10.1016/0377-0257(94)01282-M

Batchelor, G. K. (1977). Effect of Brownian-Motion on Bulk Stress in a Suspension of Spherical-Particles. *Journal of Fluid Mechanics, 83*(Nov), 97-117. doi: Doi 10.1017/S0022112077001062

Bayod, E., Mansson, P., Innings, F., Bergenstahl, B., & Tornberg, E. (2007). Low shear rheology of concentrated tomato products. Effect of particle size and time. *Food Biophysics, 2*(4), 146-157. doi: 10.1007/s11483-007-9039-2

Bengtsson, H., Wikberg, J., & Tornberg, E. (2011). Physicochemical Characterization of Fruit and Vegetable Fiber Suspensions. Ii: Effect of Variations in Heat Treatment. *Journal of Texture Studies, 42*(4), 281-290. doi: 10.1111/j.1745-4603.2010.00276.x

Beresovsky, N., Kopelman, I. J., & Mizrahi, S. (1995). The Role of Pulp Interparticle Interaction in Determining Tomato Juice Viscosity. *Journal of Food Processing and Preservation, 19*(2), 133-146. doi: DOI 10.1111/j.1745-4549.1995.tb00283.x

Blewett, J., Burrows, K., & Thomas, C. (2000). A micromanipulation method to measure the mechanical properties of single tomato suspension cells. *Biotechnology Letters, 22*(23), 1877-1883. doi: Doi 10.1023/A:1005635125829

Bond, Travis Minor and Jennifer K.). Processing Tomato Industry. 2017, from https://www.ers.usda.gov/topics/crops/vegetables-pulses/tomatoes/

Bourne, M. C. (1977). Limitations of Rheology in Food Texture Measurements. *Journal of Texture Studies, 8*(2), 219-227. doi: DOI 10.1111/j.1745-4603.1977.tb01176.x

Brady, J. F., & Bossis, G. (1985). The Rheology of Concentrated Suspensions of Spheres in Simple Shear-Flow by Numerical-Simulation. *Journal of Fluid Mechanics, 155*(Jun), 105-129. doi: Doi 10.1017/S0022112085001732

Brett, C. T., & Waldron, K. W. (1990). *Physiology and biochemistry of plant cell walls*. London ; Boston: Unwin Hyman.

Buscall, R. (2010). Wall slip in dispersion rheometry. *Journal of Rheology, 54*(6), 1177-1183. doi: 10.1122/1.3495981

Carpita, N. C., & Gibeaut, D. M. (1993). Structural Models of Primary-Cell Walls in Flowering Plants - Consistency of Molecular-Structure with the Physical-Properties of the Walls during Growth. *Plant Journal, 3*(1), 1-30. doi: DOI 10.1111/j.1365-313X.1993.tb00007.x

Chandrapala, J., Oliver, C., Kentish, S., & Ashokkumar, M. (2012). Ultrasonics in food processing - Food quality assurance and food safety. *Trends in Food Science & Technology, 26*(2), 88-98. doi: 10.1016/j.tifs.2012.01.010

Chandrapala, J., Oliyer, C., Kentish, S., & Ashokkumar, M. (2012). Ultrasonics in food processing. *Ultrasonics Sonochemistry, 19*(5), 975-983. doi: 10.1016/j.ultsonch.2012.01.010

Cheng, D. C. H. (1986). Yield Stress - a Time-Dependent Property and How to Measure It. *Rheologica Acta, 25*(5), 542-554. doi: Doi 10.1007/Bf01774406

Chin, L. H., Ali, Z. M., & Lazan, H. (1999). Cell wall modifications, degrading enzymes and softening of carambola fruit during ripening. *Journal of Experimental Botany, 50*(335), 767-775. doi: DOI 10.1093/jexbot/50.335.767

Cho, K. S., Hyun, K., Ahn, K. H., & Lee, S. J. (2005). A geometrical interpretation of large amplitude oscillatory shear response. *Journal of Rheology, 49*(3), 747-758. doi: 10.1122/1.1895801

Cho, Kwang Soo. (2016). Large Amplitude Oscillatory Shear *Viscoelasticity of Polymers: Theory and Numerical Algorithms* (pp. 545-599). Dordrecht: Springer Netherlands.

Christiaens, S., Van Buggenhout, S., Chaula, D., Moelants, K., David, C. C., Hofkens, J., Hendrickx, M. E. (2012). In situ pectin engineering as a tool to tailor the consistency and syneresis of carrot puree. *Food Chemistry, 133*(1), 146-155. doi: 10.1016/j.foodchem.2012.01.009

Christiaens, S., Van Buggenhout, S., Houben, K., Chaula, D., Van Loey, A. M., & Hendrickx, M. E. (2012). Unravelling process-induced pectin changes in the tomato cell wall: An integrated approach. *Food Chemistry, 132*(3), 1534-1543. doi: 10.1016/j.foodchem.2011.11.148

Cloitre, M., & Bonnecaze, R. T. (2017). A review on wall slip in high solid dispersions. *Rheologica Acta, 56*(3), 283-305. doi: 10.1007/s00397-017-1002-7

Cosgrove, D. J. (2005). Growth of the plant cell wall. *Nature Reviews Molecular Cell Biology, 6*(11), 850-861. doi: Doi 10.1038/Nrm1746

Davidson, M.W. (2015). Plant cell wall. Retrieved Oct 11, 2017, from http://micro.magnet.fsu.edu/cells/plants/cellwall.html

Day, L., Xu, M., Oiseth, S. K., Hemar, Y., & Lundin, L. (2010). Control of Morphological and Rheological Properties of Carrot Cell Wall Particle Dispersions through Processing. *Food and Bioprocess Technology, 3*(6), 928-934. doi: DOI 10.1007/s11947-010-0346-0

Day, L., Xu, M., Oiseth, S. K., Lundin, L., & Hemar, Y. (2010). Dynamic rheological properties of plant cell-wall particle dispersions. *Colloids and Surfaces B-Biointerfaces, 81*(2), 461-467. doi: 10.1016/j.colsurfb.2010.07.041

Day, L., Xu, M., Oiseth, S. K., & Mawson, R. (2012). Improved mechanical properties of retorted carrots by ultrasonic pre-treatments. *Ultrasonics Sonochemistry, 19*(3), 427-434. doi: 10.1016/j.ultsonch.2011.10.019

De Roeck, A., Duvetter, T., Fraeye, I., Van der Plancken, I., Sila, D. N., Van Loey, A., & Hendrickx, M. (2009). Effect of high-pressure/high-temperature processing on chemical pectin conversions in relation to fruit and vegetable texture. *Food Chemistry, 115*(1), 207-213. doi: 10.1016/j.foodchem.2008.12.016

Deguchi, S., Tsujii, K., & Horikoshi, K. (2006). Cooking cellulose in hot and compressed water. *Chemical Communications*(31), 3293-3295. doi: 10.1039/b605812d

Delmer, D. P. (1987). Cellulose Biosynthesis. *Annual Review of Plant Physiology and Plant Molecular Biology, 38*, 259-290.

DenOuden, F. W. C., & vanVliet, T. (1997). Particle size distribution in tomato concentrate and effects on rheological properties. *Journal of Food Science, 62*(3), 565-567.

Diaz, J. V., Anthon, G. E., & Barrett, D. M. (2009). Conformational Changes in Serum Pectins during Industrial Tomato Paste Production. *Journal of Agricultural and Food Chemistry, 57*(18), 8453-8458. doi: 10.1021/jf901207w

Donaldis, A. (2004). Food for thought. *Nature Materials, 3*(9), 579-581. doi: Doi 10.1038/Nmat1207

Duvarci, O. C., Yazar, G., & Kokini, J. L. (2017). The comparison of LAOS behavior of structured food materials (suspensions, emulsions and elastic networks). *Trends in Food Science & Technology, 60*, 2-11. doi: 10.1016/j.tifs.2016.08.014

Duvetter, T., Sila, D. N., Van Buggenhout, S., Jolie, R., Van Loey, A., & Hendrickx, M. (2009). Pectins in Processed Fruit and Vegetables: Part I - Stability and Catalytic Activity of Pectinases. *Comprehensive Reviews in Food Science and Food Safety, 8*(2), 75-85. doi: 10.1111/j.1541-4337.2009.00069.x

Dzuy, N. Q., & Boger, D. V. (1983). Yield Stress Measurement for Concentrated Suspensions. *Journal of Rheology, 27*(4), 321-349. doi: Doi 10.1122/1.549709

Einstein, A. (1906). A new determination of the molecular dimensions. *Annalen Der Physik, 19*(2), 289-306.

Errington, N., Tucker, G. A., & Mitchell, J. R. (1998). Effect of genetic down-regulation of polygalacturonase and pectin esterase activity on rheology and composition of tomato juice. *Journal of the Science of Food and Agriculture, 76*(4), 515-519. doi: Doi 10.1002/(Sici)1097-0010(199804)76:4<515::Aid-Jsfa979>3.0.Co;2-X

Espinosa-Munoz, L., Renard, C. M. G. C., Symoneaux, R., Biau, N., & Cuvelier, G. (2013). Structural parameters that determine the rheological properties of apple puree. *Journal of Food Engineering, 119*(3), 619-626. doi: DOI 10.1016/j.jfoodeng.2013.06.014

Evans, I. D., & Lips, A. (1990). Concentration-Dependence of the Linear Elastic Behavior of Model Microgel Dispersions. *Journal of the Chemical Society-Faraday Transactions, 86*(20), 3413-3417. doi: Doi 10.1039/Ft9908603413

Ewoldt, R. H., Hosoi, A. E., & McKinley, G. H. (2008). New measures for characterizing nonlinear viscoelasticity in large amplitude oscillatory shear. *Journal of Rheology, 52*(6), 1427-1458. doi: 10.1122/1.2970095

FAO. (2014). Food and Agriculture Organization of United Nations Statistics. Retrieved Aug, 2017, from http://www.fao.org/faostat/en/#data/QC/visualize

Farkade, V. D., Harrison, S. T. L., & Pandit, A. B. (2006). Improved cavitational cell disruption following pH pretreatment for the extraction of beta-galactosidase from Kluveromyces lactis. *Biochemical Engineering Journal, 31*(1), 25-30. doi: 10.1016/j.bej.2006.05.015

FDA. (2017). *Food for human consumption: canned vegetables: tomato concentrates*. (Code of federal regulations. 21CFR155.191). Retrieved from https://www.accessdata.fda.gov/scripts/cdrh/cfdocs/cfCFR/CFRSearch.cfm?fr=155.191.

Figoni, P. I., & Shoemaker, C. F. (1983). Characterization of Time-Dependent Flow Properties of Mayonnaise under Steady Shear. *Journal of Texture Studies, 14*(4), 431-442. doi: DOI 10.1111/j.1745-4603.1983.tb00360.x

Fischer, P., & Windhab, E. J. (2011). Rheology of food materials. *Current Opinion in Colloid & Interface Science, 16*(1), 36-40. doi: DOI 10.1016/j.cocis.2010.07.003

Fraiha, M., Biagi, J. D., & Ferraz, A. C. D. (2011). Rheological behavior of corn and soy mix as feed ingredients. *Ciencia E Tecnologia De Alimentos, 31*(1), 129-134.

Frusciante, L., Carli, P., Ercolano, M. R., Pernice, R., Di Matteo, A., Fogliano, V., & Pellegrini, N. (2007). Antioxidant nutritional quality of tomato. *Molecular Nutrition & Food Research, 51*(5), 609-617. doi: 10.1002/mnfr.200600158

Fuchigami, M. (1987). Relationship between Pectic Compositions and the Softening of the Texture of Japanese Radish Roots during Cooking. *Journal of Food Science, 52*(5), 1317-1320. doi: DOI 10.1111/j.1365-2621.1987.tb14072.x

Fuchs, M., & Ballauff, M. (2005). Flow curves of dense colloidal dispersions: Schematic model analysis of the shear-dependent viscosity near the colloidal glass transition. *Journal of Chemical Physics, 122*(9). doi: Artn 09470710.1063/1.1859285

Gaffe, J., Tieman, D. M., & Handa, A. K. (1994). Pectin Methylesterase Isoforms in Tomato (Lycopersicon-Esculentum) Tissues - Effects of Expression of a Pectin Methylesterase Antisense Gene. *Plant Physiology, 105*(1), 199-203.

Goose, Peter G., & Binsted, Raymond. (1973). *Tomato paste and other tomato products* (2nd ed.). London,: Food Trade Press.

Gould, W.A. (1974). *Tomato Production, Processing and Quality Education*: Westfort, connecticut The AVI Publishing.

Gould, W.A. (1983). *Tomato production, processing, and quality evaluation*: AVI Pub. Co.

Gould, W.A. (1992). *Tomato Production, Processing and Technology*: Woodhead Publishing.

Greve, L. C., Mcardle, R. N., Gohlke, J. R., & Labavitch, J. M. (1994). Impact of Heating on Carrot Firmness - Changes in Cell-Wall Components. *Journal of Agricultural and Food Chemistry, 42*(12), 2900-2906. doi: Doi 10.1021/Jf00048a048

Greve, L. C., Shackel, K. A., Ahmadi, H., Mcardle, R. N., Gohlke, J. R., & Labavitch, J. M. (1994). Impact of Heating on Carrot Firmness - Contribution of Cellular Turgor. *Journal of Agricultural and Food Chemistry, 42*(12), 2896-2899. doi: Doi 10.1021/Jf00048a047

Hand, D. B., Moyer, J. C., Ransford, J. R., Hening, J. C., & Whittenberger, R. T. (1955). Effect of Processing Conditions on the Viscosity of Tomato Juice. *Food Technology, 9*(5), 228-235.

Handa, A. K., Tieman, D. M., Mishra, K. K., Thakur, B. R., & Singh, R. K. (1996). Role of pectin methylesterase in tomato fruit ripening and quality attributes of processed tomato juice. *Pectins and Pectinases, 14*, 355-368. doi: Doi 10.1016/S0921-0423(96)80267-X

Harriman, R. W., Tieman, D. M., & Handa, A. K. (1991). Molecular-Cloning of Tomato Pectin Methylesterase Gene and Its Expression in Rutgers, Ripening Inhibitor, Nonripening, and Never Ripe Tomato Fruits. *Plant Physiology, 97*(1), 80-87. doi: Doi 10.1104/Pp.97.1.80

Heuvelink, J.M. Costa and E. (2005). Introduction: the tomato crop and industry. In E. Heuvelink (Ed.), *Tomatos*. Cambridge, MA: CABI Publishing.

Hsu, K. C. (2008). Evaluation of processing qualities of tomato juice induced by thermal and pressure processing. *Lwt-Food Science and Technology, 41*(3), 450-459. doi: DOI 10.1016/j.lwt.2007.03.022

Hurtado, M. C., Greve, L. C., & Labavitch, J. M. (2002). Changes in cell wall pectins accompanying tomato (Lycopersicon esculentum Mill.) paste manufacture. *Journal of Agricultural and Food Chemistry, 50*(2), 273-278. doi: 10.1021/jf010849e

Hyun, K., Kim, S. H., Ahn, K. H., & Lee, S. J. (2002). Large amplitude oscillatory shear as a way to classify the complex fluids. *Journal of Non-Newtonian Fluid Mechanics, 107*(1-3), 51-65. doi: Pii S0377-0257(02)00141-6. Doi 10.1016/S0377-0257(02)00141-6

Hyun, K., Wilhelm, M., Klein, C. O., Cho, K. S., Nam, J. G., Ahn, K. H., McKinley, G. H. (2011). A review of nonlinear oscillatory shear tests: Analysis and application of large amplitude oscillatory shear (LAOS). *Progress in Polymer Science, 36*(12), 1697-1753. doi: 10.1016/j.progpolymsci.2011.02.002

Ishii, T. (1997). O-acetylated oligosaccharides from pectins of potato tuber cell walls. *Plant Physiology, 113*(4), 1265-1272. doi: DOI 10.1104/pp.113.4.1265

Jackman, R. L., & Stanley, D. W. (1995). Perspectives in the Textural Evaluation of Plant Foods. *Trends in Food Science & Technology, 6*(6), 187-194. doi: Doi 10.1016/S0924-2244(00)89053-6

Janoria, M. P., & Rhodes, A. M. (1974). Juice Viscosity as Related to Various Juice Constituents and Fruit Characters in Tomatoes. *Euphytica, 23*(3), 553-562. doi: Doi 10.1007/Bf00022476

Joyner, H. S., & Meldrum, A. (2016). Rheological study of different mashed potato preparations using large amplitude oscillatory shear and confocal microscopy. *Journal of Food Engineering, 169*, 326-337. doi: 10.1016/j.jfoodeng.2015.08.032

Khan, S. A., Schnepper, C. A., & Armstrong, R. C. (1988). Foam Rheology .3. Measurement of Shear-Flow Properties. *Journal of Rheology, 32*(1), 69-92. doi: Doi 10.1122/1.549964

Kim, H., Hyun, K., Kim, D. J., & Cho, K. S. (2006). Comparison of interpretation methods for large amplitude oscillatory shear response. *Korea-Australia Rheology Journal, 18*(2), 91-98.

Knoerzer, Kai, Juliano, Pablo, & Smithers, Geoffrey W. (2016). *Innovative Food Processing Technologies: Extraction, Separation, Component Modification and Process Intensification*: Woodhead Publishing.

Krall, S. M., & McFeeters, R. F. (1998). Pectin hydrolysis: Effect of temperature, degree of methylation, pH, and calcium on hydrolysis rates. *Journal of Agricultural and Food Chemistry, 46*(4), 1311-1315. doi: Doi 10.1021/Jf970473y

Krieger, I. M., & Dougherty, T. J. (1959). A Mechanism for Non-Newtonian Flow in Suspensions of Rigid Spheres. *Transactions of the Society of Rheology, 3*, 137-152.

Krulis, M., & Rohm, H. (2004). Adaption of a vane tool for the viscosity determination of flavoured yoghurt. *European Food Research and Technology, 218*(6), 598-601. doi: 10.1007/s00217-004-0916-3

Leon Garcia, Milena Maria. (2013). *Impact of Microwave Processing on Quality of High Value Shelf Stable Fruit Products.* (Master of Science Open Access Theses), Purdue University.

Liu, H. J., Sun, Y., & Simmons, C. A. (2013). Determination of local and global elastic moduli of valve interstitial cells cultured on soft substrates. *Journal of Biomechanics, 46*(11), 1967-1971. doi: 10.1016/j.jbiomech.2013.05.001

Lopez-Sanchez, P., Nijsse, J., Blonk, H. C., Bialek, L., Schumm, S., & Langton, M. (2011). Effect of mechanical and thermal treatments on the microstructure and rheological properties of carrot, broccoli and tomato dispersions. *J Sci Food Agric, 91*(2), 207-217. doi: 10.1002/jsfa.4168

Luh, B. S., & Daoud, H. N. (1971). Effect of Break Temperature and Holding Time on Pectin and Pectic Enzymes in Tomato Pulp. *Journal of Food Science, 36*(7), 1039-&.

Mahaffy, R. E., Park, S., Gerde, E., Kas, J., & Shih, C. K. (2004). Quantitative analysis of the viscoelastic properties of thin regions of fibroblasts using atomic force microscopy. *Biophysical Journal, 86*(3), 1777-1793. doi: Doi 10.1016/S0006-3495(04)74245-9

Maron, Samuel H., & Pierce, Percy E. (1956). Application of ree-eyring generalized flow theory to suspensions of spherical particles. *Journal of Colloid Science, 11*(1), 80-95. doi: https://doi.org/10.1016/0095-8522(56)90023-X

Marsh, G. L., Buhlert, J. E., & Leonard, S. J. (1980). Effect of Composition Upon Bostwick Consistency of Tomato Concentrate. *Journal of Food Science, 45*(3), 703-&. doi: DOI 10.1111/j.1365-2621.1980.tb04137.x

Marsh, George L., Buhlert, James, & Leonard, Sherman. (1977). EFFECT OF DEGREE OF CONCENTRATION AND OF HEAT TREATMENT ON CONSISTENCY OF TOMATO PASTES AFTER DILUTION. *Journal of Food Processing and Preservation, 1*(4), 340-346. doi: 10.1111/j.1745-4549.1977.tb00335.x

Mason, T. G., Bibette, J., & Weitz, D. A. (1995). Elasticity of Compressed Emulsions. *Physical Review Letters, 75*(10), 2051-2054. doi: DOI 10.1103/PhysRevLett.75.2051

Mason, T. G., & Weitz, D. A. (1995). Linear Viscoelasticity of Colloidal Hard-Sphere Suspensions near the Glass-Transition. *Physical Review Letters, 75*(14), 2770-2773. doi: DOI 10.1103/PhysRevLett.75.2770

Massa, A., Gonzalez, C., Maestro, A., Labanda, J., & Ibarz, A. (2010). Rheological Characterization of Peach Purees. *Journal of Texture Studies, 41*(4), 532-548. doi: 10.1111/j.1745-4603.2010.00240.x

Matsumoto, S., & Sherman, P. (1981). A Preliminary-Study of W/O/W Emulsions with a View to Possible Food Applications. *Journal of Texture Studies, 12*(2), 243-257. doi: DOI 10.1111/j.1745-4603.1981.tb01234.x

McCann, M. C., & Roberts, K. (1996). Plant cell wall architecture: the role of pectins. *Pectins and Pectinases, 14*, 91-107. doi: Doi 10.1016/S0921-0423(96)80249-8

Meeker, S. P., Bonnecaze, R. T., & Cloitre, M. (2004). Slip and flow in pastes of soft particles: Direct observation and rheology. *Journal of Rheology, 48*(6), 1295-1320. doi: 10.1122/1.1795171

Mendoza, C. I., & Santamaria-Holek, I. (2009). The rheology of hard sphere suspensions at arbitrary volume fractions: An improved differential viscosity model. *Journal of Chemical Physics, 130*(4). doi: Artn 044904

10.1063/1.3063120

Mezzenga, R., Schurtenberger, P., Burbidge, A., & Michel, M. (2005). Understanding foods as soft materials. *Nature Materials, 4*(10), 729-740. doi: Doi 10.1038/Nmat1496

Mizrahi, S. (1997). Irreversible shear thinning and thickening of tomato juice. *Journal of Food Processing and Preservation, 21*(4), 267-277. doi: DOI 10.1111/j.1745-4549.1997.tb00782.x

Moelants, K. R. N., Cardinaels, R., Jolie, R. P., Verrijssen, T. A. J., Van Buggenhout, S., Van Loey, A. M., . . . Hendrickx, M. E. (2014). Rheology of Concentrated Tomato-Derived Suspensions: Effects of Particle Characteristics. *Food and Bioprocess Technology, 7*(1), 248-264. doi: DOI 10.1007/s11947-013-1070-3

Moelants, K. R. N., Cardinaels, R., Van Buggenhout, S., Van Loey, A. M., Moldenaers, P., & Hendrickx, M. E. (2014). A Review on the Relationships between Processing, Food Structure, and Rheological Properties of Plant-Tissue-Based Food Suspensions. *Comprehensive Reviews in Food Science and Food Safety, 13*(3), 241-260. doi: 10.1111/1541-4337.12059

Moelants, K. R. N., Jolie, R. P., Palmers, S. K. J., Cardinaels, R., Christiaens, S., Van Buggenhout, S., Hendrickx, M. E. (2013). The Effects of Process-Induced Pectin Changes on the Viscosity of Carrot and Tomato Sera. *Food and Bioprocess Technology, 6*(10), 2870-2883. doi: 10.1007/s11947-012-1004-5

Moresi, M., & Liverotti, C. (1982). Economic-Study of Tomato Paste Production. *Journal of Food Technology, 17*(2), 177-192.

Morrison, Faith A. (2001). *Understanding rheology*. New York: Oxford University Press.

Mueller, S., Llewellin, E. W., & Mader, H. M. (2010). The rheology of suspensions of solid particles. *Proceedings of the Royal Society a-Mathematical Physical and Engineering Sciences, 466*(2116), 1201-1228. doi: 10.1098/rspa.2009.0445

Nelson, P. E., & Hoff, J. E. (1969). Tomato Volatiles - Effect of Variety Processing and Storage Time. *Journal of Food Science, 34*(1), 53-&. doi: DOI 10.1111/j.1365-2621.1969.tb14361.x

Noomhorm, A., & Tansakul, A. (1992). Effect of Pulper-Finisher Operation on Quality of Tomato Juice and Tomato Puree. *Journal of Food Process Engineering, 15*(4), 229-239. doi: 10.1111/j.1745-4530.1992.tb00154.x

O'Donnell, C. P., Tiwari, B. K., Bourke, P., & Cullen, P. J. (2010). Effect of ultrasonic processing on food enzymes of industrial importance. *Trends in Food Science & Technology, 21*(7), 358-367. doi: 10.1016/j.tifs.2010.04.007

Ofoli, R. Y., Morgan, R. G., & Steffe, J. F. (1987). A Generalized Rheological Model for Inelastic Fluid Foods. *Journal of Texture Studies, 18*(3), 213-230. doi: DOI 10.1111/j.1745-4603.1987.tb00899.x

Oliveira, K. H., de Souza, J. A. R., & Monteiro, A. R. (2008). Rheological characterization of ice cream. *Ciencia E Tecnologia De Alimentos, 28*(3), 592-598. doi: Doi 10.1590/S0101-20612008000300014

Palin, R., & Geitmann, A. (2012). The role of pectin in plant morphogenesis. *Biosystems, 109*(3), 397-402. doi: 10.1016/j.biosystems.2012.04.006

Quemada, D. (1977). Rheology of Concentrated Disperse Systems and Minimum Energy-Dissipation Principle .1. Viscosity-Concentration Relationship. *Rheologica Acta, 16*(1), 82-94. doi: Doi 10.1007/Bf01516932

Quemada, D. (1998). Rheological modelling of complex fluids. I. The concept of effective volume fraction revisited. *European Physical Journal-Applied Physics, 1*(1), 119-127. doi: DOI 10.1051/epjap:1998125

Radmacher, M., Fritz, M., Kacher, C. M., Cleveland, J. P., & Hansma, P. K. (1996). Measuring the viscoelastic properties of human platelets with the atomic force microscope. *Biophysical Journal, 70*(1), 556-567.

Rani, U., & Bains, G. S. (1987). Flow Behavior of Tomato Ketchups. *Journal of Texture Studies, 18*(2), 125-135. doi: DOI 10.1111/j.1745-4603.1987.tb00574.x

Rao, M. A. (1977a). Measurement of Flow Properties of Fluid Foods - Developments, Limitations, and Interpretation of Phenomena. *Journal of Texture Studies, 8*(3), 257-282. doi: DOI 10.1111/j.1745-4603.1977.tb01181.x

Rao, M. A. (1977b). Rheology of Liquid Foods - Review. *Journal of Texture Studies, 8*(2), 135-168. doi: DOI 10.1111/j.1745-4603.1977.tb01173.x

Rao, M. A. (1987). Predicting the Flow Properties of Food Suspensions of Plant-Origin. *Food Technology, 41*(3), 85-88.

Rao, M. A., Bourne, M. C., & Cooley, H. J. (1981). Flow Properties of Tomato Concentrates. *Journal of Texture Studies, 12*(4), 521-538. doi: DOI 10.1111/j.1745-4603.1981.tb00265.x

Rao, M. A., & Qiu, C. G. (1989). Rheological Properties of Plant Food Dispersions. *Acs Symposium Series, 405*, 149-171.

Rao, V. N. M., Harrington, W. J., Hamann, D. D., & Humphries, E. G. (1975). Flow Behavior of Non-Newtonian Power Law Foods Using a Concentric Cylinder Viscometer. *Transactions of the Asae, 18*(6), 1193-1196.

Redgwell, R. J., Curti, D., & Gehin-Delval, C. (2008). Physicochemical properties of cell wall materials from apple, kiwifruit and tomato. *European Food Research and Technology, 227*(2), 607-618. doi: 10.1007/s00217-007-0762-1

Rickman, J. C., Barrett, D. M., & Bruhn, C. M. (2007). Nutritional comparison of fresh, frozen and canned fruits and vegetables. Part 1. Vitamins C and B and phenolic compounds. *Journal of the Science of Food and Agriculture, 87*(6), 930-944. doi: 10.1002/jsfa.2825

Robinson, W. B., Kimball, L. B., Ransford, J. R., Moyer, J. C., & Hand, D. B. (1956). Factors Influencing the Degree of Settling in Tomato Juice. *Food Technology, 10*(2), 109-112.

Saha, B. C. (2003). Hemicellulose bioconversion. *Journal of Industrial Microbiology & Biotechnology, 30*(5), 279-291. doi: 10.1007/s10295-003-0049-x

Sankaran, A. K., Nijsse, J., Bialek, L., Bouwens, L., Hendrickx, M. E., & Van Loey, A. M. (2015). Effect of Enzyme Homogenization on the Physical Properties of Carrot Cell Wall Suspensions. *Food and Bioprocess Technology, 8*(6), 1377-1385. doi: 10.1007/s11947-015-1481-4

Schuvens, E. P. H. M., van Vliet, T., & van Dijk, C. (1998). Effect of processing conditions on the composition and rheological properties of applesauce. *Journal of Texture Studies, 29*(2), 123-143.

Sehgal, C., Sutherland, R. G., & Verrall, R. E. (1980). Sonoluminescence of No-Saturated and No2-Saturated Water as a Probe of Acoustic Cavitation. *Journal of Physical Chemistry, 84*(4), 396-401. doi: Doi 10.1021/J100441a010

Selvendran, R. R. (1985). Developments in the Chemistry and Biochemistry of Pectic and Hemicellulosic Polymers. *Journal of Cell Science*, 51-88.

Selvendran, R. R., & Oneill, M. A. (1987). Isolation and Analysis of Cell-Walls from Plant-Material. *Methods of Biochemical Analysis, 32*, 25-153. doi: Doi 10.1002/9780470110539.Ch2

Servais, C., Ranc, H., & Roberts, I. D. (2003). Determination of chocolate viscosity. *Journal of Texture Studies, 34*(5-6), 467-497. doi: DOI 10.1111/j.1745-4603.2003.tb01077.x

Seth, J. R., Cloitre, M., & Bonnecaze, R. T. (2006). Elastic properties of soft particle pastes. *Journal of Rheology, 50*(3), 353-376. doi: 10.1122/1.2186982

Seymour, G. B., Colquhoun, I. J., Dupont, M. S., Parsley, K. R., & Selvendran, R. R. (1990). Composition and Structural Features of Cell-Wall Polysaccharides from Tomato Fruits. *Phytochemistry, 29*(3), 725-731. doi: Doi 10.1016/0031-9422(90)80008-5

Seymour, G. B., Harding, S. E., Taylor, A. J., Hobson, G. E., & Tucker, G. A. (1987). Polyuronide Solubilization during Ripening of Normal and Mutant Tomato Fruit. *Phytochemistry, 26*(7), 1871-1875. doi: Doi 10.1016/S0031-9422(00)81719-7

Sharma, P., Dessev, T. T., Munro, P. A., Wiles, P. G., Gillies, G., Golding, M., . . . Janssen, P. (2015). Measurement techniques for steady shear viscosity of Mozzarella-type cheeses at high shear rates and high temperature. *International Dairy Journal, 47*, 102-108. doi: 10.1016/j.idairyj.2015.03.005

Sherman, P. (1970). *Industrial Rheology*. New York: Academic Press.

Shomer, I., Lindner, P., & Vasiliver, R. (1984). Mechanism Which Enables the Cell-Wall to Retain Homogenous Appearance of Tomato Juice. *Journal of Food Science, 49*(2), 628-633. doi: DOI 10.1111/j.1365-2621.1984.tb12485.x

Sierou, A., & Brady, J. F. (2001). Accelerated Stokesian Dynamics simulations. *Journal of Fluid Mechanics, 448*, 115-146.

Sila, D. N., Smout, C., Elliot, F., Van Loey, A., & Hendrickx, M. (2006). Non-enzymatic depolymerization of carrot pectin: Toward a better understanding of carrot texture during thermal processing. *Journal of Food Science, 71*(1), E1-E9.

Sila, D. N., Smout, C., Vu, S. T., Van Loey, A., & Hendrickx, M. (2005). Influence of pretreatment conditions on the texture and cell wall components of carrots during thermal processing. *Journal of Food Science, 70*(2), E85-E91.

Sila, D. N., Van Buggenhout, S., Duvetter, T., Fraeye, I., De Roeck, A., Van Loey, A., & Hendrickx, M. (2009). Pectins in Processed Fruit and Vegetables: Part II - Structure-Function Relationships. *Comprehensive Reviews in Food Science and Food Safety, 8*(2), 86-104. doi: 10.1111/j.1541-4337.2009.00070.x

Sim, H. G., Ahn, K. H., & Lee, S. J. (2003). Large amplitude oscillatory shear behavior of complex fluids investigated by a network model: a guideline for classification. *Journal of Non-Newtonian Fluid Mechanics, 112*(2-3), 237-250. doi: 10.1016/S0377-0257(03)00102-2

Snabre, P., & Mills, P. (1996). Rheology of weakly flocculated suspensions of viscoelastic particles .2. *Journal De Physique Iii, 6*(12), 1835-1855.

Steele, N. M., McCann, M. C., & Roberts, K. (1997). Pectin modification in cell walls of ripening tomatoes occurs in distinct domains. *Plant Physiology, 114*(1), 373-381.

Stein, E. R., & Brown, H. E. (1975). Gel filtration and disc gel electrophoresis of tomato pectic substances. *J Agric Food Chem, 23*(3), 526-529.

Tabilo-Munizaga, G., & Barbosa-Canovas, G. V. (2005). Rheology for the food industry. *Journal of Food Engineering, 67*(1-2), 147-156. doi: DOI 10.1016/j.jfoodeng.2004.05.062

Takada, N., & Nelson, P. E. (1983). A New Consistency Method for Tomato Products - the Precipitate Weight Ratio. *Journal of Food Science, 48*(5), 1460-1462. doi: DOI 10.1111/j.1365-2621.1983.tb03516.x

Tan, B. H., Tam, K. C., Lam, Y. C., & Tan, C. B. (2004). Dynamics and microstructure of charged soft nano-colloidal particles. *Polymer, 45*(16), 5515-5523. doi: 10.1016/j.polymer.2004.05.055

Tanglertpaibul, T., & Rao, M. A. (1987a). Flow Properties of Tomato Concentrates - Effect of Serum Viscosity and Pulp Content. *Journal of Food Science, 52*(2), 318-321. doi: DOI 10.1111/j.1365-2621.1987.tb06602.x

Tanglertpaibul, T., & Rao, M. A. (1987b). Rheological Properties of Tomato Concentrates as Affected by Particle-Size and Methods of Concentration. *Journal of Food Science, 52*(1), 141-145. doi: DOI 10.1111/j.1365-2621.1987.tb13991.x

Taylor, J. E., Van Damme, I., Johns, M. L., Routh, A. F., & Wilson, D. I. (2009). Shear Rheology of Molten Crumb Chocolate. *Journal of Food Science, 74*(2), E55-E61. doi: DOI 10.1111/j.1750-3841.2008.01041.x

Thakur, B. R., Singh, R. K., & Handa, A. K. (1995). Effect of Homogenization Pressure on Consistency of Tomato Juice. *Journal of Food Quality, 18*(5), 389-396. doi: DOI 10.1111/j.1745-4557.1995.tb00389.x

Thakur, B. R., Singh, R. K., & Handa, A. K. (1996). Effect of an antisense pectin methylesterase gene on the chemistry of pectin in tomato (Lycopersicon esculentum) juice. *Journal of Agricultural and Food Chemistry, 44*(2), 628-630. doi: Doi 10.1021/Jf950461h

Thakur, B. R., Singh, R. K., & Handa, A. K. (1997). Chemistry and uses of pectin - A review. *Critical Reviews in Food Science and Nutrition, 37*(1), 47-73.

Thakur, B. R., Singh, R. K., & Nelson, P. E. (1996). Quality attributes of processed tomato products: A review. *Food Reviews International, 12*(3), 375-401.

Thakur, B. R., Singh, R. K., Tieman, D. M., & Handa, A. K. (1996). Tomato product quality from transgenic fruits with reduced pectin methylesterase. *Journal of Food Science, 61*(1), 85-&. doi: DOI 10.1111/j.1365-2621.1996.tb14731.x

Thibault, J. F., Renard, C. M. G. C., Axelos, M. A. V., Roger, P., & Crepeau, M. J. (1993). Studies of the Length of Homogalacturonic Regions in Pectins by Acid-Hydrolysis. *Carbohydrate Research, 238*, 271-286. doi: Doi 10.1016/0008-6215(93)87019-O

Thomas, C.R., Zhang, Z., & Cowen, C. (2000). Micromanipulation measurements of biological materials. *Biotechnology Letters, 22*(7), 531-537. doi: 10.1023/a:1005644412588

Tiback, E., Langton, M., Oliveira, J., & Ahrne, L. (2014). Mathematical modeling of the viscosity of tomato, broccoli and carrot purees under dynamic conditions. *Journal of Food Engineering, 124*, 35-42. doi: 10.1016/j.jfoodeng.2013.09.031

Tieman, D. M., & Handa, A. K. (1994). Reduction in Pectin Methylesterase Activity Modifies Tissue Integrity and Cation Levels in Ripening Tomato (Lycopersicon-Esculentum Mill) Fruits. *Plant Physiology, 106*(2), 429-436.

Tieman, D. M., Harriman, R. W., Ramamohan, G., & Handa, A. K. (1992). An Antisense Pectin Methylesterase Gene Alters Pectin Chemistry and Soluble Solids in Tomato Fruit. *Plant Cell, 4*(6), 667-679.

Trappe, V., & Sandkuhler, P. (2004). Colloidal gels - low-density disordered solid-like states. *Current Opinion in Colloid & Interface Science, 8*(6), 494-500. doi: DOI 10.1016/j.cocis.2004.01.002

Tschoegl, Nicholas W. (1989). *The phenomenological theory of linear viscoelastic behavior : an introduction*. Berlin ; New York: Springer-Verlag.

UCLA. (1996). Tomato anatomy. from http://www-plb.ucdavis.edu/labs/rost/Tomato/Reproductive/anat.html

USDA. (2012). Economic Research Service, October 09, 2012. Vegetables & Pulses, Tomato. from http://www.ers.usda.gov/topics/crops/vegetables-pulses/tomatoes.aspx#processing

Valencia, C., Sanchez, M. C., Ciruelos, A., Latorre, A., Franco, J. M., & Gallegos, C. (2002). Linear viscoelasticity of tomato sauce products: influence of previous tomato paste processing. *European Food Research and Technology, 214*(5), 394-399. doi: DOI 10.1007/s00217-002-0501-6

Van Buggenhout, S., Sila, D. N., Duvetter, T., Van Loey, A., & Hendrickx, M. (2009). Pectins in Processed Fruits and Vegetables: Part III - Texture Engineering. *Comprehensive Reviews in Food Science and Food Safety, 8*(2), 105-117. doi: 10.1111/j.1541-4337.2009.00071.x

Van Buren, J. P. (1979). THE CHEMISTRY OF TEXTURE IN FRUITS AND VEGETABLES. *Journal of Texture Studies, 10*(1), 1-23. doi: 10.1111/j.1745-4603.1979.tb01305.x

van der Vaart, K., Depypere, F., De Graef, V., Schall, P., Fall, A., Bonn, D., & Dewettinck, K. (2013). Dark chocolate's compositional effects revealed by oscillatory rheology. *European Food Research and Technology, 236*(6), 931-942. doi: 10.1007/s00217-013-1949-2

van der Vaart, K., Rahmani, Y., Zargar, R., Hu, Z. B., Bonn, D., & Schall, P. (2013). Rheology of concentrated soft and hard-sphere suspensions. *Journal of Rheology, 57*(4), 1195-1209. doi: 10.1122/1.4808054

Vanburen, J. P. (1979). Chemistry of Texture in Fruits and Vegetables. *Journal of Texture Studies, 10*(1), 1-23.

Vanderwerff, J. C., & Dekruif, C. G. (1989). Hard-Sphere Colloidal Dispersions - the Scaling of Rheological Properties with Particle-Size, Volume Fraction, and Shear Rate. *Journal of Rheology, 33*(3), 421-454.

Vincken, J. P., Schols, H. A., Oomen, R. J. F. J., McCann, M. C., Ulvskov, P., Voragen, A. G. J., & Visser, R. G. F. (2003). If homogalacturonan were a side chain of rhamnogalacturonan I. Implications for cell wall architecture. *Plant Physiology, 132*(4), 1781-1789. doi: 10.1104/pp.103.022350

Waldron, K. W., Parker, M. L., & Smith, A. C. (2003). Plant Cell Walls and Food Quality. *Comprehensive Reviews in Food Science and Food Safety, 2*(4), 128-146. doi: 10.1111/j.1541-4337.2003.tb00019.x

Weltmann, R. N. (1943). Breakdown of thixotropic structure as function of time. *Journal of Applied Physics, 14*(7), 343-350. doi: Doi 10.1063/1.1714996

Whitney, S. E. C., Gothard, M. G. E., Mitchell, J. T., & Gidley, M. J. (1999). Roles of cellulose and xyloglucan in determining the mechanical properties of primary plant cell walls. *Plant Physiology, 121*(2), 657-663. doi: Doi 10.1104/Pp.121.2.657

Whittenberger, R. T., & Nutting, G. C. (1958). High Viscosity of Cell Wall Suspensions Prepared from Tomato Juice. *Food Technology, 12*(8), 420-424.

Willats, W. G. T., McCartney, L., Mackie, W., & Knox, J. P. (2001). Pectin: cell biology and prospects for functional analysis. *Plant Molecular Biology, 47*(1-2), 9-27. doi: Doi 10.1023/A:1010662911148

Willenbacher, N., & Georgieva, K. (2013). Rheology of Disperse Systems. *Product Design and Engineering: Formulation of Gels and Pastes*, 7-49. doi: Book_Doi 10.1002/9783527654741

Wu, B. (2011). *Tomato product viscosity is determined by the physical properties of the pulp*. (M.s.), Purdue University. Retrieved from http://login.ezproxy.lib.purdue.edu/login?url=http://gateway.proquest.com/openurl?url_ver=Z39.882004&rft_val_fmt=info:ofi/fmt:kev:mtx:dissertation&res_dat=xri:pqm&rft_dat=xri:pqdiss:1510030

Wu, J., Gamage, T. V., Vilkhu, K. S., Simons, L. K., & Mawson, R. (2008). Effect of thermosonication on quality improvement of tomato juice. *Innovative Food Science & Emerging Technologies, 9*(2), 186-195. doi: 10.1016/j.ifset.2007.07.007

Xu, S. Y., Shoemaker, C. F., & Luh, B. S. (1986). Effect of Break Temperature on Rheological Properties and Microstructure of Tomato Juices and Pastes. *Journal of Food Science, 51*(2), 399-&. doi: DOI 10.1111/j.1365-2621.1986.tb11140.x

Yan, Y., Zhang, Z. B., Stokes, J. R., Zhou, Q. Z., Ma, G. H., & Adams, M. J. (2009). Mechanical characterization of agarose micro-particles with a narrow size distribution. *Powder Technology, 192*(1), 122-130. doi: 10.1016/j.powtec.2008.12.006

Yoo, B., & Rao, M. A. (1994). Effect of Unimodal Particle-Size and Pulp Content on Rheological Properties of Tomato Puree. *Journal of Texture Studies, 25*(4), 421-436. doi: DOI 10.1111/j.1745-4603.1994.tb00772.x

# CHAPTER 3. EFFECTS OF SOLUBLE PECTIN ON THE VISCOSITY OF RECONSTITUTED TOMATO SUSPENSIONS

## 3.1 Introduction

As one of the most cultivated vegetable crops worldwide, tomato had a global production of about 170.8 million tons in 2014 (FAO, 2014). In general, tomatoes are processed into tomato paste before any further manufacturing (Abu-Jdayil, Banat, Jumah, Al-Asheh, & Hammad, 2004), and 80% of produced tomatoes in US are consumed as processed products such as tomato sauce, juice or ketchup (Rickman, Barrett, & Bruhn, 2007). Most tomato products are suspensions of plant cell wall particles dispersed in a continuous serum phase (Moelants, Cardinaels, Jolie, et al., 2014; Rao, 1987). The rheological properties of the suspension are influenced by the concentration of the particles in the suspension, the attributes of those particles (i.e., size distribution, morphology and deformability), and by properties of the serum phase (Moelants, Cardinaels, Jolie, et al., 2014; Moelants et al., 2013; Yoo & Rao, 1994).

Pectin contributes to the structural makeup of the plant cell wall material along with cellulose microfibrils and hemicellulose (Palin & Geitmann, 2012; Sankaran et al., 2015). Pectin molecules consist mainly of polymerized galacturonic acid (GalA) subunits, many of which are methyl-esterified at the C-6 position (Rinaudo, 1988). It has been hypothesized that cell wall pectin becomes soluble in the serum phase via depolymerization and demethoxylation caused by severe thermal treatment and enzymatic activity (Sila et al., 2009; Tiback, Langton, Oliveira, & Ahrne, 2014; Van Buggenhout, Sila, Duvetter, Van Loey, & Hendrickx, 2009). It has been also suggested that both the concentration and chemical properties of the solubilized pectin may influence the viscosity of the serum phase. Many studies have shown that an increase in serum viscosity can be achieved with increasing pectin content (Moelants, Cardinaels, Van Buggenhout,

et al., 2014; Moelants et al., 2013; Tanglertpaibul & Rao, 1987). A few studies have also demonstrated the effects of pectin properties, such as degree of methoxylation (DM), molar mass distribution, composition and conformation, on serum viscosity (Diaz, Anthon, & Barrett, 2009; Moelants et al., 2013). Moelants et al. (2013) investigated the influence of the galacturonic acid (GalA) content and the properties of pectin (specifically DM and size distribution) after thermal treatment and high-pressure homogenization on the viscosity of the serum phase. It was concluded that the characteristics of the pectin soluble in the serum phase only had a limited effect on the rheological properties of tomato suspensions.

Recently, it has become of interest to many researchers the characteristics of particles derived from plant cell wall material and their influence on typical foods, such as juices, pastes, etc. Results of those researches have shown that the physical properties of the cell wall materials, hereby called particles, are important physical characteristics that strongly depend on the treatment applied to process them and have a large influence on the rheological properties of the derived products. Various processes such as thermal and mechanical treatments have been employed to produce suspensions with different particle physical properties (e.g. size, morphology, and deformability) (Appelqvist, Cochet-Broch, Poelman, & Day, 2015; Day, Xu, Oiseth, Hemar, & Lundin, 2010; Lopez-Sanchez, Nijsse, et al., 2011; Moelants, Cardinaels, Jolie, et al., 2014). However, plant cell wall composition, particle structure, as well as serum soluble pectin often change simultaneously during food processing, which poses difficulties for the analysis of the effect of process on the resulting mechanical properties of the final products (Moelants, Cardinaels, Van Buggenhout, et al., 2014). Studies on the mechanisms of particle modifications have been suggested as a key way to understand the effects of the tomato particles on the viscosity of the final products and separation of particles with further reconstitution of

suspensions approaches have been used in several studies (Moelants, Cardinaels, Jolie, et al., 2014; Moelants, Cardinaels, Van Buggenhout, et al., 2014; Yoo & Rao, 1994). The idea behind the formation of reconstituted suspensions is to better understand the role of each component of the suspension such as the particle attributes and the viscosity of the suspension medium on the viscosity of tomato products. Thus, based on several reconstitution procedures described in the literature, well-characterized suspensions in terms of particle size, particle content of the particle phase and the characteristics of soluble pectin in the serum phase could be established in the present study.

The Bostwick consistometer is a simple device developed by E.P. Bostwick, which is widely used by the tomato industry and has been specifically employed to evaluate the consistency of tomato products (Barrett, Garcia, & Wayne, 1998). Although of notable use in many applications and quality control, values determined with this instrument are merely empirical and cannot be used to infer physicochemical characteristics of these suspensions. On the other hand, rheometer has been extensively used for determining the viscosity of tomato products. Cone-plate geometry is commonly used for viscosity measurement of tomato juice or relatively thin samples (Barrett et al., 1998). To characterize the rheological profile of concentrated suspensions containing particles having large sizes, a vane geometry (Day et al., 2010; Lopez-Sanchez & Farr, 2012; Lopez-Sanchez, Nijsse, et al., 2011; Moelants, Cardinaels, Jolie, et al., 2014; Tiback et al., 2014) or parallel plates with rough surfaces (Sankaran et al., 2015) has been chosen to eliminate wall slip effect which commonly occurs in these suspensions. In addition of minimizing problems of slip, settling of significantly large particles from suspensions is another occurring measuring artifact that can be minimized using the vane geometry.

In the present study, tomato suspensions were reconstituted from pulp (i.e. particles) obtained from commercial tomato sauce and pectin solutions prepared with different concentrations and types of pectin. The influence of particle concentration, pectin concentration in the serum, and pectin DM, on the rheological characteristics of the tomato suspensions were examined. To account for potential artifacts related to the fundamental rheological characterization of suspensions, yet to compare to an industry-relevant technique, the rheology of the reconstituted suspensions was measured by two geometries (vane and cone-plate) and by the Bostwick consistometer. Therefore, the main objective of this work was to evaluate the effects of soluble pectin on the rheological properties of tomato suspensions determined by different rheological methods.

## 3.2 Materials and Methods

### 3.2.1 Preparation of Pectin Solutions

High DM pectin (DM=70%, HDM) and medium DM pectin (DM= 52%, MDM) were purchased from CP Kelco Ltd. (GA, USA) and used for the preparation of pectin solutions that were used as the sera of the reconstituted suspensions.

Pectin samples were dissolved in deionized distilled water by continuous stirring for 4 hours to prepare the pectin solutions. A pectin content of 2.6 mg/mL in the serum for Hot Break tomato juice has been reported by Wu and was used as a reference value (Wu, 2011). Pectin solutions having pectin concentrations of 25%, 50%, 100%, 200% and 400% of the chosen reference (2.6 mg/mL) were prepared using both HDM and MDM pectins. The samples were labeled as HDM (or MDM) Pectin_25%, Pectin_50%, Pectin_100%, Pectin_200% and Pectin_400%.

### 3.2.2 Preparation of Reconstituted Tomato Suspensions

Tomato sauce (Gold Red, IN, USA) was purchased from a local market. It was centrifuged (Beckman AvantiTM J-251, CA, USA) at 13,000 *g* at 10 ℃ for 30 min. Then the serum was discarded and replaced with an equal amount of deionized distilled water. Then it was stirred homogeneously and centrifuged again. The pulp was stored for 2 hours for further preparations. To prepare all suspensions, an express blender (Ninja Englewood NJ100Express Chopper, MA, USA) was employed for 2 minutes.

#### 3.2.2.1 Pulp% Suspension Series

Pulps were reconstituted in tomato suspensions using deionized distilled water and 5 different pulp fractions (pulp%): 5, 10, 15, 20, 25 and 30 wt. %. The pulp% was calculated as:

$$\text{pulp\%} = \frac{\text{weight of pulp}}{\text{weight of pulp and water (or pectin solution)}} \times 100\% \tag{3.1}$$

#### 3.2.2.2 Pectin% Suspension Series

20% pulp% reconstituted suspensions were prepared using the different pectin solutions and the extracted pulp. As noted the pulp% used for the suspensions containing dissolved pectin with different concentrations was the same and equal to 20%. Hence, rheological differences among the samples in this series are attributed to the characteristics of the serum, which was varied by the pectin content and DM.

### 3.2.3 Bostwick Consistency

The consistency of the suspensions was measured using a standard Bostwick consistometer (CSC Scientific Company, VA, USA). The suspension maintained at room temperature (i.e. 25 ℃) was placed in the instrument chamber. The instrument gate was released

while simultaneously initiating the stopwatch. The distance travelled by the suspension (±0.1 cm) after 30 s was recorded. Measurements were performed in triplicate.

### 3.2.4 Rheological Measurements

The rheological measurements were carried out in a stress controlled rheometer (ARG2; TA Instruments, DE, USA) using vane and cone-plate geometries. The four-blade vane geometry has a diameter of 28 mm and a height of 42 mm, respectively. To avoid effects of changes in the sample structure and consequently rheological results due to loading, the sample was subjected to a pre-shearing step at a shear rate of 100 1/s for 60 s followed by 2 min rest period prior to measurements(Moelants, Cardinaels, Jolie, et al., 2014). The cone-plate geometry has a 2-degree cone angle and a 40 mm diameter. All measurements were performed at least in triplicate at a constant temperature of 25 ℃.

### 3.2.5 Particle Size Measurements

The particle size distribution of the suspension was measured by laser light scattering using a Malvern Mastersizer 2000 instrument (Malvern Instruments Ltd, Worcestershire, UK). Prior to measurements, all samples were stirred in a dispersion unit at a speed of 2000 RPM. Approximately 2 ml of each sample were pipetted into a diluting accessory (Hydro 2000 MU) filled with 800 ml of deionized distilled water to achieve an obscuration of 10-15% to minimize multiple scattering effects. All measurements were performed in triplicate and the particle size distribution was calculated from the intensity profile of the scattered light based on the Mie theory using the instrument software (Mastersizer2000, version 5.40). The parameters: $D[v,0.1]$, $D[v,0.5]$ and $D[v,0.9]$ (μm) were recorded for each sample, also the volume based ($D[4, 3]$) and area-based ($D[3, 2]$) diameters were obtained according to the following equations:

$$D[4,3] = \frac{\sum_i n_i d_i^4}{\sum_i n_i d_i^3} \tag{3.2}$$

$$D[3,2] = \frac{\sum_i n_i d_i^3}{\sum_i n_i d_i^2} \tag{3.3}$$

where $n_i$ is the number of particles of diameter $d_i$.

### 3.2.6 Statistical Analysis

All the measurements were performed in triplicate and the results were given as mean of three measurements ± standard deviation. The rheological data was analyzed using Trios (TA Instruments, DE, USA).

Rheological data of pectin solutions exhibited Newtonian behavior and were accurately described by the Newton equation for viscosity:

$$\tau = \mu\dot{\gamma} \tag{3.4}$$

where $\tau$ = shear stress (Pa), $\mu$ = viscosity (Pa.s), and $\dot{\gamma}$ = shear rate ($s^{-1}$)

Rheological data from the suspensions was described by the power law model given by the following equation:

$$\tau = k\dot{\gamma}^n \tag{3.5}$$

where $k$ = consistency index ($Pa.s^n$), and $n$ the flow index (-))

Statistical analysis was carried out using SAS 9.3 software package (SAS Institute, Inc., NC, USA). All pairwise comparisons were tested using Tukey method. The level of significance was set at $p<0.05$.

## 3.3 Results and Discussion

### 3.3.1 Particle Size Characterization

The particle size distributions of all the reconstituted suspensions with different concentration of particles (pulp%) are given in Table 3.1. It can be seen that particle sizes in all suspensions were larger than the particle size of the commercial tomato sauce. Differences may be explained due to the centrifugation process that may have caused aggregation of particles. Thermal and mechanical treatments are commonly used to change the physical properties of plant cell materials, potentially from changes in the cell particle size (Moelants, Cardinaels, Van Buggenhout, et al., 2014). For instance, it has been reported that application of a hot break process to tomatoes resulted in smaller particle size in comparison with the size of cell-wall-derived particles formed in a cold break process (Lopez-Sanchez, Nijsse, et al., 2011). Those differences in particle size results are probably due to different shear forces and temperatures used in these two processes. Furthermore, high-pressure homogenization (HPH) is able to generate small particles and even cell fragments (Lopez-Sanchez, Nijsse, et al., 2011; Moelants, Cardinaels, Jolie, et al., 2014). Since no physical treatment are involved in this study, as expected the particle size distribution in each reconstituted suspension was practically similar (Table 3.1). Becker et al. (1972) reported that the tomato cell size dimensions varied between 400 and 1000 μm. Lopez-Sanchez et al. (2012; 2011) calculated the average tomato cell diameter from light microscopy images and found it was between 350 and 450 μm and the $D[3, 2]$ of individual tomato cell was about 233 μm. In Moelants's report (2014), $D[v,0.5]$ of particle ranged from 300 to 400 μm and they were assumed as intact cells or even cell clusters. Therefore, based on the size distribution parameters reported in Table 3.1 it can be concluded that the reconstituted tomato suspensions used in this study comprise mainly intact cells and some cell fragments.

Table 3.2 illustrates the particle size distribution properties of reconstituted suspensions with a particle concentration of 20% and prepared with serum having different pectin concentrations and different types of pectin. As shown in Table 3.2, there was no major difference among the size distribution characteristics of these suspensions. The overall average particle sizes ($D[v,0.5]$ or $D[3, 2]$) of particles in suspensions prepared with pectin at all concentrations were slightly larger than those in suspensions prepared with a medium without pectin (pulp% suspension series) for the same particle concentration of 20%. Given the characteristics of the suspensions, these differences could be attributed to the presence of solubilized pectin in the suspension serum. It is thought that negatively charged pectin molecules could increase the interaction between particles and cell fragments. As a result, $D[v,0.1]$ increased because of the possible tiny fragment bonding to large particles. The effect of pectin on the particle surface and the rheological properties of suspensions formed with particles originated from plant cell material have been discussed recently (Tiback et al., 2014). However, it is necessary further visualization and location of the pectin on the particle surface.

Moelants et al. (2014) concluded there was no a clear effect of particle size on the rheological properties of cell-wall-derived food suspensions because as particle size changes, particle morphology and size distribution may be also changing. The type of particle including cell clusters, single cells and cell fragments is another important factor influencing the relationship between particle size and the suspension rheology. Appelqvist et al. (2015) determined viscosity profiles of these three particle types and concluded the interaction between the particles varied with the critical packing volume of each type of particle. It must be noted that the parenchyma cells of tomato tissues are highly deformable and not exactly spherical, and the assumptions on which the laser diffraction measurements are based (Den Ouden & Van Vliet,

2002), so the absolute values of particle sizes obtained from this measurement should be treated with caution. However, the trend appears to indicate that a qualitative analysis of these results is appropriate.

### 3.3.2 Viscosity of Pectin Solutions

The flow curves of the different pectin solutions measured with the vane geometry are illustrated in Figures 3.1A and 3.1B. The viscosities of both HDM and MDM pectin solutions were less than 0.1 Pa.s and practically independent of shear rate in the range 0.1 to 100 $s^{-1}$. It can be noted that for solutions of low pectin concentrations (both HDM and MDM) the viscosities of the solutions were low, and the use of the vane geometry resulted in an apparent shear thickening at shear rates larger than 10 $s^{-1}$ (Figures 3.1A and 3.1B). That effect was likely caused by flow instabilities or secondary flows known as Taylor instability, which have been reported when testing is done in concentric-cylinder geometries at high shear rates around $10^3$ $s^{-1}$ for liquids with viscosity close to 0.001 Pa.s (Ewoldt, Johnston, & Caretta, 2015). Results shown in Figures 3.1A and 3.1B appear that secondary flow is exacerbated by the vane geometry and becomes noticeable at lower shear rates (10 $s^{-1}$). When the concentration of pectin in the solutions was increased, their viscosities increased accordingly and the instability effects observed at higher shear rate disappeared (see viscosity data for the 200% and 400% solutions for both HDM and MDM pectin in Figures 3.1A and 3.1B). These instabilities were not observed when the cone-plate geometry was used to test these solutions (Figures 3.1C and 3.1D). When comparing the values of viscosity obtained with the two geometries, the use of the vane geometry provided slightly lower values than those obtained with the cone-plate geometry at high pectin concentrations (i.e. 200% and 400%), whereas at 100% or lower pectin concentrations (i.e. 25% and 50%) the two geometries yielded almost identical viscosity values.

In general, it was observed that the behavior of all solutions was Newtonian and viscosities increased with both pectin concentration and the DM (compare Figures 3.1A with 3.1B, and Figures 3.1C with 3.1D). Thus, the sera of the reconstituted tomato juice can be considered a Newtonian fluid. The results observed in this study are in agreement with the rheological behavior of sera obtained from tomato products processed by the hot- break (HB) and the cold-break (CB) treatments by Wu (Wu, 2011). Tanglerpaibul and Rao (1987) also reported a linear relationship between the serum viscosity and pectin concentration. In their study, the pectin concentration range used (0.16% to 0.80%) was similar to the range of pectin concentration used in the present study for the sera preparation. Pectin has been thought to be the most important component affecting the viscosity of the serum phase rather than solubilized sugars, salts and organic acids (Anthon, Diaz, & Barrett, 2008; Moelants, Cardinaels, Van Buggenhout, et al., 2014). Moelants et al. (2013) reported that the DM of pectin in tomato sera varied from 58.1% to 66.6% depending on the treatments received. Therefore, in the present study it was appropriate using pectin with DM 52% and 70% to prepare the tomato sera used in the reconstitution of the tomato dispersions.

For further comparison of the effect of pectin content and DM, absolute viscosity (Pa.s) was compared by using the Tukey test (Table 3.3). It can be observed that pectin concentration is the dominant factor affecting the viscosity of the serum. An increase in pectin concentration led to a rise in the viscosity of the pectin solution, which is in line with some previous reports related to tomato serum viscosity (Luh, Sarhan, & Wang, 1984; Moelants et al., 2013; Tanglertpaibul & Rao, 1987). The degree of methylation (DM) also showed an influence on the viscosity of pectin solutions. For the same pectin content, high DM pectin solutions exhibited larger viscosity than solutions prepared with medium DM pectin. Differences were very significant when the pectin

content was high (i.e. the 400% solution). This could be explained by its structure: the increased methoxyl esters on the poly-GlaA chains in high DM pectin solutions enhanced the probability of interaction and entanglement between the pectin chains, which led to a higher viscosity.

The data obtained from the cone-plate geometry was considered more accurate because it is an ideal geometry to study the rheology of solutions of polymeric systems. Reconstituted tomato suspensions formed by resuspending separated particles are a different scenario concerning rheological measurements and the cone and plate geometry may not be suitable for these systems (discussed later in this chapter).

### 3.3.3 Viscosity of Reconstituted Suspensions with Pectin Solutions

All reconstituted suspensions were prepared by combining solutions of pectin described in the previous section and the same amount of pulp fraction (20%) obtained from commercial tomato sauce. A content of 20% was used because it is close to the tomato pulp content of commercial tomato sauces. All suspensions showed a shear thinning behavior, which is characteristic of most suspensions comprising plant-cell-wall-derived materials. This behavior is also indicative of the structural characteristics the cell particles and potential changes during rheological testing (Morrison, 2001). However, the two geometries yielded completely opposite trends. Viscosity measured by the vane geometry (Figures 3.2A and 3.2B) slightly increased with increasing pectin content; whereas it decreased when the cone-plate geometry was used (Figures 3.2C and 3.2D). The flow curves were described by the power law model given by Equation 3.5. The consistency coefficient ($k$) from the power law model determined from the flow curves depicted in Figure 3.2, which is an indication of the suspension viscosity, are compared by the Tukey test, and results are given in Table 3.4.

As illustrated in Figures 3.2A and 3.2B there are slight differences in the viscosity of prepared suspensions tested with the vane geometry regardless of the concentration of the pectin in the sera or the degree of pectin methylation. However, results obtained with the cone-plate geometry showed noticeable differences that depended on the concentration and type of the pectin (Figures 3.2C and 3.2D). These results were less reproducible and there was evidence of phase separation during testing. Results did not seem to follow a defined trend and they were even showing that the measured viscosity of the suspension was lower for serum with higher pectin concentrations. In contrast, results obtained with the vane geometry showed expected results indicating that reconstituted suspensions prepared with highest pectin content (400%) had larger viscosities (noted by the larger *k* values reported in Table 3.4), and only when the pectin content was high (i.e. 200% and 400%) there was a significant effect of the degree of methylation, e.g., suspensions prepared with HDM pectin exhibited higher *k* values than suspensions prepared with MDM pectin. Conversely, reconstituted suspensions tested with the cone-plate geometry and containing the highest pectin content (400%) exhibited significant smaller *k* values, and there was no clear difference between suspensions prepared with HDM and MDM pectin, which appears to be contradictory. Variability in the results was also larger using the cone-plate geometry. It has been recognized that for testing non-homogeneous systems like suspensions, typical tests used in commercial rheometers could yield erroneous results due to phase separation, wall slippage, destructuring of organized media, and fouling of the measuring gap. Therefore, geometries that promote mixing of suspended materials, such as the vane geometry used in this study or helical ribbon types geometries, are recommended for testing suspensions (La Fuente et al., 1998). Hence, in the present study the vane geometry was considered as a superior measurement system to eliminate wall slip, particle setting and phase

separation, artifacts that commonly occur when testing suspensions (Lopez-Sanchez & Farr, 2012). With the vane geometry, if the gap between the vane and the sample-holding cup is large enough to ensure the inclusion of large particles, it is possible to measure the rheological properties of suspensions comprising particles with wide size distributions (Dzuy & Boger, 1983). Conversely, by using the cone-plate and parallel plate geometries, the sample is loaded on a plate's surface and the set gap is relatively narrow (from a few microns to 1 mm) to minimize measurement errors, but that is easily promoting the phase separation of the suspended particles leading to unstable measurements.

During testing with the cone-plate geometry, it was noted that some liquid was squeezed out of the suspension when the geometry was raised from the set gap, particularly in samples with low pectin concentration in the serum, and similar to the pectin content of commercial tomato sauce, which further reinforces the concept that the cone-plate geometry was not suitable for characterizing the rheology of tomato suspensions. Pectin has the ability to form a gel-like configuration that serves as a binding component tying tomato parenchyma cells together (Aguilera & Stanley, 1999; Palin & Geitmann, 2012). Solubilized pectin in the liquid phase can loosely bond to the cell wall (particles) through noncovalent and nonionic bonds (Moelants, Cardinaels, Van Buggenhout, et al., 2014). Beresovsky et al. (1995) reported the solubilized pectin increased the inter-particle interaction. Therefore in the present study, the role of soluble pectin could be considered more as that of a stabilizer, increasing the particle interaction and bonding the liquid phase and particle phase together, thus decreasing water exudation (i.e. phase separation) when the suspensions are tested. Thus, at low pectin content, the reconstituted suspensions were unstable and prone to artifacts especially under conditions imposed by systems that use small gaps such as the cone-plate geometry. During measurement, the cone-plate

geometry was squeezing out liquid from the suspension, and, as a result, the solid phase of the sample became more concentrated and the measured viscosity correspondingly increased. At high pectin contents, only a small amount of liquid was squeezed out of the sample, and the relatively greater water content of the sample when compared to those with lower pectin concentration led to an apparently lesser and more representative viscosity of the reconstituted suspensions.

Apart from artifacts due to the exudation of fluid, the cone-plate geometry also exhibited noticeable wall slip during measurements of 20% tomato pulp reconstituted suspensions. That is illustrated by the sudden decrease in shear stress with increasing rate rates (Figure 3.3). Shear stress does not increase significantly with shear rates, and for high shear rates, even an unexpected decrease is observed. This may be the result of changes in the structure of the material or significant slippage. Regardless, it is a clear artifact that invalidates the rheological measurements. Wall slip is commonly found during the testing of two phase systems such as suspensions due to displacement of the solid or disperse phase away from the solid boundaries with high shear stresses. This displacement of the solid particles reduces the concentration of particles in the contact area, leading to an unexpected drop in the shear stress with increasing shear rate (Barnes, 1995). Suspensions with lower pectin content were more vulnerable to wall slip while suspensions with the highest pectin content in the sera (e.g. pectin_400%) did appear to indicate less wall slip while testing with the cone and plate geometry. It could be explained by aggregation of the cell particles. At low pectin concentration, phase separation in the suspension was favored and therefore wall slippage. On the other hand, high pectin concentrations increased serum viscosity which reduced phase separation and wall slip. Since wall slip and phase

separation occurred when the cone-plate geometry was used, only the data from vane geometry will be discussed in next sections.

### 3.3.4 Effect of the Pulp Fraction on the Viscosity of the Reconstituted Tomato Suspensions

Flow curves of reconstituted suspensions having different particle fractions (%pulp) are illustrated in Figure 3.4. In these samples, the serum phase was replaced with deionized distilled water so the pectin concentration of the serum was zero. Viscosity data was obtained with the vane geometry where it becomes clear that all suspensions exhibited shearing thinning behavior.

Particle concentration, sometimes called water-insoluble solids (WIS), pulp content, or particle weight fraction, has a major impact on the rheological behavior suspensions comprising cell wall material (Moelants, Cardinaels, Jolie, et al., 2014; Moelants et al., 2013). The power law rheological model was used to describe the rheology of these suspensions and the parameters *k* and *n* were obtained and related to the particle concentration of the suspensions (Moelants, Cardinaels, Jolie, et al., 2014; Tanglertpaibul & Rao, 1987; Yoo & Rao, 1994). As illustrated in Figure 3.5, the *k* values and pulp% were well described by a power law equation with a high correlation coefficient using the vane geometry ($R^2$=0.99). *k* values increased significantly with increasing concentration of the tomato particles in the suspensions, which is in agreement with other investigations (Lopez-Sanchez & Farr, 2012; Moelants, Cardinaels, Jolie, et al., 2014; Rao, Bourne, & Cooley, 1981; Yoo & Rao, 1994). This result demonstrated that the particle concentration had the largest effect on the viscosity of suspension. The power index obtained was 2.43 , which was close to that obtained by Tanglertpaibul and Rao's (1987) but lower than the reported by Yoo and Rao (1994), probably due to the different rheological measurements employed for the suspension characterization and particle size of the samples. In Yoo and Rao's work, the particle sizes of two samples were 340 and 710 μm while in the present study it was

about 285 μm. However, in the suspension series used in this work, the effect of particle size on rheological characteristics of the suspensions was not considered because the samples were all reconstituted suspensions from the same original stock and not modified by any chemical or physical process. Table 3.1 also shows that the particle sizes of the different reconstituted suspensions were very similar. It should be noted that although the viscosity of solubilized pectin solution within the tomato suspension showed no indication of contributing significantly to the total viscosity, the role of soluble pectin in the suspension should not be ignored. As discussed in section 3.3, particle aggregation in the suspension due to insufficient stabilizer (i.e. pectin) could be causing changes in flow behavior. Soluble pectin has shown the function of increasing the suspension stability to the action of shear forces by promoting the interaction between tomato particles.

### 3.3.5 Relationship between Fundamental Rheological Measurements and the Empirical Bostwick Consistency Measurement

Bostwick consistency measurements were carried out for all the reconstituted dispersions and a simple linear regression was obtained between the consistency index *k* obtained from tests using the vane and the cone-plate geometries and the Bostwick consistency (Figure 3.6). As illustrated in the figure the consistency index *k* determined from measurements obtained with the cone-plate geometry had a poor correlation with the Bostwick consistency ($R^2$=0.54), whereas the correlation obtained from the vane geometry was significantly improved ($R^2$=0.91). The rheological measurement using the cone-plate geometry was set with a very small gap (60 μm), and during the loading and measurement the particles in the suspensions were deformed and the sample was prone to phase separation and wall slip when the soluble pectin content was low.

McCarthy and Seymour (1994) proposed an empirical relationship to relate the Bostwick distance to apparent viscosity of tomato products. The correlation was $L=c(\eta/\rho)^{-1/5}$, where $\eta$ is the

apparent viscosity measured by viscometry, $\rho$ is the density of the sample, $c$ is constant for a given testing time and $L$ is the Bostwick measured distance plus 0.05m. Based on this analysis, Milczarek and McCarthy (2006) reported a high correlation ($R^2$=0.96) between $L$ and $(\eta/\rho)^{-1/5}$. In our study, the density difference was ignored and only a simple linear regression was fitted between viscosity and Bostwick distance, so the $R^2$ was a little lower than the reported value (0.96). Another reason could be that the Bostwick consistometer has its own limitations and cannot fully reflect changes of microstructure of the suspensions during measurement. In the present study, the Bostwick consistency remained almost the same when the serum phase (pectin content and DM) of the suspensions was changed, which decreased the correlation with the consistency index $k$ obtained by vane geometry. The Bostwick consistency measurements could not detect consistency changes due to possible particle interaction enhanced by soluble pectin. Therefore, the vane geometry should be encouraged to use for the rheological measurement of plant-cell-wall-derived suspension system.

## 3.4 Conclusions

The pectin solutions were Newtonian fluids and their viscosity increased with pectin content and DM. All reconstituted suspensions showed similar shear thinning behavior, and can be well fitted by the power law model. The influence of the soluble pectin on the rheology of reconstituted suspensions seemed limited and only at high pectin content the suspensions had a significant higher viscosity. DM showed a less important effect in improving the suspension viscosity. The particle concentration turned out to be the dominant factor in determining the suspension viscosity. The particle size also affected the suspension viscosity and could be altered by pectin. In presence of solubilize pectin, the increasing particle interaction led to a slightly larger particle size.

The comparison of rheological measurements with Bostwick consistency gave more insights of functions of soluble pectin in the suspension system. *k* values obtained using the vane geometry had a good correlation with Bostwick consistency ($R^2$=0.91). Therefore, the vane geometry should be preferred to evaluate the rheology of plant-cell-wall-derived suspensions. Wall slip happened when using cone-plate due to phase separation and can be avoided by increasing the pectin concentration. In summary, although the reconstituted serum viscosity is too low to significantly influence the rheology of suspension system compared to the dominant factor—particle phase, the soluble pectin still have major effects on maintaining the system stability and increasing the particle interaction. Further studying the role of pectin in the particle microstructure and the transition from structural pectin to soluble pectin will be desired and is expected to generate more information about the rheological properties of the system.

## 3.5 Figures and Tables

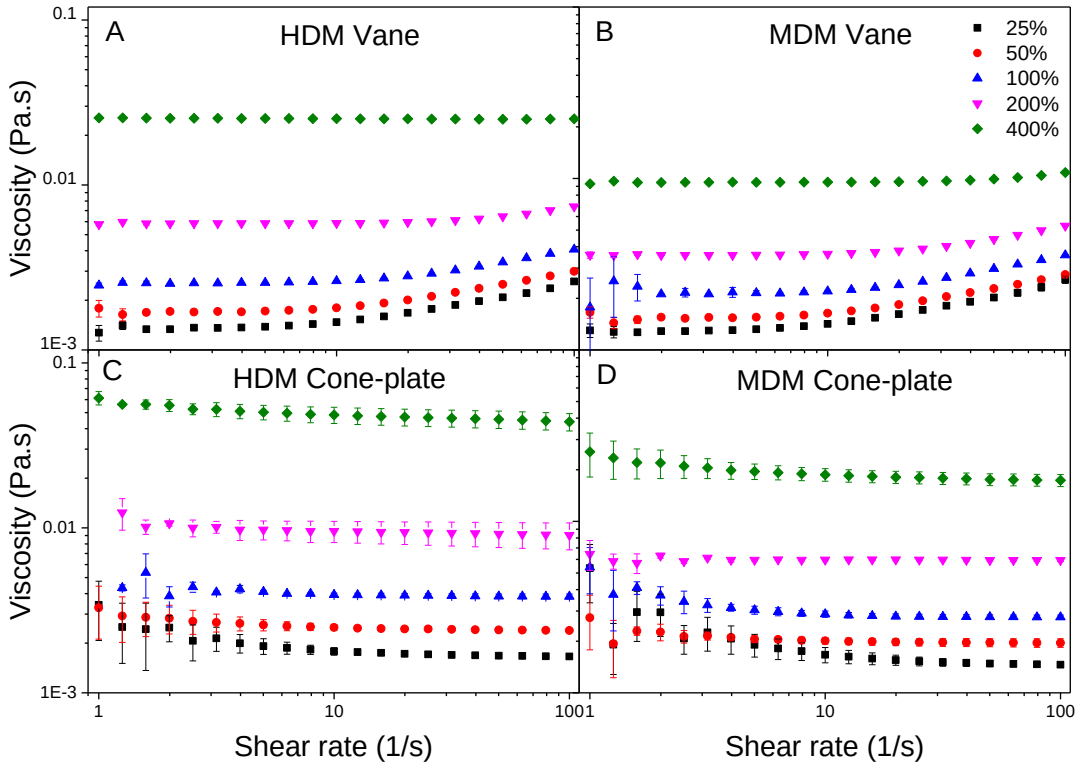


Figure 3.1 Viscosity versus shear rate plots of solutions prepared with different pectin concentrations and DM. The vane and the cone-plate geometries were used for the measurements. (A) HDM pectin solutions using vane geometry, (B) MDM pectin solutions using vane geometry, (C) HDM pectin solutions using cone-plate geometry, (D) MDM pectin solutions using cone-plate geometry.

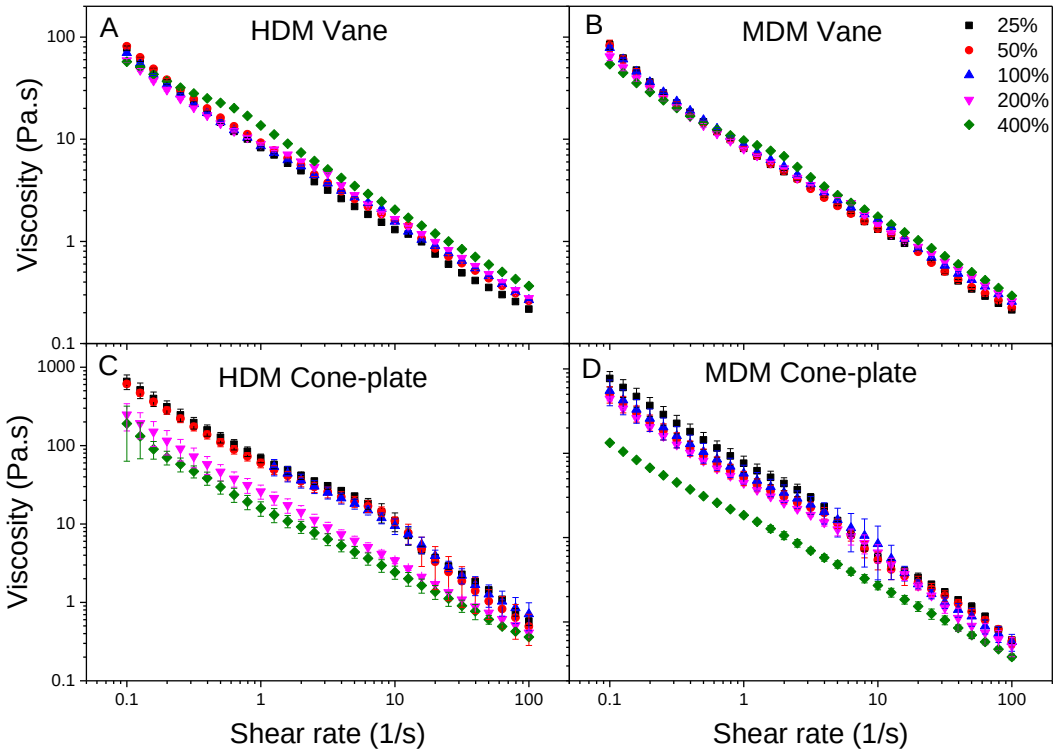


Figure 3.2 Viscosity versus shear rate plots of reconstituted suspensions prepared with sera having different pectin concentrations and DM. The concentration of tomato particles (% pulp) in the dispersions was 20% and the vane and cone-plate geometries were used for the measurements. (A) HDM pectin suspensions using vane geometry, (B) MDM pectin suspensions using vane geometry, (C) HDM pectin suspensions using cone-plate geometry, (D) MDM pectin suspensions cone-plate geometry.

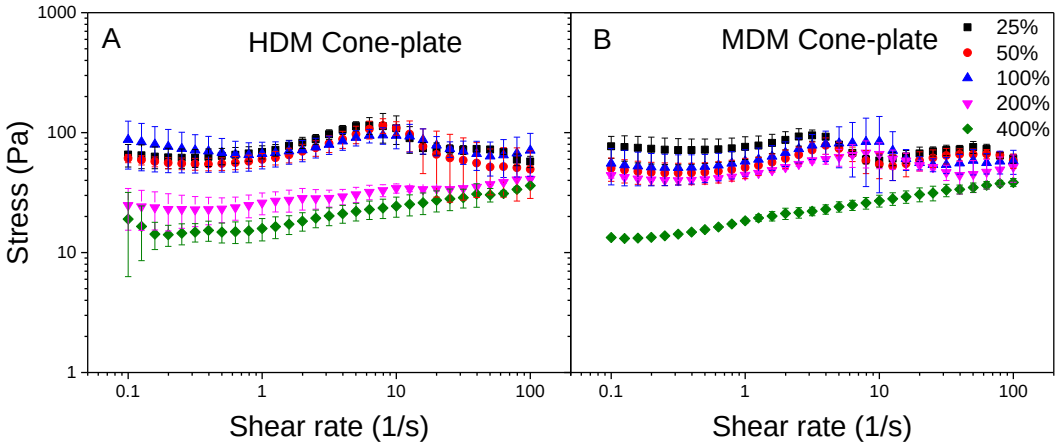


Figure 3.3 Shear stress versus shear rate plots of reconstituted suspensions prepared with serum of different pectin concentrations and DM, obtained using the cone and plate geometry. (A) Suspensions prepared with HDM pectin (B) Suspensions prepared with MDM pectin.

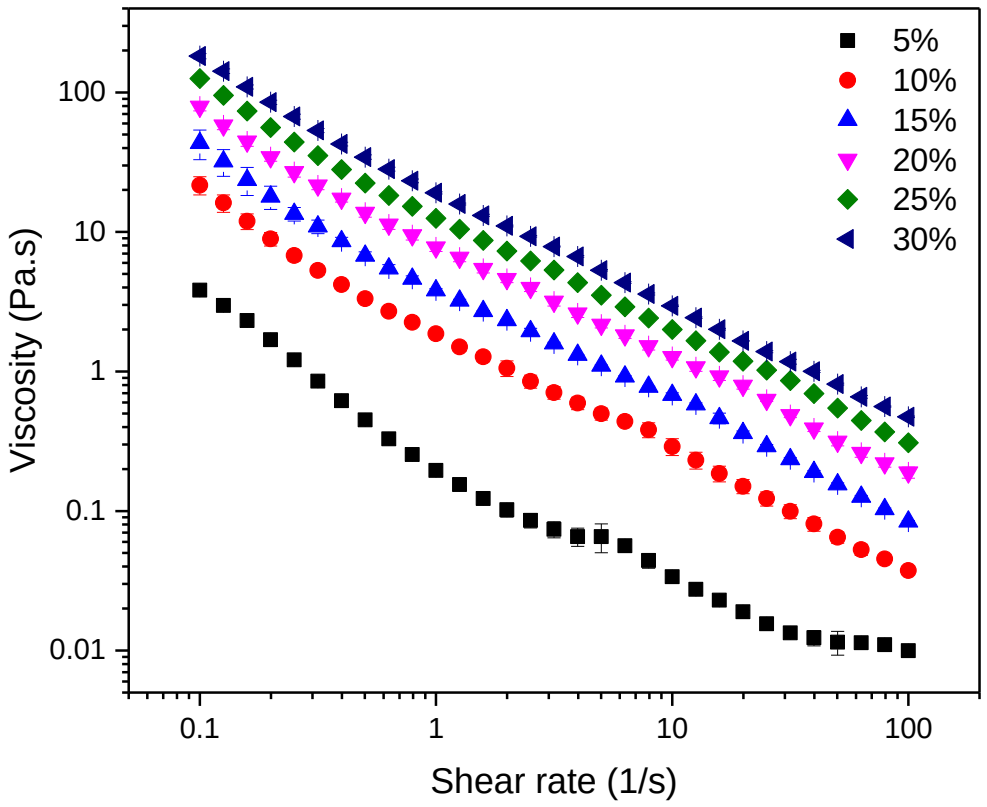


Figure 3.4 Viscosity versus shear rate curves of reconstituted suspensions with different pulp fraction using vane geometry. In these suspensions, the serum phase was reconstituted with deionized distilled water and the pectin concentration of the serum was 0.

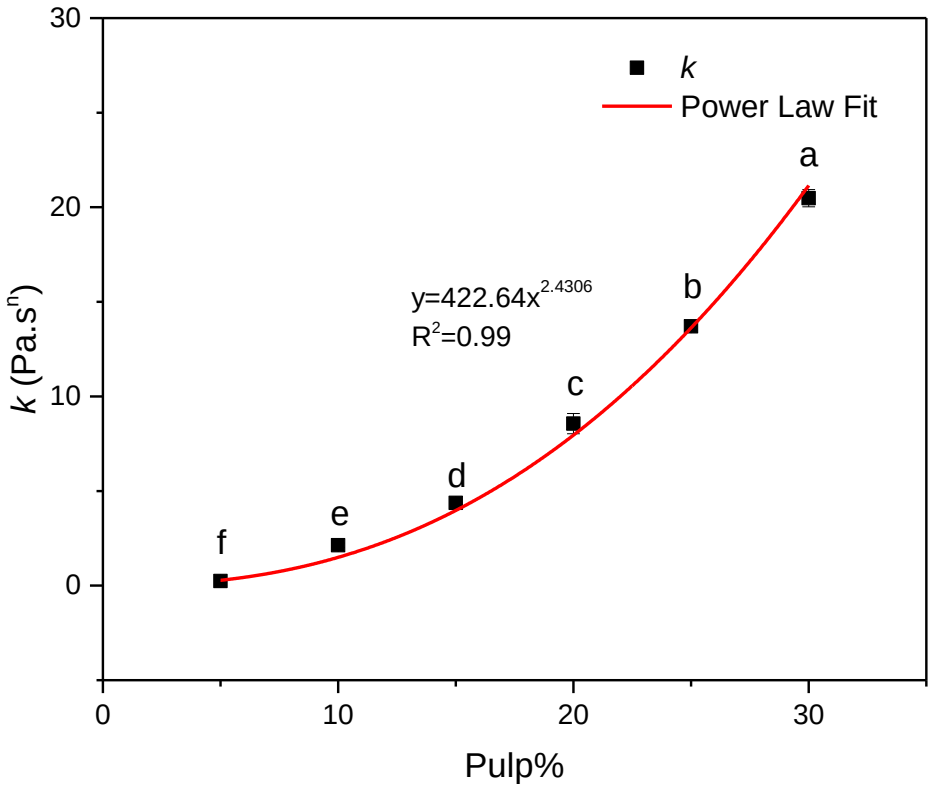


Figure 3.5 Consistency index (*k)* values as a function of the concentration of tomato particles (pulp %). A power law trend line is also included in the figure. Solid line represents power law trend line. The range of shear rate used in the fitting was 0.1 to 100 $s^{-1}$. Values of *k* calculated from the instrument software (TRIOS) were compared by Tukey grouping and means with the same letter are not significantly different.

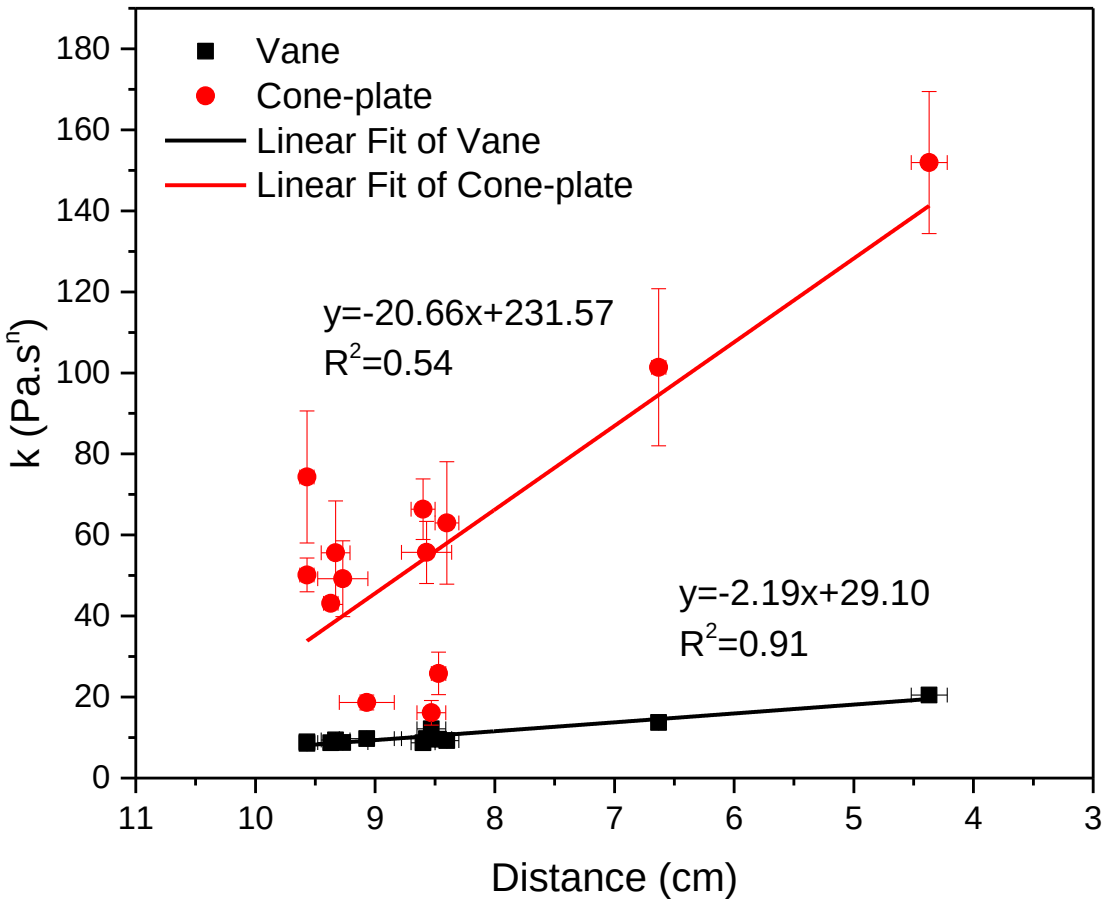


Figure 3.6 Relationship between *k* value and Bostwick consistency (measured by the distance moved by the sample) for all reconstituted suspensions. Solid lines represent the linear fits.

Table 3.1 Particle size (± standard deviation) of commercial tomato sauce and reconstituted suspensions having different concentration of particles (pulp%). In the reconstituted suspensions, the serum phase was deionized distilled water and the pectin concentration was 0. Data were classified by Tukey grouping and means with the same letter are not significantly different.

| Sample | $D[v,0.1]$ (μm) | $D[v,0.5]$ (μm) | $D[v,0.9]$ (μm) | $D[3, 2]$ (μm) | $D[4, 3]$ (μm) |
|---|---|---|---|---|---|
| Tomato sauce | 95.7 ±1.4 d | 264.6 ±3.6 b | 588.8 ±5.4 a | 168.3 ±2.3 c | 306.9 ±3.3 b |
| Pulp%_5% | 103.4 ±0.5 bc | 283.9 ±1.5 ab | 602.2 ±5.6 a | 175.0 ±0.7 b | 321.5 ±1.7 ab |
| Pulp%_10% | 111.1 ±0.8 a | 294.6 ±3.4 a | 617.2 ±5.6 a | 187.1 ±1.8 a | 332.1 ±3.2 a |
| Pulp%_15% | 103.1 ±0.7 bc | 282.4 ±1.6 ab | 608.1 ±3.1 a | 175.6 ±1.3 b | 322.8 ±1.6 ab |
| Pulp%_20% | 104.8 ±1.1 b | 284.7 ±4.6 ab | 604.6 ±10.3 a | 178.0 ±2.8 b | 322.8 ±4.9 ab |
| Pulp%_25% | 101.3 ±0.6 c | 282.2 ±1.2 ab | 607.2 ±7.5 a | 174.2 ±0.8 b | 321.4 ±2.1 ab |
| Pulp%_30% | 102.8 ±0.5 bc | 284.7 ±3.5 ab | 605.5 ±10.6 a | 176.4 ±1.6 b | 322.7 ±4.2 ab |

Table 3.2 Particle size (± standard deviation) of reconstituted suspensions prepared with pectin solutions having different concentrations and different DM. Concentration of particles in the suspension was 20% (%Pulp). Data were tested by Tukey grouping and means with the same letter are not significantly different.

| Sample | $D[v,0.1]$ (μm) | $D[v,0.5]$ (μm) | $D[v,0.9]$ (μm) | $D[3, 2]$ (μm) | $D[4, 3]$ (μm) |
|---|---|---|---|---|---|
| HDM_25% | 107.5 ±0.9 a | 285.2 ±2.9 ab | 608.7 ±6.7 a | 180.0 ±2.1 c | 324.5 ±3.2 a |
| HDM_50% | 108.4 ±0.6 a | 290.0 ±0.3 ab | 617.4 ±2.6 a | 182.8 ±0.3 bc | 329.2 ±0.5 a |
| HDM_100% | 107.5 ±0.6 a | 283.8 ±2.4 b | 605.8 ±3.9 a | 179.7 ±1.3 c | 323.2 ±2.3 a |
| HDM_200% | 108.1 ±1.7 a | 283.5 ±2.6 b | 602.7 ±4.5 a | 180.6 ±2.5 c | 322.5 ±2.5 a |
| HDM_400% | 108.6 ±1.0 a | 285.9 ±3.3 ab | 609.4 ±8.1 a | 183.2 ±3.2 abc | 325.3 ±3.7 a |
| MDM_25% | 108.7 ±1.2 a | 291.6 ±1.5 ab | 616.1 ±5.4 a | 183.9 ±1.3 abc | 329.8 ±2.0 a |
| MDM_50% | 110.1 ±0.4 a | 292.9 ±3.2 a | 614.3 ±5.4 a | 188.9 ±0.9 ab | 330.5 ±2.9 a |
| MDM_100% | 110.3 ±1.1 a | 288.2 ±2.9 ab | 600.0 ±7.3 a | 189.0 ±2.1 a | 324.9 ±3.2 a |
| MDM_200% | 108.6 ±1.6 a | 287.2 ±5.9 ab | 604.6 ±14.0 a | 183.0 ±3.7 abc | 324.9 ±6.5 a |
| MDM_400% | 108.2 ±0.4 a | 289.1 ±3.3 ab | 611.1 ±4.2 a | 182.0 ±1.5 c | 327.3 ±2.8 a |

Table 3.3 Absolute viscosity ( $\mu$ ) ( $\pm$ standard deviation) of pectin solutions. The shear rate range is 0.1 to 100 $s^{-1}$. Data generated from the same geometry were tested by Tukey grouping and means with the same letter are not significantly different. At high pectin concentrations 200% and 400%, the vane geometry provides slightly lower values than those obtained with the cone-plate geometry whereas at pectin concentrations 25%, 50% and 100% the two geometries give almost the same viscosity values.

| Sample (DM type and +Content) | Vane Geometry Viscosity (Pa.s) | Cone-plate Geometry Viscosity (Pa.s) |
|---|---|---|
| HDM_25% | $2.3\times10^{-3} \pm 5.4\times10^{-5}$ f | $1.7\times10^{-3} \pm 2.2\times10^{-5}$ d |
| HDM_50% | $2.7\times10^{-3} \pm 3.8\times10^{-5}$ ef | $2.4\times10^{-3} \pm 4.9\times10^{-5}$ d |
| HDM_100% | $3.7\times10^{-3} \pm 1.5\times10^{-5}$ de | $3.9\times10^{-3} \pm 1.2\times10^{-4}$ cd |
| HDM_200% | $6.9\times10^{-3} \pm 2.2\times10^{-5}$ c | $9.1\times10^{-3} \pm 1.6\times10^{-3}$ c |
| HDM_400% | $2.5\times10^{-2} \pm 6.5\times10^{-5}$ a | $4.5\times10^{-2} \pm 5.4\times10^{-3}$ a |
| MDM_25% | $2.3\times10^{-3} \pm 1.1\times10^{-4}$ f | $1.5\times10^{-3} \pm 5.6\times10^{-5}$ d |
| MDM_50% | $2.5\times10^{-3} \pm 3.3\times10^{-5}$ ef | $2.0\times10^{-3} \pm 1.1\times10^{-4}$ d |
| MDM_100% | $3.3\times10^{-3} \pm 1.8\times10^{-5}$ ef | $2.8\times10^{-3} \pm 7.9\times10^{-5}$ d |
| MDM_200% | $4.8\times10^{-3} \pm 3.3\times10^{-5}$ d | $5.9\times10^{-3} \pm 9.3\times10^{-5}$ cd |
| MDM_400% | $9.6\times10^{-3} \pm 1.3\times10^{-3}$ b | $1.8\times10^{-2} \pm 2.0\times10^{-3}$ b |

Table 3.4 Consistency coefficient ($k$) (± standard deviation) of reconstituted suspensions prepared with different pectin concentrations and DM. The concentration of tomato particles (%pulp) in the suspensions was 20% and the vane and cone-plate geometries were used for the measurements. For the vane geometry, the shear rate used in the fitting was 0.1 to 100 $s^{-1}$ whereas for the cone-plate geometry a valid range had to be selected from a shear rate of 1 $s^{-1}$ to the shear rate at which wall slip started. Data generated from the same geometry were tested by Tukey grouping and means with the same letter are not significantly different.

| Sample (DM+Content) | Vane Geometry Consistency Coefficient ($k$) ($Pa.s^n$) | Cone-plate Geometry Consistency Coefficient ($k$) ($Pa.s^n$) |
|---|---|---|
| HDM_25% | 8.7 ±0.2 d | 66.4 ±7.5 ab |
| HDM_50% | 9.7 ±0.3 b | 55.7 ±7.7 ab |
| HDM_100% | 9.3 ±0.1 bcd | 63.0 ±15.1 ab |
| HDM_200% | 9.6 ±0.2 b | 25.8 ±5.2 cd |
| HDM_400% | 12.2 ±0.1 a | 16.1 ±3.1 d |
| MDM_25% | 8.9 ±0.2 cd | 74.3 ±16.3 a |
| MDM_50% | 8.8 ±0.4 d | 49.2 ±9.4 abc |
| MDM_100% | 9.4 ±0.1 bc | 55.6 ±12.8 ab |
| MDM_200% | 8.7 ±0.3 d | 43.1 ±1.3 bcd |
| MDM_400% | 9.7 ±0.2 b | 18.7 ±1.9 d |

## 3.6 References

Abu-Jdayil, B., Banat, F., Jumah, R., Al-Asheh, S., & Hammad, S. (2004). A comparative study of rheological characteristics of tomato paste and tomato powder solutions. *International Journal of Food Properties, 7*(3), 483-497. doi: 10.1081/Jfp-120040203

Aguilera, José Miguel, & Stanley, David W. (1999). *Microstructural principles of food processing and engineering* (2nd ed.). Gaithersburg, MD: Aspen Publishers.

Anthon, G. E., Diaz, J. V., & Barrett, D. M. (2008). Changes in pectins and product consistency during the concentration of tomato juice to paste. *Journal of Agricultural and Food Chemistry, 56*(16), 7100-7105. doi: 10.1021/jf8008525

Appelqvist, I. A. M., Cochet-Broch, M., Poelman, A. A. M., & Day, L. (2015). Morphologies, volume fraction and viscosity of cell wall particle dispersions particle related to sensory perception. *Food Hydrocolloids, 44*, 198-207. doi: 10.1016/j.foodhyd.2014.09.012

Barnes, H. A. (1995). A Review of the Slip (Wall Depletion) of Polymer-Solutions, Emulsions and Particle Suspensions in Viscometers - Its Cause, Character, and Cure. *Journal of Non-Newtonian Fluid Mechanics, 56*(3), 221-251. doi: Doi 10.1016/0377-0257(94)01282-M

Barrett, D. M., Garcia, E., & Wayne, J. E. (1998). Textural modification of processing tomatoes. *Critical Reviews in Food Science and Nutrition, 38*(3), 173-258. doi: Doi 10.1080/10408699891274192

Becker, R., Wagner, J. R., Miers, J. C., Dietrich, W. C., & Nutting, M. D. (1972). Consistency of Tomato Products .7. Effects of Acidification on Cell-Walls and Cell Breakage. *Journal of Food Science, 37*(1), 118-&. doi: DOI 10.1111/j.1365-2621.1972.tb03399.x

Beresovsky, N., Kopelman, I. J., & Mizrahi, S. (1995). The Role of Pulp Interparticle Interaction in Determining Tomato Juice Viscosity. *Journal of Food Processing and Preservation, 19*(2), 133-146. doi: DOI 10.1111/j.1745-4549.1995.tb00283.x

Day, L., Xu, M., Oiseth, S. K., Hemar, Y., & Lundin, L. (2010). Control of Morphological and Rheological Properties of Carrot Cell Wall Particle Dispersions through Processing. *Food and Bioprocess Technology, 3*(6), 928-934. doi: 10.1007/s11947-010-0346-0

Den Ouden, F. W. C., & Van Vliet, T. (2002). Effect of concentration on the rheology and serum separation of tomato suspensions. *Journal of Texture Studies, 33*(2), 91-104.

Diaz, J. V., Anthon, G. E., & Barrett, D. M. (2009). Conformational Changes in Serum Pectins during Industrial Tomato Paste Production. *Journal of Agricultural and Food Chemistry, 57*(18), 8453-8458. doi: 10.1021/jf901207w

Dzuy, N. Q., & Boger, D. V. (1983). Yield Stress Measurement for Concentrated Suspensions. *Journal of Rheology, 27*(4), 321-349. doi: Doi 10.1122/1.549709

Ewoldt, R. H., Johnston, M. T., & Caretta, L. M. (2015). Experimental Challenges of Shear Rheology: How to Avoid Bad Data. *Complex Fluids in Biological Systems: Experiment, Theory, and Computation*, 207-241. doi: 10.1007/978-1-4939-2065-5_6

FAO. (2014). Food and Agriculture Organization of United Nations Statistics. Retrieved Aug, 2017, from http://www.fao.org/faostat/en/#data/QC/visualize

La Fuente, E. B., Nava, J. A., Lopez, L. M., Medina, L., Ascanio, G., & Tanguy, P. A. (1998). Process viscometry of complex fluids and suspensions with helical ribbon agitators. *Canadian Journal of Chemical Engineering, 76*(4), 689-695.

Lopez-Sanchez, P., & Farr, R. (2012). Power Laws in the Elasticity and Yielding of Plant Particle Suspensions. *Food Biophysics, 7*(1), 15-27. doi: DOI 10.1007/s11483-011-9238-8

Lopez-Sanchez, P., Nijsse, J., Blonk, H. C., Bialek, L., Schumm, S., & Langton, M. (2011). Effect of mechanical and thermal treatments on the microstructure and rheological properties of carrot, broccoli and tomato dispersions. *J Sci Food Agric, 91*(2), 207-217. doi: 10.1002/jsfa.4168

Lopez-Sanchez, P., Svelander, C., Bialek, L., Schumm, S., & Langton, M. (2011). Rheology and Microstructure of Carrot and Tomato Emulsions as a Result of High-Pressure Homogenization Conditions. *Journal of Food Science, 76*(1), E130-E140. doi: 10.1111/j.1750-3841.2010.01894.x

Luh, B. S., Sarhan, M. A., & Wang, Z. (1984). Pectins and Fibers in Processing Tomatoes. *Food Technology in Australia, 36*(2), 70-73.

Mccarthy, K. L., & Seymour, J. D. (1994). Gravity Current Analysis of the Bostwick Consistometer for Power-Law Foods. *Journal of Texture Studies, 25*(2), 207-220. doi: DOI 10.1111/j.1745-4603.1994.tb01327.x

Milczarek, R. R., & McCarthy, K. L. (2006). Relationship between the Bostwick measurement and fluid properties. *Journal of Texture Studies, 37*(6), 640-654. doi: DOI 10.1111/j.1745-4603.2006.00075.x

Moelants, K. R. N., Cardinaels, R., Jolie, R. P., Verrijssen, T. A. J., Van Buggenhout, S., Van Loey, A. M., . . . Hendrickx, M. E. (2014). Rheology of Concentrated Tomato-Derived Suspensions: Effects of Particle Characteristics. *Food and Bioprocess Technology, 7*(1), 248-264. doi: DOI 10.1007/s11947-013-1070-3

Moelants, K. R. N., Cardinaels, R., Van Buggenhout, S., Van Loey, A. M., Moldenaers, P., & Hendrickx, M. E. (2014). A Review on the Relationships between Processing, Food Structure, and Rheological Properties of Plant-Tissue-Based Food Suspensions. *Comprehensive Reviews in Food Science and Food Safety, 13*(3), 241-260. doi: 10.1111/1541-4337.12059

Moelants, K. R. N., Jolie, R. P., Palmers, S. K. J., Cardinaels, R., Christiaens, S., Van Buggenhout, S., . . . Hendrickx, M. E. (2013). The Effects of Process-Induced Pectin Changes on the Viscosity of Carrot and Tomato Sera. *Food and Bioprocess Technology, 6*(10), 2870-2883. doi: 10.1007/s11947-012-1004-5

Morrison, Faith A. (2001). *Understanding rheology*. New York: Oxford University Press.

Palin, R., & Geitmann, A. (2012). The role of pectin in plant morphogenesis. *Biosystems, 109*(3), 397-402. doi: 10.1016/j.biosystems.2012.04.006

Rao, M. A. (1987). Predicting the Flow Properties of Food Suspensions of Plant-Origin. *Food Technology, 41*(3), 85-88.

Rao, M. A., Bourne, M. C., & Cooley, H. J. (1981). Flow Properties of Tomato Concentrates. *Journal of Texture Studies, 12*(4), 521-538. doi: DOI 10.1111/j.1745-4603.1981.tb00265.x

Rickman, J. C., Barrett, D. M., & Bruhn, C. M. (2007). Nutritional comparison of fresh, frozen and canned fruits and vegetables. Part 1. Vitamins C and B and phenolic compounds. *Journal of the Science of Food and Agriculture, 87*(6), 930-944. doi: 10.1002/jsfa.2825

Rinaudo, M. (1988). The Role of the Chemical-Structure of Pectins on the Interaction with Calcium. *Abstracts of Papers of the American Chemical Society, 195*, 23-Cell.

Sankaran, A. K., Nijsse, J., Bialek, L., Bouwens, L., Hendrickx, M. E., & Van Loey, A. M. (2015). Effect of Enzyme Homogenization on the Physical Properties of Carrot Cell Wall Suspensions. *Food and Bioprocess Technology, 8*(6), 1377-1385. doi: 10.1007/s11947-015-1481-4

Sila, D. N., Van Buggenhout, S., Duvetter, T., Fraeye, I., De Roeck, A., Van Loey, A., & Hendrickx, M. (2009). Pectins in Processed Fruit and Vegetables: Part II - Structure-Function Relationships. *Comprehensive Reviews in Food Science and Food Safety, 8*(2), 86-104. doi: 10.1111/j.1541-4337.2009.00070.x

Tanglertpaibul, T., & Rao, M. A. (1987). Flow Properties of Tomato Concentrates - Effect of Serum Viscosity and Pulp Content. *Journal of Food Science, 52*(2), 318-321. doi: DOI 10.1111/j.1365-2621.1987.tb06602.x

Tiback, E., Langton, M., Oliveira, J., & Ahrne, L. (2014). Mathematical modeling of the viscosity of tomato, broccoli and carrot purees under dynamic conditions. *Journal of Food Engineering, 124*, 35-42. doi: 10.1016/j.jfoodeng.2013.09.031

Van Buggenhout, S., Sila, D. N., Duvetter, T., Van Loey, A., & Hendrickx, M. (2009). Pectins in Processed Fruits and Vegetables: Part III - Texture Engineering. *Comprehensive Reviews in Food Science and Food Safety, 8*(2), 105-117. doi: 10.1111/j.1541-4337.2009.00071.x

Wu, B. (2011). *Tomato product viscosity is determined by the physical properties of the pulp.* (M.s.), Purdue University. Retrieved from http://login.ezproxy.lib.purdue.edu/login?url=http://gateway.proquest.com/openurl?url_ver=Z39.882004&rft_val_fmt=info:ofi/fmt:kev:mtx:dissertation&res_dat=xri:pqm&rft_dat=xri:pqdiss:1510030

Yoo, B., & Rao, M. A. (1994). Effect of Unimodal Particle-Size and Pulp Content on Rheological Properties of Tomato Puree. *Journal of Texture Studies, 25*(4), 421-436. doi: DOI 10.1111/j.1745-4603.1994.tb00772.x

# CHAPTER 4. EFFECTS OF PROCESSING CONDITIONS ON THE RHEOLOGICAL PROPERTIES OF TOMATO SUSPENSIONS (I): ULTRASOUND AND SHEAR

## 4.1 Introduction

The primary plant cell wall material consists of three main polysaccharides: pectin, cellulose microfibril and hemicellulose (Palin & Geitmann, 2012; Sankaran, Nijsse, Bialek, et al., 2015). The pectin matrix, which is abundant in the middle lamella, determines cell to cell adhesion that contributes to the firmness and elasticity of the tissue (Fuchigami, 1987). The structural integrity and the mechanical properties of the cell wall material as well as the internal turgor of that material generated by osmosis effects play a central role in the viscosity and sensorial quality of such foods (Jackman & Stanley, 1995; Waldron, Parker, & Smith, 2003).

Most food processes promote softening the texture of products by decreasing the turgor pressure and changing the structure of plant cell wall (Ilker & Szczesniak, 1990; Knoerzer, Juliano, & Smithers, 2016). The three main polysaccharides mentioned above exhibit different characteristics when subjected to processings (Knoerzer et al., 2016). For example, the pectin matrix is more susceptible to both chemical and enzymatic degradations whereas the hemicellulose-cellulose network remains almost intact (Terefe, Buckow, & Versteeg, 2014). Therefore, the manipulation of the cell wall pectin by various processes has been used to control the structural and textual properties of derived products (Day, Xu, Oiseth, & Mawson, 2012). Thermal processing, including both hot-break (HB) and cold-break (HB) treatments, is commonly used to produce tomato products. On one hand, the pectinolytic enzymes including pectinmethylesterase (PME) and polygalacturonase (PG) can be inactivated by high temperatures (e.g. at the hot-break temperature >90 ℃); therefore the enzymatic pectin degradation and the

associated cell wall weakening effects are inhibited at these high temperatures (Moelants, Cardinaels, Van Buggenhout, et al., 2014). PME removes the methyl groups from the pectin biopolymer; PG depolymerizes the pectin backbone resulting in pectin solubilization (Day et al., 2012; Moelants, Cardinaels, Van Buggenhout, et al., 2014). On the other hand, during the CB treatment, which uses temperatures lower than those used in the HB treatment, cell wall pectin can be further demethoxylesterified and depolymerized since an optimal temperature for PME and PG activities is around 50 to 60 ℃ depending on the plant source (Verlent, Hendrickx, Verbeyst, & Van Loey, 2007; Verlent, Van Loey, Smout, Duvetter, & Hendrickx, 2004). Moreover, thermal treatment also causes cell firmness loss through disruption of cell membrane (loss of turgor pressure) and promotes pectin thermal degradation (Greve, Mcardle, Gohlke, & Labavitch, 1994). During thermal treatment, pectin degradation via β-elimination and acid hydrolysis provokes pectin depolymerization and thermosolubilizaiton. β-elimination is the favored reaction, while acid hydrolysis is negligible since the pH of tomato suspension is between 4 to 5 (Moelants, Cardinaels, Van Buggenhout, et al., 2014). Pectin thermal degradation, particularly in the middle lamella, weakens the intercellular adhesion and causes cell separation, and thereby affects the rheology of the plant-cell-wall-based food suspensions (Van Buggenhout, Sila, Duvetter, Van Loey, & Hendrickx, 2009). Therefore, although the traditional thermal processing has worked effectively in increasing the shelf life of these types of products, it compromises their sensory quality and eating pleasure (Day et al., 2012).

In previous studies, thermal treatments often combined with mechanical treatments were applied to yield suspensions with different particle sizes and morphologies (Appelqvist, Cochet-Broch, Poelman, & Day, 2015; Day, Xu, Oiseth, Hemar, & Lundin, 2010; Rao & Qiu, 1989). Homogenization has been reported to modify not only the particle size but also the particle

properties such as the aspect ratio, shape, and the orientation of particles, thus increasing the viscosity of suspensions made with these particles, when they are compared to samples that are not homogenized (Bayod, Mansson, Innings, Bergenstahl, & Tornberg, 2007). Recent study also showed that shear treatment has different effect on the particle structure and rheological properties depending on the type of plant cell walls.

Ultrasound has been used as an alternative processing option to conventional thermal approaches (Chandrapala, Oliver, Kentish, & Ashokkumar, 2012). When an ultrasound wave passes through a liquid medium, it generates an effect known as acoustic cavitation (AC) which locally results in very high temperatures (around 5500 ℃), high pressure (500 MPa), and enormous shear forces at the point where the bubbles collapse (Chandrapala, Oliyer, Kentish, & Ashokkumar, 2012; Sehgal, Sutherland, & Verrall, 1980). The multiple physical and biochemical effects caused by cavitation can lead changes in the structure of cell wall materials through the breakdown of weak intermolecular interaction forces and disintegration of particles and cellular compartments (Farkade, Harrison, & Pandit, 2006). Research reported to date was mainly focused on the effect of ultrasound on PME and PG inactivation (Wu, Gamage, Vilkhu, Simons, & Mawson, 2008), for which protein denaturation was assumed to be the main cause of inactivation (O'Donnell, Tiwari, Bourke, & Cullen, 2010; Wu et al., 2008). Controlling the viscosity by ultrasound has been successfully applied to many food systems, most of which have been applied to starch-based products such as corn, potato, tapioca, and sweet potato (Chandrapala, Oliyer, et al., 2012). Recently, ultrasound treatment has been reported to improve the structural and textural properties of non-starchy cell wall materials including carrot and peas (Day et al., 2012; Knoerzer et al., 2016). However, there are few reports on the application of ultrasound to improve the rheological properties of plant-cell-wall-based suspensions, in

particular taking into account the changes on the mechanical and ultrastructural properties of the particles forming the suspensions.

This study used tomato as a typical vegetable product, and the main objective was to investigate the effects of processing conditions including thermal, shear and ultrasound on the rheological properties of suspensions, which were determined by steady shear and oscillatory shear experiments. In addition, particle characterization was performed by examining particle size and microstructure changes and related them to the mechanical strength of the particles and rheology of the suspensions. The pectin in the suspensions was further extracted and quantified to understand its potential role in the rheology of such plant cell wall suspensions.

## 4.2 Materials and Methods

### 4.2.1 Materials

#### 4.2.1.1 Sample Preparation

Fresh tomatoes were purchased from a local market (Indiana, USA) and the same batch was used for the preparation of all samples. Tomatoes were washed and cut into approximate 2 cm followed by a blending process (Ninja Englewood NJ100Express Chopper, MA, USA) for 1 min. About 300 ml of the resulting tomato suspensions were packed in plastic bags (20cm x 14.9cm x 4.7cm, Ziploc, USA). The water was pre-heated by a circulator heater (Anova Precision Cooker, CA, USA) and the packed tomato suspensions were added to simulate break stage. Two break temperatures were chosen, 65 ℃ for 20 min as the cold break process and 90 ℃ for 20 min as the hot break process. After thermal treatment, seeds and large skin pieces were removed by using a hand crank food mill fitted with 1/16” screen (OXO Good Grips Food Mill, OXO, New York, NY). The samples collected were HB and CB samples, respectively.

One part of the break samples received ultrasound treatment, while other part received a high shear treatment. The ultrasound treatment was applied using an ultrasonic converter (Branson 102 Ultrasonics, Danbury, CT, USA) for 3 min and set at Micro tip limit 8, Duty cycle 50%. The treated samples were labelled as hot break ultrasound (HBU) and cold break ultrasound (CBU). The shear treatment was conducted by using a high speed homogenizer (IKA T-25 Ultra-Turrax, Wilmington, NC, USA) set at 2 levels: high shear force (13500 rpm/min) and low shear force (6500 rpm/min). These treatments generated four samples: hot break high shear (HBH), hot break low shear (HBL), cold break high shear (CBH) and cold break low shear (CBL). A schematic of the sample preparation is presented in Figure 4.1. In total, eight samples, counting the two controls HB and CB samples were analyzed in the study.

To obtain sera, each sample was centrifuged (Beckman AvantiTM J-251, CA, USA) at 13,000 *g* at 10 ℃ for 20 min. Then the supernatant was filtered through a filter paper ((Whatman No.1) and collected as sera.

#### 4.2.1.2 Chemical Reagents

Chemical reagents were obtained from multiple sources as follows: inositol was obtained from Calbiochem (Calbiochem, Los Angeles, CA). D-Galacturonic acid (GalA), D-Glucose (Glc), D-Fructose (Fru), D-Sucrose (Suc), hexane, deuterium oxide ($D_2O$) were obtained from Sigma-Aldrich (Sigma-Aldrich, Co., St. Louis, MO). Acetone, methanol and acetic acid were purchased from J. T. Baker (J.T. Baker Chemical Co., Phillipsburg, NJ). Tri-Sil reagent ® was purchased from Pierce Co. (Rockford, IL). Citrus pectin was purchased from USB Corporation (Cleveland, OH).

### 4.2.2 Rheological Measurements

To characterize the rheological properties of the samples, both steady shear and oscillatory shear experiments were performed. The rheological measurements were carried out on a stress controlled rheometer (ARG2; TA Instruments, DE, USA) using the vane geometry. The four blade vane geometry has a diameter of 28 mm and a height of 42 mm. To eliminate the effects of the loading history on the structure, the sample was subjected to a pre-shearing step at a shear rate of 100 $s^{-1}$ for 60 s followed by 2 min rest period before all measurements (Moelants, Cardinaels, Jolie, et al., 2014). A new sample was used for each measurement and the sample was covered during the testing to eliminate loss of water.

To determine the viscosity profile, steady shear experiments were conducted by applying a shear rate sweep from 0.1 to 100 $s^{-1}$. For oscillatory shear experiments, first a strain sweep was performed at constant frequency 1 Hz to determine the Linear Viscoelastic Region (LVR). The storage modulus (G') and loss modulus (G") were recorded in the LVR. Then a frequency sweep from 0.1 to 30 Hz was carried out at a constant strain of 0.1% (which is in LVR).

The viscosity of the tomato sera was measured on the same rheometer using a 2 ° cone-plate geometry with a diameter of 40 mm. The procedure was performed following the method described in Chapter 3.

All measurements were performed at least in triplicate at a constant temperature of 25 ℃.

### 4.2.3 Particle Size Measurements

The particle size distribution in the suspension was measured by laser light scattering using a Malvern Mastersizer 2000 instrument (Malvern Instruments Ltd, Worcestershire, UK). Prior to the measurements, all samples were stirred in a water-continuous diluting accessory unit (Hydro 2000 MU) at a speed of 2000 RPM. Samples (approximately 2 ml) were diluted 400-fold

in ultrapure water to minimize multiple scattering effects. The particle size distribution was calculated from the intensity profile of the scattered light based on the Mie theory using the instrument software (Mastersizer2000, version 5.40). Volume median diameter value *D*[v,0.5] was used as the average particle size. Measurements were performed at least three times and the mean values of *D*[v,0.5] are reported.

### 4.2.4 Compression Experiment

Compression experiment was carried out on the same rheometer according to the method described by Sankaran et al. (2015). A parallel plate with 40 mm diameter was used for the measurement. After the sample was loaded onto the peltier plate, the geometry was lowered to the setting gap 1000 μm. The same pre-shear was applied as mentioned in section 4.2.2. The normal force was recorded by applying a direct compressive strain on the suspension as the geometry was lowered to a gap of 100 μm at a speed of 10 μm/s. The peak force was determined from the force-time plot. Measurements were conducted by triplicate and average values are reported.

### 4.2.5 Cryo-Scanning Electron Microscopy

Suspension samples were mounted on specimen holders with a slot of approximately 1mm of the sample rising above the holder surface, then frozen by plunging into liquid nitrogen slush and cryo transferred into the preparation chamber of the Gatan Alto 2500 system set for −185 ℃ (Pleasanton, CA, USA). Tomato samples were fractured with the preparation chamber knife and transferred to the FEI NovaNano SEM (Hillsborough, Oregon, USA) and placed on the cryo stage set for sublimation of surface ice at −90 ℃. Fractured surfaces where sublimated and imaged until sufficient structure was observed and then returned to the Gatan cryo preparation chamber for 120 seconds of sputter coating using a platinum target and temperature of −185 ℃.

During sputter coating, the SEM cryo stage was lowered to −140 ℃ to prepare for final imaging. Upon completion of 120 seconds of sputtering, the sample was reinserted onto the NovaNano SEM cryo stage and images of fractured surfaces were captured.

### 4.2.6 Color Scores

The color of the samples was assessed by a colorimeter (LabScan XE, HunterLab, Reston, Virginia, USA). The 2 °standard observer was chosen and the values of Hunter L, a, b color scale were calculated by the software EasyMatch QC. Values of $L^*$, $a^*$, and $b^*$ were measured to describe a three-dimensional color space and interpreted as follows: $L^*$ indicates lightness read from 0 (completely opaque or "black") to 100 (completely transparent or "white"). $a^*$ value indicates greenness (-) and redness (+), and $b^*$ value represents blueness (-) and yellowness (+).

The color score (TPS) was calculated based on Equation 4.1, which was approved by USDA and developed for the evaluation of color of processed tomato paste/puree (Barrett & Anthon, 2008).

$$TPS = -40.926 + 1.061a + 9.473b - 0.376b^2 \quad (4.1)$$

### 4.2.7 Chemical Analyses of Pectin

#### 4.2.7.1 Nuclear Magnetic Resonance ($^1$H NMR) of Sera

40 mL serum from each sample was further dialyzed using a 3000 MWCO (molecular weight cut-off) membrane (Spectrum Labs, Rancho Dominguez, CA). The dialyzed sera were then lyophilized for $^1$H NMR spectroscopy analyses. Approximately 10 mg lyophilized sample was dissolved in 1 mL $D_2O$ followed by freeze-drying. This procedure was repeated once more for an additional $D_2O$ exchange. The final lyophilized product was then dissolved in 1 mL $D_2O$ for NMR analysis. $H^1$-NMR spectra were obtained at ambient temperature using a Varian Unity

INOVA 300 NMR spectrometer (Varian Inc., Palo Alto, CA). Glc, Fru, GalA and citrus pectin were used as standards to identify resonance peaks.

4.2.7.2 Isolation of Cell Wall Material (alcohol insoluble residue, AIR)

AIR isolation process was based on the method reported by McFeeters and Armstrong (1984). 30 g tomato sample was mixed with 150 mL 95% (v/v) ethanol using a magnetic stirrer for 5 min. Subsequently, the suspension was filtered (Whatman No.1 filter paper) on a Buchner funnel. The residue was collected and suspended in 75 mL 95% (v/v) for 5 min. After another filtration procedure, the cell wall residue remixed with 75 mL acetone and then went through a final filtration. The residue was collected and referred as AIR (alcohol insoluble residue). The AIR sample was dried in a vacuum oven at 25 ℃ overnight and stored in a desiccator until use.

4.2.7.3 Pectin Fractionation

AIR was further fractionated into 3 pectin fractions according to the method described by Christiaens et al. (2012). Water-soluble pectin (WSP), chelator-soluble pectin (CSP), and sodium-carbonate-soluble pectin (NSP) were obtained by subsequently extracting the AIR sample with different solvents. 0.25 g AIR was first stirred in 45 mL boiling water for 5min. After cooling down, the suspension was filtered, and the filtrate was collected and adjusted to 50 mL as WSP fraction. 50 mL chelator-soluble pectin (CSP) fraction was further obtained by re-suspending residue in 45 mL 0.05 M cyclohexane-trans-1, 2-diamine tetra-acetic acid (CDTA) in 0.1 M potassium acetate pH 6.5 for 6 h followed by the same filtration and supplement steps. The final pectin fraction is sodium-carbonate-soluble pectin (NSP) fraction, which was prepared by re-incubating the residue in 45 mL 0.05 M $Na_2CO_3$ containing 0.02 M $NaBH_4$ for 16 h at 4 ℃, and subsequently for 6 h at 28 ℃. The mixture was filtered, and the volume of the filtrate was adjusted to 50 mL. All pectin fractions were frozen and stored at -80 ℃.

4.2.7.4 Pectin Content

The pectin content was determined by gas chromatographic (GC) analysis of trimethylsilyl (TMS) methyl glycoside derivatives, which were prepared as described by McNeill et al. (1982). 1 mL mixture comprised of 3 mg AIR and 1 mg inositol internal standard was prepared and dried under a stream of $N_2$ gas. Then, 450 µL of 2M methanolic-HCl was added to the mixture for methanolysis at 80 ℃ for 16h. After evaporation of methanolic-HCl using $N_2$ gas, 200 µL of Tri-Sil reagent was added and heat at 80 ℃ for 20 minutes. After cooling down, the trimethylsilyl methylglycoside derivatives were dissolved in 1 mL hexane and ready for GC testing. A standard curve for GalA was created to estimate the pectin content in the samples.

4.2.8 Statistical Analysis

All the measurements were performed in triplicate and the results are given as mean of three measurements ± standard deviation. The rheological data was analyzed using Trios (TA Instruments, DE, USA).

The rheological data from the tomato suspensions was described by the power law model given by the following equation:

$$\tau = k\dot{\gamma}^n \tag{4.2}$$

where $k$= consistency index (Pa.s$^n$), and $n$ the flow index (-))

Statistical analysis was carried out using SAS 9.3 software package (SAS Institute, Inc., NC, USA). All pairwise comparisons were tested using Tukey method. The level of significance was set at $p < 0.05$.

## 4.3 Results and discussion

### 4.3.1 Particle Size and Microstructure

The particle size data of the eight samples is illustrated in Figure 4.2. The average particle sizes of HB and CB were about 475 μm, and did not show significant differences. However, the ultrasound and high shear treatments dramatically reduced the particle size while the low shear didn't cause any size changes in particles. In the present study, HB and CB were obtained without significant shear forces applied after the break stage. This suggests that thermal processing alone doesn't lead to the reduction in particle size, but the further mechanic disruption does.

Thermal treatments result in the soften of plant cell wall tissue and partial loss of turgor pressure (Greve, Shackel, et al., 1994). It causes β-elimination of pectin in the cell wall that provokes pectin depolymerization and thermosolubilization. As the bonding agent pectin degrades, the degree of cell detachments depends on the intensity of the thermal conditions applied. For example, carrot cells started to separate from tissue at 80 ℃ (Sila, Smout, Vu, Van Loey, & Hendrickx, 2005), and clear separation of individual cells was observed at 100 ℃ (Day, Xu, Oiseth, Hemar, et al., 2010). According to Day et al. (2010), particle size and microstructure after mechanical shear was determined by the starting structure of the cell wall tissues. HB samples were assumed to have a softer tissue structure than CB samples due to a higher temperature applied. Therefore, samples derived from the HB treatment had a smaller size compared to samples derived from the CB treatment after same intense mechanic disruption (i.e. ultrasound and high shear treatments). In industry production and many previous studies (Day, Xu, Oiseth, Hemar, et al., 2010; Lopez-Sanchez et al., 2011; Moelants, Cardinaels, Jolie, et al., 2014), strong shear forces are usually applied after the break procedure, so the HB samples

always have smaller sizes compared to the CB treated samples. However, in the present study this particle size difference only was observed in the ultrasound and high shear treatments.

Ultrasound treatment significantly decreased the particle size of both HB and CB samples. The average particle sizes of HBU and CBU were 304 and 330 μm, which decreased by 35.9% and 31.3% the particle size of the HB and CB samples, respectively. Ultrasound could promote degradation of pectin in the middle lamella, which accelerated the cell detachments resulting in much smaller particle size. The particle size reduction caused by high shear treatment is different. Rather than cell separation, it was more like cell wall tissue rupture. The average particle sizes of HBH and CBH were 442 and 460 μm, which were only decreased by 7.0% and 4.2% from HB and CB, respectively. These values were too small compared to the reduction caused by ultrasound, which proves that the ways that cell separated were different between these two treatments. The low shear almost didn't change the particle size. Instead, the particles were rearranged in a more efficient packing, which would contribute to the mechanical strength of these particles (discussed later).

The microstructures of particles generated from these treatments determined by cryo-SEM are illustrated in Figure 4.3. Without the presence of shear forces (e.g. blending) involved after break processes, HB and CB had similar morphologies. Lopez-Sanchez et al. (2011) reported the same results on a study analyzing the microstructures and rheological properties of tomato suspensions. When blending was applied before both thermal treatments (70 and 90 ℃), the microstructures obtained contained mostly large cell structures similar to the non-heated (only blended) sample. It was explained by the thermal input which could be insufficient to reduce cell adhesion. However, after ultrasound treatment the samples had smoother surface and contained more intact cells without broken edges. This result confirmed that cell detachment

through middle lamella was favored under ultrasound treatment. By this way, the plant cells can still maintain structural integrity and turgor pressure, which contribute to enhance the mechanical properties of the formed particles. During cryo-SEM measurements, freezing and sublimation would leave a concentrated mass of material in the particles. In ultrasound treated samples, small material spots were observed inside of the cells. This could be polysaccharide (i.e. pectin) solubilized by ultrasound and precipitated during the sample dehydration. This structure would greatly increase the turgor pressure as well as elasticity of the particles. By contrast, high shear treatments led to cell breakage. The cell wall tissue was intensely mechanical disrupted with many cells broken having irregular morphologies. Such particle structure already lost integrity and turgor pressure. The cellular and particular structural differences generated by these treatments directly affect the rheological properties of the derived suspensions. This is discussed in the following sections.

### 4.3.2 Viscosity of Suspensions

All suspensions showed shear thinning behavior (Figure 4.4), which is the characteristic of most plant cell wall derived suspensions and indicative of structural changes in the cell particles during rheological testing (Morrison, 2001). For further comparison of the viscosities, the consistency coefficients *k* obtained from the power law model were compared by using the Tukey test (Figure 4.5). Break temperature showed its influence on the viscosity. The HB treatment yielded a suspension with a relatively higher viscosity than that obtained from the CB treatment. This result well echoed previous studies (Goodman, Fawcett, & Barringer, 2002; Valencia et al., 2002). Thermal treatments lead to the rupture of cell membrane and an initial loss of cell firmness (Greve, Shackel, et al., 1994), which results in softer plant-cell-wall-based particles (Moelants, Cardinaels, Van Buggenhout, et al., 2014). It also causes β-elimination of

pectin in the cell wall that provokes pectin depolymerization and thermosolubilization. Such changes in cell wall biopolymers alter the cell wall structure and physical properties of particles, consequently changing the rheological properties of suspensions containing them. In addition, thermal treatments affect the way cells are separated (cell separation compared with cell wall breakage) and the shape of particles during the following mechanical destruction (Greve, Mcardle, et al., 1994; Ormerod, Ralfs, Jackson, Milne, & Gidley, 2004). Day et al. (2010) and Lopez-Sanchez et al. (2011) reported that hot-break samples had smaller sizes, smooth surfaces without broken edges which indicated the cell separation was favored through middle lamella at intense heat treatments. Some researchers also suggested that thermal treatments influenced the activity of pectinolytic enzymes which in turn changed the rheological properties of the suspensions. The effect of thermal treatment is through the changes of particle phase and serum phase to alter the rheology.

Applying ultrasound significantly increased the viscosity of tomato suspensions. In particular, for the CB treated samples, the ultrasound treatment produced samples (i.e. CBU) with higher *k*-values (i.e. viscosity) than those of the HB samples (Figure 4.5). This suggests the ultrasound could be considered as a potentially alternative treatment to the traditional HB treatment to increase viscosity while maintaining superior consumption quality and a low energy input for their production. Wu et al. (2008) reported a similar improvement of viscosity in tomato juice by ultrasound. It was explained by the observed particle size reduction which resulted in a larger interfacial area and stronger interparticle interactions. The particles also had a smaller particle size in the present study while kept structural integrity compared to shear treated samples. Ultrasound can enhance heat and mass transfer processes and thus has been used extensively in the extraction of natural products (Chemat, Zill-e-Huma, & Khan, 2011). Yildirim,

Oner, and Bayram (2011) evaluated water diffusion of chickpeas during soaking assisted with ultrasound and found it significantly increased in extraction yield with increasing of ultrasound power at low frequency (i.e. 25 KHz). Ultrasound could accelerate pectin dissolution in the middle lamella resulting cell separation, which led to a reduced size. Also, more cells remained intact compared to the conventional shear treatments because the cell tended to separate through middle lamella. This typical structure helped to trap soluble pectin in the cells under ultrasound treatment, which could, in turn, maintain the turgor pressure as well as the elasticity of the particles. Turgor generated within the cells by osmosis is one of the main factors which control the structural integrity and the texture of plant cell wall tissues (Jackman & Stanley, 1995). During most of the food processing operations, turgor pressure is lost due to tissue disruption which leads to a softer texture (Knoerzer et al., 2016). Day et al. (2012) suggested that the turgor pressure was in a gradual decrease fashion at early stage of ultrasound application, which minimized the impact of sudden pressure loss. In addition, ultrasound increased the solubilized pectin diffusion in the cell wall, some of which could be accumulated in the cell wall or intact inner cells. These altered cell particle properties together with reduced particle size may explain that the viscosity was significantly increased by the ultrasound treatment.

The shear treatment influenced the viscosity by creating cell wall particles with distinct microstructures. The high shear treatment caused a significant decrease in viscosity whereas the low shear treatment resulted in a similar viscosity compared to break samples (HB or CB). Tomato cell wall tissue is softer in contrast to other plant sources such as carrot and broccoli, and even simple blending before any thermal treatment was sufficient to produce suspensions with single cells both intact and broken (Lopez-Sanchez et al., 2011). The high shear treatment could further break down the plant tissue and cells resulting in a reduction in particle size and also loss

of cell integrity and elasticity, which led to a lower viscosity. The low shear treatment seemed not to change particle size and microstructure. It was more like a rearrangement of particles in the suspension, so the viscosity remained unchanged. Reduced particle size could increase the probability of interparticle interaction due to a larger interfacial area; however the interaction depends on the particle properties. Although both treatments reduced the particle size by comparing results from ultrasound and high shear treatments, ultrasound increased the viscosity of suspensions while the other one decreased it. This result demonstrated the cell integrity and elasticity is crucial on affecting viscosity of plant-cell-wall-based suspensions.

### 4.3.3 Viscoelastic Properties of Suspensions

Strain-sweep results performed on HB and CB samples are illustrated in Figure 4.6. The linear viscoelastic range where the storage modulus (G') and loss modulus (G") are independent of the applied strain was determined in the range 0.01 to 2%. In agreement with previous studies, for all samples studied G' was higher than G", at a strain range <2%, indicating a “weak gel” response (Lopez-Sanchez et al., 2011; Verlent, Hendrickx, Rovere, Moldenaers, & Van Loey, 2006). At higher strains (>2%), both G' and G" started to decrease, and reached a cross-over point, which suggested that the suspensions had a more viscous behavior at higher strains (Day, Xu, Oiseth, Lundin, & Hemar, 2010). Qualitatively, the same strain-sweep behavior was observed for other ultrasound treated and shear treated samples (figures not shown). To study the effect of processing on the network properties of suspension, the G' and G" value measured at 0.1% strain (within the LVR) for all the samples are illustrated in Figure 4.7. HB samples exhibited higher G' values than those of the CB samples. Furthermore, for the same break sample (HB or CB), it is clearly shown that the ultrasound treatment increased the G' values of the suspensions while high shear treatment decreased it. Although samples produced by the low

shear treatment had higher G' values than samples produced by the high shear treatment, their G' values were still insignificantly lower than those measured in original break samples (HB or CB). The results are in good agreement with the viscosity data, which indicates that the viscosity may be influenced by the elasticity of the suspensions.

The frequency sweep test performed on the suspensions are presented in Figure 4.8, which shows G' and G" values as a function of frequency for a 0.1% strain (which is within LVR ). G' and G" values showed an increasing trend with increased in the applied frequency. All suspensions exhibited a weak gel behavior with G' values greater than G" by less than 10-folds regardless of the frequency. This is a typical rheological behavior of concentrated fruit and vegetable suspensions and similar to the previous studies on such as apple (Espinosa-Munoz, Renard, Symoneaux, Biau, & Cuvelier, 2013), peach (Massa, Gonzalez, Maestro, Labanda, & Ibarz, 2010), tomato (Valencia et al., 2002) and carrot (Day, Xu, Oiseth, Hemar, et al., 2010; Day, Xu, Oiseth, Lundin, et al., 2010). The ultrasound treated samples (HBU, CBU) always presented higher G' values than the other samples; however the high shear treated samples (HBH, CBH) showed significant lower G' values. These trends are very similar to the viscosity measurements which could further confirm there may be a relationship between the viscosity of the suspensions and the elasticity of the plant-cell-wall-derived particles forming the suspension.

Suspension is composed of a serum and solid or particle phases. It is well known that the viscoelastic properties could be significantly improved by increasing the solid content of suspensions. Espinosa-Munoz (2013) observed a 4 times increase in G' as raising dry insoluble solid content from 11 g/kg to 21 g/kg in apple puree. Day et al. (2010) found three solid concentration regions in carrot cell wall suspensions. In the middle range G' and dry solid content can be described by a power law model with power indexes in a range from 3.0 to 6.3

depending on the different particle morphologies (i.e. cell clusters, single cells and cell fragments). In this study, the dry solid content was in the range 3.9% to 4.1%, and there was no significant difference among the samples. Therefore, the difference in the viscoelastic properties could be attributed mainly to the variations in the size and particle properties caused by the different processing conditions.

### 4.3.4 Mechanical Strength of Suspensions

Figure 4.9 shows a typical force-time plot generated from the compression test. The initial gap was set as 1000 μm, because it was reported at that gap the strain applied only cause water squeezed out of the system while maintaining the cellulose network of cell wall unchanged (Lopez-Sanchez et al., 2014). The flat plate geometry was lowered down at a constant rate of 10 μm/s until the final setting gap of 100 μm. Subsequently, the gap was held for 160 s while recording the normal force gathered by the force transducer of the rheometer. Since the average particle size of suspension was much larger than 100 μm, it is assumed that the strain is directly applied to particles and the deformation of the particles is considerable large. Lopez-Sanchez et al. (2014) were the first to propose the rheometer setup for studying the micromechanics of cellulose networks, and they suggested that there were two mechanisms associated to the force responses under a compressive strain: particle deformation and water transport through the cell wall. According to a micromanipulation study of single tomato suspension cells conducted by Blewett et al.(2000), the peak force is a parameter that indicates cell wall elasticity.

Therefore, peak forces were obtained from force-time curves and compared as shown in Figure 4.10. Similar viscoelastic and viscosity values reported in previous sections, HB samples showed a larger peak force response than that of the CB samples. Ultrasound treatment increased the peak forces of the break samples. In particular, for the HB sample this increase was

significant (HB vs. HBU). However, shear treatments led to opposite results, which depended on the intensity of shear used; the peak forces of the treated samples were significantly decreased by high shear, whereas slight raised by application of low shear treatments.

Turgor pressure and the structural integrity are essential for maintaining the mechanic strength of plant cell wall tissues (Blewett et al., 2000; Cosgrove, 1997; Jackman & Stanley, 1995). During the compression test, liquid was observed flowing out radially from the samples. In a more integral structure the liquid would be better confined in the cell tissue, which would be more resistant to the loading pressure and will be more evident at higher peak forces. As discussed in previous sections, the HB treatment favored cell separation through middle lamella instead of cell wall breakage, so the HB treated samples had more intact, smaller and smoother cells compared to that of the CB samples. This structure difference could explain why the HB samples exhibited higher mechanic strength (peak force) than the CB samples. Ultrasound could further create large amounts of smaller intact cells via pectin dissolution in the middle lamella. Therefore, it will further increase the measured peak force. Although high shear yielded small particles, most cells might probably already lost turgor and structural integrity. The cell tissues had low water retention and demonstrated a significant smaller peak force. In contrast, low shear didn't cause a particle size reduction for the break samples (Figure 4.2, HB vs. HBL; CB vs. CBL). It more likely created a rearrangement of particles in the samples. Thus, peak forces response was slight raised due to a more efficient particle packing in the system.

It also has been noticed that the mechanical strength of the suspensions has a relationship with their rheological properties (i.e. viscosity and viscoelasticity). For instance, the HBU sample had higher mechanical strength also produced suspensions with a higher viscosity and

storage modulus. It directly relates the rheology to the particle strength which needs to be further investigated in the future.

### 4.3.5 Chemical Analyses of Pectin

#### 4.3.5.1 Proton NMR (1H-NMR) Analysis of Sera

Proton NMR was used to study the serum composition. The H-4 protons of homogalacturonan, i.e., pectin (α-1, 4 GalA), have a resonance in the region of 4.3 to 4.5 ppm; the exact resonance distribution depends on the degree of methylation (Rosenbohm, Lundt, Christensen, & Young, 2003). The anomeric proton is in the region from 5.0 to 5.2 ppm. Figure 4.11 shows that the representative NMR spectra of the sera did have resonances in these regions, which confirms that pectin is present in the serum. The resonances at ~5.2 ppm and ~4.6 ppm are characteristic of the anomeric protons of free Glc, in the equilibrium ratio of the α and β anomeric configurations. The resonances in region of 3.3 to 4.2 ppm are characteristic of the ring protons of carbohydrates, and the resonances between 2.0 and 3.0 ppm indicate the presence of organic acids, such as citric acid. Comparison of these spectra to standards demonstrates that free Glc and Fru are also present in the dialyzed tomato sera though in a minor quantity. All dialyzed seta almost presented an identical spectra profile, which suggests that all the samples have sera with a similar composition. The results showed that the dialyzed sera were mainly composed of galacturonic residues, and there was no difference between the samples treated by the different thermal, shear and ultrasound treatments. Past work on HB and CB tomato samples (Chong, Simsek, & Reuhs, 2009) also showed a similar result indicating that there is no difference in the quality of total pectin extracted from the entire product.

4.3.5.2 Pectin Content of Suspensions

The GalA content representing the pectin content was determined by GC and the data is illustrated in Figure 4.12. WSP is loosely bound to the cell wall through non-covalent and non-ionic bonds (Selvendran & Oneill, 1987). In the present study, it was the biggest fraction which accounted for 60-80% of the total pectin that was determined from the combined three fractions. CSP mainly contains ionically cross-linked pectin usually bonding with $Ca^{2+}$ in middle lamella (Sila, Smout, Elliot, Van Loey, & Hendrickx, 2006), and approximately a CSP fraction of 20-30% was obtained in the study. NSP is predominantly linked to cell wall polysaccharides through covalent ester bonds (Chin, Ali, & Lazan, 1999; Christiaens, Van Buggenhout, Houben, et al., 2012). It only accounted for a minor portion (<3%). Christiaens et al. (2012) reported a relative low WSP (~36%) and high NSP (~31%) in high temperature blanched tomato samples compared to results obtained in this work. It could be related to the ripeness of tomato fruits as well as the measurement of pectin content. These authors were using a colorimetric method described by Blumenkrantz and Asboe-Hansen (1973) where the pectin had to be hydrolyzed with sulfuric acid and could overestimate its calculated content.

HB and CB samples had similar pectin content in the three fractions. Although a higher temperature could enhance pectin thermal degradation and solubilization (Greve, Mcardle, et al., 1994), HB only had a slight higher pectin content in the WSP fraction than CB samples. However, ultrasound and shear treatments dramatically increased this water-soluble pectin fraction. As discussed ultrasound promotes pectin degradation through middle lamella and that could be the cause of such as increase. As the bonding agent pectin was solubilized and went into serum phase, the cell wall tissues were detached producing smaller particles. Shear treatments also increase the soluble pectin by mechanical disrupting the particles, which can leach out the pectin that is trapped in the particles.

The results also demonstrated that soluble pectin was not the key factor affecting the viscosity of suspensions, because all further mechanical disruption would increase this portion including high shear that produced suspensions with decreased viscosity. Therefore these results are reinforcing the hypothesis that the change of water-soluble pectin wasn't the main cause explaining viscosity differences in the tomato products. As a cell wall component, changes of pectin fraction reflected the cell wall and particle structure changes upon treatment. The WSP increase was a result of particle structural changes, and the later was the true cause that explains the observed viscosity difference.

### 4.3.6 Viscosity of Sera

As shown in Figure 4.13, the viscosities of the isolated sera indicate a Newtonian behavior. For the applied shear rate range (0.1 to 100 $s^{-1}$), the viscosity of sera was low (1.0 mPa.s) and remained unchanged at different shear rates tested. In addition, the sera from different samples all exhibited a similar viscosity value, which indicates the contribution of sera to the overall viscosity of the tomato products is not significant, which is probably due to the limited amount and the relatively low viscosity values of the sera present in the samples. Pectin is the most important component affecting the viscosity of the serum phase rather than solubilized sugars, salts and organic acids (Anthon, Diaz, & Barrett, 2008; Moelants, Cardinaels, Van Buggenhout, et al., 2014). In Chapter 3, the effects of soluble pectin on the overall viscosity have been demonstrated as negligible. The serum viscosity values obtained in this chapter were close to the viscosity of pectin solutions prepared with the lowest pectin concentration (i.e. 25%). It can be inferred that the pectin content in the sera are low, and even though there are some differences caused by processing conditions; therefore pectin contribution to the viscosity of suspensions is negligible compared to that of the particle phase.

### 4.3.7 Color Scores

Color is one of the most important aspects of commercial tomato products (Min & Zhang, 2003). Color in tomatoes is due to the presence of carotenoids. Lycopene is the major carotenoid which accounts for 83% of the total pigment (Gould, 1992). The carotenoids in tomatoes are subject to degradation during processing which leads to color loss of derived products (Hayes, G Smith, & E. J. Morris, 1998). The color scores of the samples were calculated and are illustrated in Figure 4.14. HB samples showed a lower color scores than those of the CB samples. It has been well known that the color of tomato juice degraded more rapidly with increasing temperature (Gould, 1992), and one of the advantages of CB over HB is that the CB final products retain a more natural color (Hsu, 2008). By applying ultrasound or shear treatments, the color of the samples was significantly deteriorated especially for high shear treatments. It has been noticed that the samples originated from HB always had a lower color scores than that from CB (i.e. HBU<CBU, HBH<CBH, and HBL<CBL). It suggests that the initial break stage has a great effect on the color loss. Carotenoids in the HB sample are easier to extract due to a softer tissue structure and therefore can be faster degraded during subsequent processing. The main cause for color loss is oxidation (Thakur, Singh, & Nelson, 1996), which can be accelerated by application of high shear forces. This high mechanical disruption could severely rupture the cell wall tissue as well as incorporate more oxygen. More carotenoids could leach out and react with oxygen, thus leading to a significant color loss.

## 4.4 Conclusions

In the present study, tomato suspensions with various particle morphologies and strengths were obtained by using a combination of thermal treatment and ultrasound or high shear treatment. Although the color was significantly lost during the process, the rheological attributes

of the suspensions showed different aspects depending on the particle phase created. Cellular and particular structural differences generated by these treatments directly affected the rheological properties of the suspensions (see Figure 4.15). Results showed that thermal treatment alone didn’t change the particle size; however subsequent ultrasound and high shear treatments dramatically reduced the suspension particle size. As visualized by cryo-SEM, the ultrasound treated suspensions had more intact cells into which solubilized pectin could be trapped, resulting in particles with an increased mechanical strength. By contrast, high shear treatments led to cell rupture and therefore a loss of structural integrity and turgor pressure. Particle mechanical strength was determined directly by a compression experiment and the peak forces were in good agreement with the rheological properties of suspensions produced with these particles. Tomato suspensions with a higher viscosity could be created by the ultrasound treatment, while the high shear treatment produced suspensions with lower viscosity. The storage modulus (G') of suspensions showed a similar trend and had a positive correlation with their viscosities, which indicates that the rheology of the tomato suspensions is influenced by the mechanical properties of the particles.

The serum phase of the suspensions confirmed the little contribution of its chemical composition to the overall rheology of the suspension. The isolated sera exhibited Newtonian behavior with identical viscosity values. Proton NMR showed that dialyzed sera were mainly composed of galacturonic residues, and the spectra profiles of samples were almost identical, indicating a similar serum composition. The water-soluble pectin (WSP) fraction of the suspensions became larger after ultrasound and shear treatments. Changes in pectin are the consequences of alteration of particle phase. This result suggests that pectin was leached out from particles which caused the changes of in the particle mechanical properties. Future work

should be focused on the role of the mechanic properties of the cell wall particles on the rheology of tomato suspension.

## 4.5 Figures and Tables

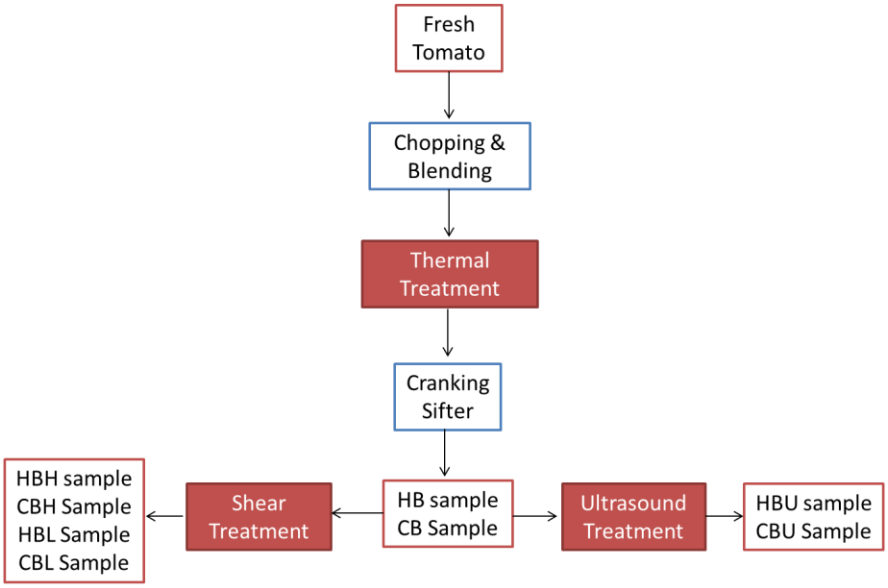


Figure 4.1 Schematic overview of sample preparation. In total, eight samples were prepared in the study.

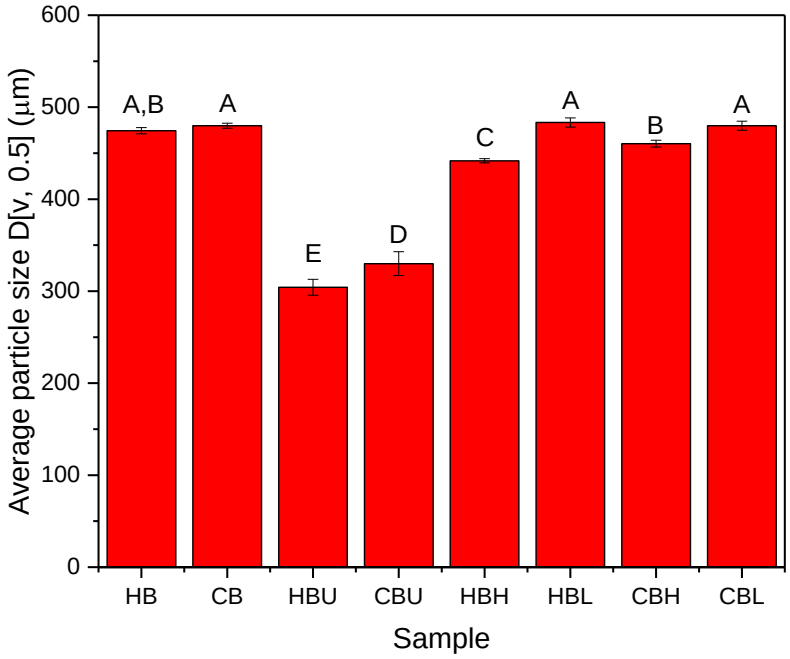


Figure 4.2 Average particle size *D*[v, 0.5] measured by static light scattering. Data were compared by Tukey grouping and means with the same letter are not significantly different.

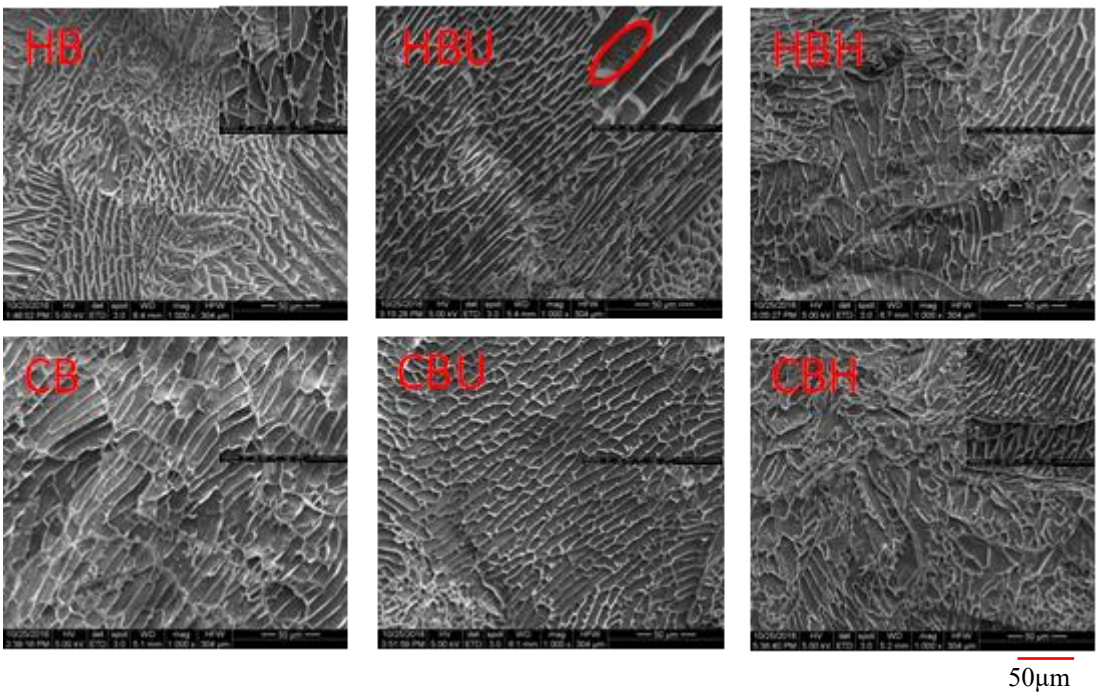


Figure 4.3 Cryo-SEM images of thermal, ultrasound and high shear treated samples. The large images have a magnification of 1000 X, and the images inserted have a magnification of 3000X. Small material spots (indicated by red circles) were observed in ultrasound treated samples (HBU), and it could be soluble pectin freeze-dried during the measurement. Scale bar is 50 μm.

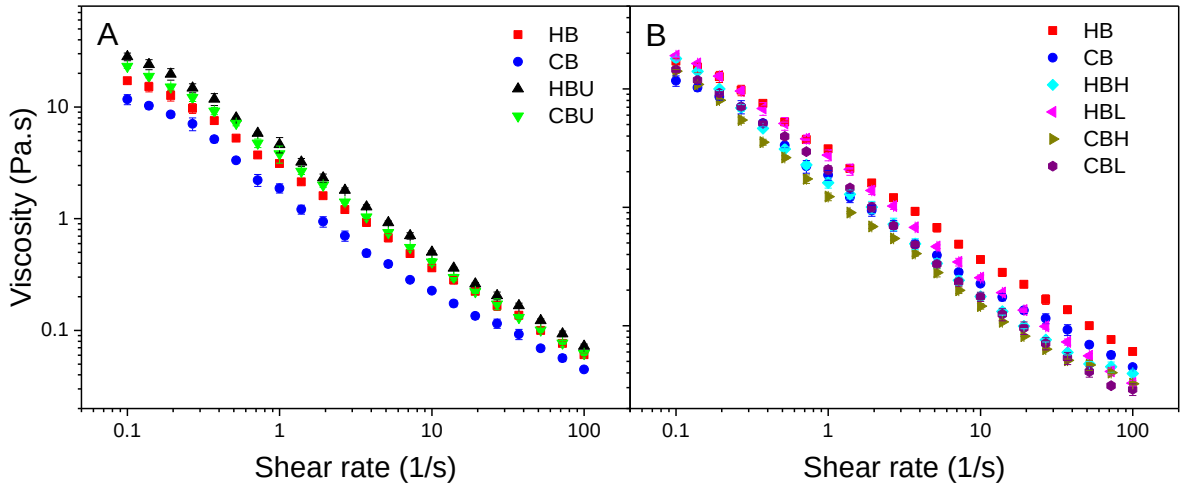


Figure 4.4 Viscosity versus shear rate plots of tomato suspensions received ultrasound and shear treatments. (A) Ultrasound treated; (B) Shear treated.

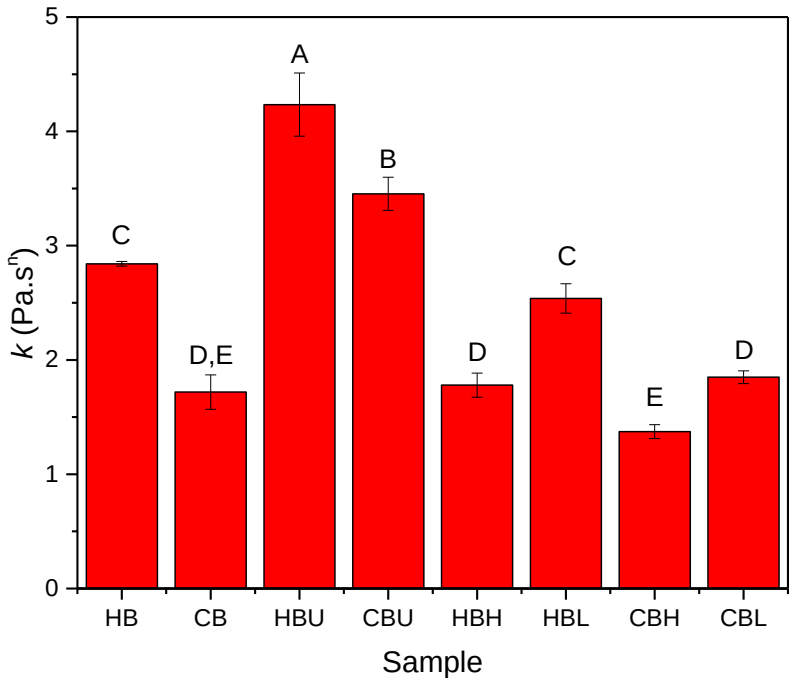


Figure 4.5 Consistency coefficient (*k*) of tomato suspensions obtained from ultrasound and shear treatments. The *k* values were obtained from the flow curves by the Trios software. The shear rate range for fitting was 0.1-100 $s^{-1}$. Data were tested by Tukey grouping and means with the same letter are not significantly different.

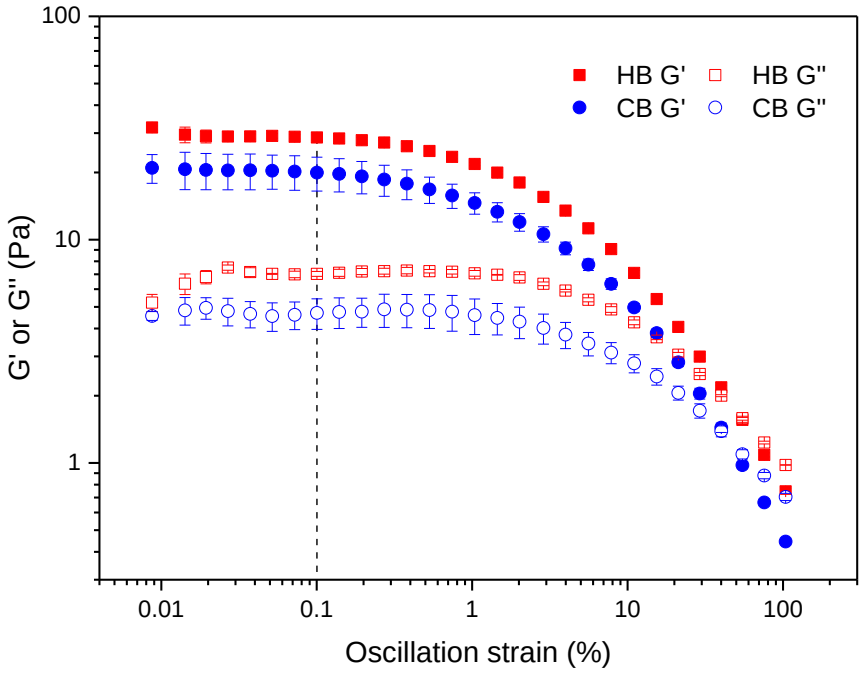


Figure 4.6 Strain sweeps for HB and CB samples. From these results, the linear range was determined to be in the range 0.01 to 2%. Other samples received ultrasound or shear treatments had similar linear ranges. Strain% 0.1% was chosen to compare the viscoelastic properties of the samples.

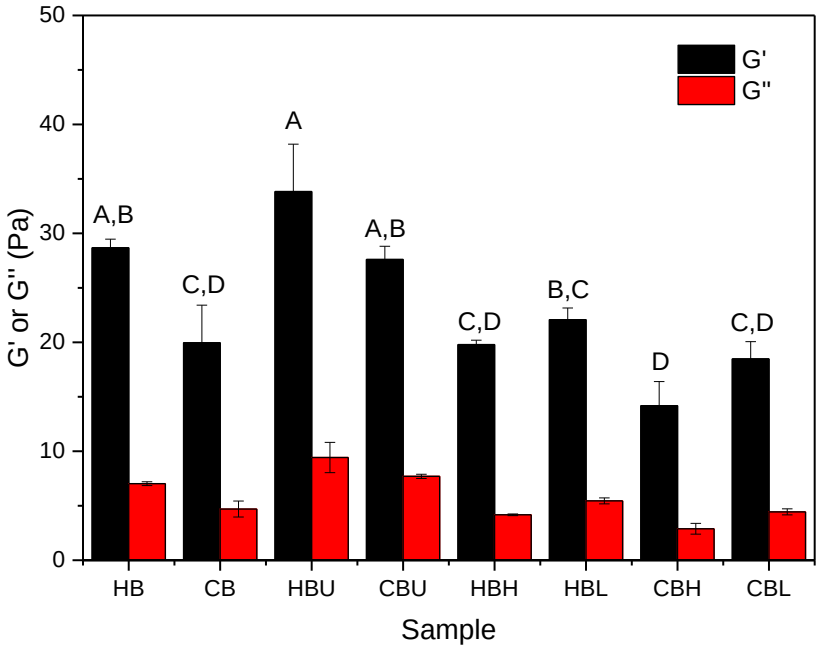


Figure 4.7 Comparison of storage modulus (G') and loss modulus (G'') measured at the LVR for or all samples. Data were analyzed by Tukey grouping and means with the same letter are not significantly different.

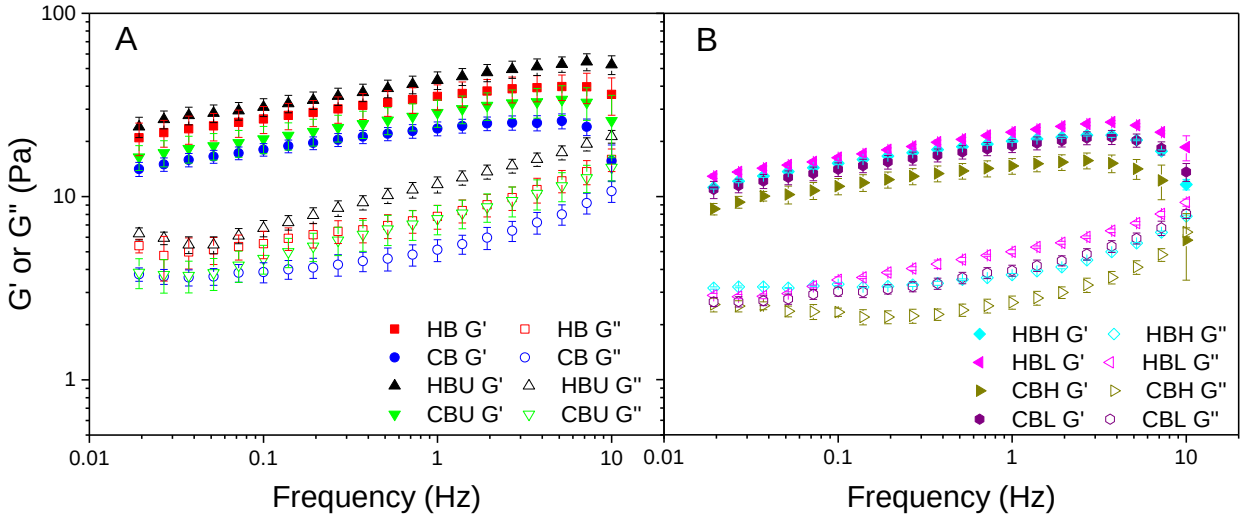


Figure 4.8 Frequency sweep plots of tomato suspensions received (A) ultrasound and (B)shear treatments.

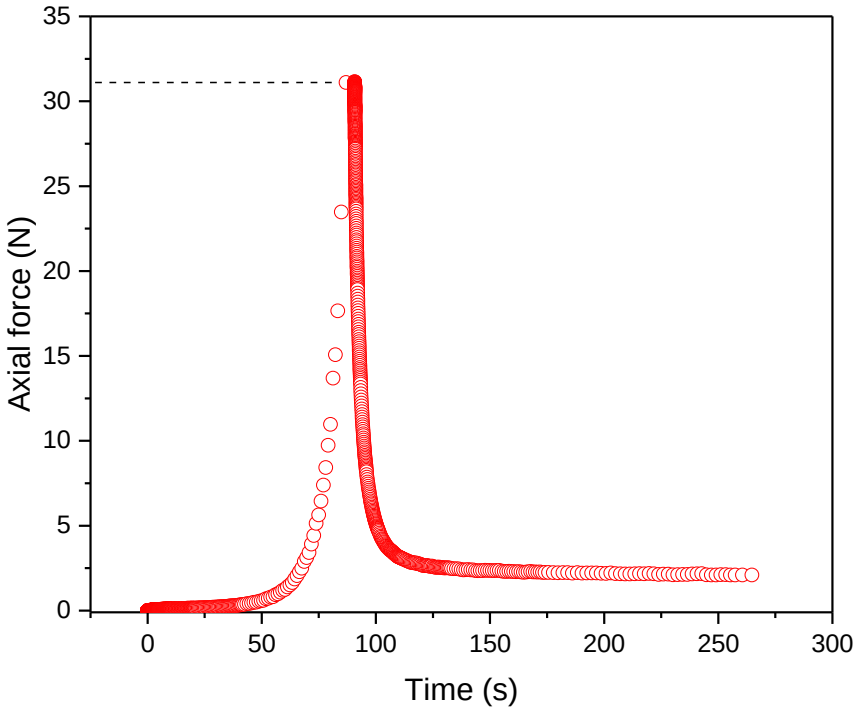


Figure 4.9 Typical force-time curves for tomato suspensions. Each samples showed unique peak force which indicates the cell wall elasticity.

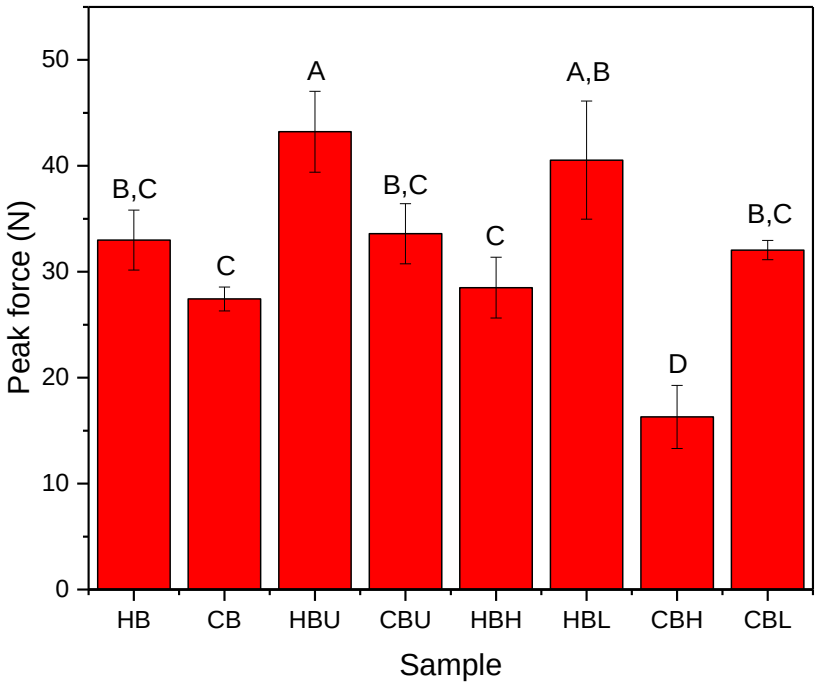


Figure 4.10 Peak force comparison of tomato suspensions. Data were tested by Tukey grouping, and means with the same letter are not significantly different.

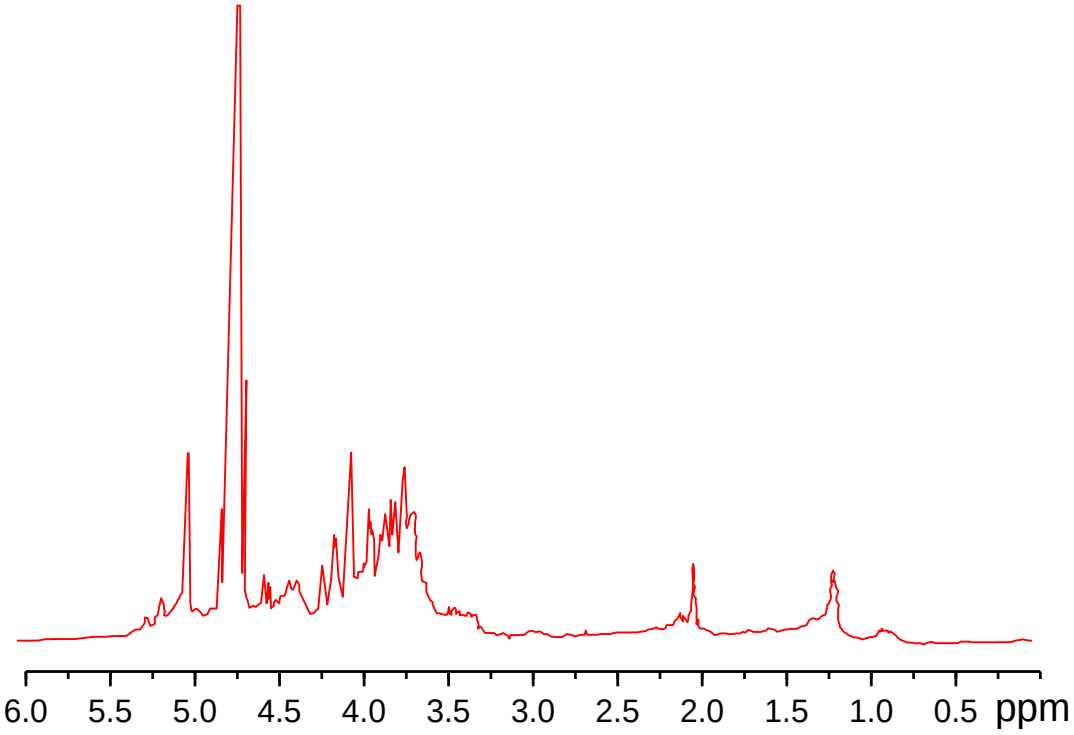


Figure 4.11 Representative $^{1}$H-NMR spectrum of dialyzed tomato serum showing the resonances of pectin. The pectin anomeric is in the region from δ 5.0 to δ 5.2, and the H4 resonances are from δ 4.3-4.5, depending on the degree of methylation.

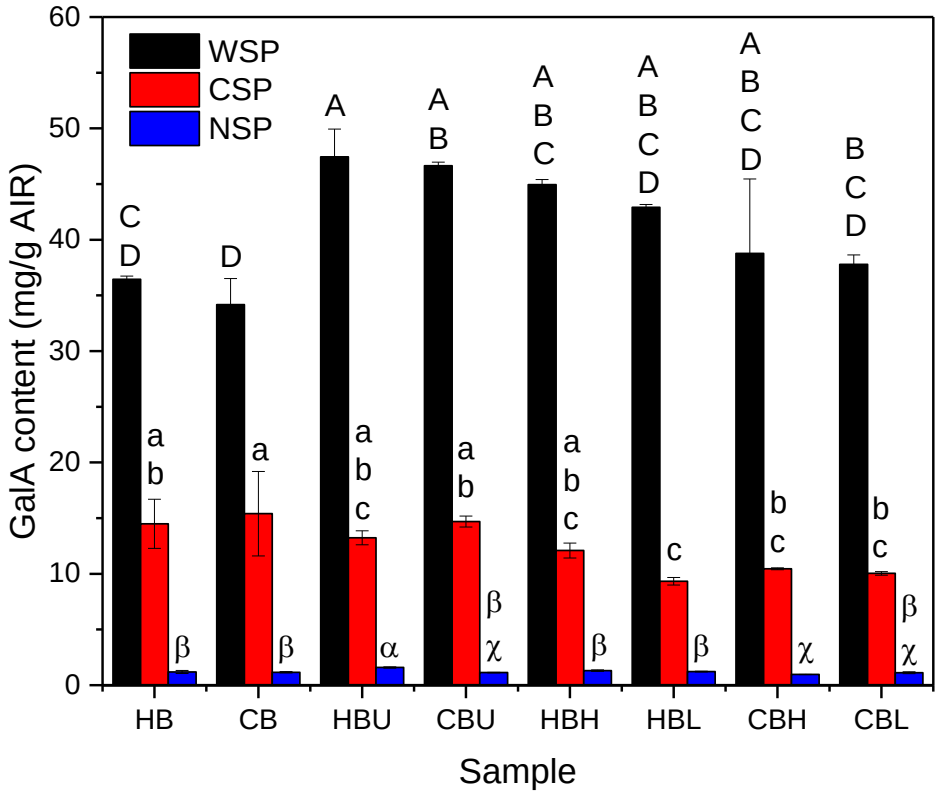


Figure 4.12 GalA contents of three pectin fractions extracted from tomato suspensions. WSP: Water-soluble pectin; CSP: Chelator-soluble pectin; NSP: $Na_2CO_3$-soluble pectin. Data were analyzed by Tukey grouping, and means with the same letter are not significantly different.

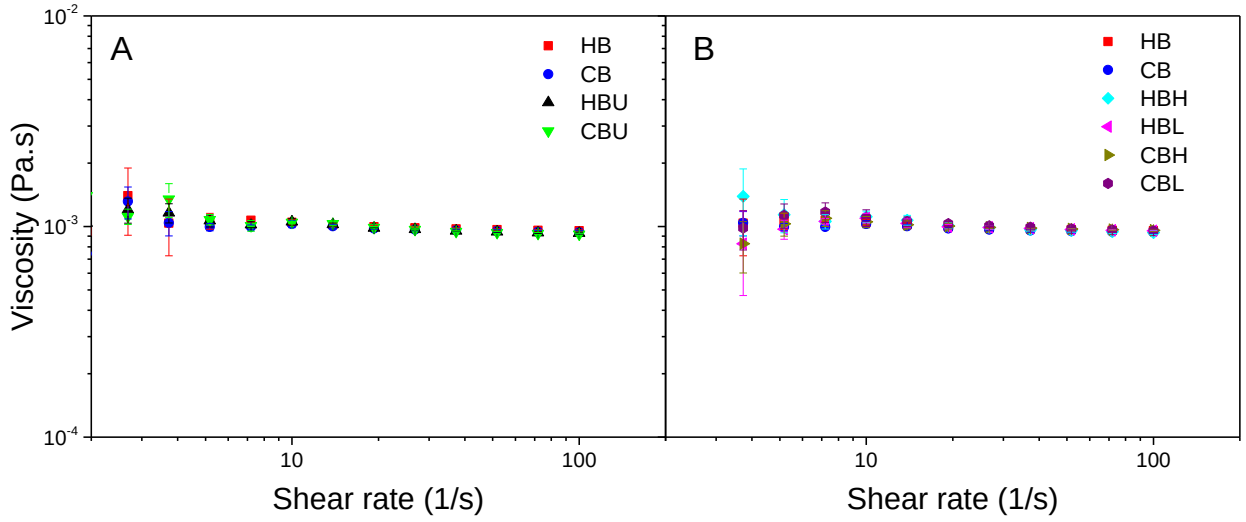


Figure 4.13 Viscosity versus shear rate plots of tomato sera centrifuged from suspensions received ultrasound and shear treatments. (A) Ultrasound treated; (B) Shear treated.

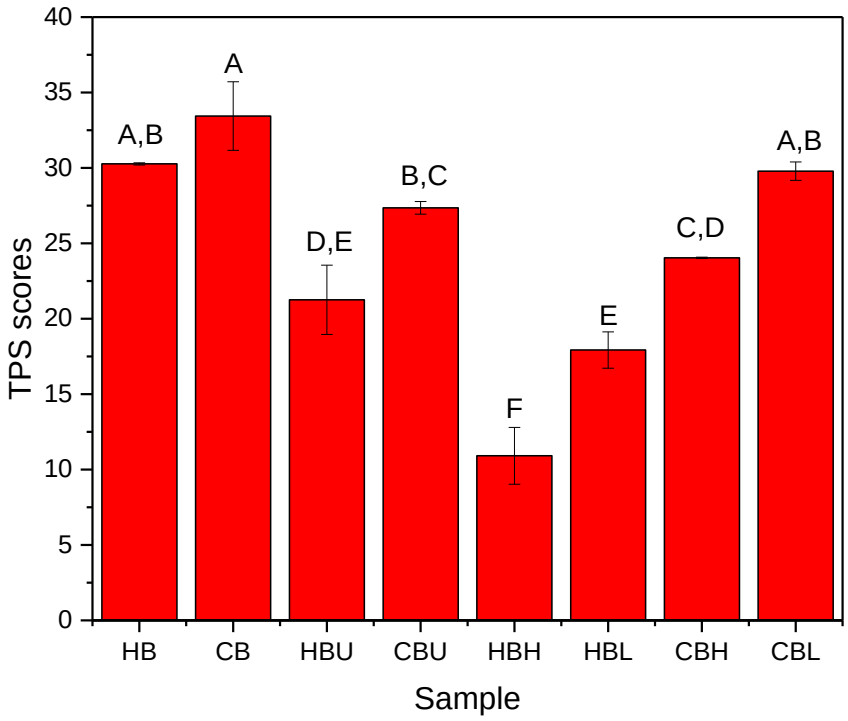


Figure 4.14 TPS scores comparison. A higher score means a better color retention. Data were tested by Tukey grouping, and means with the same letter are not significantly different.

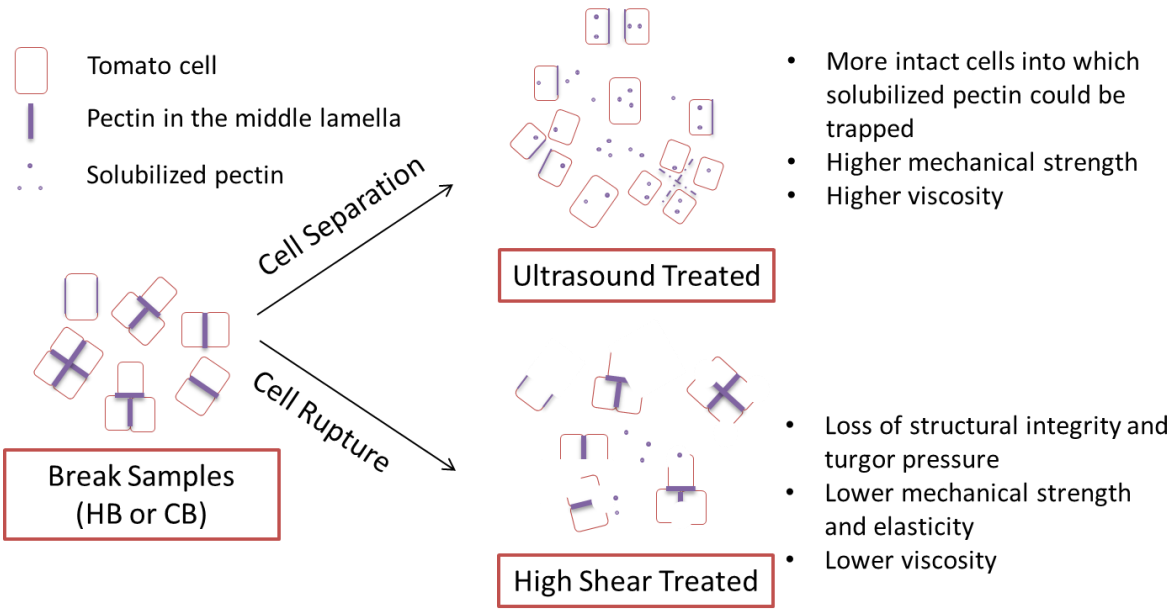


Figure 4.15 Schematic plot of particle formation upon the treatments of ultrasound and high shear. By applying ultrasound, cell separation through the middle lamella was favored, so more cells were still remained intact. Ultrasound also promoted the pectin solubilization, and the soluble pectin would be trapped within the cell which increased the turgor pressure. This microstructure contributed to a higher mechanical strength of the particles, as well as a higher viscosity. High shear treatments caused cell rupture. Most cells were broken, and already lost structural integrity and turgor pressure. It caused lower mechanical strength and elasticity of particles, and therefore a lower viscosity.

## 4.6 References

Anthon, G. E., Diaz, J. V., & Barrett, D. M. (2008). Changes in pectins and product consistency during the concentration of tomato juice to paste. *Journal of Agricultural and Food Chemistry, 56*(16), 7100-7105. doi: 10.1021/jf8008525

Appelqvist, I. A. M., Cochet-Broch, M., Poelman, A. A. M., & Day, L. (2015). Morphologies, volume fraction and viscosity of cell wall particle dispersions particle related to sensory perception. *Food Hydrocolloids, 44*, 198-207. doi: 10.1016/j.foodhyd.2014.09.012

Barrett, Diane M., & Anthon, Gordon E. (2008). Color Quality of Tomato Products *Color Quality of Fresh and Processed Foods* (Vol. 983, pp. 131-139): American Chemical Society.

Bayod, E., Mansson, P., Innings, F., Bergenstahl, B., & Tornberg, E. (2007). Low shear rheology of concentrated tomato products. Effect of particle size and time. *Food Biophysics, 2*(4), 146-157. doi: 10.1007/s11483-007-9039-2

Blewett, J., Burrows, K., & Thomas, C. (2000). A micromanipulation method to measure the mechanical properties of single tomato suspension cells. *Biotechnology Letters, 22*(23), 1877-1883. doi: Doi 10.1023/A:1005635125829

Blumenkr.N, & Asboehan.G. (1973). New Method for Quantitative-Determination of Uronic Acids. *Analytical Biochemistry, 54*(2), 484-489. doi: Doi 10.1016/0003-2697(73)90377-1

Chandrapala, J., Oliver, C., Kentish, S., & Ashokkumar, M. (2012). Ultrasonics in food processing - Food quality assurance and food safety. *Trends in Food Science & Technology, 26*(2), 88-98. doi: 10.1016/j.tifs.2012.01.010

Chandrapala, J., Oliyer, C., Kentish, S., & Ashokkumar, M. (2012). Ultrasonics in food processing. *Ultrasonics Sonochemistry, 19*(5), 975-983. doi: 10.1016/j.ultsonch.2012.01.010

Chemat, F., Zill-e-Huma, & Khan, M. K. (2011). Applications of ultrasound in food technology: Processing, preservation and extraction. *Ultrasonics Sonochemistry, 18*(4), 813-835. doi: 10.1016/j.ultsonch.2010.11.023

Chin, L. H., Ali, Z. M., & Lazan, H. (1999). Cell wall modifications, degrading enzymes and softening of carambola fruit during ripening. *Journal of Experimental Botany, 50*(335), 767-775. doi: DOI 10.1093/jexbot/50.335.767

Chong, Hui H., Simsek, Senay, & Reuhs, Bradley L. (2009). Analysis of cell-wall pectin from hot and cold break tomato preparations. *Food Research International, 42*(7), 770-772. doi: 10.1016/j.foodres.2009.02.025

Christiaens, S., Van Buggenhout, S., Chaula, D., Moelants, K., David, C. C., Hofkens, J., . . . Hendrickx, M. E. (2012). In situ pectin engineering as a tool to tailor the consistency and syneresis of carrot puree. *Food Chemistry, 133*(1), 146-155. doi: 10.1016/j.foodchem.2012.01.009

Christiaens, S., Van Buggenhout, S., Houben, K., Chaula, D., Van Loey, A. M., & Hendrickx, M. E. (2012). Unravelling process-induced pectin changes in the tomato cell wall: An integrated approach. *Food Chemistry, 132*(3), 1534-1543. doi: 10.1016/j.foodchem.2011.11.148

Cosgrove, D. J. (1997). Relaxation in a high-stress environment: the molecular bases of extensible cell walls and cell enlargement. *Plant Cell, 9*(7), 1031-1041. doi: 10.1105/tpc.9.7.1031

Day, L., Xu, M., Oiseth, S. K., Hemar, Y., & Lundin, L. (2010). Control of Morphological and Rheological Properties of Carrot Cell Wall Particle Dispersions through Processing. *Food and Bioprocess Technology, 3*(6), 928-934. doi: DOI 10.1007/s11947-010-0346-0

Day, L., Xu, M., Oiseth, S. K., Lundin, L., & Hemar, Y. (2010). Dynamic rheological properties of plant cell-wall particle dispersions. *Colloids and Surfaces B-Biointerfaces, 81*(2), 461-467. doi: 10.1016/j.colsurfb.2010.07.041

Day, L., Xu, M., Oiseth, S. K., & Mawson, R. (2012). Improved mechanical properties of retorted carrots by ultrasonic pre-treatments. *Ultrasonics Sonochemistry, 19*(3), 427-434. doi: 10.1016/j.ultsonch.2011.10.019

Espinosa-Munoz, L., Renard, C. M. G. C., Symoneaux, R., Biau, N., & Cuvelier, G. (2013). Structural parameters that determine the rheological properties of apple puree. *Journal of Food Engineering, 119*(3), 619-626. doi: DOI 10.1016/j.jfoodeng.2013.06.014

Farkade, V. D., Harrison, S. T. L., & Pandit, A. B. (2006). Improved cavitational cell disruption following pH pretreatment for the extraction of beta-galactosidase from Kluveromyces lactis. *Biochemical Engineering Journal, 31*(1), 25-30. doi: 10.1016/j.bej.2006.05.015

Fuchigami, M. (1987). Relationship between Pectic Compositions and the Softening of the Texture of Japanese Radish Roots during Cooking. *Journal of Food Science, 52*(5), 1317-1320. doi: DOI 10.1111/j.1365-2621.1987.tb14072.x

Goodman, C. L., Fawcett, S., & Barringer, S. A. (2002). Flavor, viscosity, and color analyses of hot and cold break tomato juices. *Journal of Food Science, 67*(1), 404-408. doi: DOI 10.1111/j.1365-2621.2002.tb11418.x

Gould, Wilbur A. (1992). CHAPTER 17 - Color and Color Measurement *Tomato Production, Processing and Technology (Third Edition)* (pp. 297-312): Woodhead Publishing.

Greve, L. C., Mcardle, R. N., Gohlke, J. R., & Labavitch, J. M. (1994). Impact of Heating on Carrot Firmness - Changes in Cell-Wall Components. *Journal of Agricultural and Food Chemistry, 42*(12), 2900-2906. doi: Doi 10.1021/Jf00048a048

Greve, L. C., Shackel, K. A., Ahmadi, H., Mcardle, R. N., Gohlke, J. R., & Labavitch, J. M. (1994). Impact of Heating on Carrot Firmness - Contribution of Cellular Turgor. *Journal of Agricultural and Food Chemistry, 42*(12), 2896-2899. doi: Doi 10.1021/Jf00048a047

Hayes, W. A., G Smith, P., & E. J. Morris, A. (1998). *The Production and Quality of Tomato Concentrates* (Vol. 38).

Hsu, Kuo-Chiang. (2008). Evaluation of processing qualities of tomato juice induced by thermal and pressure processing. *LWT-Food Science and Technology, 41*(3), 450-459.

Ilker, R., & Szczesniak, A. S. (1990). Structural and Chemical Bases for Texture of Plant Foodstuffs. *Journal of Texture Studies, 21*(1), 1-36. doi: DOI 10.1111/j.1745-4603.1990.tb00462.x

Jackman, R. L., & Stanley, D. W. (1995). Perspectives in the Textural Evaluation of Plant Foods. *Trends in Food Science & Technology, 6*(6), 187-194. doi: Doi 10.1016/S0924-2244(00)89053-6

Knoerzer, Kai, Juliano, Pablo, & Smithers, Geoffrey W. (2016). *Innovative Food Processing Technologies: Extraction, Separation, Component Modification and Process Intensification*: Woodhead Publishing.

Lopez-Sanchez, P., Nijsse, J., Blonk, H. C. G., Bialek, L., Schumm, S., & Langton, M. (2011). Effect of mechanical and thermal treatments on the microstructure and rheological properties of carrot, broccoli and tomato dispersions. *Journal of the Science of Food and Agriculture, 91*(2), 207-217. doi: Doi 10.1002/Jsfa.4168

Lopez-Sanchez, P., Rincon, M., Wang, D., Brulhart, S., Stokes, J. R., & Gidley, M. J. (2014). Micromechanics and Poroelasticity of Hydrated Cellulose Networks. *Biomacromolecules, 15*(6), 2274-2284. doi: 10.1021/bm500405h

Massa, A., Gonzalez, C., Maestro, A., Labanda, J., & Ibarz, A. (2010). Rheological Characterization of Peach Purees. *Journal of Texture Studies, 41*(4), 532-548. doi: 10.1111/j.1745-4603.2010.00240.x

Mcfeeters, R. F., & Armstrong, S. A. (1984). Measurement of Pectin Methylation in Plant-Cell Walls. *Analytical Biochemistry, 139*(1), 212-217. doi: Doi 10.1016/0003-2697(84)90407-X

McNeil, Michael, Darvill, Alan G., Åman, Per, Franzén, Lars-Erik, & Albersheim, Peter. (1982). [1] Structural analysis of complex carbohydrates using high-performance liquid chromatography, gas chromatography, and mass spectrometry *Methods in Enzymology* (Vol. 83, pp. 3-45): Academic Press.

Min, S, & Zhang, QH. (2003). Effects of Commercial‐scale Pulsed Electric Field Processing on Flavor and Color of Tomato Juice. *Journal of Food Science, 68*(5), 1600-1606.

Moelants, K. R. N., Cardinaels, R., Jolie, R. P., Verrijssen, T. A. J., Van Buggenhout, S., Van Loey, A. M., . . . Hendrickx, M. E. (2014). Rheology of Concentrated Tomato-Derived Suspensions: Effects of Particle Characteristics. *Food and Bioprocess Technology, 7*(1), 248-264. doi: 10.1007/s11947-013-1070-3

Moelants, K. R. N., Cardinaels, R., Van Buggenhout, S., Van Loey, A. M., Moldenaers, P., & Hendrickx, M. E. (2014). A Review on the Relationships between Processing, Food Structure, and Rheological Properties of Plant-Tissue-Based Food Suspensions. *Comprehensive Reviews in Food Science and Food Safety, 13*(3), 241-260. doi: 10.1111/1541-4337.12059

Morrison, Faith A. (2001). *Understanding rheology*. New York: Oxford University Press.

O'Donnell, C. P., Tiwari, B. K., Bourke, P., & Cullen, P. J. (2010). Effect of ultrasonic processing on food enzymes of industrial importance. *Trends in Food Science & Technology, 21*(7), 358-367. doi: 10.1016/j.tifs.2010.04.007

Ormerod, A. P., Ralfs, J. D., Jackson, R., Milne, J., & Gidley, M. J. (2004). The influence of tissue porosity on the material properties of model plant tissues. *Journal of Materials Science, 39*(2), 529-538. doi: Doi 10.1023/B:Jmsc.0000011508.02563.93

Palin, R., & Geitmann, A. (2012). The role of pectin in plant morphogenesis. *Biosystems, 109*(3), 397-402. doi: 10.1016/j.biosystems.2012.04.006

Rao, M. A., & Qiu, C. G. (1989). Rheological Properties of Plant Food Dispersions. *Acs Symposium Series, 405*, 149-171.

Rosenbohm, C., Lundt, I., Christensen, T. M. I. E., & Young, N. W. G. (2003). Chemically methylated and reduced pectins: preparation, characterisation by H-1 NMR spectroscopy, enzymatic degradation, and gelling properties. *Carbohydrate Research, 338*(7), 637-649. doi: Pii S0008-6215(02)00440-8

Sankaran, A. K., Nijsse, J., Bialek, L., Bouwens, L., Hendrickx, M. E., & Van Loey, A. M. (2015). Effect of Enzyme Homogenization on the Physical Properties of Carrot Cell Wall Suspensions. *Food and Bioprocess Technology, 8*(6), 1377-1385. doi: 10.1007/s11947-015-1481-4

Sankaran, A. K., Nijsse, J., Cardinaels, R., Bialek, L., Shpigelman, A., Hendrickx, M., . . . Van Loey, A. M. (2015). Effect of Enzymes on Serum and Particle Properties of Carrot Cell Suspensions. *Food Biophysics, 10*(4), 428-438. doi: 10.1007/s11483-015-9403-6

Sehgal, C., Sutherland, R. G., & Verrall, R. E. (1980). Sonoluminescence of No-Saturated and No2-Saturated Water as a Probe of Acoustic Cavitation. *Journal of Physical Chemistry, 84*(4), 396-401. doi: Doi 10.1021/J100441a010

Selvendran, R. R., & Oneill, M. A. (1987). Isolation and Analysis of Cell-Walls from Plant-Material. *Methods of Biochemical Analysis, 32*, 25-153. doi: Doi 10.1002/9780470110539.Ch2

Sila, D. N., Smout, C., Elliot, F., Van Loey, A., & Hendrickx, M. (2006). Non-enzymatic depolymerization of carrot pectin: Toward a better understanding of carrot texture during thermal processing. *Journal of Food Science, 71*(1), E1-E9.

Sila, D. N., Smout, C., Vu, S. T., Van Loey, A., & Hendrickx, M. (2005). Influence of pretreatment conditions on the texture and cell wall components of carrots during thermal processing. *Journal of Food Science, 70*(2), E85-E91.

Terefe, N. S., Buckow, R., & Versteeg, C. (2014). Quality-Related Enzymes in Fruit and Vegetable Products: Effects of Novel Food Processing Technologies, Part 1: High-Pressure Processing. *Critical Reviews in Food Science and Nutrition, 54*(1), 24-63. doi: 10.1080/10408398.2011.566946

Thakur, B. R., Singh, R. K., & Nelson, P. E. (1996). Quality attributes of processed tomato products: A review. *Food Reviews International*, *12*(3), 375-401.

Valencia, C., Sanchez, M. C., Ciruelos, A., Latorre, A., Franco, J. M., & Gallegos, C. (2002). Linear viscoelasticity of tomato sauce products: influence of previous tomato paste processing. *European Food Research and Technology, 214*(5), 394-399. doi: DOI 10.1007/s00217-002-0501-6

Van Buggenhout, S., Sila, D. N., Duvetter, T., Van Loey, A., & Hendrickx, M. (2009). Pectins in Processed Fruits and Vegetables: Part III - Texture Engineering. *Comprehensive Reviews in Food Science and Food Safety, 8*(2), 105-117. doi: 10.1111/j.1541-4337.2009.00071.x

Verlent, I., Hendrickx, M., Rovere, P., Moldenaers, P., & Van Loey, A. (2006). Rheological properties of tomato-based products after thermal and high-pressure treatment. *Journal of Food Science, 71*(3), S243-S248.

Verlent, I., Hendrickx, M., Verbeyst, L., & Van Loey, A. (2007). Effect of temperature and pressure on the combined action of purified tomato pectinmethylesterase and polygalacturonase in presence of pectin. *Enzyme and Microbial Technology, 40*(5), 1141-1146. doi: 10.1016/j.enzmictec.2006.08.021

Verlent, I., Van Loey, A., Smout, C., Duvetter, T., & Hendrickx, M. E. (2004). Purified tomato polygalacturonase activity during thermal and high-pressure treatment. *Biotechnology and Bioengineering, 86*(1), 63-71. doi: 10.1002/bit.10920

Waldron, K. W., Parker, M. L., & Smith, A. C. (2003). Plant Cell Walls and Food Quality. *Comprehensive Reviews in Food Science and Food Safety, 2*(4), 128-146. doi: 10.1111/j.1541-4337.2003.tb00019.x

Wu, J., Gamage, T. V., Vilkhu, K. S., Simons, L. K., & Mawson, R. (2008). Effect of thermosonication on quality improvement of tomato juice. *Innovative Food Science & Emerging Technologies, 9*(2), 186-195. doi: 10.1016/j.ifset.2007.07.007

Yildirim, A., Oner, M. D., & Bayram, M. (2011). Fitting Fick's model to analyze water diffusion into chickpeas during soaking with ultrasound treatment. *Journal of Food Engineering, 104*(1), 134-142. doi: 10.1016/j.jfoodeng.2010.12.005

# CHAPTER 5. EFFECTS OF PROCESSING CONDITIONS ON THE RHEOLOGICAL PROPERTIES OF TOMATO SUSPENSIONS (II): CONCENTRATION

## 5.1 Introduction

About 80% of tomatoes in the U.S. are consumed as tomato processed products (Heuvelink, 2005). In general, most tomatoes are processed into tomato pastes (i.e. concentrates) before any further manufacturing (Abu-Jdayil, Banat, Jumah, Al-Asheh, & Hammad, 2004). Tomato sauce and ketchup are the most commonly consumed processed forms which are originated/diluted from tomato concentrates (Rickman, Barrett, & Bruhn, 2007). The concentration process comes after "break" step and also uses intense thermal conditions to evaporate the water from the juice to produce the paste. The purposes of the concentration process are for long-term storage and easy transportation. Concentrated paste can be stored for one year or more and is used as the starting material for the production of other value-added products (Anthon, Diaz, & Barrett, 2008).

Typically, this process takes from half hour to more than 2 h of heating at moderate temperatures under reduced pressure in either batch-type system or continuous evaporation system (Apaiah & Barringer, 2001). However, it has been known for years that the subsequent dilution for production of tomato products at a set concentration is accompanied by a loss of the product consistency (Tanglertpaibul & Rao, 1987b). This is a major economic cost for the industry since more concentration of solids is required to add in order to achieve the same viscosity as the original form before concentration (Thakur, Singh, & Nelson, 1996). There is considerable literature on the influence of the concentration process on the rheological properties of tomato products (Anthon et al., 2008; Diaz, Anthon, & Barrett, 2009; Sanchez, Valencia,

Ciruelos, Latorre, & Gallegos, 2003; Valencia et al., 2002). However, the causes for this problem have not been found yet, although some hypotheses have been proposed. Hurtado et al. (2002) suggested pectin hydrolysis during the high evaporation temperature was the cause. Marsh et al. (1977) proposed irreversible deleterious changes in the particles due to high osmotic and ionic strength led to a drop in viscosity. Beresovsky et al. (1995) and Mizrahi (1997) attributed the viscosity loss to mechanical shear applied to the juice during pumping. According to Anthon et al. (2008), there was little or no change in the total pectin content during the concentration of both HB and CB juices. However, insoluble pectin was decreased which was possible to result in a higher Bostwick value, but these two phenomena were not directly connected because occurred at different times. For instance, the insoluble pectin decreased at the late stages of the concentration, whereas the consistency was lost at the initial stage of the process. Furthermore, Beresovsky et al. (1995) found that a loss of consistency still happened without applying heat or vacuum to the evaporator which indicated that mechanical effects other than thermal effects were responsible for the consistency loss. Therefore, Anthon et al. (2008) suggested that the reduction in the particle size and precipitate ratio could be the main causes to the loss in consistency.

The overall objective of this chapter was to investigate the changes in rheological properties of tomato products during the concentration process at an industrial plant. This study tried to analyze the problem from a new perspective that considered the properties of the particles to explain the consistency loss issue after concentration. This information should provide strategies to design better processing conditions and alternatives to improve the quality of the tomato products.

## 5.2 Materials and Methods

### 5.2.1 Tomato Juice and Pastes from Processing Plant

The tomato samples were provided by ConAgra Foods Inc. (Oakdale, CA) from a paste processing plant in November 2015. The paste samples were collected from the same batch during processing. Unconcentrated tomato juice from which the pastes were made was also sampled. They were aseptically packed and shipped to the Purdue lab overnight. The sample labeling is shown in Table 5.1. These paste samples were from the same origin tomato fruits but had different initial consistency when packed due to minor variation in the concentration process. For instant, Paste 1 designated as P1, had a Bostwick consistency of 2.6 cm at packing. The Bostwick value of original juice was measured in the lab immediately after arrival also shown in the table. The paste samples were stored in a cool room (5 ℃) and all measurements took place within one month after manufacture.

### 5.2.2 Tomato Suspension Preparation

Since unconcentrated original juice had a soluble solid content of 4.0 °Brix, the pastes were diluted with deionized water to reconstitute juices (i.e. suspensions) of 4.0 °Brix. Mixing was performed following the method described by Anthon et al. (2008). Additional water or paste was blended as necessary to adjust the samples to 4.0 °Brix. The suspension labeling is also listed in Table 5.1.

### 5.2.3 General Properties

#### 5.2.3.1 Solid Content

The solid contents were determined by a vacuum oven. About 5 g samples were transferred to the pre-weighed drying foil dishes and dried for 12 hours at 60 ℃ in a vacuum

oven. The total weight of dish plus sample was recorded before and after drying. The moisture content or percent dry solids were determined.

5.2.3.2 °Brix

The °Brix value was measured by an Abbe refractometer at room temperature. The soluble solids reading was on temperature compensated. The reconstituted juices were adjusted a soluble solid content to 4.0 °Brix.

5.2.3.3 Bostwick Consistency

The Bostwick consistency was determined for the original juice as well as reconstituted juices. The method was described in Chapter 3.

5.2.3.4 Isolation of Tomato Cell Wall Material

The Alcohol Insoluble Residue (AIR) isolation was carried out for unconcentrated original juice and reconstituted juices based on the method reported by McFeeters and Armstrong (1984), which was described in detail in Chapter 4. The AIR was dried in a vacuum oven at 25 °C overnight and stored in a desiccator.

5.2.4 Rheology Measurements

Rheological measurements were carried out in a stress controlled rheometer (ARG2; TA Instruments, DE, USA). For the original juice and reconstituted juices, both steady-state shear and dynamic oscillatory shear experiments were performed using a vane geometry with a diameter of 28 mm and a height of 42 mm. The methods were described in Chapter 4. For pastes, the viscoelastic properties were determined using a parallel plate geometry with a diameter of 40 mm. A strain sweep in a range from 0.1 to 100% (strain%) was performed at a constant frequency of 1 Hz to determine the linear viscoelastic region (LVR). The Small Amplitude

Oscillatory Shear (SAOS) test was then carried out using a frequency sweep from 0.1 to 10 Hz at a constant strain of 0.1% (which is in LVR). All measurements were performed at least in triplicate at a constant temperature of 25 ℃.

### 5.2.5 Particle Size

The particle size of the original juice and reconstituted juices were determined by laser light scattering using a Malvern Mastersizer 2000 instrument (Malvern Instruments Ltd, Worcestershire, UK). The procedure was described in Chapter 3.

### 5.2.6 Statistical Analysis

All the measurements were performed in triplicate and the results are given as mean of three measurements ± standard deviation. Statistical analysis was carried out using SAS 9.3 software package (SAS Institute, Inc., NC, USA). All pairwise comparisons were tested using the Tukey method. The level of significance was set at $p < 0.05$.

## 5.3 Results and Discussion

### 5.3.1 General Product Properties

Solid contents of original juice (OJ), pastes (P1, P2, P3 and P4) and reconstituted juices (RJ1, RJ2, RJ3 and RJ4) are shown in Figure 5.1. The pastes after concentration process all had a high solid content greater than 25%, which showed no significant differences in comparison by Tukey grouping. Although the reconstituted juices after dilution had the some °Brix values (i.e. 4) as OJ, the solid content in the reconstituted juices were considerably higher. Marsh et al. (1977) reported that high solute concentration found in pastes compressed the particles which were not fully re-expanded upon dilution. Heutink (1986) also claimed that tomato cells were collapsed after concentration process and were not able to re-absorb water and re-expand to the initial state.

Results in this work suggest that condensed solutes are also trapped within the particles and cannot be fully re-solubilized in the following dilution at ambient temperature. It partially acts as insoluble solids and therefore more paste needs to be added to bring the °Brix value back to 4. This result is in good agreement with the data reported by Marsh et al. (1977), where they strongly suggested an additional heating step to reduce the inefficient resorption. Solid content is one of the most important factors that influence the rheological properties of cell-wall-derived suspensions (Espinosa-Munoz, Renard, Symoneaux, Biau, & Cuvelier, 2013). The solid content of RJ4 was 5.8%, which was significantly higher than that of other reconstituted suspensions (i.e. RJ1, RJ2 and RJ3). This difference would lead to variation in consistency and rheology in the following tests. It should be pointed out, although the initial Bostwick consistencies of pastes at packing were provided, these values could not fully represent the texture of samples. According to Marsh et al. (1977), the Bostwick values became very small as the solid content increases to 15% and therefore the actual value cannot be precisely determined by the Bostwick consistometer. The paste in the present study contained more than 25% solids, so other parameters such as solid content and particle size should be also considered when comparing the properties of diluted suspensions.

Bostwick values of original juice and reconstituted juices are compared in Figure 5.2. Although OJ had much lower solid content, it still exhibited a lower Bostwick value meaning a more optimum consistency. The solid content measured in the study includes water soluble and insoluble parts, and the contribution of soluble material (i.e. soluble pectin) to the overall viscosity has been demonstrated as very limited in Chapter 3. To understand the effects of solids, AIR was extracted and compared in the same figure. The AIR is often referred to as cell wall material and has been shown to have a high positive correlation to the viscosity of tomato juice

(Janoria & Rhodes, 1974). However, it gave an opposite result here. OJ had the lowest AIR weight but exhibited a lower Bostwick consistency than reconstituted juices. This result seemed controversy; however could be explained by changes on the properties of the particles. Particle volume fraction is one of the most important parameters that influence the suspension rheology (Mueller, Llewellin, & Mader, 2010). However, plant cell wall particles are soft, highly deformable and non-spherical, and several studies use weight such as particle concentration or solid content instead of volume to describe their rheological properties. It is meaningful for comparison only if the particles are the same. However during the concentration process, the physical properties of the particles were greatly altered, which were not the same as the particles from OJ. Thus, it explains that OJ still can show a lower Bostwick consistency even though its AIR weight and solid content are significantly lower compared to those of reconstituted juices. By contrast, all the pastes were produce from the same concentration procedure, so the particles did not show major differences among the reconstituted juices. Therefore, as AIR weight increased from RJ1 to RJ4 Bostwick values showed a decreasing trend. The only discrepancy was RJ1, which was determined to have the lowest AIR weight; however failed to present a highest Bostwick value. It may be due to the minor differences in particle properties among paste particles (i.e. P1, P2, P3 and P4). These results indicate solid content/AIR is just one of the major factors that control the product consistency. Other parameters such as particle size and particle properties are showing the same importance, which are discussed in the next sections.

### 5.3.2 Particle Size

The particle size of original juice and reconstituted juices measured by static light scattering are presented in Table 5.2. Values of $D[v,0.1]$, $D[v,0.5]$ and $D[v,0.9]$ of OJ were significantly higher than those of the reconstituted juices. These parameters indicate the particle

diameter at which reaches 10, 50 and 90% of the particle volume, respectively. The *D*[3, 2] (area-based diameter) and *D*[4, 3] (volume-based diameter) of the OJ particle, which were 180.2 and 365.2 μm, also showed higher values compared to those of the reconstituted juices. However, the difference between the *D*[3, 2] of OJ and RJ4 particles was not significant. It is observed that the values of these five parameters for the RJ4 particles were considerably higher than those of other reconstituted juices. The *D*[4, 3] value is strongly biased towards the very largest particles in the distribution, whereas the *D*[3, 2] value is more associated with smaller-sized particles (Bayod, Mansson, Innings, Bergenstahl, & Tornberg, 2007; Lopez-Sanchez et al., 2011). This result suggests that two mechanisms may exist during the concentration process. The particles "shrink" at the initial stage showing a significant drop in particle size compared to OJ. As the concentration process continues the particles, especially small particles, could be further condensed and then strongly bonded together and therefore exhibits a larger particle size. This is evidenced by a higher *D*[3, 2] value of RJ4 particle.

A decreased average particle size was reported due to the concentration process (Den Ouden & Van Vliet, 2002). Thus, the consistency loss could be explained by the reduced volume fraction occupied by the smaller particles (Kalamaki et al., 2003). Anthon et al. (2008) also showed that the reduction in precipitate ratio during concentration, which further confirmed that the volume fraction could be the one of the main causes to the loss in consistency. The present study illustrates a high correlation between particle size and consistency. A higher value of average particle size (i.e. *D*[*v*,0.5], *D*[3, 2] or *D*[4, 3]) indicates a better Bostwick consistency (Table 5.2 and Figure 5.2). It should be noted that as the particles were reduced in volume during the concentration, their properties were altered as well. This also contributes to the observed differences in the measured Bostwick consistency.

When tomato juice is concentrated to paste, the particles are showing a reduction in volume and a condensation in their weight into much smaller particle size as solutes are concentrated within the particles. When the paste is diluted back to juice, the particles cannot be fully re-expanded and the concentrated solute is only partially re-solubilized. Therefore, more paste is needed to adjust the soluble solid content back to original °Brix. This process reduces the particle volume to achieve a higher concentrated weight. The individual particles in the reconstituted juices are assumed to have a smaller volume and higher density. Although these suspensions contain more solid, they probably still have a relatively lower volume fraction compared to original juice. Another alteration caused by concentration is the particle properties, which are discussed later. These combined effects could explain the viscosity loss during the concentration process.

### 5.3.3 Viscosity

The viscosity of original juice and reconstituted juices is shown in Figure 5.3. As expected, the viscosity of OJ was significantly higher than those of the reconstituted juices. In addition, S4 showed a higher viscosity compared to other reconstituted suspensions. These results are in line with the results of Bostwick consistency (Figure 5.2). However, in the Bostwick consistency measurements, significant differences between reconstituted juices were obtained, which were not observed by the rheometer measurements. The Bostwick values are the travelled distance based on the gravity of the material (Mccarthy & Seymour, 1994), and its magnitude increases exponentially with concentration (Marsh et al., 1977). It is only a single point measurement and cannot be used to infer physicochemical characteristics of the tested material (Tanglertpaibul & Rao, 1987a). In the present study the solid contents of the samples

varied significantly in the reconstituted juices to achieve the required °Brix, which could explain the differences observed between these two methods.

From the viscosity curve, it is noticed that the reconstituted juices changed the flow behavior at a shear rate > 50 $s^{-1}$ which indicates a change in the sample structure; whereas the structure of the OJ sample appeared to remain the same at the shear rate ranged applied. The inset plot serves to demonstrate the difference between the OJ and RJ3 samples. The RJ3 sample changed the flow behavior at a shear rate of 50 $s^{-1}$, exhibiting an abrupt increase in viscosity followed by a slowly decrease. By contrast, the slope of OJ flow curve was maintained even in the high shear rate range. These results suggest that the particle structure and properties are not the same in these two suspension systems. In the reconstituted juices, the particles are derived from pastes that have been subjected to a concentration. The aim of concentration is to evaporate large liquid volume for long-term storage and easy transportation. However, at the meantime it probably causes a reduction in particle volume and a concentration in particle weight into smaller size. It has been proposed that the particles undergone irreversible deleterious changes resulted from high osmotic and ionic strength (Reid, Kotte, Kalamaki, & Ibanez, 2006). Reconstituted suspensions (i.e. juices) from pastes are not stable systems, and serum separation commonly occurs. Den Ouden and Van Vliet (2002) reported serum separation became severer if the reconstituted juice was prepared from a concentrated paste having a higher °Brix value. Generally, cell-wall-derived suspensions show a shear thinning behavior: viscosity decreases with increasing shear rate. In the present study, as shear rate increases to a high range, the particles in reconstituted juices are probably aggregated together thus exhibiting an abrupt increasing or a flat flow curve. This result indicates that the changes of particle structure and

properties are also important causes of consistency loss. It can alter the flow behavior and affect the rheological properties of more diluted products.

### 5.3.4 Viscoelasticity of Original Juice and Reconstituted Juices

The viscoelastic properties of OJ and reconstituted juices were determined by performing dynamic oscillatory shearing tests. A strain-sweep from 0.1 to 100% (strain %) was first carried out at a constant frequency 1 Hz and shown in Figure 5.4. The linear viscoelastic (LVR) region was below 1%. In the LVR, all samples showed that the storage modulus G' was higher than the loss modulus G" indicating a 'weak gel' behavior (Verlent, Hendrickx, Rovere, Moldenaers, & Van Loey, 2006). OJ exhibited considerably higher moduli G' and G" values in LVR than those of the reconstituted juices. There were also small differences between the reconstituted juices. In order to quantitatively compare the viscoelastic properties of OJ and the reconstituted juices, G' and G" values at 0.1% strain were obtained from Figure 5.4 and replotted in Figure 5.5. As expected, the differences between OJ and the reconstituted juices were significant. Although there were no significantly differences between viscoelastic moduli of the reconstituted suspensions, the slight small differences in the storage modulus followed the order RJ4>RJ3>RJ1>RJ2, which is the same to the comparisons in the particle size, consistency, and viscosity. This result indicates both volume fraction and particle properties (i.e. elasticity or mechanical strength) are important factors in determining the rheological properties of the suspensions.

A frequency sweep from 0.01 to 10 Hz was then performed and the results are presented in Figure 5.6. G' and G" showed a slightly increasing trend in the range of frequencies tested with G' values greater than G" by more than 10-folds regardless of the frequency, which is a typical rheological behavior of concentrated fruit and vegetable suspensions (Day, Xu, Oiseth,

Hemar, & Lundin, 2010; Day, Xu, Oiseth, Lundin, & Hemar, 2010). Similar to the results from the strain sweep test, OJ sample always showed higher G' values than those of the reconstituted juices. It has been reported that the viscoelastic properties have a positive correlation with the solid content of vegetable- and fruit-derived suspensions (Day, Xu, Oiseth, Hemar, et al., 2010; Espinosa-Munoz et al., 2013). In such systems, solid content is usually used instead of volume fraction due to the soft and highly deformable nature of the cell wall particles. In the present study, OJ showed significantly higher viscoelasticity although it contained lesser solid content compared to the reconstituted suspensions. The result of the suspension viscoelasticity is a combined effect of the particle volume fraction and the particle properties. It seems that the particles in the original juice occupy a larger phase volume fraction and/or have higher elasticity. After the concentration process, the particles are reduced in particle volume and concentrated their particle weight into much smaller size. Although more solids need to be put in the reconstituted juices, OJ might still have a larger particle volume fraction. Furthermore, the particle properties have been changed, which alters the particle interaction and further affects the rheology. This hypothesis needs further studies on the properties of particles to confirm it.

### 5.3.5 Viscoelasticity of Pastes

Pastes obtained from the concentration process had similar solid content, so their viscoelastic properties were expected to yield useful information regarding the properties of particles forming them. A strain sweep was performed on the pastes and results are illustrated in Figure 5.7. The pastes exhibited a similar LVR as the suspensions (Figure 5.5); however G' and G" values were two orders of magnitude higher. It indicates that particles dominate the rheological behaviors of these paste systems. A decrease in both G' and G" to eventually reach a cross-over point in the non-linear range was observed with further increasing the strain (>1%).

The cross-over strain was about 8% for P1 and 2% for P4. It moved to a low strain range from P1 to P4. This result indicates that particles forming the paste P1 promote a larger number of strain bearing entanglements compared to the P4 particles (Day, Xu, Oiseth, Lundin, et al., 2010). The moduli measured in the LVR were compared by Tukey's grouping and the result shows that there was no significant difference between these pastes. The four pastes are final concentrated products obtained in a commercial concentration evaporation process, so the small differences observed are likely due to the minor differences in the processing conditions. It indicates that the pastes are formed by particles with similar properties that differ from those of the original tomato juice.

The frequency sweep was conducted on the pastes and results are illustrated in Figure 5.9. It can be observed in the figure that G' values were greater than G" values, indicating that elastic behavior of these pastes. Similar to the strain sweep results, G' values only exhibited an insignificant decrease trend from P1 to P4, with paste P4 showing a slightly lower value than those of other pastes. Particles in pastes are highly packed and deformed, and in such systems the elasticity of individual particles determines the bulk viscoelasticity (Stokes & Frith, 2008). Therefore, this result confirms that particles forming the different pastes should have the similar elasticity. Although there is only minor difference, it has been noticed that the paste P4 which has the lowest G' can form reconstituted juice (i.e. RJ4) with a slight higher G' than those of other reconstituted juices. It can be explained by the high solid content of the RJ4 sample. During reconstitution/dilution from paste to juice, the amount of paste to put depends on the soluble solid content of suspension. The particles cannot re-absorb water and fully re-expand to the original shape after concentration process (Heutink, 1986). If the particles were more affected during concentration, they would be less re-expended upon dilution and more solids

were required to achieve the original °Brix value (i.e. 4). The facts that the paste P4 shows lower G', as well as the reconstituted juice RJ4 (diluted from P4) contains significantly higher solids (Figure 5.1), suggest P4 particles were most altered by concentration. The minor differences in particle properties among the paste samples, however, could result in huge differences in compensation of soluble solid content and viscosity loss in producing diluted tomato products. These results also indicate that both particle volume fraction (i.e. concentration) and particle properties are essential to the rheology of cell-wall-derived suspensions.

## 5.4 Conclusions

In this study, four tomato pastes from a commercial processing plant were diluted back with deionized water to reconstitute these concentrates in suspensions that had the same °Brix values than the original juice. The solid content, AIR weight and particle size were determined for the original juice and reconstituted juices, and correlated with the results of Bostwick consistency and rheological properties. Although the original juice had a much lower solid content and AIR weight, it still exhibited a better consistency and a higher viscosity in comparison with the reconstituted juices. The particle size showed a high correlation with consistency and viscosity. Average particle size of the original juice was significantly reduced by the concentration process. The viscoelastic properties of the original juice also showed higher moduli values, which indicate that the properties of the particles are altered by the concentration process.

It can be concluded that both particle volume fraction and particle properties have a major effect on the rheological properties of cell-wall-derived suspensions (see Figure 5.10). When original tomato juice is concentrated to a paste, the particles reduced in volume and concentrated their weight into much smaller particle size. The concentration process not only

reduces the particle volume but also negatively alters the particle mechanical properties. The individual particles in the reconstituted suspensions have a smaller size and lower elasticity. Even though these suspensions contain more solids, they probably still have a relatively lower volume fraction and elasticity compared to original juice, therefore exhibiting a lower consistency and viscosity. Furthermore, after concentration the particles cannot fully return to the original shape when they are reconstituted from the concentrate, and the solute is only partially re-solubilized upon dilution to juice. This explains that more paste is needed to be added in order to adjust the °Brix back to that of the original juice. Although there were minor differences of particle elasticity among the paste samples, it caused significant impacts on the subsequent dilution for production of tomato products (i.e. reconstituted juices). These results illustrate the predominant role of the particles on the rheological behavior of products. However, this study didn't directly compare the particles in pastes and unconcentrated original juice in terms of viscoelasticity and mechanical strength, which need to be further investigated in the future.

## 5.5 Figures and Tables

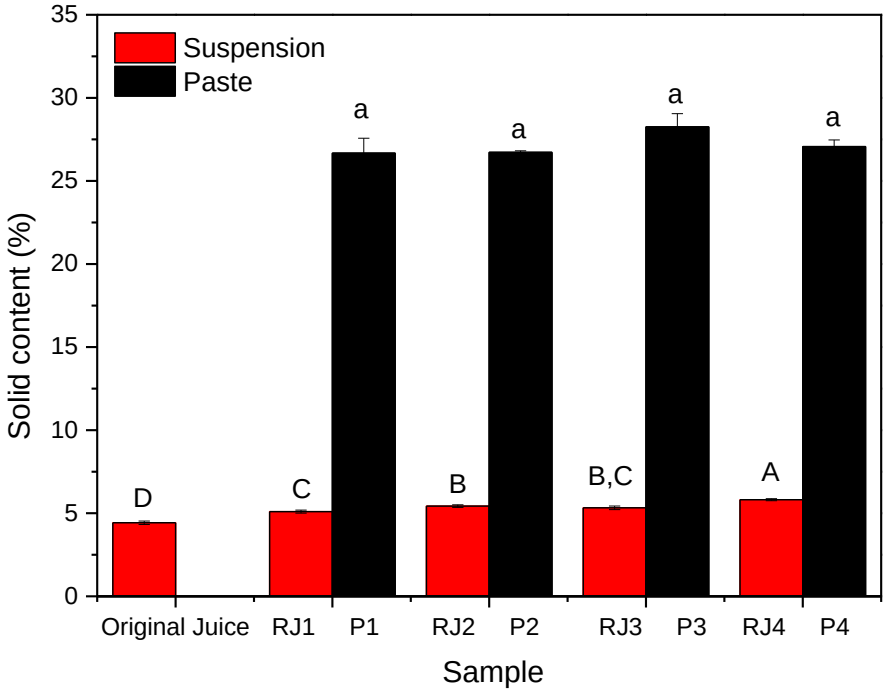


Figure 5.1 Solid contents of original juice (OJ), pastes (P1, P2, P3 and P4) and reconstituted juices (RJ1, RJ2, RJ3 and RJ4). Data were classified by Tukey grouping method, and means with the same letter are not significantly different.

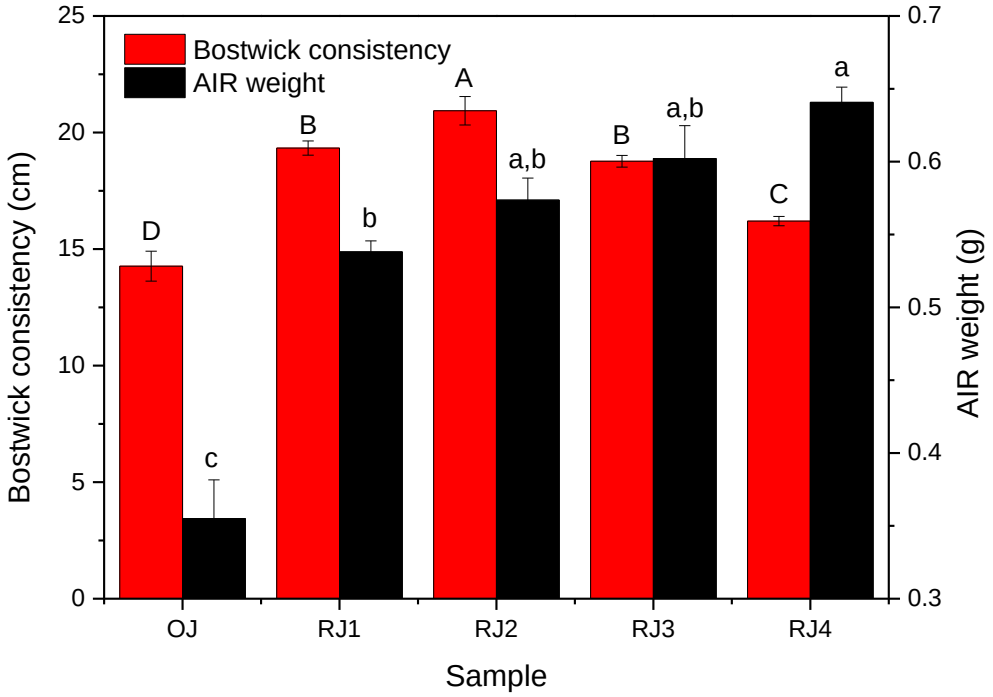


Figure 5.2 Bostwick values and AIR weights of original juice and reconstituted juices/suspensions. AIR was extracted from 30 g suspensions. Data were classified by Tukey grouping method and means with the same letter are not significantly different.

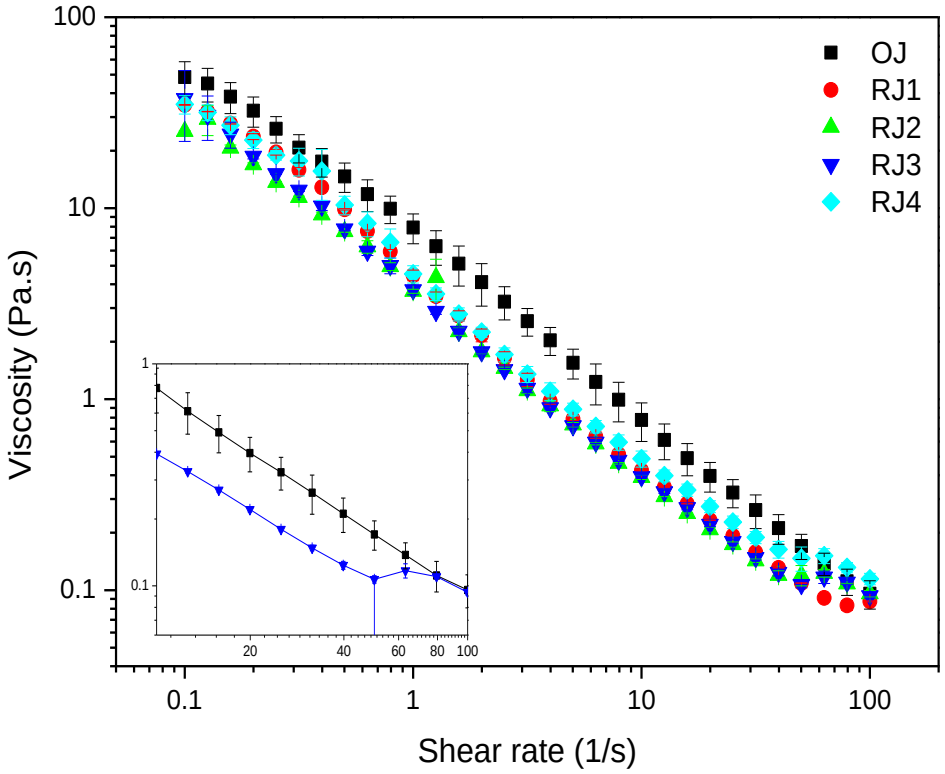


Figure 5.3 Viscosity curves of original juice and reconstituted juices/suspensions. The insert plot shows the different flow behavior between OJ and S3. S3 changes slope at a shear rate of 50 $s^{-1}$, whereas the slope of OJ flow curve keeps the same.

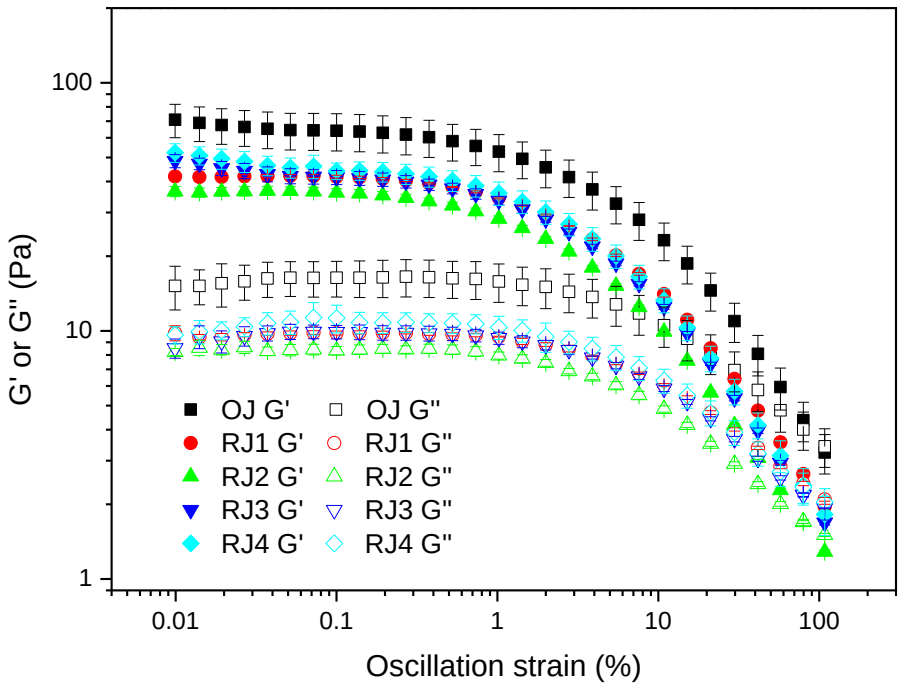


Figure 5.4 Strain sweep tests of original juice and reconstituted juice at a constant frequency 1 Hz. The shear strain range was 0.1% to 100% and the testing temperature was 25 $^{o}$C.

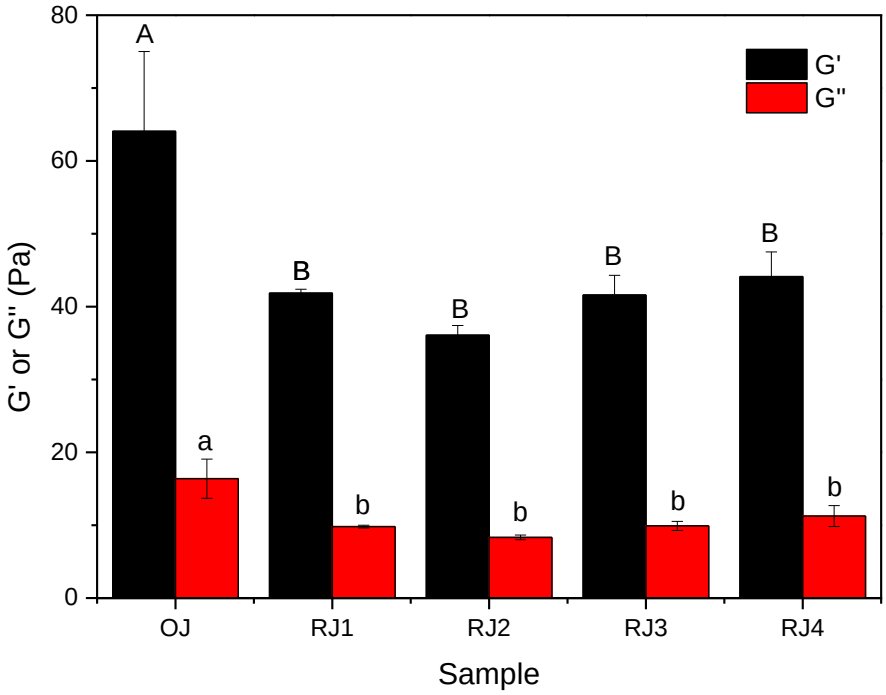


Figure 5.5 Comparison of storage modulus (G') and loss modulus (G") in the LVR of original juice and reconstituted juices/suspensions. Data were classified by Tukey grouping method and means with the same letter are not significantly different.

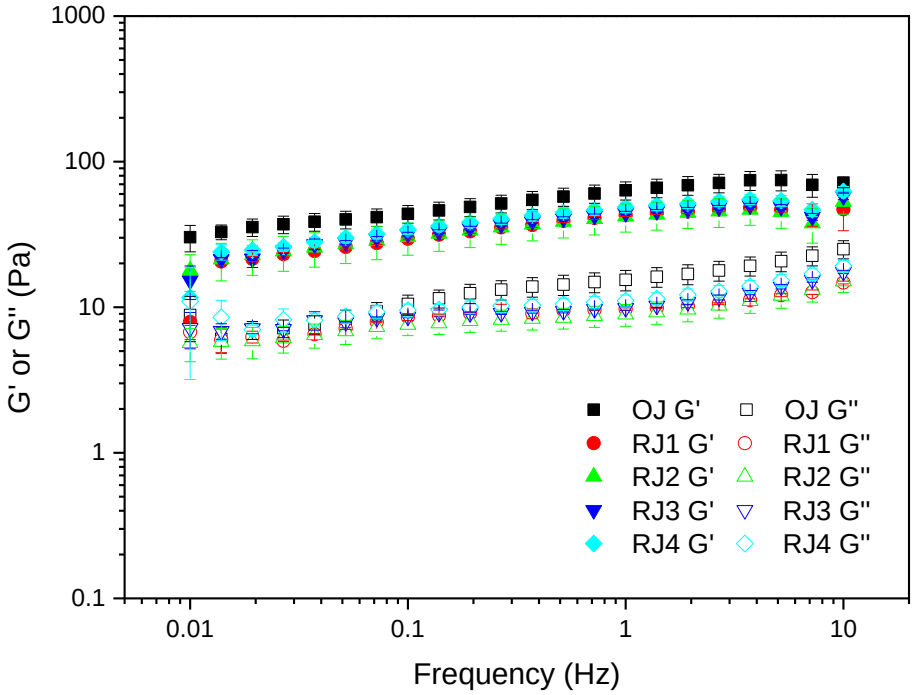


Figure 5.6 Frequency sweep tests of original juice and reconstituted juices at a constant strain% 0.1% (in LVR). The frequency range was 0.01 to 10 Hz and the testing temperature was 25 $^{o}$C.

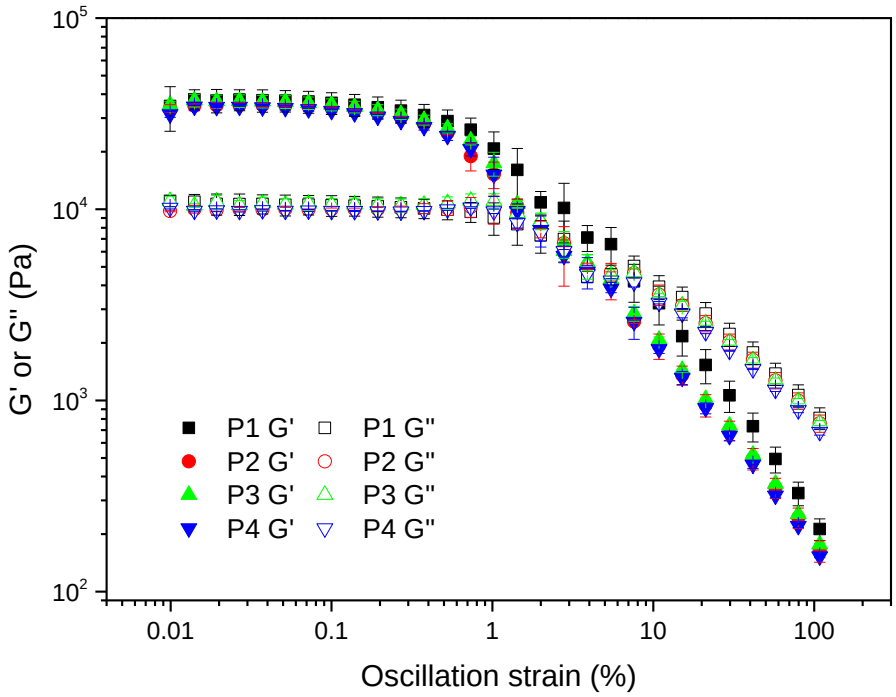


Figure 5.7 Strain sweep tests of pastes from concentration process at a constant frequency 1 Hz. The shear strain range was 0.1% to 100% and the testing temperature was 25 $^{o}$C.

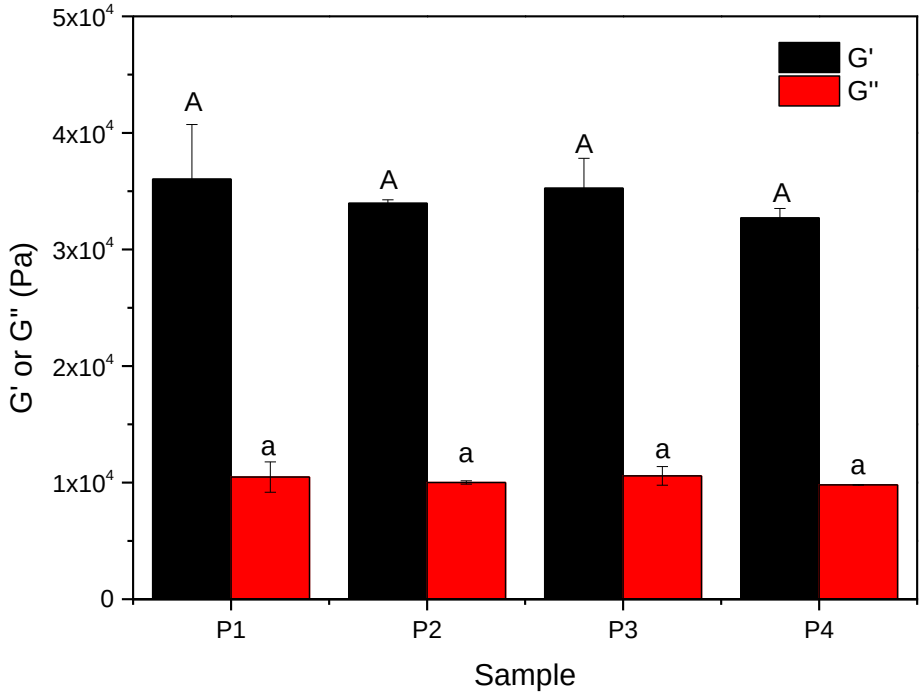


Figure 5.8 Comparisons of storage modulus (G') and loss modulus (G'') in the LVR of pastes from concentration process. Data were classified by Tukey grouping method and means with the same letter are not significantly different.

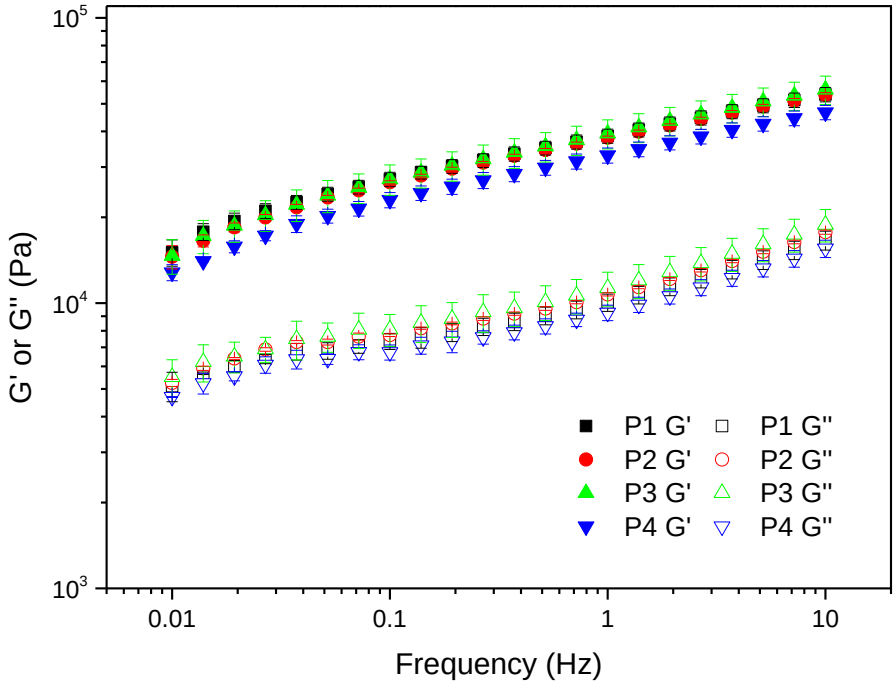


Figure 5.9 Frequency sweep tests on pastes obtained from the commercial concentration process. The frequency range was 0.01 to 10 Hz at a constant strain% 0.1% (in LVR). Testing temperature was 25 $^{o}$C.

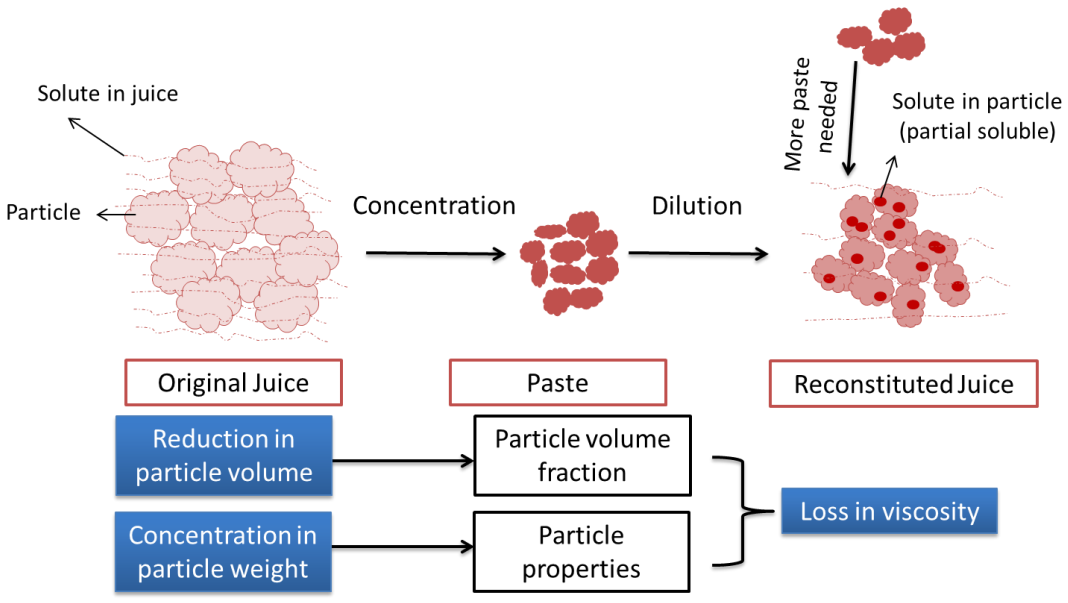


Figure 5.10 Schematic plot of particle changes during concentration and subsequent dilution process. During the industrial concentration process from tomato juice to paste, it caused a reduction in particle volume and concentrated their weight into much smaller particle size. This process not only reduced the particle volume fraction but also negatively changed the particle mechanical properties. The individual particles in the reconstituted juices had a smaller size and lower elasticity. Therefore, it caused a loss in viscosity. Furthermore, after concentration the particles cannot fully re-expend to the original shape upon dilution, and the solute is only partially re-solubilized. In order to achieve the same soluble solid content as OJ, more paste was needed.

Table 5.1 Sample labeling for the experiments. Tomato juice and paste were from the same origin batch. The Bostwick values of pastes were determined when they were packed in the plant. These pastes were diluted to tomato juices in the lab to have the same solid contents as the original juice (i.e. 4 °Brix).

| Sample from plant | Bostwick consistency (cm) | Paste name | Suspension name (diluted from paste) |
|---|---|---|---|
| Original juice | 14.3 | N/A | OJ |
| Paste 1 | 2.6 | P1 | RJ1 |
| Paste 2 | 2.2 | P2 | RJ2 |
| Paste 3 | 1.9 | P3 | RJ3 |
| Paste 4 | 1.6 | P4 | RJ4 |

Table 5.2 Particle size (± standard deviation) of original juice and reconstituted juices prepared from commercial pastes. Data were classified by Tukey grouping method and means with the same letter are not significantly different.

| Sample | $D[v,0.1]$ (μm) | $D[v,0.5]$ (μm) | $D[v,0.9]$ (μm) | $D[3, 2]$ (μm) | $D[4, 3]$ (μm) |
|---|---|---|---|---|---|
| OJ | 132.0 ± 0.2 a | 330.2 ± 2.4 a | 665.0 ± 9.6 a | 180.2 ± 5.2 a | 365.2 ± 3.3 a |
| RJ1 | 98.6 ± 2.6 d | 270.6 ± 3.0 cd | 553.1 ± 19.3 bc | 142.5 ± 1.9 c | 301.8 ± 7.4 c |
| RJ2 | 99.6 ± 0.7 d | 263.9 ± 1.8 d | 534.0 ± 4.0 c | 146.8 ± 1.9 c | 293.3 ± 2.1 c |
| RJ3 | 111.7 ± 1.9 c | 279.7 ± 6.9 c | 539.4 ± 17.2 c | 162.2 ± 1.6 b | 305.0 ± 8.5 c |
| RJ4 | 118.6 ± 0.9 b | 282.4 ± 3.0 b | 583.8 ± 15.6 b | 174.1 ± 4.9 a | 326.4 ± 5.4 b |

## 5.6 References

Abu-Jdayil, B., Banat, F., Jumah, R., Al-Asheh, S., & Hammad, S. (2004). A comparative study of rheological characteristics of tomato paste and tomato powder solutions. *International Journal of Food Properties, 7*(3), 483-497. doi: 10.1081/Jfp-120040203

Anthon, G. E., Diaz, J. V., & Barrett, D. M. (2008). Changes in pectins and product consistency during the concentration of tomato juice to paste. *Journal of Agricultural and Food Chemistry, 56*(16), 7100-7105. doi: 10.1021/jf8008525

Apaiah, R. K., & Barringer, S. A. (2001). Quality loss during tomato paste production versus sauce storage. *Journal of Food Processing and Preservation, 25*(4), 237-250. doi: DOI 10.1111/j.1745-4549.2001.tb00458.x

Bayod, E, Mansson, P, Innings, F, Bergenstahl, B, & Tornberg, E. (2007). Low shear rheology of concentrated tomato products. Effect of particle size and time. *Food Biophysics, 2*(4), 146-157. doi: 10.1007/s11483-007-9039-2

Beresovsky, N., Kopelman, I. J., & Mizrahi, S. (1995). The Role of Pulp Interparticle Interaction in Determining Tomato Juice Viscosity. *Journal of Food Processing and Preservation, 19*(2), 133-146. doi: DOI 10.1111/j.1745-4549.1995.tb00283.x

Day, L., Xu, M., Oiseth, S. K., Hemar, Y., & Lundin, L. (2010). Control of Morphological and Rheological Properties of Carrot Cell Wall Particle Dispersions through Processing. *Food and Bioprocess Technology, 3*(6), 928-934. doi: DOI 10.1007/s11947-010-0346-0

Day, L., Xu, M., Oiseth, S. K., Lundin, L., & Hemar, Y. (2010). Dynamic rheological properties of plant cell-wall particle dispersions. *Colloids and Surfaces B-Biointerfaces, 81*(2), 461-467. doi: 10.1016/j.colsurfb.2010.07.041

Den Ouden, F. W. C., & Van Vliet, T. (2002). Effect of concentration on the rheology and serum separation of tomato suspensions. *Journal of Texture Studies, 33*(2), 91-104.

Diaz, J. V., Anthon, G. E., & Barrett, D. M. (2009). Conformational Changes in Serum Pectins during Industrial Tomato Paste Production. *Journal of Agricultural and Food Chemistry, 57*(18), 8453-8458. doi: 10.1021/jf901207w

Espinosa-Munoz, L., Renard, C. M. G. C., Symoneaux, R., Biau, N., & Cuvelier, G. (2013). Structural parameters that determine the rheological properties of apple puree. *Journal of Food Engineering, 119*(3), 619-626. doi: DOI 10.1016/j.jfoodeng.2013.06.014

Heutink, R. (1986). *Tomato juices and tomato juice concentrates: a study of factors contributing to their gross viscosity*.

Heuvelink, J.M. Costa and E. (2005). Introduction: the tomato crop and industry. In E. Heuvelink (Ed.), *Tomatos*. Cambridge, MA: CABI Publishing.

Hurtado, M. C., Greve, L. C., & Labavitch, J. M. (2002). Changes in cell wall pectins accompanying tomato (Lycopersicon esculentum Mill.) paste manufacture. *Journal of Agricultural and Food Chemistry, 50*(2), 273-278. doi: 10.1021/jf010849e

Janoria, M. P., & Rhodes, A. M. (1974). Juice Viscosity as Related to Various Juice Constituents and Fruit Characters in Tomatoes. *Euphytica, 23*(3), 553-562. doi: Doi 10.1007/Bf00022476

Kalamaki, M. S., Harpster, M. H., Palys, J. M., Labavitch, J. M., Reid, D. S., & Brummell, D. A. (2003). Simultaneous transgenic suppression of LePG and LeExp1 influences rheological properties of juice and concentrates from a processing tomato variety. *Journal of Agricultural and Food Chemistry, 51*(25), 7456-7464. doi: 10.1021/jf034164l

Lopez-Sanchez, P., Nijsse, J., Blonk, H. C. G., Bialek, L., Schumm, S., & Langton, M. (2011). Effect of mechanical and thermal treatments on the microstructure and rheological properties of carrot, broccoli and tomato dispersions. *Journal of the Science of Food and Agriculture, 91*(2), 207-217. doi: Doi 10.1002/Jsfa.4168

Marsh, George L., Buhlert, James, & Leonard, Sherman. (1977). Effect of degree of concentration and of heat treatment on consistency of tomato pastes after dilution. *Journal of Food Processing and Preservation, 1*(4), 340-346. doi: 10.1111/j.1745-4549.1977.tb00335.x

Mccarthy, K. L., & Seymour, J. D. (1994). Gravity Current Analysis of the Bostwick Consistometer for Power-Law Foods. *Journal of Texture Studies, 25*(2), 207-220. doi: DOI 10.1111/j.1745-4603.1994.tb01327.x

Mcfeeters, R. F., & Armstrong, S. A. (1984). Measurement of Pectin Methylation in Plant-Cell Walls. *Analytical Biochemistry, 139*(1), 212-217. doi: Doi 10.1016/0003-2697(84)90407-X

Mizrahi, S. (1997). Irreversible shear thinning and thickening of tomato juice. *Journal of Food Processing and Preservation, 21*(4), 267-277. doi: DOI 10.1111/j.1745-4549.1997.tb00782.x

Mueller, S., Llewellin, E. W., & Mader, H. M. (2010). The rheology of suspensions of solid particles. *Proceedings of the Royal Society a-Mathematical Physical and Engineering Sciences, 466*(2116), 1201-1228. doi: 10.1098/rspa.2009.0445

Reid, D., Kotte, K., Kalamaki, M., & Ibanez, M. (2006). The contribution of water removal to the phenomenon of "consistency loss" associated with juice concentrate products. 664.

Rickman, J. C., Barrett, D. M., & Bruhn, C. M. (2007). Nutritional comparison of fresh, frozen and canned fruits and vegetables. Part 1. Vitamins C and B and phenolic compounds. *Journal of the Science of Food and Agriculture, 87*(6), 930-944. doi: 10.1002/jsfa.2825

Sanchez, M. C., Valencia, C., Ciruelos, A., Latorre, A., & Gallegos, C. (2003). Rheological properties of tomato paste: Influence of the addition of tomato slurry. *Journal of Food Science, 68*(2), 551-554. doi: DOI 10.1111/j.1365-2621.2003.tb05710.x

Stokes, J. R., & Frith, W. J. (2008). Rheology of gelling and yielding soft matter systems. *Soft Matter, 4*(6), 1133-1140. doi: 10.1039/b719677f

Tanglertpaibul, T., & Rao, M. A. (1987a). Flow Properties of Tomato Concentrates: Effect of Serum Viscosity and Pulp Content. *Journal of Food Science, 52*(2), 318-321. doi: 10.1111/j.1365-2621.1987.tb06602.x

Tanglertpaibul, T., & Rao, M. A. (1987b). Rheological Properties of Tomato Concentrates as Affected by Particle-Size and Methods of Concentration. *Journal of Food Science, 52*(1), 141-145. doi: DOI 10.1111/j.1365-2621.1987.tb13991.x

Thakur, B. R., Singh, R. K., & Nelson, P. E. (1996). Quality attributes of processed tomato products: A review. *Food Reviews International, 12*(3), 375-401.

Valencia, C, Sanchez, MC, Ciruelos, A, Latorre, A, Franco, JM, & Gallegos, C. (2002). Linear viscoelasticity of tomato sauce products: influence of previous tomato paste processing. *European Food Research and Technology, 214*(5), 394-399. doi: 10.1007/s00217-002-0501-6

Verlent, I., Hendrickx, M., Rovere, P., Moldenaers, P., & Van Loey, A. (2006). Rheological properties of tomato-based products after thermal and high-pressure treatment. *Journal of Food Science, 71*(3), S243-S248.

# CHAPTER 6. EFFECTS OF PARTICLE PROPERTIES ON RHEOLOGY OF TOMATO SUSPENSIONS

## 6.1 Introduction

Plant cell walls are complex composite materials made up by three main polysaccharides which can form cross-linking with different proteins and phenolic compounds (Carpita & Gibeaut, 1993), building structural systems that can control the mechanical properties that the plants need for their growth. Each component adds its functions to the individual cells or jointed tissues in terms of structural strength, rigidity, flexibility and porosity (Carpita & Gibeaut, 1993). The structural integrity and texture of cell wall material are mainly determined by its mechanical properties, cell adhesion and the internal turgor generated by osmosis (Jackman & Stanley, 1995; Waldron, Parker, & Smith, 2003). They also play a central role in the sensorial quality of foods derived from plant cell wall. Recently, the understanding of structure of plant cell wall material in relation to the textural properties of derived foods has become of research interest to both academia and industry given the importance of plants in human nutrition (Sankaran et al., 2015).

Pectin is a major cell wall component that can “glue” tomato cells together, so changes in pectin structure are crucial in determining the textural properties of tomato tissue (Christiaens et al., 2012). Cell wall pectin can be degraded via demethoxylation and depolymerization by both enzymatic and chemical conversion reactions (Vanburen, 1979). Pectin degradation due to PME enzymes can modify the cell wall structure by releasing the methyl groups from the pectin backbone at C-6 position during the ripening process (Errington, Tucker, & Mitchell, 1998). Genetic engineering of crops using recombinant technology has provided promising means to alter in vivo levels of these enzymes for creating “designer” pectin that promotes desired texture on processed tomato products (Thakur, Singh, & Handa, 1996; Thakur, Singh, Tieman, & Handa,

1996; Tieman, Harriman, Ramamohan, & Handa, 1992). Some studies have shown that reduction in PME activity exhibited remarkable improvements in various qualities of processed tomato products over wild type (Thakur, Singh, & Handa, 1996; Thakur, Singh, Tieman, et al., 1996; Tieman et al., 1992). However, few of them have assessed the changes on tissue structure and particle phases induced by genetic modified PME pectin, and therefore its relation to the textural properties.

To understand the effects of the tomato particles on the rheology of suspensions containing these particles, many studies were conducted via bulk characterization. However, results are still inconclusive concerning the effects of the particle properties. Studies at the individual particle level are needed for better understanding such systems. Atomic force microscopy (AFM) has been used to study tomato plant cell wall material. However, the majority of these studies have focused on imaging the structure of pectin molecules isolated from tomato tissue (Kirby, MacDougall, & Morris, 2008; Round, Rigby, MacDougall, & Morris, 2010; Round, Rigby, MacDougall, Ring, & Morris, 2001). Recently, AFM has been proposed for studying the mechanical properties of single particles in colloidal system even including biological cells (Mahaffy, Park, Gerde, Kas, & Shih, 2004; Radmacher, Fritz, Kacher, Cleveland, & Hansma, 1996). The Young's modulus of the particles can be obtained by fitting the force-indentation curve to the Hertz model.

In this chapter, the effects of reduced PME activity on the cell wall tissue and particle structure were discussed. The viscoelastic properties of the particle phase were also characterized in bulk. Furthermore, an AFM based approach was developed to study the mechanical properties of individual particle and therefore to determine their influence on bulk rheology. These studies explored the functions of tomato particles on the rheology of these systems considering both bulk

and individual scales. It is expected that the gained knowledge will provide a comprehensive understanding of these systems.

## 6.2 Materials and Methods

### 6.2.1 Materials

#### 6.2.1.1 Tomato Transgenic Lines and Sample preparation

Selected tomato transgenic lines of Ohio 8245 cultivar with PME activity ranging from 12% to 100% of the wild type tomato were grown in a controlled greenhouse environment at Purdue University (West Lafayette, IN) during the spring of 2014. The transgenic tomato fruits were denoted by their PME activity (Table 1.1). Fully ripened tomato fruits (twelve days after breaker stage) were collected and then processed into suspensions. Fresh fruits were washed and placed into boiling water for 15 s. This short blanching procedure was aimed to remove the skin without cooking the tomato flesh. The fruits were then cut into 2 cm pieces followed by a gentle blending process using a household food processor (Ninja Englewood NJ100Express Chopper, MA, USA) for 30 s. Then, samples were transferred into a cranking food mill with 1/16" screen in order to remove the seeds. The samples were collected for further analyses.

#### 6.2.1.2 Samples for AFM Measurements

HB and CB samples from Red Gold Inc. (Elwood, Indiana facility) were chosen for AFM measurements. Information of these samples was given in Chapter 7.

### 6.2.2 General Properties

The precipitate weight ratio was measured as per Takada and Nelson (1983). Approximately 50 g suspensions made from transgenic lines were centrifuged at 12,800 *g* at 4 ℃ for 30 min (Beckman AvantiTM J-251 centrifuge, Beckman Coulter Inc., Fullerton, CA). The

pulp was collected for cryo-SEM and SAOS measurements. The precipitate weight ratio was calculated as the ratio of the weight of pulp (wet) to the weight of suspension.

The moisture contents of pulp were determined by a vacuum oven method, described in Chapter 5.

### 6.2.3 Cryo-Scanning Electron Microscopy

Cryo SEM (Nova NanoSEM, Hillsborough, Oregon, USA) at temperatures in the range −100 to −140 ℃ at a voltage of 3.0 kV was used to analyze the microstructure of transgenic tomato particles. The procedure was described in detail in Chapter 4. Pore size of the samples from the cryo-SEM images was analyzed using ImageJ.

### 6.2.4 Viscoelasticity of the Transgenic Tomato Pulp

Viscoelasticity measurements were carried out on a stress controlled rheometer (ARG2; TA Instruments, DE, USA) using a parallel plate geometry with a diameter of 40 mm. A same pre-shear procedure was performed on each sample following the method described in Chapter 3. A strain sweep from 0.1 to 100% (strain %) was performed at a constant frequency of 1 Hz to determine the linear viscoelastic region (LVR) of the samples. The Small Amplitude Oscillatory Shear (SAOS) test was then carried out using a frequency sweep from 0.05 to 100 Hz at a constant strain of 0.1%, which was in the LVR. All measurements were performed at least in triplicate at a constant temperature of 25 ℃.

### 6.2.5 AFM Measurements for Individual Particles

#### 6.2.5.1 Mica Surface Chemical Modification

To make mica surface positively charged, it was modified with 3-Aminopropyl triethoxysilane (APTES, Aldrich 440140). The reaction is shown schematically in Figure 6.1.

Ten mica sheets (Ted Pella, Redding, CA ) were well dispersed in 75mL toluene (Fisher) in a three-neck flask. The water residue was removed by azeotropic distillation in toluene under a nitrogen atmosphere. Subsequently, 0.1 mL of APTES was dropwisely added. The mica sheets were then refluxed overnight in the reaction mixture under nitrogen atmosphere. The APTES functionalized mica sheets were separated and were washed with toluene three times. The obtained APTES functionalized mica sheets were dried under a vacuum oven overnight. The amino groups becomes positively charged in a wide range of pH after exposure to the water solution, which would adhere strongly to tomato cells having negative charges due to the pectin residues.

#### 6.2.5.2 Sample Preparation for AFM

Selected HB and CB samples were diluted 10 times using ultrapure water. 50 μL of the suspension samples were then deposited on the surface of the modified mica fixed to a glass slide. An air flow was used to help drying the sample, and the samples were stored overnight in a desiccator for use the following day.

#### 6.2.5.3 AFM Force Measurements

Force measurements were performed with a MFP-3D AFM (Asylum Research, Santa Barbara, CA). The interaction force was detected using a triangular silicon nitride probe with a pyramid tip (SiNi, gold/chromium coating, 0.06 N/m force constant, 10 kHz resonant frequency, Innovative Solutions Bulgaria Ltd, Sofia, Bulgaria). AFM was conducted in contact force mode and the environmental vibrations were minimized by use of a vibration table (Herzan TS-150, Laguna Hills, CA).

Before testing, InvOLS (Inverse Optical Lever Sensitivity), virtual deflection, and cantilever spring constant were calibrated according to the protocol reported by Thomas,

Burnham, Camesano, and Wen (2013). Calibration in liquid was also conducted for the InvOLS and virtual deflection due to the cantilever sensitivity in the liquid environment. A thermal-tune method was used for the calibration of spring constant. After the glass slide was loaded and secured onto the AFM stage, a small drop of ultrapure water (50 μL) was applied to the mica as well as the tip of the AFM cantilever. The AFM head was then lowered until the tip was immersed in the water drop. The top-view camera was used to position the cantilever above the selected individual particle.

The force-indentation measurements were performed using the following setting: force distance 1 to 5 μm, scan rate 0.1 to 0.5 Hz and velocity 1 to 5 μm/s. The force curves were obtained as the tip was moved toward and away from the particle surface. Young's modulus was calculated by fitting the force-indentation data to the Hertz model. At least 20 points were chose for each sample for the single force-indentation measurements. Force-map mode was applied to illustrate the overall distribution of stiffness of a single particle. The settings of the indentation parameters were the similar as those chosen for single force measurement. The data analysis was carried out using Asylum Research software (IGOR Pro Platform, Asylum Research, Santa Barbara, CA).

## 6.3 Results and Discussion

### 6.3.1 Moisture Distributions of the Transgenic Tomato Suspensions

The precipitate weight ratio of the suspensions is presented in Table 6.2. As PME activity decreased, the precipitate weight ratio showed an increasing trend, with 212 (lowest PME activity, 12%) had a significant higher ratio than that of OWT (PME activity, 100%). Higher precipitate weight ratio usually associates with a higher consistency of the product (Takada & Nelson, 1983), so the transgenic lines are expected to have a higher viscosity than that of OWT.

It has been reported that 85-90% reduction in PME activity in transgenic fruits displayed a maximum increase in juice and serum viscosity, and precipitate weight ratio (Takada & Nelson, 1983; Thakur, Singh, Tieman, et al., 1996). No heat and intense shear were involved in the sample preparation, so the differences between the transgenic lines are mainly caused by the plant tissue structures modified by PME. Generally, hot-break and cold-break tomato suspensions from industrial processing have a precipitate weight ratio of 8-12% using the same centrifugation process (Chapter 7), which is much lower than the values obtained in this work. It could be explained by the fact that the tissue structures are altered significantly by industrial processing, mainly due to the presence of high temperature and shear. These conditions greatly soften and disrupt the cell wall membrane (Van Buggenhout, Sila, Duvetter, Van Loey, & Hendrickx, 2009), which leads to a lower precipitate ratio. The moisture content in the pulp is also reported in Table 6.2. The value ranged from 90 to 93% and a non-obvious trend was found in these transgenic lines.

Moisture distributions of the transgenic samples are calculated and compared in Figure 6.2. Transgenic line 212 contained considerably higher dry solid content (2.8%) than other lines (~1.8%). More notably, all transgenic tomatoes exhibited higher water holding capacity of pulps. For instance, Line 212 pulp structure can capture moisture which accounted for 26.8% of the total suspension weight; whereas for OWT it was only 16.0%. This result indicates the microstructures of tissue are significantly affected by the various PME activities. PME catalyzes the specific hydrolysis of the C-6 methyl ester bond of GalA residues, releasing methanol and creating negatively charged carboxyl groups (Sila et al., 2009). The demethylated pectin is a preferred substrate for polygalacturonase (PG), which causes pectin further depolymerization and solubilization, and consequently changes the tissue structure (Moelants et al., 2013).

Demethylated pectin also resists β-elimination, a chemical conversion that depolymerizes pectin. However, this reaction usually occurs at high temperature (>80 °C). Therefore, pectin enzymatic conversions (PME and PG) are responsible for the changes of tissue structure. A higher PME activity (i.e. OWT) indicates a higher pectin degradation rate, and therefore a weaker tissue structure and water holding capacity. Pulps of transgenic tomatoes with low PME activity can hold water so well that it can prevent serum separation, a phenomenon that commonly occurs in juice and sauce products. Thakur, Singh, Tieman, et al. (1996) reported that tomato ketchup made from tomatoes with low PME activity exhibited significant improvements in quality attributes, with lowed serum separation compared to products obtained from tomatoes with high PME activity.

### 6.3.2 Microstructure of the Transgenic Tomato Particles

The particles of transgenic tomatoes were studied with cryo-SEM to determine the effect of PME activity on the microstructures of cell wall tissue. During cryo-SEM measurements, the freezing process would extract water from the surroundings and leave a concentrated mass of material shown as a network structure (Lopez-Sanchez et al., 2011). A lot of intact cells (black arrow) are still observed in the image with a magnification of 3000 X (Figure 6.3 left), probably due to the mild processing used in the sample preparation. Some cells were broken and merged together resulting in a bigger pore size (indicated by the red arrow). From the image with a magnification of 10000 X (Figure 6.3 right), the fine structure of middle lamella was clearly seen (black arrow). These areas are rich in a pectin matrix, which determines cell to cell adhesion and therefore contributes to the firmness and elasticity of the tissue (Fuchigami, 1987). The hairy structure in the middle lamella was probably structural pectin bonding neighboring cells together. These structures are critical to the texture of tissue and rheology of derived products. The cells

would become loosely attached as the pectin structures are degraded by enzymatic activity or processing (red arrow). The cell wall weakening is also the consequence of such effects. As cell wall strength is lost, cells tended to rupture under the action of external stresses, and they are observed as cells having bigger pore sizes. This structure is denoted by a red arrow shown in Figure 6.3 left.

The microstructures of transgenic tomato particles varied according to the PME activity of tomatoes and they are presented in Figure 6.4 (upper row). Plant cells from low PME lines were closely packed together and showed small pore sizes, while the tissue from high PME lines were greatly disrupted and exhibited large pore sizes formed by non-intact cells. Thermal and mechanical processes applied usually affect the microstructure of plant cell wall tissue. Homogenized samples have been identified to have more cell fragments due to disruption compared to non-homogenized samples (Lopez-Sanchez et al., 2011). In the present study, the treatments applied to the samples were the same for all transgenic tomato lines. Therefore, the differences in microstructure solely depend on the mechanical strength of cell walls, which can be weakened by PME activity. Cells with less strength are vulnerable to the applied processing, and they could rupture easily and resulting in tissues with bigger pore sizes. The pore sizes of the samples were calculated using ImageJ and can be compared in Figure 6.4 (lower row). The threshold was set as 20 $\mu m^2$ with an upper limit of 200 $\mu m^2$, so only the pore size falling into the range from 20 to 200 $\mu m^2$ was counted by ImageJ. As shown in Figure 6.5, there were more pores counted by ImageJ in the low PME activity samples, for instance transgenic line 212 and 253. While for high PME samples such as 263 and OWT, the cells were disrupted resulting in bigger pore sizes due to the weak cell wall strength. Since some of those pores size exceeded 200 $\mu m^2$, fewer pores were counted. The average pore sizes of cell wall of transgenic tomato lines

were further compared and also illustrated in Figure 6.5. As PME activity increased, the pore size of the tissue showed an increasing trend. Because many pores were formed by different numbers of disrupted cells (two or more) instead of uniformed single cells, the variations were relatively large. It should be noted that many pores larger than 200 $\mu m^2$ were not counted, which is mostly present in transgenic lines with high PME activity. The results indicate transgenic tomatoes with 85-90% reduced PME activity (i.e. lines 212 and 253) have cell wall structures with a stronger mechanical strength to resist intense processing, which explains the better water holding capacity described in section 6.3.1.

### 6.3.3 Viscoelasticity of Transgenic Tomato Pulps

Frequency sweep tests performed on tomato pulps are presented in Figure 6.6, which shows the viscoelastic properties of transgenic tomato pulps have very significant differences. G' values were higher than G" values in the applied frequency range, indicating a dominant solid-like behavior; i.e., a weak gel structure, which is a typical rheological behavior of concentrated fruit and vegetable suspensions (Day, Xu, Oiseth, Hemar, & Lundin, 2010; Day, Xu, Oiseth, Lundin, & Hemar, 2010). Both G' and G" of transgenic pulps showed an increasing trend with PME activity. For instance, OWT exhibited higher values than that of transgenic line 212. Higher G' and G" indicate that particles are relatively more rigid in nature. It has been reported that the viscoelastic properties of suspensions is significantly increased by increasing the solid content of the suspensions (Espinosa-Munoz, Renard, Symoneaux, Biau, & Cuvelier, 2013). However in the present study the solid content (wet %) decreased as PME activity increased, which appears to be contradictory to the viscoelasticity results. An explanation for these results is that differences in particle properties (i.e. mechanical strength) caused by PME activity are responsible for these measured viscoelastic properties. Figure 6.7 shows that liquid is squeezed

out from the OWT pulp (PME activity 100%) during the test, which indicates it has less water holding capacity compared to the pulps obtained from low PME activity tomatoes. As a result of the water syneresis, the particles in the pulp become more concentrated and therefore the measured G' and G" correspondingly increase. Conversely, pulps with low PME activities (i.e. 212 and 253) have stronger and relatively intact cell walls, and therefore no liquid is exuded which is leading to an apparently lesser measured viscoelasticity in these pulps.

The viscoelastic properties of tomato products have been investigated in many studies (Bayod, Mansson, Innings, Bergenstahl, & Tornberg, 2007; Bayod, Willers, & Tornberg, 2008; Lopez-Sanchez et al., 2011; Redgwell, Curti, & Gehin-Delval, 2008). However, most of these studies were focused on the viscoelastic property of concentrated tomato suspensions instead of tomato pulps centrifuged from suspensions. The viscoelastic characteristics of the tomato cell wall structure can be greatly influenced by the thermal input, mechanical forces, and enzymatic activities (Lopez-Sanchez et al., 2011). Although there are artifacts in the viscoelastic measurements of high PME pulps, the data clearly shows that PME activity has a significant impact on the particle structure as well as the rheological behavior of suspensions containing those particles. Further studies are needed to explain the correlation between those two.

### 6.3.4 Mechanical Properties of Individual Particles

The mechanical properties of individual tomato particles were determined by AFM. Figure 6.8 illustrates a typical plot of the test in which the interaction force between the cantilever tip and an individual particle is presented as a function of the sample indentation. The cantilever approaches the particle from point a, approximately 2 μm above the sample. Until the tip contacts the particle at point b, the interaction force remains zero. After that, the tip continues indenting the particle until the cantilever deflection reaches a set value at point c. Then the

cantilever retracts from the maximum deformation point to the point d (contact point), where it often pulled downwards due to tip-particle adhesion (Thomas et al., 2013). As the tip further withdraws from point d to the original starting point e, the force measured returns to zero. Hysteresis was observed between the extending and retracting curves, which is characteristic of viscoelastic deformable systems (G. Gillies, Prestidge, & Attard, 2002; Graeme Gillies & Prestidge, 2004). It indicates a relaxation time required to recover the particle's original position. The area inside the hysteresis loop demonstrates the energy dissipated during the testing. According to Bremmell, Evans, and Prestidge (2006), the area of hysteresis increased with drive velocity from 0.6 to 2.8 μm/s, explained by the limited time for relaxation at the faster approach rates. They also claimed that hydrodynamic effects were not the cause for the observed hysteresis, which was in agreement with the study of oil droplet reported by Nespolo, Chan, Grieser, Hartley, and Stevens (2003) where the different velocities in the range 0.04 to 3.7 μm/s were applied. For biological samples, the drive velocity is usually set within the range of 1-10 μm/s to eliminate hydrodynamic effects (Thomas et al., 2013). In the present study, the drive velocity was set the same for all samples in the range of 1-5 μm/s to be able to compare e results.

The force acting between the tip and particle was calculated by the AFM software using the Hooke's law:

$$F = k \cdot D \tag{6.1}$$

where $F$ is interaction force, $k$ is the cantilever spring constant and $D$ is the deflection of the cantilever. The force ($F$) versus sample indentation ($\delta$) data in the linear range was fitted to the Hertz model:

$$F = \frac{2E \tan\theta}{\pi(1-v^2)}\delta^2 \tag{6.2}$$

where $E$ is Young's modulus; $\delta$ is sample deformation (i.e., indentation), $v$ is Poisson ratio, and $\theta$ is half cone angle (i.e. 35 °). Please note this is a modified equation for the pyramid tip used in the present study.

$E$ was obtained by fitting the first 400 nm of the force-indentation curve to the Hertz model. The force response exhibited significant nonlinear viscoelastic behavior beyond 400 nm, where this model is not applicable. The Hertz model assumes linearly elastic material and is widely used to characterize elastic response of bio-materials (Alonso & Goldmann, 2003; Casademunt, 2001). In the present study, 20 single force measurements were performed evenly in a 40 μm by 40 μm area of a single particle surface. However, due to large particle size (i.e. ~250 μm) and the heterogeneous nature of the particle, the variation of fitted $E$ was considerable large. Therefore, AFM force-mapping was carried out and a typical stiffness map is presented in Figure 6.9. The local Young's modulus varied from values less than 100 Pa to values around 30 kPa, which is similar to the values measured on of most biological tissues and cells. Solon, Levental, Sengupta, Georges, and Janmey (2007) reported that the stiffness of fibroblasts determined by AFM was between 500 Pa and 40 kPa. It should be noted that the elastic response of particle depends on the tip velocity. Particle exhibits elastic behavior at short time scale while it shows viscus behavior at long time scale. Thus, the difference in Young's modulus is only meaningful and comparable when the data are obtained by the same tip velocity (Thomas et al., 2013).

To compare the Young's modulus distribution of HB and CB particles, the local Young's modulus was extract from AFM force map and presented in the histogram shown in Figure 6.10.

The median values of the Young's modulus were obtained by fitting the histogram using Gaussian function. The HB particle had a median Young's modulus of 14.1 kPa, which was significantly higher than that of CB particle (1.4 kPa). The HB particle also showed a wider distribution of Young modulus than the CB particles. This result is the first one to show the difference between HB and CB treatment on individual particles. Thus, the mechanical properties of individual particles seem to explain differences observed from bulk rheology measurements on suspensions. It confirms that the rheological difference between HB and CB originates from observed particles.

## 6.4 Conclusions

In this study the effects of tomatoes variety with reduced PME activity on the cell wall microstructure and the viscoelastic properties of the particle phase on tomato suspensions were investigated. As PME activity decreased, the precipitate weight ratio of the produced suspensions increased. Suppression of PME activity resulted in pulps with higher water holding capacity. Cryo-SEM imaging showed that cell wall tissues with 85-90% reduction of the PME activity were closely packed together and exhibited a smaller pore size compared to the tissue of commercially used tomatoes (OWT type). This was explained by a lower structural pectin degradation rate due to reduced PME activity, which contributed to the generation of cell wall particles with stronger mechanical strength. Conversely due to poor water holding capacity, serum separation was observed in pulps of tomato varieties having high PME activity (i.e. OWT), which was clearly visible during rheological measurement. As discussed, serum phase separation promoted serious artifacts on the rheological characterization of tomato suspensions. Furthermore, it led to an apparently higher viscoelastic behavior of the pulps, even though the solid content of OWT pulps was much lower than those of pulps prepared with tomato varieties

having lower PME activity. These results demonstrate that an 85-90% reduction in PME activity significantly strengthens the microstructures of cell wall particles, and therefore could improve the rheological properties of tomato suspensions and thus their quality.

In addition, the mechanical properties of individual HB and CB particles were studied by Atomic Force Microscopy. Measured local Young's modulus varied across individual particles and fell within the range of 0.1 kPa to 30 kPa. HB particles exhibited a higher average Young's modulus as well as a wider modulus distribution than the CB particles. Young's modulus values obtained from individual particles were related to the bulk rheology of the suspensions. Results of this chapter allowed to conclude that the differences between the rheological properties of HB and CB samples are mainly originated from differences in the mechanical properties of the particles.

## 6.5 Figures and Tables

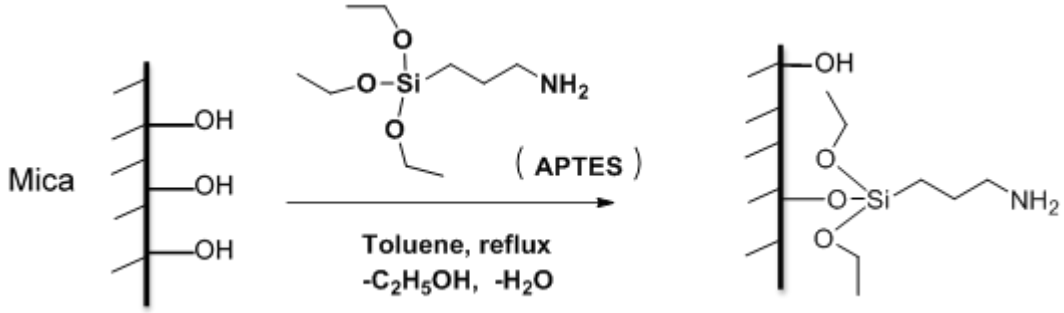


Figure 6.1 Schematic plot of mica surface modification.

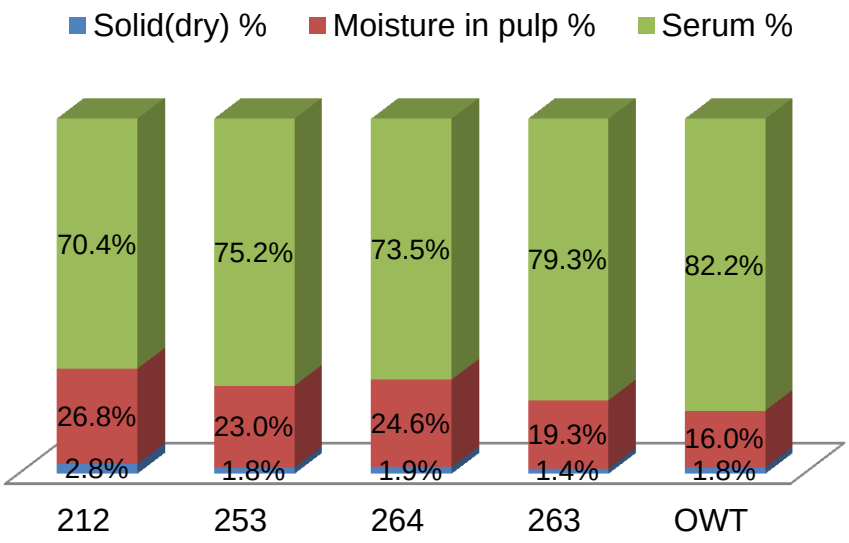


Figure 6.2 Moisture distributions of transgenic tomato suspension samples.

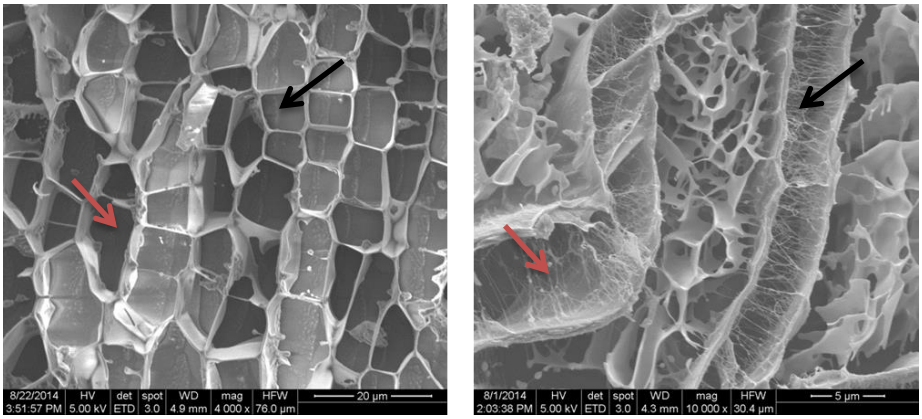

Figure 6.3 Microstructure of tomato cell wall tissues. Left: Intact cells (indicated with black arrow) and broken cells (indicated with red arrow) can be observed in the image with a magnification of 3000 X. Right: A hairy structure of pectin in the middle lamella (indicated with black arrow) image was observed with a magnification of 10000 X. The cells were ready to detach as the pectin structures were degraded by enzymatic activity or processing (indicated with red arrow).

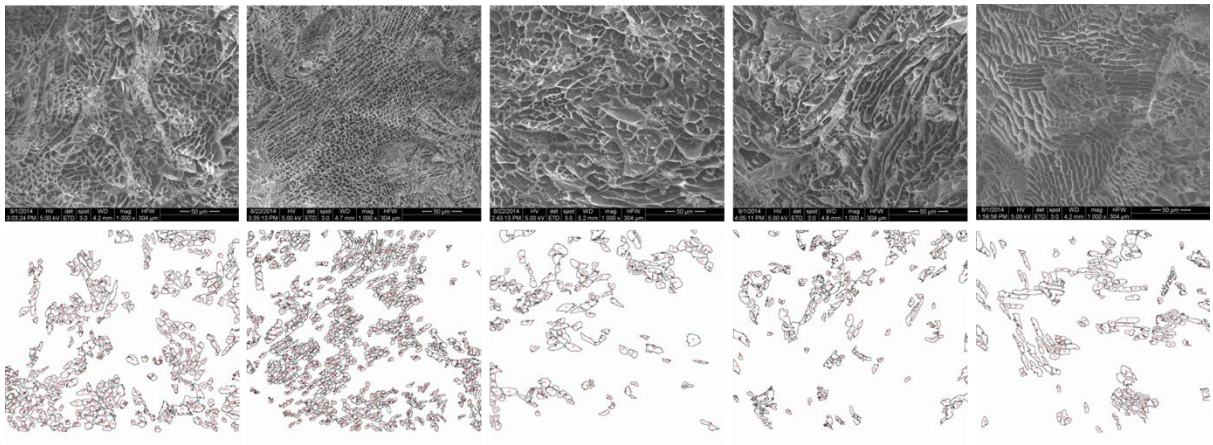

Figure 6.4 Cryo-SEM images of transgenic tomato particle tissues having different PME activities (upper row) and the pores extracted from the images using ImageJ (lower row). The images have a magnification of 1000 X, and the samples from left to right are 212, 253, 264, 263, OWT. Pores were formed by intact or non-intact cells depending on the mechanical strength of cells.

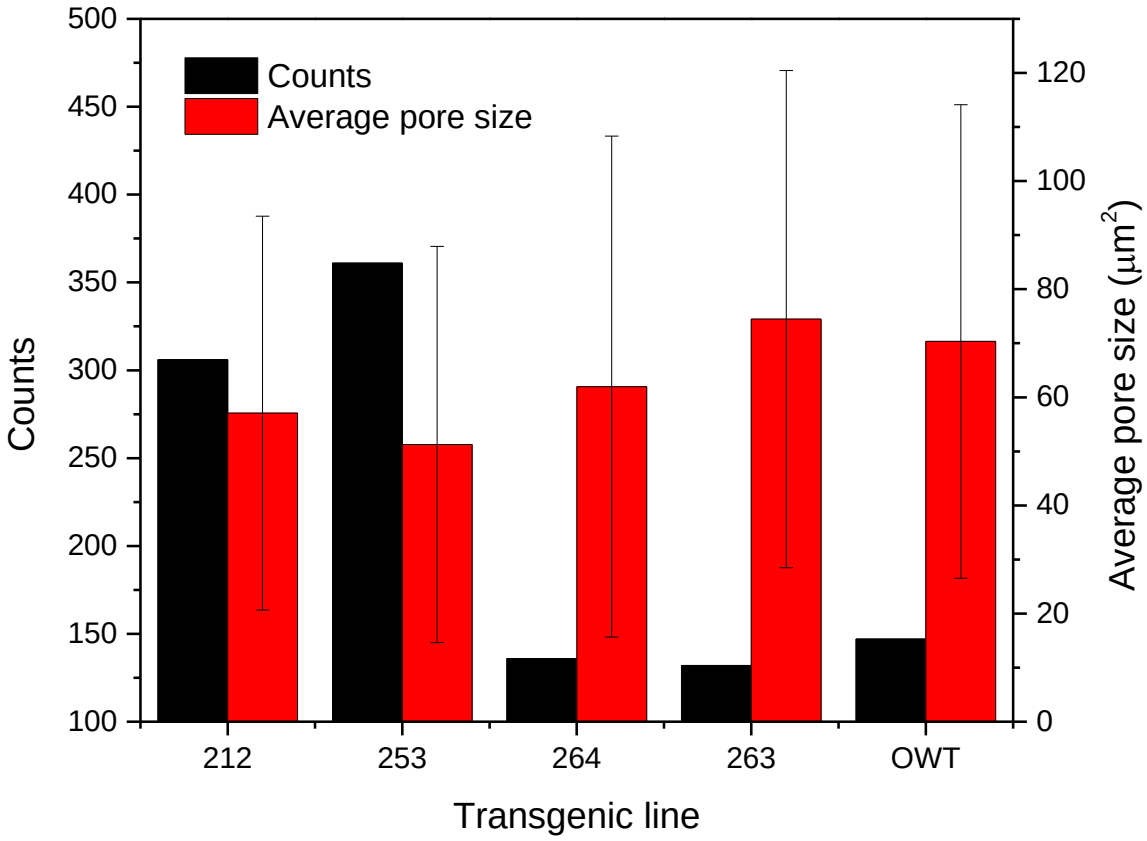


Figure 6.5 Pore counts between 20-200 $\mu m^2$ and average pore size comparisons between transgenic tomato particles. The image process and calculation were done by ImageJ on the images of 1000 X magnification.

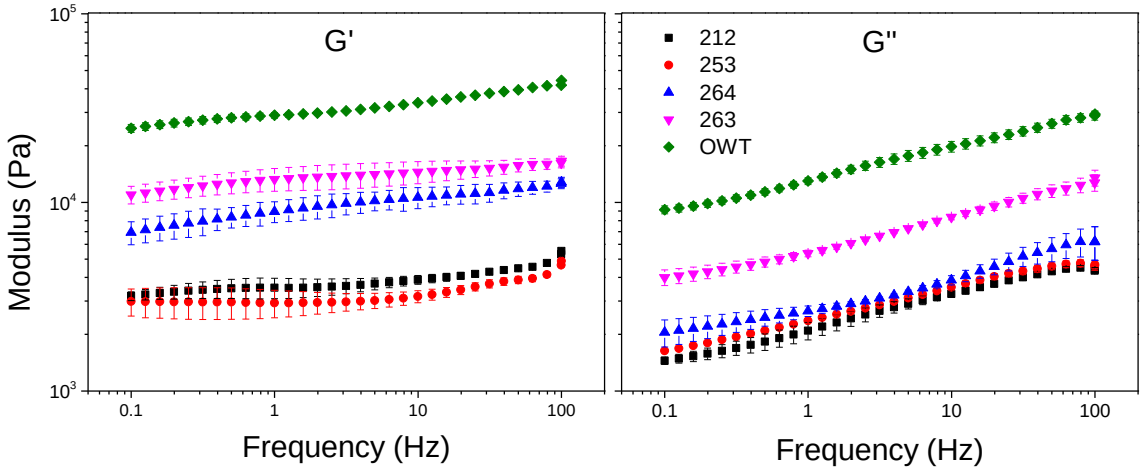


Figure 6.6 Frequency sweep tests of transgenic tomato pulps. The SAOS test was carried in a range of frequencies from 0.1 to 100 Hz at a constant strain of 0.1%. Left plot: Storage modulus G'; right plot: Loss modulus G".


Figure 6.7 Pictures of tomato pulps taken during viscoelastic measurements. Left: 212; right: OWT. The pulps show different water holding capacities. Transgenic line 212 pulp can hold water well, whereas the water is easily squeezed out from OWT pulp during testing (see arrow).

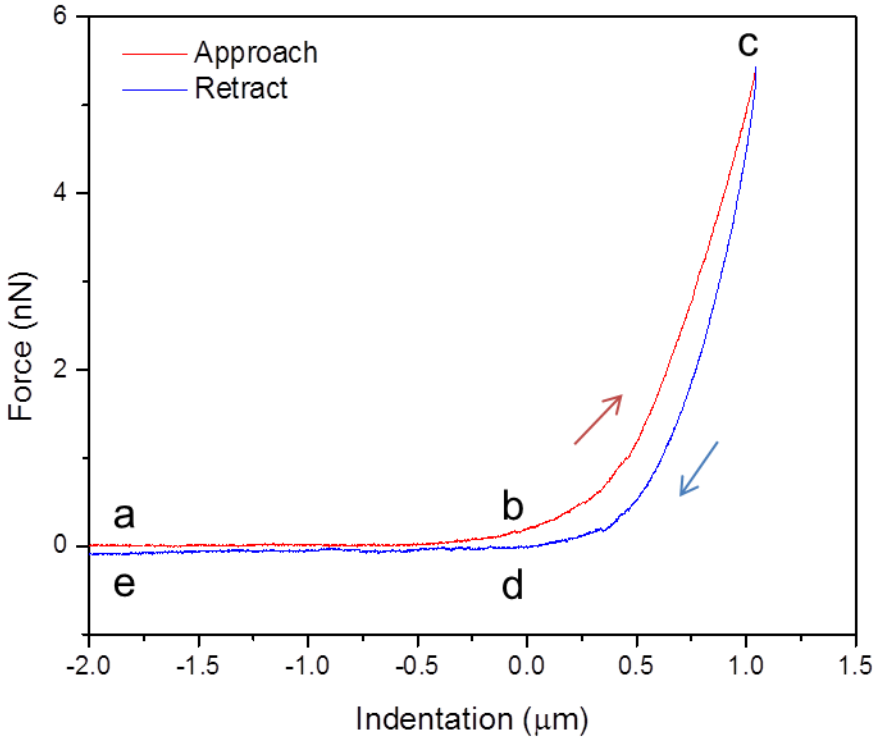


Figure 6.8 Representative force-indentation curves between cantilever tip and individual particle. The first 400 nm of extending curve date was fitted to the Hertz model to extract the Young's modulus.

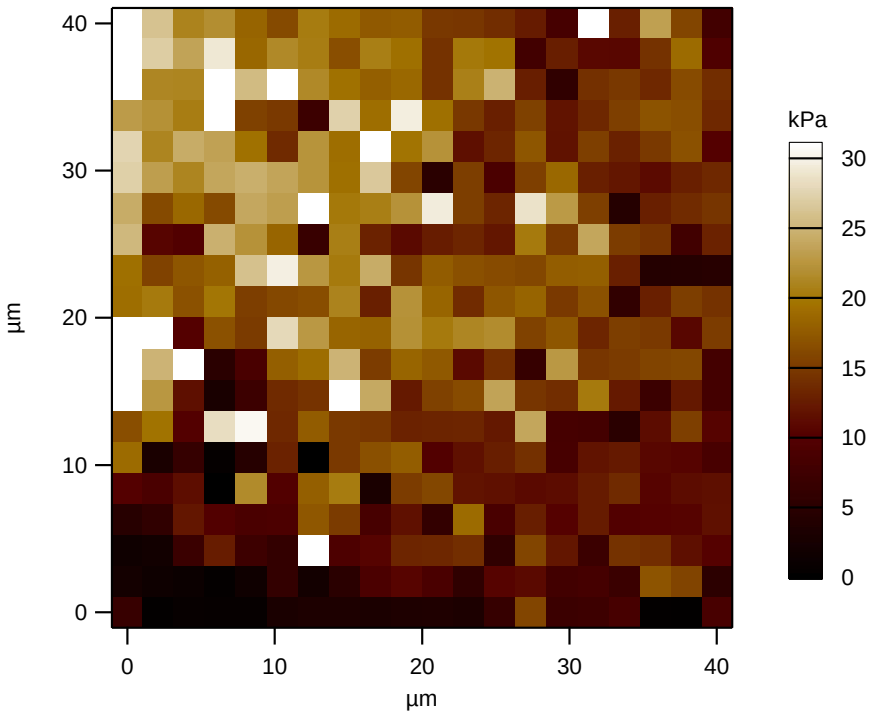


Figure 6.9 Reprehensive stiffness map of individual particles. Force-mapping was performed in a 40 µm by 40 µm area.

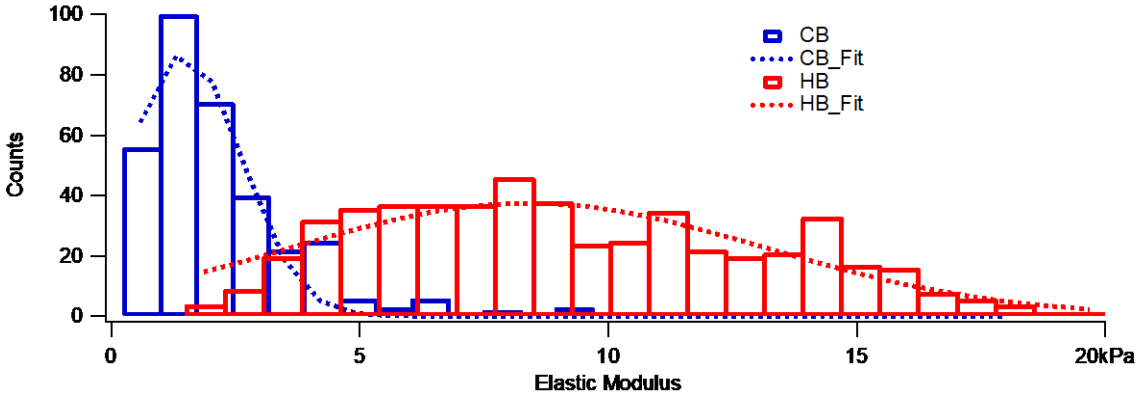


Figure 6.10 Young's modulus distribution of HB and CB particles. Dash lines represent Gaussian fit.

Table 6.1 Tomato transgenic line naming and its PME activity

| Transgenic line name | 212 | 253 | 264 | 263 | OWT |
|---|---|---|---|---|---|
| PME activity | 12% | 13% | 21% | 100% | 100% |

Table 6.2 Precipitate weight ratio and the moisture content of pulp in transgenic tomatoes

| Sample (PME activity) | 212 (12%) | 253 (13%) | 264(21%) | 263(100%) | OWT (100%) |
|---|---|---|---|---|---|
| Precipitate weight ratio (%) | 29.6±1.2 | 24.8±1.5 | 26.5±1.2 | 20.7±1.0 | 17.8±1.3 |
| Moisture content of pulp (%) | 90.6±0.0 | 92.9±0.2 | 93.0±0.1 | 93.1±0.1 | 90.0±0.1 |

## 6.6 References

Alonso, J. L., & Goldmann, W. H. (2003). Feeling the forces: atomic force microscopy in cell biology. *Life Sciences, 72*(23), 2553-2560. doi: 10.1016/S0024-3205(03)00165-6

Bayod, E, Mansson, P, Innings, F, Bergenstahl, B, & Tornberg, E. (2007). Low shear rheology of concentrated tomato products. Effect of particle size and time. *Food Biophysics, 2*(4), 146-157. doi: 10.1007/s11483-007-9039-2

Bayod, E, Willers, EP, & Tornberg, E. (2008). Rheological and structural characterization of tomato paste and its influence on the quality of ketchup. *Lwt-Food Science and Technology, 41*(7), 1289-1300. doi: 10.1016/j.lwt.2007.08.011

Bremmell, K. E., Evans, A., & Prestidge, C. A. (2006). Deformation and nano-rheology of red blood cells: An AFM investigation. *Colloids and Surfaces B-Biointerfaces, 50*(1), 43-48. doi: 10.1016/j.colsurfb.2006.03.002

Carpita, N. C., & Gibeaut, D. M. (1993). Structural Models of Primary-Cell Walls in Flowering Plants - Consistency of Molecular-Structure with the Physical-Properties of the Walls during Growth. *Plant Journal, 3*(1), 1-30. doi: DOI 10.1111/j.1365-313X.1993.tb00007.x

Casademunt, J.A. (2001). *Micromechanics of Cultured Human Bronchial Epithelial Cell Measured with Atomic Force Microscopy*. Universitat de Barcelona. Departament de Ciències Fisiològiques I. Retrieved from https://books.google.com/books?id=6d64MwEACAAJ

Christiaens, S., Van Buggenhout, S., Chaula, D., Moelants, K., David, C. C., Hofkens, J., Hendrickx, M. E. (2012). In situ pectin engineering as a tool to tailor the consistency and syneresis of carrot puree. *Food Chemistry, 133*(1), 146-155. doi: 10.1016/j.foodchem.2012.01.009

Day, L., Xu, M., Oiseth, S. K., Hemar, Y., & Lundin, L. (2010). Control of Morphological and Rheological Properties of Carrot Cell Wall Particle Dispersions through Processing. *Food and Bioprocess Technology, 3*(6), 928-934. doi: DOI 10.1007/s11947-010-0346-0

Day, L., Xu, M., Oiseth, S. K., Lundin, L., & Hemar, Y. (2010). Dynamic rheological properties of plant cell-wall particle dispersions. *Colloids and Surfaces B-Biointerfaces, 81*(2), 461-467. doi: 10.1016/j.colsurfb.2010.07.041

Errington, N., Tucker, G. A., & Mitchell, J. R. (1998). Effect of genetic down-regulation of polygalacturonase and pectin esterase activity on rheology and composition of tomato juice. *Journal of the Science of Food and Agriculture, 76*(4), 515-519. doi: Doi 10.1002/(Sici)1097-0010(199804)76:4<515::Aid-Jsfa979>3.0.Co;2-X

Espinosa-Munoz, L., Renard, C. M. G. C., Symoneaux, R., Biau, N., & Cuvelier, G. (2013). Structural parameters that determine the rheological properties of apple puree. *Journal of Food Engineering, 119*(3), 619-626. doi: DOI 10.1016/j.jfoodeng.2013.06.014

Fuchigami, M. (1987). Relationship between Pectic Compositions and the Softening of the Texture of Japanese Radish Roots during Cooking. *Journal of Food Science, 52*(5), 1317-1320. doi: DOI 10.1111/j.1365-2621.1987.tb14072.x

Gillies, G., Prestidge, C. A., & Attard, P. (2002). An AFM study of the deformation and nanorheology of cross-linked PDMS droplets. *Langmuir, 18*(5), 1674-1679. doi: 10.1021/la011461g

Gillies, Graeme, & Prestidge, Clive A. (2004). Interaction forces, deformation and nano-rheology of emulsion droplets as determined by colloid probe AFM. *Advances in Colloid and Interface Science, 108-109*(Supplement C), 197-205. doi: https://doi.org/10.1016/j.cis.2003.10.007

Jackman, R. L., & Stanley, D. W. (1995). Perspectives in the Textural Evaluation of Plant Foods. *Trends in Food Science & Technology, 6*(6), 187-194. doi: Doi 10.1016/S0924-2244(00)89053-6

Kirby, A. R., MacDougall, A. J., & Morris, V. J. (2008). Atomic force microscopy of tomato and sugar beet pectin molecules. *Carbohydrate Polymers, 71*(4), 640-647. doi: 10.1016/j.carbpol.2007.07.014

Lopez-Sanchez, P., Nijsse, J., Blonk, H. C. G., Bialek, L., Schumm, S., & Langton, M. (2011). Effect of mechanical and thermal treatments on the microstructure and rheological properties of carrot, broccoli and tomato dispersions. *Journal of the Science of Food and Agriculture, 91*(2), 207-217. doi: Doi 10.1002/Jsfa.4168

Mahaffy, R. E., Park, S., Gerde, E., Kas, J., & Shih, C. K. (2004). Quantitative analysis of the viscoelastic properties of thin regions of fibroblasts using atomic force microscopy. *Biophysical Journal, 86*(3), 1777-1793. doi: Doi 10.1016/S0006-3495(04)74245-9

Moelants, K. R. N., Jolie, R. P., Palmers, S. K. J., Cardinaels, R., Christiaens, S., Van Buggenhout, S., Hendrickx, M. E. (2013). The Effects of Process-Induced Pectin Changes on the Viscosity of Carrot and Tomato Sera. *Food and Bioprocess Technology, 6*(10), 2870-2883. doi: 10.1007/s11947-012-1004-5

Nespolo, Sarah A., Chan, Derek Y. C., Grieser, Franz, Hartley, Patrick G., & Stevens, Geoffrey W. (2003). Forces between a Rigid Probe Particle and a Liquid Interface: Comparison between Experiment and Theory. *Langmuir, 19*(6), 2124-2133. doi: 10.1021/la0260638

Radmacher, M., Fritz, M., Kacher, C. M., Cleveland, J. P., & Hansma, P. K. (1996). Measuring the viscoelastic properties of human platelets with the atomic force microscope. *Biophysical Journal, 70*(1), 556-567.

Redgwell, RJ, Curti, D, & Gehin-Delval, C. (2008). Physicochemical properties of cell wall materials from apple, kiwifruit and tomato. *European Food Research and Technology, 227*(2), 607-618. doi: 10.1007/s00217-007-0762-1

Round, A. N., Rigby, N. M., MacDougall, A. J., & Morris, V. J. (2010). A new view of pectin structure revealed by acid hydrolysis and atomic force microscopy. *Carbohydrate Research, 345*(4), 487-497. doi: 10.1016/j.carres.2009.12.019

Round, A. N., Rigby, N. M., MacDougall, A. J., Ring, S. G., & Morris, V. J. (2001). Investigating the nature of branching in pectin by atomic force microscopy and carbohydrate analysis. *Carbohydrate Research, 331*(3), 337-342. doi: Doi 10.1016/S0008-6215(01)00039-8

Sankaran, A. K., Nijsse, J., Bialek, L., Bouwens, L., Hendrickx, M. E., & Van Loey, A. M. (2015). Effect of Enzyme Homogenization on the Physical Properties of Carrot Cell Wall Suspensions. *Food and Bioprocess Technology, 8*(6), 1377-1385. doi: 10.1007/s11947-015-1481-4

Sila, D. N., Van Buggenhout, S., Duvetter, T., Fraeye, I., De Roeck, A., Van Loey, A., & Hendrickx, M. (2009). Pectins in Processed Fruit and Vegetables: Part II - Structure-Function Relationships. *Comprehensive Reviews in Food Science and Food Safety, 8*(2), 86-104. doi: 10.1111/j.1541-4337.2009.00070.x

Solon, J., Levental, I., Sengupta, K., Georges, P. C., & Janmey, P. A. (2007). Fibroblast adaptation and stiffness matching to soft elastic substrates. *Biophysical Journal, 93*(12), 4453-4461. doi: 10.1529/biophysj.106.101386

Takada, N., & Nelson, P. E. (1983). A New Consistency Method for Tomato Products - the Precipitate Weight Ratio. *Journal of Food Science, 48*(5), 1460-1462. doi: DOI 10.1111/j.1365-2621.1983.tb03516.x

Thakur, B. R., Singh, R. K., & Handa, A. K. (1996). Effect of an antisense pectin methylesterase gene on the chemistry of pectin in tomato (Lycopersicon esculentum) juice. *Journal of Agricultural and Food Chemistry, 44*(2), 628-630. doi: Doi 10.1021/Jf950461h

Thakur, B. R., Singh, R. K., Tieman, D. M., & Handa, A. K. (1996). Tomato product quality from transgenic fruits with reduced pectin methylesterase. *Journal of Food Science, 61*(1), 85-&. doi: DOI 10.1111/j.1365-2621.1996.tb14731.x

Thomas, G., Burnham, N. A., Camesano, T. A., & Wen, Q. (2013). Measuring the Mechanical Properties of Living Cells Using Atomic Force Microscopy. *Jove-Journal of Visualized Experiments*(76). doi: UNSP e5049710.3791/50497

Tieman, D. M., Harriman, R. W., Ramamohan, G., & Handa, A. K. (1992). An Antisense Pectin Methylesterase Gene Alters Pectin Chemistry and Soluble Solids in Tomato Fruit. *Plant Cell, 4*(6), 667-679.

Van Buggenhout, S., Sila, D. N., Duvetter, T., Van Loey, A., & Hendrickx, M. (2009). Pectins in Processed Fruits and Vegetables: Part III - Texture Engineering. *Comprehensive Reviews in Food Science and Food Safety, 8*(2), 105-117. doi: 10.1111/j.1541-4337.2009.00071.x

Vanburen, J. P. (1979). Chemistry of Texture in Fruits and Vegetables. *Journal of Texture Studies, 10*(1), 1-23.

Waldron, K. W., Parker, M. L., & Smith, A. C. (2003). Plant Cell Walls and Food Quality. *Comprehensive Reviews in Food Science and Food Safety, 2*(4), 128-146. doi: 10.1111/j.1541-4337.2003.tb00019.x

# CHAPTER 7. FLOW BEHAVIOR OF INDUSTRIAL PROCESSING TOAMTO SUSPENSIONS

## 7.1 Introduction

About 80% tomatoes grown in the U.S. are processed before consumption (Rickman, Barrett, & Bruhn, 2007). Foods produced from tomatoes, such as tomato sauce, juice or ketchup, are mainly suspensions thermally processed and transported as fluids by pumping to other processing unit or storage. Industrial tomato processing begins with a "break" step, which plays vital role in determining the quality of final products (Nelson & Hoff, 1969). The main purposes of the "break" step are the partial or full inactivation of degradative enzymes, such as pectin methylesterase (PME) and polygalacturonase (PG), as well as the initial softening of tissues, which is associated with loss of turgor, due to plant cell membrane disruption (Greve, Shackel, et al., 1994). A low temperature break (cold break, CB; 60 to 77 ℃) yields fresher products, whereas a high temperature break (hot break, HB; around 90 ℃) is used for producing higher viscosity products. The HB process is believed to destroy most pectolytic enzyme activity (Van Buggenhout, Sila, Duvetter, Van Loey, & Hendrickx, 2009), thereby preserving the pectic matrix.

There has been a lot research on the influence of processing conditions on the rheological properties of tomato products (Anthon, Diaz, & Barrett, 2008; Bayod, Mansson, Innings, Bergenstahl, & Tornberg, 2007; Bayod & Tornberg, 2011; Diaz, Anthon, & Barrett, 2009; Sanchez, Valencia, Ciruelos, Latorre, & Gallegos, 2003; Sharma, LeMaguer, Liptay, & Poysa, 1996; C Valencia et al., 2002). However, many of them used concentrated tomato pastes that were further diluted for the studies. Some researchers used samples prepared in the lab which couldn't reflect the intensity of continuous shearing (e.g. extraction and pumping) during industrial processing (Lopez-Sanchez et al., 2011; Moelants, Cardinaels, Jolie, et al., 2014;

Tiback, Langton, Oliveira, & Ahrne, 2014). Lopez-Sanchez et al. (2011) reported that switching the order of thermal and homogenization treatments significantly changed the final viscosity and microstructures of plant cell wall particles. It has been reported that the viscosity of the processed product increases with the increase of temperature used in the break process (Gould, 1974, 1992; Hsu, 2008; Thakur, Singh, & Nelson, 1996). Many studies have attributed this behavior to the inactivation of the pectolytic enzymes by the HB process. However, recent research from our research group has shown that the break-down and solubilization of pectin is limited and has little effect on the product composition (Chong, Simsek, & Reuhs, 2009; Chong, Simsek, & Reuhs, 2014; B. C. Wu et al., In preparation), and therefore on viscosity.

This chapter focuses on industrially processed HB and CB tomatoes, which are systematically investigated in terms of their flow behavior under steady-state and small amplitude oscillatory strain (SAOS) tests. Temperature and time dependence of HB and CB samples are characterized and compared. The particle interaction and network properties are further evaluated by rheological methods. The obtained data is able to distinguish HB and CB materials in term of their flow properties, and their impact and potential usefulness for future industrial process design are discussed.

## 7.2 Materials and Methods

### 7.2.1 Materials

#### 7.2.1.1 HB and CB Samples

Tomato samples (suspensions) were supplied by Red Gold Inc. (Elwood, Indiana facility) during the growing season (August to October, 2017). The processing temperatures for HB and CB were 93.3 and 77.2 ℃ respectively. During the production of tomato samples, 25 kg of each

tomato product (HB and CB) were collected after production and were immediately transported to the laboratory in iced containers and stored in a cold room (4 ℃) for further analysis.

### 7.2.2 General Properties

#### 7.2.2.1 Precipitate Weight Ratio

The precipitate weight ratio was measured as described by Takada and Nelson (1983). Approximately 300 g the suspensions were centrifuged at 12,800*g* for 30 min at 4 ℃ in a laboratory centrifuge (Beckman AvantiTM J-251 centrifuge, Beckman Coulter Inc., Fullerton, CA) to separate serum and pulp. The pulp was stored at 4 ℃ for further measurements afterwards. The precipitate weight ratio was calculated as the ratio of the weight of pulp (wet) to the weight of the suspension.

#### 7.2.2.2 Moisture Content

The moisture contents were determined by a vacuum oven on both suspensions and pulps of the HB and the CB samples. About 5 g of samples were transferred to the pre-weighed drying foil dishes and dried for 12 hours at 60 ℃ in the vacuum oven. The total weight of dish and sample was recorded before and after drying. The moisture content or percent dry solids of the samples were determined.

#### 7.2.2.3 °Brix

The °Brix values of HB and CB samples were measured by an Abbe refractometer at room temperature. A drop of serum was placed on to the glass prism. The viewing field was adjusted to obtain the best definition for the light and dark areas, and the °Brix value was recorded.

#### 7.2.2.4 Bostwick Consistency

The Bostwick consistency was determined immediately upon the sample's arrival. The method was described in Chapter 3.

### 7.2.3 Rheology Measurements

To characterize rheological properties, both steady-state shear and SAOS experiments were performed. The rheological measurements were carried out on a stress controlled rheometer (ARG2; TA Instruments, DE, USA) using a vane geometry with a diameter of 28 mm and a height of 42 mm. To avoid effects on the sample structure and rheological results due to its loading, a pre-shearing step was applied at a shear rate of 100 $s^{-1}$ for 60 s followed by 2 min rest period prior to measurements (Moelants, Cardinaels, Jolie, et al., 2014). To avoid sample dehydration the sample cell was covered throughout the test; all measurements were performed in triplicate.

#### 7.2.3.1 Steady-state Shear Rheology

Steady-state shear tests were performed in a shear rate range 0.1-100 $s^{-1}$ at a constant temperature of 25 ℃. The flow curve was fitted by the power law model given by the following equation:

$$\tau = k\dot{\gamma}^n \tag{7.1}$$

where $\tau$ = shear stress (Pa), $k$ = consistency index ($Pa.s^n$), $\dot{\gamma}$ = shear rate ($s^{-1}$) and $n$ the flow index (-))

#### 7.2.3.2 Dynamic Oscillatory Shear Rheology

First, a strain sweep from 0.1 to 100% (strain%) was performed at a constant frequency of 1 Hz. The storage (G') and loss moduli (G'') were recorded to determine the linear viscoelastic

region (LVR) of the sample. A SAOS test was then carried out using a frequency sweep from 0.1 to 10 Hz at a constant strain of 0.1% (which was within the LVR).

### 7.2.4 Temperature Dependence of Viscosity

The viscosity was tested at 4 different temperatures: 20, 40, 60 and 80 ℃. A logarithmic decreasing shear rate protocol (100-0.1 $s^{-1}$) was applied according to Augusto et al. (2012). The rheological data was fitted by the Herschel-Bulkley model given by the following equation:

$$\tau = \tau_0 + k\dot{\gamma}^n \tag{7.2}$$

$\tau_0$ = yield stress (Pa), and other parameters are the same as in Equation 7.1.

To evaluate the effect of temperature on the viscosity, the consistency coefficient (*k*) was modeled by the Arrhenius-type equation:

$$k = A_0 \cdot \exp(\frac{B}{T}) \tag{7.3}$$

Where $A_0$ and B are fitting parameters and T is the absolute temperature (K).

### 7.2.5 Time Dependence of Viscosity

To study the time dependence of the rheological properties, viscosity was measured every 10 s at a constant shear rate of 50 $s^{-1}$. The shear lasted for 30 min and performed at 4 different temperatures: 20, 40, 60 and 80 ℃. This test used the same rheometer setting with the pre-shear protocol described in section 7.2.3. The viscosity data was fitted to the Stretched Exponential Equation which is a general time-dependent model for fluids (Barnes, 1997; Barua & Saha, 2016):

$$\eta(t) = \eta_i + (\eta_{in} - \eta_i)(1 - e^{-t/\lambda_s}) \tag{7.4}$$

where $\eta(t)$ is apparent viscosity, $t$ is time of shearing, $\eta_i$ is initial-time viscosity, $\eta_{in}$ is infinite-time viscosity, and $\lambda_s$ is a characteristic time.

### 7.2.6 Compression Experiment

Compression experiments were carried out on the same rheometer according to the method described by Sankaran et al. (2015). A parallel plate with 40 mm diameter was used for the measurements. After the sample was loaded onto the peltier plate, the geometry was lowered to the set gap of 1000 μm. The sample was subjected a pre-shear of 5 $s^{-1}$ for 60 s followed by 2 min rest period before all measurements. The normal force was recorded by applying a direct compressive strain on the suspension as the geometry was lowered to a gap of 100 μm at a speed of 10 μm/s. The peak force was obtained from the force-time plot. Tests were conducted in triplicate and average values are reported.

### 7.2.7 Effect of Solid Content on the Rheological Properties

Pulps obtained as described in the section 7.2.2.1 were used to prepare suspension samples using deionized distilled water as the solvent medium. The samples were prepared with a wide range of solid content from 0.5 to 6.0%. Steady-state shear (section 7.2.3.1) and SAOS (section 7.2.3.2) tests were carried out on these suspensions to determine the effect of solid content of the different pulps on the suspension rheological properties. The rheological parameters of the suspensions modeled with the power law and Adam's equations were determined and used to assess the effect of solid content on particle interaction and formed network in the suspension system.

## 7.3 Results and Discussion

### 7.3.1 General Product Properties of the HB and CB Samples

The general properties of tomato suspensions processed under HB and CB conditions are presented in Table 7.1. The precipitate weight ratio of the HB sample was 10.8% and significantly higher than that of the CB sample (8.5%). Higher values of the precipitate weight ratio translate into more viscous products (Takada & Nelson, 1983), so as expected results showed that the HB sample had a higher Bostwick consistency than the CB sample. The ° Brix values was also considerably higher in the HB sample when compared to those of the CB samples, which can be explained by a higher thermal solubilization of cell wall polysaccharides promoted at elevated temperatures. Although the two samples showed no difference in moisture content in the suspension and the serum, significant higher moisture content in pulp was observed in the pulp of the HB sample.

Based on values reported in Table 7.1, moisture distribution of the samples were further determined and are compared in Figure 7.1. Mostly, the solid content consists of insoluble solids (Black pie in Figure 7.1) and soluble solids (Blue pie in Figure 7.1), and they were almost identical between the samples. The soluble solids in serum primarily were determined as being simple sugars along with organic acids and pectin (Moelants, Cardinaels, Van Buggenhout, et al., 2014). Previous studies from our group have shown that HB and CB sera were almost the same in terms of pectin content, and the contribution of the serum pectin to the suspension viscosity was limited (Chong et al., 2009; Chong et al., 2014; B. Wu, 2011). Insoluble solids are mainly dried structural materials/particles derived from cell wall that play an important role in the product textural properties, although it only accounts a small percentage (e.g. 1%). It should be noted the pulps from the HB and CB samples had significantly different water holding capacities,

demonstrated by the moisture contents in these pulps. The pulp of the HB sample can take 30% more water than that of CB samples (9.8% versus 7.5%), which indicates that HB particles are formed by cell wall material with a more intact structure and with higher capacity to hold water. And this structure may add function to the particle properties that may explain the different rheological behavior different than the CB samples.

### 7.3.2 Rheological Behavior of the HB and CB Samples

#### 7.3.2.1 Viscosity

The flow curves of the HB and CB suspensions are illustrated in Figure 7.2. The HB sample exhibited higher viscosity which is in good agreement with the results from the Bostwick consistency (Table 7.1) and previous studies (Goodman, Fawcett, & Barringer, 2002; C. Valencia et al., 2002).The consistency coefficient (*k*) was determined from the flow curves by fitting to the power law model. As expected, the *k* value of HB sample ($8.2 \pm 0.4$ Pa.s$^n$) was significantly larger than that of CB sample ($1.5 \pm 0.1$ Pa.s$^n$), whereas the flow index of the HB and CB samples were $0.17 \pm 0.00$ and $0.21 \pm 0.01$, respectively. Compared to the results of Chapter 4 where the HB and CB suspensions were made in the lab, the difference observed in the industrially processed samples was even bigger. This could be probably due to the high shear processes such as pumping and extraction to which the material is subjected in the industrial process. Thermal processes alone cause the initial tissue softening due to loss of turgor pressure (Greve, Shackel, et al., 1994; Van Buggenhout et al., 2009); however cell wall tissue disruption, which is associated to cell rupture and cell separation, occurs due the more severe mechanical treatment in the industrial process. It has been reported that thermal treatment affects the formation of particles (cell separation versus cell rupture) and the shape of the formed particles during the mechanical destruction (Greve, Mcardle, Gohlke, & Labavitch, 1994; Ormerod, Ralfs,

Jackson, Milne, & Gidley, 2004). Li et al. (2010) reported that HB samples had smaller sizes, smooth surfaces and without broken edges which indicated the cell separation was favored through middle lamella at more intense heat treatments in the presence of shear. In the present study, the HB particles exhibited better water holding capacity which confirmed this assumption. The particle properties may serve a major determinant in viscosity and needs to be further investigated.

#### 7.3.2.2 Viscoelasticity

The strain-sweep from 0.1 to 100% (strain %) was performed at constant frequency 1 Hz to determine the linear viscoelastic (LVR) region. From Figure 7.3, it was determined that the LVR range where the storage modulus (G') and loss modulus (G") are independent of the applied strain was between 0.01 to 1%. This range was slight narrower than that obtained from lab prepared HB and CB samples (see Chapter 4). In addition, the HB samples from the industrial process showed much higher G' and G" values than those measured in the samples prepared in the laboratory. In agreement with previous studies (Lopez-Sanchez et al., 2011; Verlent, Hendrickx, Rovere, Moldenaers, & Van Loey, 2006), both HB and CB samples revealed a “weak gel” behavior with G' values one order of magnitude higher than G" at the LVR. G' and G" values at 0.1% strain were compared between the two samples, and HB sample exhibited higher G' values than those of the CB sample. Upon increasing the applied strain, both G' and G" decreased until a cross-over point was reached, indicating that suspension behavior was more liquid like at larger strains (Day, Xu, Oiseth, Lundin, & Hemar, 2010).

Frequency sweep from 0.1 to 10 Hz also performed on the HB and CB samples are illustrated in Figure 7.4. Similar to the strain-sweep test, G' values were always higher than G" values by approximately 10-folds, regardless the frequency, which reinforces the assumption that

the suspensions have dominant elastic properties and can be classified as “weak gels” (Rao, 2007). G' and G" increased with increases of frequencies. These are typical rheological properties of concentrated fruit and vegetable suspensions and similar behavior has been reported for other cell wall materials (Massa, Gonzalez, Maestro, Labanda, & Ibarz, 2010; C. Valencia et al., 2002).

The viscoelasticity results are highly correlated with the viscosity data, which indicates that the viscosity is greatly influenced by the elasticity of the suspensions. It is well known that the solid content is a very important parameter affecting the rheological properties of suspensions, and in the industry the viscosity of tomato products is significantly improved by adding more tomato concentrates (i.e. solids) (Thakur et al., 1996). In the present study, the dry solid content of the HB and CB samples were the same (i.e. 4.3%). However there is a significantly difference in the moisture content of the pulps, which indicates that the resulting particle structures and the holding capacities of the pulps are distinct from the HB and CB processes. Thus, it could be concluded that are the particle properties which account for the observed differences in the rheological properties of the HB and CB samples.

To further evaluate the mechanical strength of the particles in the HB and CB suspensions, a compression experiment on these suspensions was carried out. Figure 7.5 shows force-time plots for the HB and CB suspensions. During the test, the upper plate was lowered down from 1000 μm until 100 μm while recording the normal force by the force transducer in the rheometer. Particle deformation and water transport through the cell wall are the two mechanisms associated to compression response according to Lopez-Sanchez et al. (2014), and the peak force is an indicator of cell wall elasticity (Blewett, Burrows, & Thomas, 2000). HB sample exhibited a peak force of $50.0 \pm 0.3$N, which was considerably higher than that determined

in the CB sample (35.7±0.4 N). This result indicates HB particles have a much higher mechanical strength and cell wall elasticity compared to CB sample. As discussed before, cell separation through middle lamella was favored by HB instead of cell wall breakage, so the HB sample consists of more intact and smoother cells compared to the CB sample. This structural difference allowed HB particles to hold more cell fluid. And, the HB sample maintained better a turgor pressure and structural integrity, which are essential to keep the mechanical strength of cell wall tissues (Blewett et al., 2000; Cosgrove, 1997; Jackman & Stanley, 1995).

### 7.3.3 Temperature Dependence

The flow curves expressed as shear stress versus shear rate at 20, 40, 60 and 80 ℃ are illustrated in Figure 7.6. The HB and CB suspensions exhibited a typical shear thinning behavior ($n$<1) with a yield stress ($\tau_0$). The flow curves were then fitted by Herschel-Bulkley model (Equation 7.2) and the values of the rheological parameters are presented in Table 7.2.

The yield stress is the minimum shear stress required to initiate flow (Genovese & Rao, 2005). When the applied stress is below the yield stress, the material deforms plastically like a solid but doesn't flow; however when the applied stress is above the yield stress, the material starts flowing with finite viscosity (Augusto, Falguera, Cristianini, & Ibarz, 2012). The yield stress of CB sample at 20 ℃ was 1.7 Pa, which is closed to the value reported for fruit concentrated juices such as tamarind juice (1.46 Pa) (Ahmed, Ramaswamy, & Sashidhar, 2007) and mandarin juice (1.50 Pa) (Falguera, Velez-Ruiz, Alins, & Ibarz, 2010). Augusto et al. (2012) also reported tomato juice had a yield stress of 0.94 Pa at 20 ℃. The CB sample from the industrial process has a solid content higher than that of the tomato juice product. Therefore, it has higher a yield stress than that reported for tomato juice. The HB sample showed a much higher yield stress than the CB sample, in range from 8.0 to 9.6 Pa for the testing temperatures,

which was similar to those measured in some fruit pulps (Augusto, Cristianini, et al., 2012; Massa et al., 2010). The yield stress can be observed as capacity of the material to maintain an internal structure that must be broken to make the material flows (Genovese & Rao, 2005). Thus, the difference of yield stress between HB and CB may come from differences in the particle structures, and possibly to the fact that the HB sample has a higher mechanical strength.

Values of yield stress at different temperatures depend on the products and the temperature range applied. It remains constant in some products at a specific temperature range (Massa et al., 2010), while it could show a falling behavior in others (Augusto, Cristianini, et al., 2012). In the present study, the yield stress showed a decreasing trend with temperature for both HB and CB samples and maximum values were observed at 40 ℃ for both samples. Augusto et al. (2012) reported same quasi-constant values of yield stress at 40 ℃ (11-13 Pa) in siriguela pulp. However, it was followed by a dramatic drop, which was not observed in the present study.

The flow index ($n$) increased nearly linearly with increases of temperature, indicating the suspensions were less shear thinning as temperature increased. A linear function was chosen to model the changes of the flow index with temperature as shown in Figure 7.7. The fit equations were $n = -0.824 + 0.00473T$ ($R^2$=0.80) for the HB sample, and $n = -0.235 + 0.00307T$ for the CB sample ($R^2$=0.81). The flow index ($n$) is usually considered as a constant during temperature changes (Rao, 2007). According to Augusto et al. (2012), the $n$ value of tomato juice remained unchanged with increasing temperatures in a range from 20 to 80 ℃. However, their study on siriguela pulp revealed that $n$ followed an increasing trend with temperature (2012). It seems that their relationship depends on the suspension system: in a concentrated suspension (i.e. pulp) the $n$ value increases with temperature whereas in a more diluted suspension (i.e. a juice) the $n$ value remains constant.

To evaluate the effect of temperature on the viscosity, the consistency coefficient ($k$) as a function of temperature was modeled by the Arrhenius-like equation (Equation 7.3). As illustrated in Figure 7.8, $k$ values were well fitted using the Arrhenius-like equation, with $R^2$ =0.98 for the HB sample and 0.95 for the CB sample. The $k$ value decreased with increasing temperature, which is a typical behavior for cell-wall-based suspensions. Massa et al. (2010) attributed it to a less developed structure at elevated temperature due to particle motion. It has been noticed that the $k$ value of HB sample exhibited a more dramatic drop from 20 to 80 ℃. This indicates HB may have a more integral structure, with a potential to be disrupted by higher temperatures. The B value of HB sample (41137.0) was higher than that of CB sample (27589.3). Higher values of the parameter B means that high temperature is required to ensure a change in viscosity happens. Thus, it indicates that the internal structure of the HB suspension is more resistant to increase of temperature compared to the CB suspension. Some studies reported the empirical parameter B of plant cell wall based suspensions ranged from thousands to one hundred thousand varied with the plant source (Akbulut, Coklar, & Ozen, 2008; Barbana & El-Omri, 2012). Solid content also influences this parameter. Tomato juice was reported to have an B value of 7353.3 (Augusto, Falguera, et al., 2012), while in tomato pasted it falls to the range of 9000 to 13000 (Dak, Verma, & Jaaffrey, 2008). In the present study, the solid content is the same for the HB and CB suspensions. The difference in the temperature dependence is probably caused by the differences in the particle structures in the suspension systems.

### 7.3.4 Time Dependence

The time dependence behavior was evaluated by applying a constant shear ($\dot{\gamma}$ =50 $s^{-1}$) for 30 min. HB and CB suspensions exhibited a thixotropic behavior as shown in Figure 7.9. The viscosity versus time curve was well fitted by the Stretch Exponential model and the values of

parameters are presented in Table 7.3. In this model, the parameter $\eta_i$ is the viscosity at the beginning of shearing. $\eta_{in}$ is infinite-time viscosity, which refers to the equilibrium viscosity, at the time the internal structure of the sample is broken down. Both $\eta_i$ and $\eta_{in}$ decreased with increases of temperature from 20 to 80 ℃. This type of temperature dependence behavior was discussed in the previous section. However the viscosity drop after each shearing was approximately 0.03 Pa.s for the HB sample and 0.012 Pa.s for the CB sample. Thus, this viscosity decrease was almost a constant at the different temperatures, which indicates the time dependence behavior of these suspensions doesn't vary much with temperature. $\lambda_s$ is a characteristic time required to reach the equilibrium. For the HB sample, $\lambda_s$ increased from 491.4s to 1140.4s with rising temperature. Conversely, CB sample showed a decreasing trend, with $\lambda_s$ changing from 1039.9 s to 606.6s with increasing temperatures. The thixotropic equilibrium is governed by a balance of microstructure built-up and break-down (Barnes, 1997). Brownian or particle motion, which is accelerated by high temperature, can cause collision of particles building the structure up, whereas the shear stress leads the microstructure to break-down by erosion (Barnes, 1997). Enhancing either mechanism would accelerate the equilibrium process. Mewis and Schryvers (1996) reported that $\lambda_s$ was negatively correlated with $\eta_i \cdot \dot{\gamma} / \eta_{cont.}$, where $\eta_{cont.}$ is the viscosity of the continuous phase which also changes with temperature. At the present study, the shear rate was a constant, so the apparent viscosity $\eta_i$ is an indicator of shear stress that is associated with the microstructure break-down. As temperature increased, $\eta_i$ decreased therefore inhibiting microstructure break-down. On the other hand, the particle motion was extensively accelerated by higher temperatures. The HB sample had a much higher initial

viscosity compare to that of the CB sample. In addition, as discussed before the HB particle structure was more resistant to changes in temperatures, and its particle motion needed a higher temperature to initiate. Therefore, it could be assumed that the shear stress induced microstructure break-down dominates the equilibrium in the HB suspension. As $\eta_i$ (or shear stress) decreases with temperature, $\lambda_s$ showed a rising trend. By contrast, the CB suspension is dominated by a build-up mechanism due to the low initial viscosity and the presence of the shear stress. Increasing temperatures promotes particle collision that helps build up the structure, and therefore decreases the value of $\lambda_s$ as shown in Table 7.3.

In order to compare results, the stress versus time curve was fitted by the Weltman model (1943) and Figoni and Shoemaker model (1983), both widely used in characterization of thixotropic behavior in foods. The fitting curves are shown in Figure 7.10 and the values of parameters are presented in Tables 7.4 and 7.5. In the Weltman model (Equation 7.5), the parameter A is the shear stress value at *t*=1s, while B is a positive value that in thixotropic fluids is related to their stress decay (Rao, 2007). From Figure 7.10, this model seemed to overestimate the initial stress and therefore it results in a relatively low $R^2$ (Table 7.4). The Figoni and Shoemaker model (Equation 7.6) is the Stretch Exponential model in stress form, with the parameter $\tau_e$ being the equilibrium shear stress, $\tau_0$ is the initial shear stress, and *k* is related to the stress decay time. As expected, these values followed a similar trend than that followed by the Stretch Exponential model and shared the some $R^2$. Both models successfully predicted a stress decay or thixotropic behavior in tomato HB and CB suspensions, and gave more information about the equilibrium state and time. Thus, it should be preferred to use in these cell wall based suspensions over the Weltman model.

$$\tau = A - B \cdot \ln t \tag{7.5}$$

$$\tau = \tau_e + (\tau_0 - \tau_e) \cdot e^{-k \cdot t} \tag{7.6}$$

### 7.3.5 Effect of Solid Content and Particle Interaction

To evaluate the effects of particle concentration and associated interactions on the rheology of the suspensions, a series of HB and CB suspensions prepared with different solid contents ranging from 0.5 to 4.0% were prepared and their viscosity and viscoelasticity were measured. Figure 7.11 shows the apparent viscosity at shear rate 50 $s^{-1}$ of the HB and CB suspensions with varying solid contents. At low particle concentration (solid %< 1.0%), the apparent viscosity increased linearly with the solid content. In diluted suspension system where the particles have limited contact, the volume occupied by the individual particles mainly determines the viscosity of the suspension (Day, Xu, Oiseth, Hemar, et al., 2010). Since HB and CB had similar volume fractions at the low concentration range (see Figure 7.13), a small viscosity difference was observed between HB and CB suspensions. As the solid content increases, particles start to contact each other and form networks that result in more interaction between particles. Therefore, the viscosity showed a power law increase with solid content. In this range, the viscosity of HB suspensions was always higher than that of CB suspensions at the some solid content. This would be indicating that the HB particles have higher mechanical strength and elasticity than CB particles. In other words they would be less deformable. As the solid content approaches to 4.0%, the particles in the suspensions are highly packed and could be more or less deformed by deformation and/or flow depending on their mechanical strengths.

To further investigate the contribution of particle interactions on the rheology of the suspension, G' and G" values were obtained by preforming strain sweep and then plotted against solid content as shown in Figure 7.12. The complex modulus $G^*$ defined as $(G'^2 + G''^2)^{1/2}$ was also

calculated and plotted in the same figure. Because the G' values were about one order of magnitude higher than G" values, $G^*$ and G' were overlapped in the plots. Two regions distinguished by a transition concentration ($c^*$) are observed in Figure 7.12. The concentration at which the transition occurred was 1.75% for the HB sample and 2.25% for the CB sample. Below $c^*$, $G^*$ increased sharply with solid concentration (c); while above $c^*$, a much slower rise was observed. Another parameter, the critical concentration ($c^{**}$) defined as the concentration at which a plateau is observed, can be identified in the figure. Normally the rheological behavior of suspensions is modeled as a function of the particle volume fraction. However, it is hard to directly determine the volume fraction of plant cell wall particles due to their soft nature and high deformability. According to Day, Xu, Oiseth, Lundin, et al. (2010), the volume fraction can be assumed to be one when $G^*$ is at the plateau. The relative volume fraction ($\phi$) was defined to relate the particle concentration to volume. It was calculated by dividing c by $c^{**}$, and the critical volume fraction ($\phi_c$) was further calculated as $c^*/c^{**}$. Figure 7.13 shows $G^*$ as a function of $\phi$ at two different ranges differentiated by the value of $\phi_c$. In the first range, where $\phi < \phi_c$, the data can be modeled by a power-law equation given as $G^* \propto \phi^a$. In the other range, where $\phi > \phi_c$, $G^*$ was reaching the plateau and was modeled by an empirical equation proposed by Adams, Frith, and Stokes (2004):

$$G^* = A\left[1-(\frac{\phi_c}{\phi})^{1/3}\right] \tag{7.7}$$

where A is an adjustable parameter representing the physical properties of the suspension.

The values of the parameters fitted from the above two equations are presented in Table 7.6. In the case of the HB suspension, a power constant $a$ of $4.0 \pm 0.2$ was obtained, which was higher than that obtained for the CB suspension ($3.3 \pm 0.1$). This power law equation has been used for modeling elastic properties of particle networks and $a$ is related to the interaction

between particles as well as their shapes. The higher *a* value of the HB suspension could correspond to a stronger particle interaction in the system, which greatly depends on the particle properties (i.e. elasticity, mechanical strength). The Adams model described well the viscoelasticity behavior of tomato suspensions at high particle concentrations (Adams et al., 2004). The parameter $\phi_c$ was obtained as $0.44 \pm 0.02$ for the HB suspension and $0.51 \pm 0.02$ for CB suspension, which are close to values determined from Figure 7.12. Day, Xu, Oiseth, Lundin, et al. (2010) reported that values of $\phi_c$ for carrot and broccoli cell wall materials were 0.56 and 0.49, which are similar to the values of tomato obtained in the present study. The constant A represents the elasticity of the particles. The result indicates that HB suspensions are formed by particles that are more elastic, which is in line with the steady state shear and oscillatory shear results discussed in previous sections. In the plateau range, the particles are highly packed and deformed. The HB suspensions exhibited a higher plateau value compared to that of the CB suspensions. According to Stokes and Frith (2008), the individual particle elasticity determines the plateau $G^*$, and concentrated phases from the same particles should have the same values. From the measured plateaus it can be concluded that individual particles from the HB samples should have a larger elasticity than that of particles obtained from the CB samples. Therefore, the differences observed between the measured bulk rheologies (i.e. HB vs. CB) are originated from the different mechanical strengths of the individual particles forming these systems.

## 7.4 Conclusions

The flow behavior of HB and CB tomato suspensions from industry processed products were studied under steady-state and SAOS tests . The viscosity and viscoelastic properties of the HB sample were considerably higher than those of the CB sample, which could be explained by a better water holding capacity and a stronger mechanical strength of the HB particles. In

addition, the rheological differences between industrial produced HB and CB suspensions were relatively bigger, when compared to those of suspensions produced in the lab setting (Chapter 4). This is probably due to the high shear used in the industrial process which can further disrupt cell wall tissue into smaller sizes.

HB and CB suspensions exhibited temperature dependence and their flow curves were fitted to the Herschel-Bulkley model. The yield stress ($\tau_0$) showed decreased with temperature and maximum values were observed at 40 ℃ for both suspensions. The consistency coefficient (*k*) decreased with increasing temperatures, and was well described by an Arrhenius-like equation. The empirical parameter B of HB sample (41137.0) was higher than that of CB sample (27589.3), indicating HB has a structure more resistant to the changes of temperature. The difference in the temperature dependence of the suspension is likely to be caused by the particle structures in these suspension systems.

HB and CB suspensions exhibited thixotropic behavior and the viscosity versus time curve was well described by the Stretch Exponential equation. The characteristic time ($\lambda_s$) for the HB sample increased from 491.4 s to 1140.4s with increases of temperature while it decreased from 1039.9 s to 606.6s with increases of temperature for the CB suspensions. The thixotropic equilibrium is governed by a balance of microstructure build-up and break-down. The results indicate that the shear stress induced microstructure break-down dominates the equilibrium in the HB system whereas the temperature accelerated build-up governs the equilibrium in the CB system. The differences were caused by the particle structure and were related to the initial viscosity of the suspensions. Weltman model and Figoni and Shoemaker models were applied for modeling purpose and to compare results. Weltman model

overestimated the initial stress and therefore the other two models are recommended to use for cell wall derived suspensions.

Particle interactions showed great effects on the rheological properties of HB and CB suspensions, which depended on particle concentration and volume fraction. At low particle concentrations (solid % < 1.0%), the HB and CB suspensions had the same apparent viscosity because the particles have limited contact. As particle concentration increases, particles start to contact each other and the viscosity shower an increase with solid concentration that followed a power law relationship. The complex modulus ($G^*$) was further modeled as a function of relative volume fraction by power law and Adams' equations at two different ranges defined by the critical volume fraction ($\phi_c$). The HB sample was described by a higher power *a* parameter as well as a higher A parameter in the Adams' equation. These results demonstrate that HB suspensions have particles with larger mechanical strength and elasticity and stronger particle interaction than the particles forming CB suspensions.

## 7.5 Figures and Tables

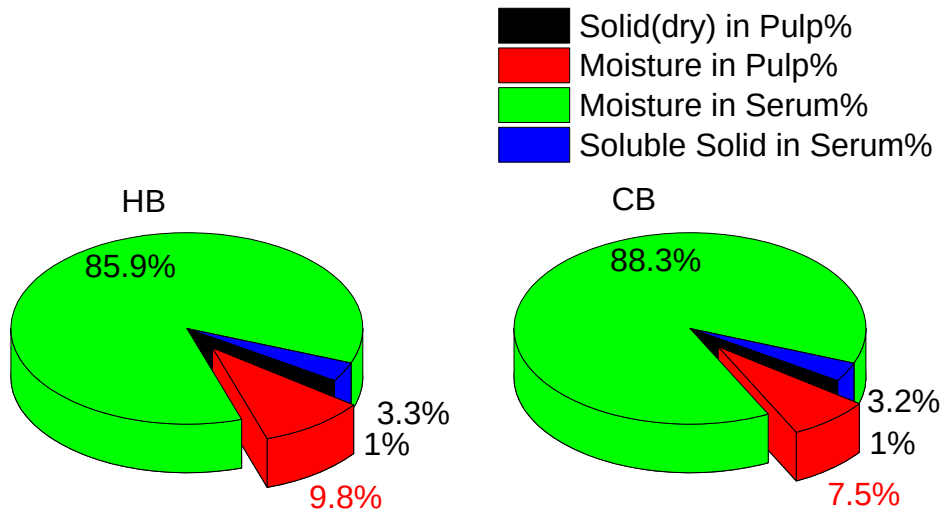


Figure 7.1 Moisture distributions in the HB and CB samples.

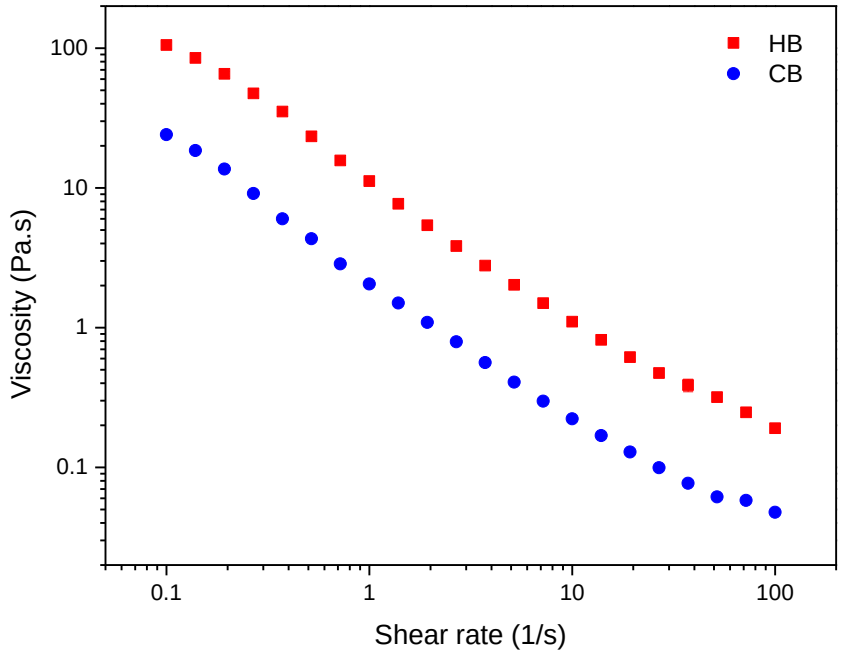


Figure 7.2 Flow curves of HB and CB samples from industrial processing.

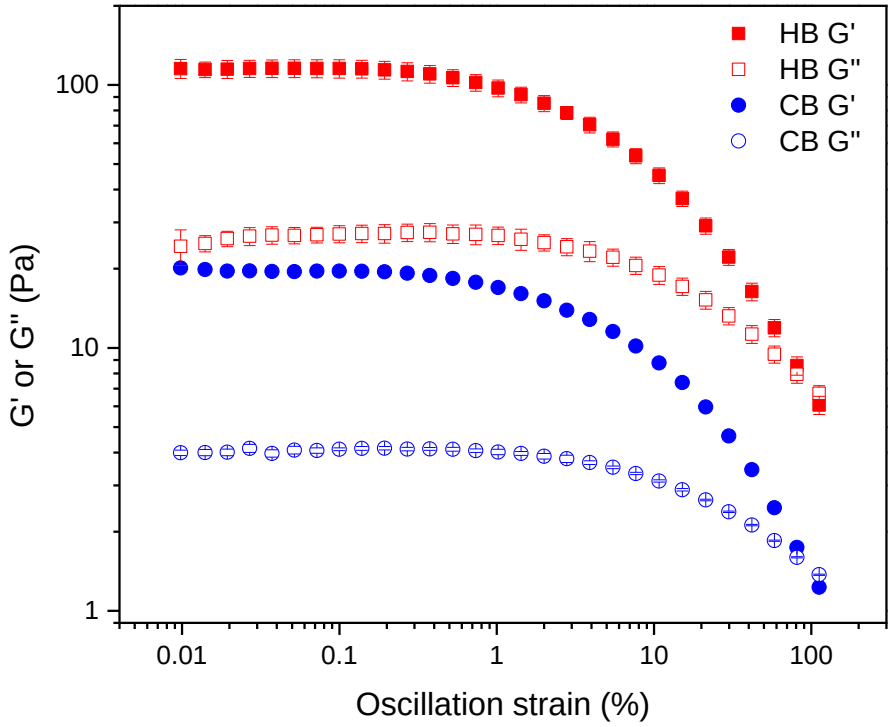


Figure 7.3 Strain sweep tests of HB and CB samples from industrial processing.

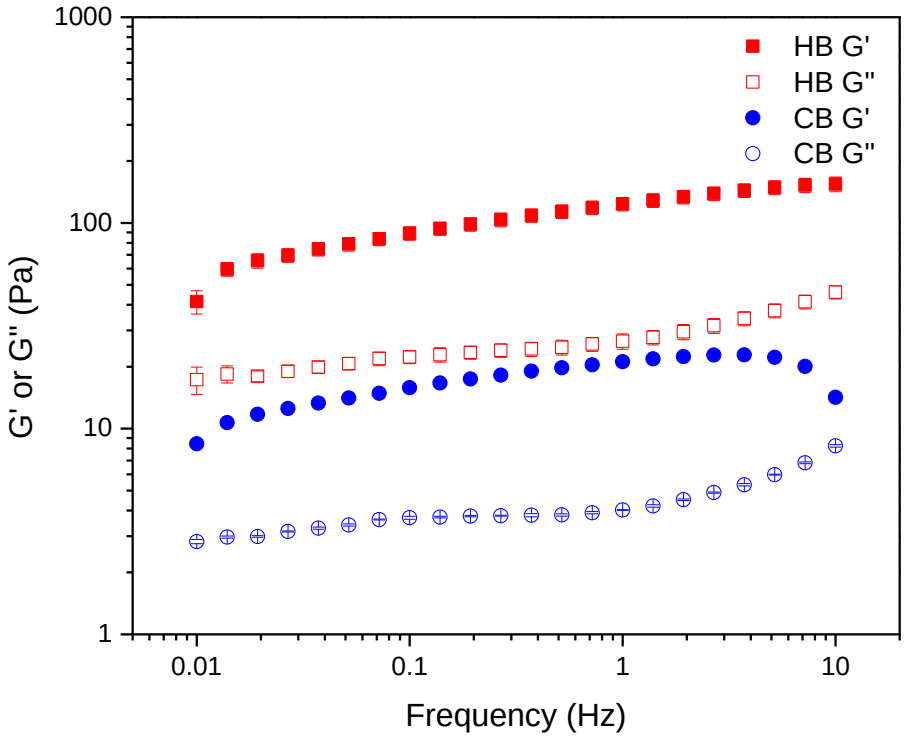


Figure 7.4 Frequency sweep tests of HB and CB samples from industrial processing.

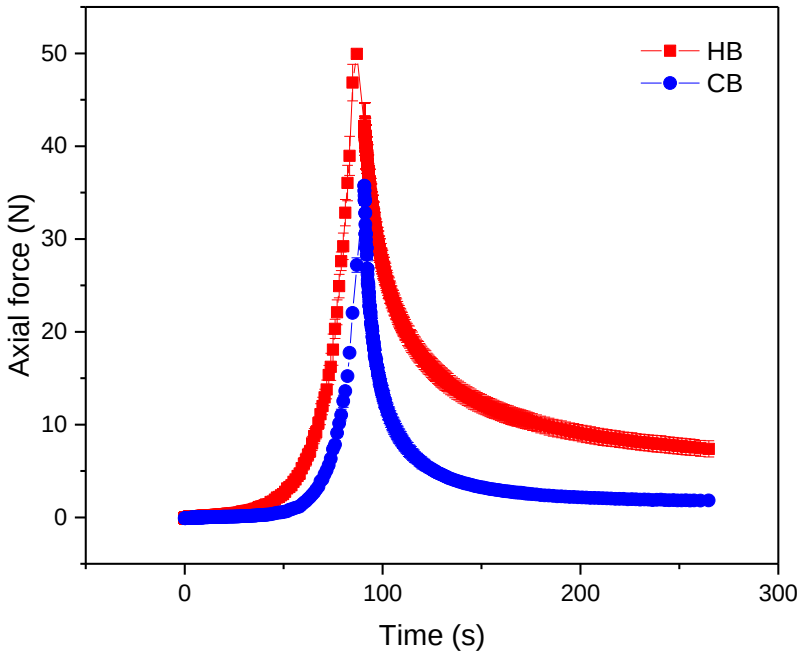


Figure 7.5 Peak force of HB and CB samples obtained from an industrial process.

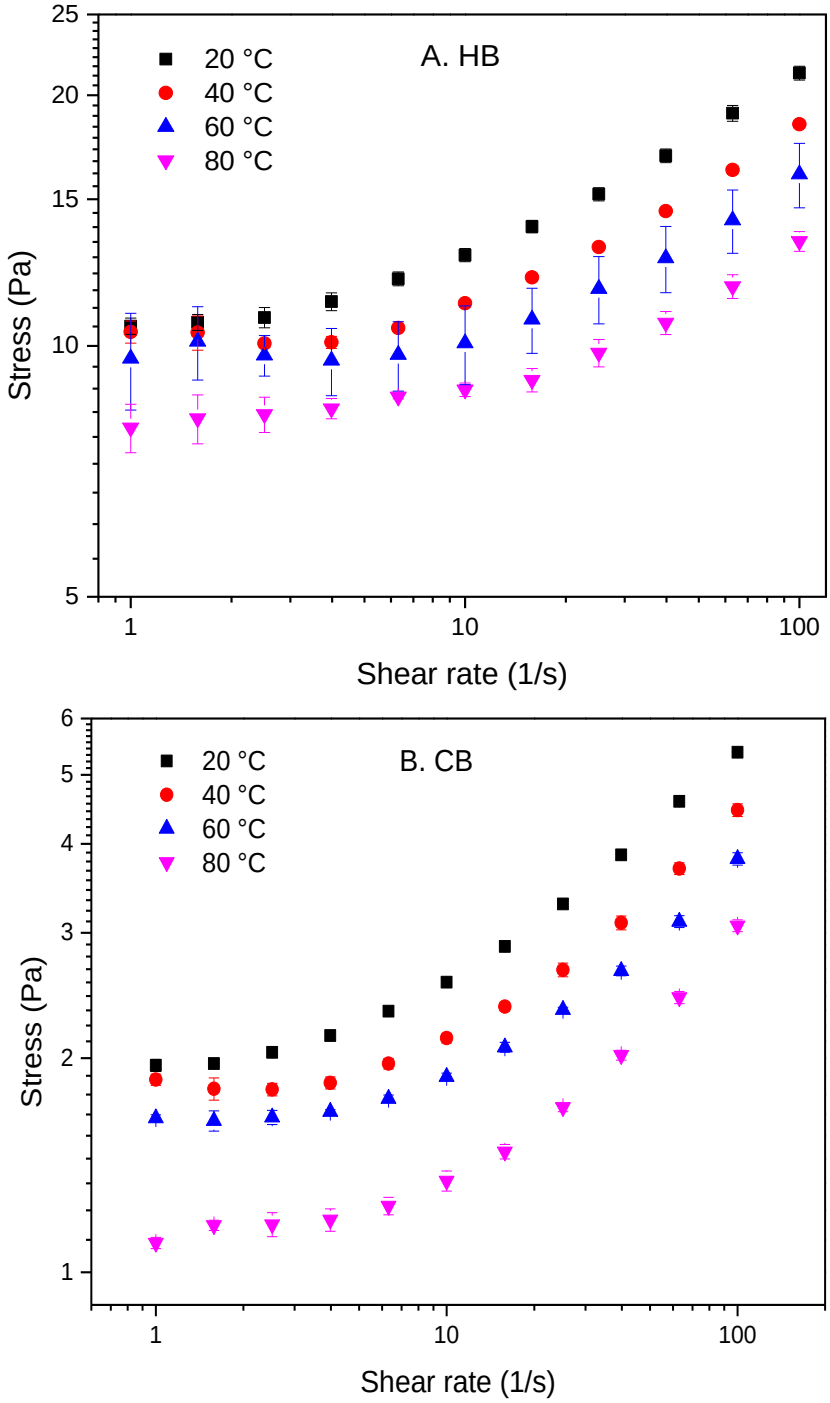


Figure 7.6 Stress versus shear rate of HB and CB samples obtained from an industrial process. Flow curves were determined at 20, 40, 60 and 80 ℃.

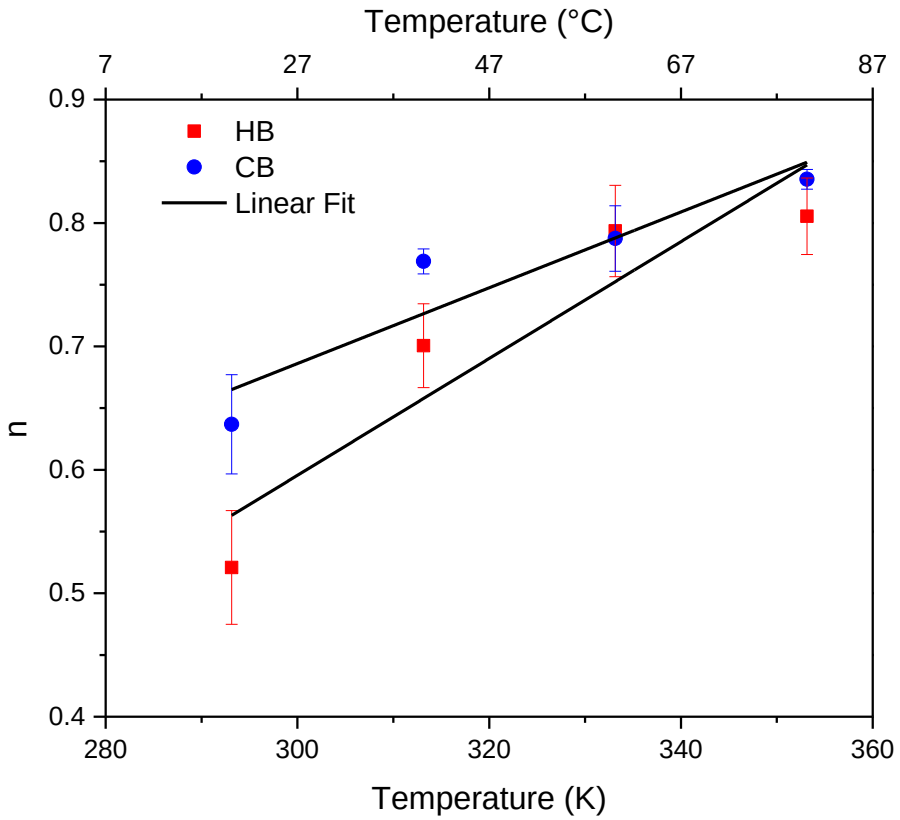


Figure 7.7 *n* values in Herschel Bulkley model as a function of temperature. Black lines represent linear fit.

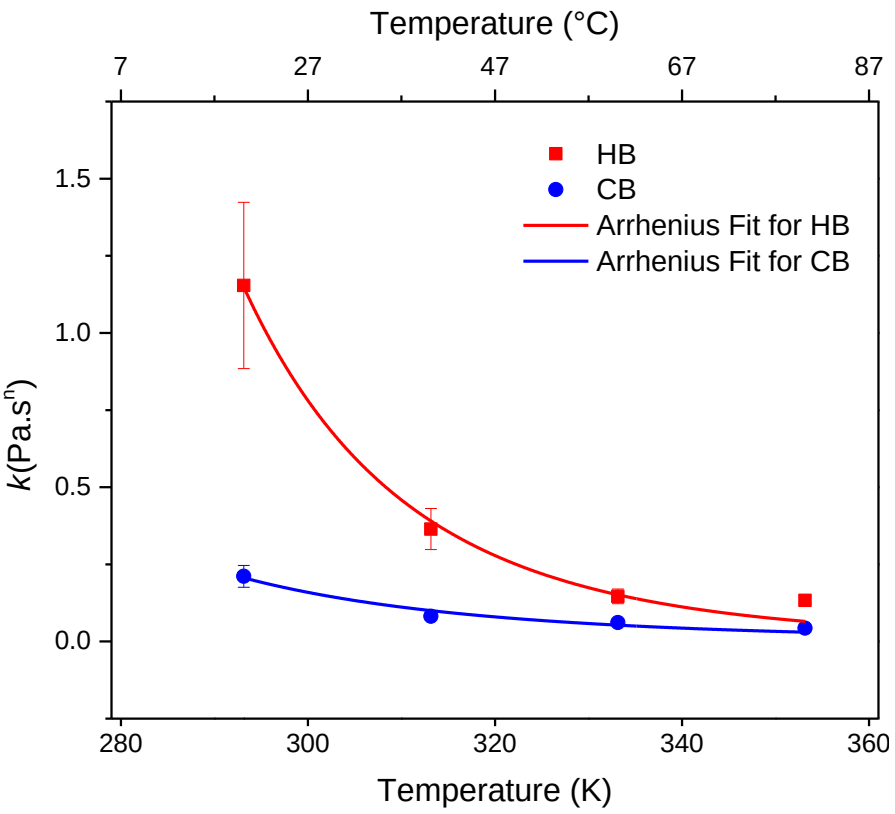


Figure 7.8 Consistency coefficient ($k$) as a function of temperature fitted by an Arrhenius-like equation. Black lines represent Arrhenius fit.

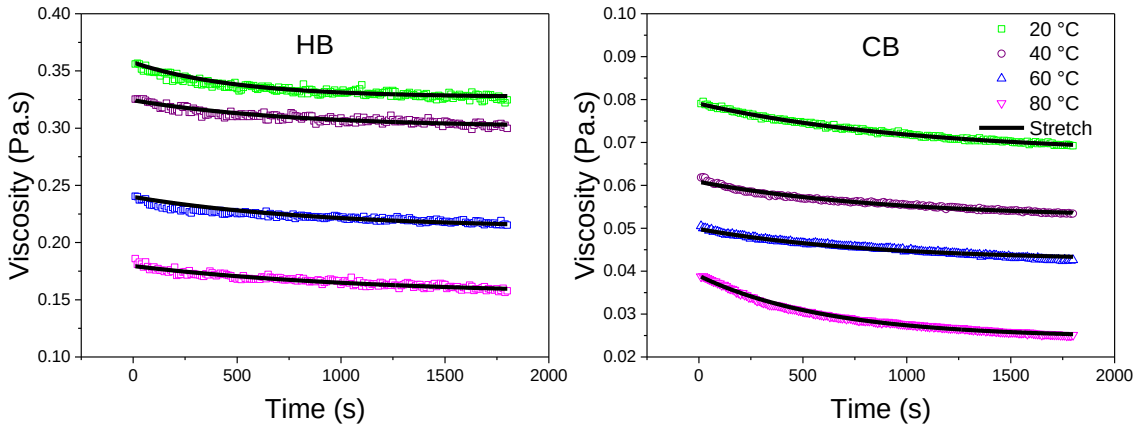


Figure 7.9 Thixotropic behavior of HB and CB samples from industrial processing at 20, 40, 60 and 80 ℃ modeled by the Stretch Exponential equation. Black lines represent Stretch Exponential fit

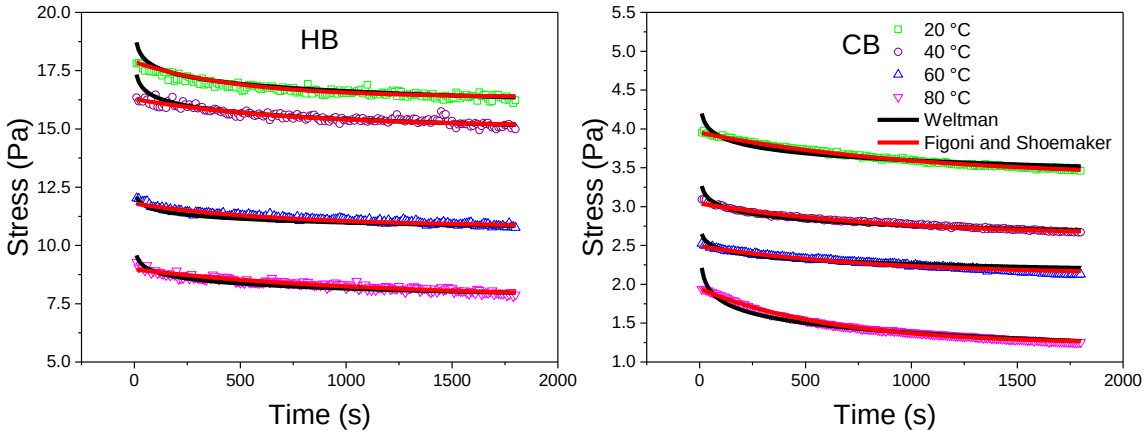


Figure 7.10 Stress decay of HB and CB samples from industrial processing at 20, 40, 60 and 80 ℃ modeled by Weltman equation and Figoni and Schoemaker equation. Black lines represent Weltman fit, and red lines represent Figoni and Schoemaker fit.

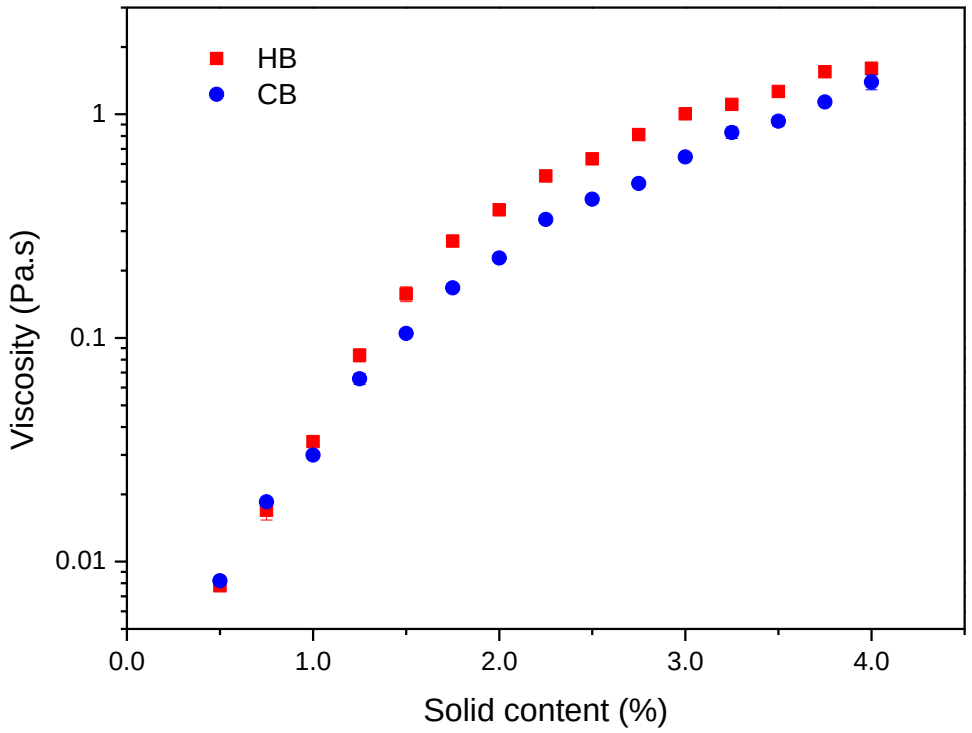


Figure 7.11 Apparent viscosity at shear rate 50 $s^{-1}$ of HB and CB suspensions as a function of particle concentration.

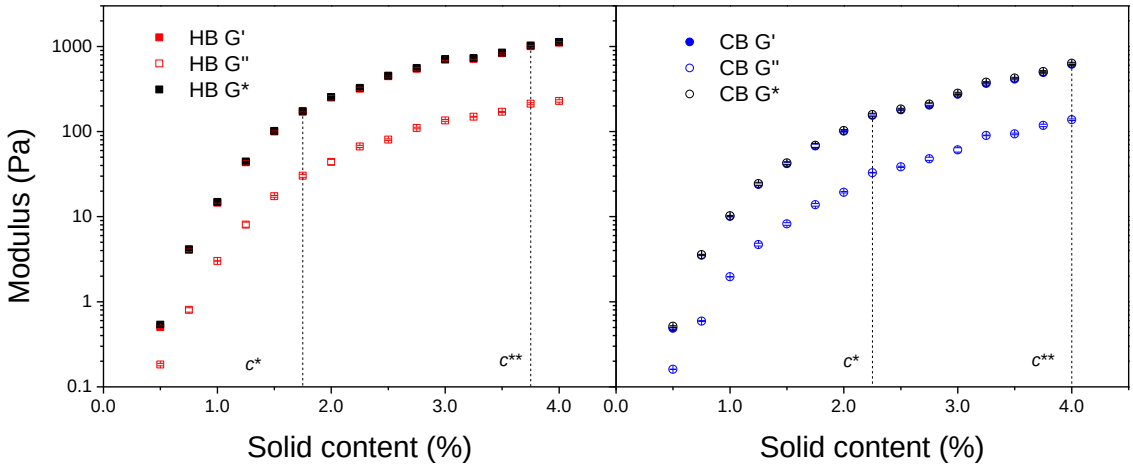


Figure 7.12 Storage modulus G', loss modulus G" and complex modulus $G^*$ at 0.1% strain and 1 Hz frequency as functions of particle concentration for the HB and CB suspensions. The transition concentration and critical concentration are indicated in the plots.

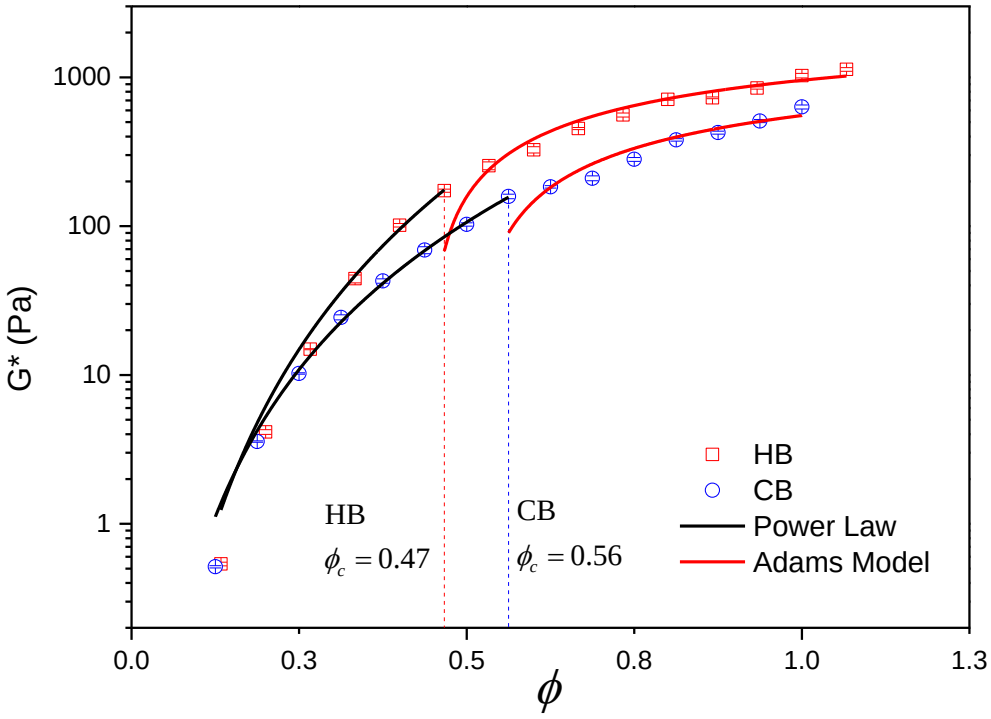


Figure 7.13 Complex modulus $G^*$ as a function of relative volume fraction $\phi$ for HB and CB suspensions. Below the critical volume fraction $\phi_c$, the data was fitted to the power law model (Black lines, $R^2$ > 99% ); while above critical volume fraction $\phi_c$, the data was fitted to the Adams model (Red lines, $R^2$ > 90% )

Table 7.1 General product properties of the HB and CB samples.

| | Precipitate weight ratio (%) | °Brix | Bostwick Consistency (cm) | Moisture content (%) | | |
|---|---|---|---|---|---|---|
| | | | | Suspension | Pulp | Serum |
| HB | 10.8±0.6 a | 4.2±0.1 a | 9.2±0.2 a | 95.7±0.0 | 90.7±0.0 a | 96.3±0.0 |
| CB | 8.5±0.6 b | 3.9±0.0 b | 12.3±0.6 b | 95.7±0.0 | 88.2 ±0.3 b | 96.1±0.0 |

Data was tested by Two Sample t-test ($p$=0.05), and means with different letters indicate significant difference, $p < 0.05$.

Table 7.2 Values of parameters (±standard deviation) for fitting Herschel-Bulkley model.

| $T$ (℃) | $\tau_0$ (Pa) | | $k$ (Pa.s$^n$) | | $n$ | |
|---|---|---|---|---|---|---|
| | HB | CB | HB | CB | HB | CB |
| 20 | 9.10±0.49 | 1.68±0.06 | 1.15±0.27 | 0.21±0.04 | 0.52±0.05 | 0.64±0.04 |
| 40 | 9.55±0.12 | 1.68±0.04 | 0.36±0.07 | 0.08±0.00 | 0.70±0.03 | 0.77±0.01 |
| 60 | 9.39±0.97 | 1.53±0.03 | 0.15±0.02 | 0.06±0.01 | 0.84±0.04 | 0.79±0.03 |
| 80 | 7.96±0.32 | 1.06±0.03 | 0.13±0.01 | 0.04±0.00 | 0.81±0.03 | 0.84±0.01 |

$R^2$>95% for each fit

Table 7.3 Values of parameters (±standard deviation) and the $R^2$ for fitting Stretch Exponential model.

| $T$ (℃) | Stretch Exponential model $\eta(t) = \eta_i + (\eta_{in} - \eta_i)(1 - e^{-t/\lambda_s})$ | | | | | | | |
|---|---|---|---|---|---|---|---|---|
| | $\eta_i$ (Pa.s) | | $\eta_{in}$ (Pa) | | $\lambda_s$ (s) | | $R^2$ | |
| | HB | CB | HB | CB | HB | CB | HB | CB |
| 20 | 0.36±0.00 | 0.079±0.000 | 0.33±0.00 | 0.067±0.000 | 494.1±39.8 | 1039.9±27.4 | 95.5% | 99.5% |
| 40 | 0.32±0.00 | 0.061±0.000 | 0.30±0.00 | 0.052±0.000 | 765.2±66.5 | 903.6±38.0 | 87.3% | 98.2% |
| 60 | 0.24±0.00 | 0.050±0.000 | 0.21±0.00 | 0.043±0.000 | 895.0±48.9 | 836.9±41.9 | 97.5% | 97.9% |
| 80 | 0.18±0.00 | 0.039±0.000 | 0.15±0.02 | 0.025±0.000 | 1140.4±133.6 | 606.6±9.1 | 91.8% | 99.5% |

Table 7.4 Values of parameters (±standard deviation) and the $R^2$ for fitting Weltman model.

| $T$ (℃) | Weltman Model $\tau = A - B \cdot \ln t$ | | | | | |
|---|---|---|---|---|---|---|
| | A (Pa) | | B (Pa.s) | | $R^2$ | |
| | HB | CB | HB | CB | HB | CB |
| 20 | 19.76±0.05 | 4.51±0.02 | 0.45±0.01 | 0.13±0.00 | 93.1% | 91.0% |
| 40 | 18.29±0.10 | 3.52±0.01 | 0.42±0.02 | 0.11±0.00 | 80.8% | 95.8% |
| 60 | 12.64±0.03 | 2.84±0.01 | 0.24±0.00 | 0.08±0.00 | 93.6% | 93.5% |
| 80 | 10.29±0.01 | 2.63±0.02 | 0.31±0.00 | 0.18±0.00 | 99.4% | 95.2% |

Table 7.5 Values of parameters (±standard deviation) and the $R^2$ for fitting Figoni and Shoemaker model.

| $T$ (℃) | Figoni and Shoemaker model $\tau = \tau_e + (\tau_0 - \tau_e) \cdot e^{-k \cdot t}$ | | | | | | | |
|---|---|---|---|---|---|---|---|---|
| | $\tau_e$ (Pa) | | $\tau_0$ (Pa) | | $k$ ($s^{-1}$) | | $R^2$ | |
| | HB | CB | HB | CB | HB | CB | HB | CB |
| 20 | 16.36±0.03 | 3.37±0.01 | 17.88±0.03 | 3.95±0.00 | 0.0020±0.0002 | 0.0010±0.0000 | 95.5% | 99.5% |
| 40 | 15.08±0.05 | 2.62±0.01 | 16.28±0.03 | 3.04±0.00 | 0.0013±0.0001 | 0.0011±0.0000 | 87.3% | 98.2% |
| 60 | 10.80±0.03 | 2.13±0.01 | 11.80±0.02 | 2.49±0.00 | 0.0014±0.0001 | 0.0012±0.0001 | 97.5% | 97.9% |
| 80 | 7.72±0.07 | 1.23±0.00 | 9.00±0.02 | 1.95±0.00 | 0.0009±0.0001 | 0.0016±0.0000 | 91.8% | 99.5% |

Table 7.6 Transition and critical concentrations used to calculate relative volume fraction and values of parameters for fitting the power law and Adams equations

| | $c^*$ (%) | $c^{**}$ (%) | $a$ | A | $\phi_c$ |
|---|---|---|---|---|---|
| HB | 1.75 | 3.75 | 4.0±0.2 | 4023.0±274.6 | 0.44±0.02 |
| CB | 2.25 | 4.00 | 3.3±0.1 | 2748.0±303.5 | 0.51±0.03 |

$R^2$>99% for the power law fitting and > 90% for the Adams model fitting

## 7.6 References

Adams, S., Frith, W. J., & Stokes, J. R. (2004). Influence of particle modulus on the rheological properties of agar microgel suspensions. *Journal of Rheology, 48*(6), 1195-1213. doi: 10.1122/1.1773782

Ahmed, J., Ramaswamy, H. S., & Sashidhar, K. C. (2007). Rheological characteristics of tamarind (Tamarindus indica L.) juice concentrates. *Lwt-Food Science and Technology, 40*(2), 225-231. doi: 10.1016/j.lwt.2005.11.002

Akbulut, M., Coklar, H., & Ozen, G. (2008). Rheological Characteristics of Juniperus drupiacea Fruit Juice (pekmez) Concentrated by Boiling. *Food Science and Technology International, 14*(4), 321-328. doi: 10.1177/1082013208097193

Anthon, GE, Diaz, JV, & Barrett, DM. (2008). Changes in pectins and product consistency during the concentration of tomato juice to paste. *Journal of Agricultural and Food Chemistry, 56*(16), 7100-7105. doi: 10.1021/jf8008525

Augusto, P. E. D., Cristianini, M., & Ibarz, A. (2012). Effect of temperature on dynamic and steady-state shear rheological properties of siriguela (Spondias purpurea L.) pulp. *Journal of Food Engineering, 108*(2), 283-289. doi: 10.1016/j.jfoodeng.2011.08.015

Augusto, P. E. D., Falguera, V., Cristianini, M., & Ibarz, A. (2012). Rheological Behavior of Tomato Juice: Steady-State Shear and Time-Dependent Modeling. *Food and Bioprocess Technology, 5*(5), 1715-1723. doi: 10.1007/s11947-010-0472-8

Barbana, C., & El-Omri, A. (2012). Viscometric Behavior of Reconstituted Tomato Concentrate. *Food and Bioprocess Technology, 5*(1), 209-215. doi: 10.1007/s11947-009-0270-3

Barnes, Howard A. (1997). Thixotropy—a review. *Journal of Non-Newtonian Fluid Mechanics, 70*(1), 1-33. doi: https://doi.org/10.1016/S0377-0257(97)00004-9

Barua, B., & Saha, M. C. (2016). Incorporating Density and Temperature in the Stretched Exponential Model for Predicting Stress Relaxation Behavior of Polymer Foams. *Journal of Engineering Materials and Technology-Transactions of the Asme, 138*(1). doi: Artn 01100110.1115/1.4031426

Bayod, E, Mansson, P, Innings, F, Bergenstahl, B, & Tornberg, E. (2007). Low shear rheology of concentrated tomato products. Effect of particle size and time. *Food Biophysics, 2*(4), 146-157. doi: 10.1007/s11483-007-9039-2

Bayod, E, & Tornberg, E. (2011). Microstructure of highly concentrated tomato suspensions on homogenisation and subsequent shearing. *Food Research International, 44*(3), 755-764. doi: 10.1016/j.foodres.2011.01.005

Blewett, J., Burrows, K., & Thomas, C. (2000). A micromanipulation method to measure the mechanical properties of single tomato suspension cells. *Biotechnology Letters, 22*(23), 1877-1883. doi: Doi 10.1023/A:1005635125829

Chong, H. H., Simsek, S., & Reuhs, B. L. (2009). Analysis of cell-wall pectin from hot and cold break tomato preparations. *Food Research International, 42*(7), 770-772. doi: 10.1016/j.foodres.2009.02.025

Chong, H. H., Simsek, S., & Reuhs, B. L. . (2014). Chemical Properties of Pectin from Industry Hot and Cold Break Tomato Products. *Food and Nutrition Sciences, Vol.05No.13*, 6. doi: 10.4236/fns.2014.513126

Cosgrove, D. J. (1997). Relaxation in a high-stress environment: the molecular bases of extensible cell walls and cell enlargement. *Plant Cell, 9*(7), 1031-1041. doi: 10.1105/tpc.9.7.1031

Dak, M., Verma, R. C., & Jaaffrey, S. N. A. (2008). Rheological Properties of Tomato Concentrate. *International Journal of Food Engineering, 4*(7). doi: Artn 1110.2202/1556-3758.1470

Day, L., Xu, M., Oiseth, S. K., Hemar, Y., & Lundin, L. (2010). Control of Morphological and Rheological Properties of Carrot Cell Wall Particle Dispersions through Processing. *Food and Bioprocess Technology, 3*(6), 928-934. doi: DOI 10.1007/s11947-010-0346-0

Day, L., Xu, M., Oiseth, S. K., Lundin, L., & Hemar, Y. (2010). Dynamic rheological properties of plant cell-wall particle dispersions. *Colloids and Surfaces B-Biointerfaces, 81*(2), 461-467. doi: 10.1016/j.colsurfb.2010.07.041

Diaz, J. V., Anthon, G. E., & Barrett, D. M. (2009). Conformational Changes in Serum Pectins during Industrial Tomato Paste Production. *Journal of Agricultural and Food Chemistry, 57*(18), 8453-8458. doi: 10.1021/jf901207w

Falguera, V., Velez-Ruiz, J. F., Alins, V., & Ibarz, A. (2010). Rheological behaviour of concentrated mandarin juice at low temperatures. *International Journal of Food Science and Technology, 45*(10), 2194-2200. doi: 10.1111/j.1365-2621.2010.02392.x

Figoni, P. I., & Shoemaker, C. F. (1983). Characterization of Time-Dependent Flow Properties of Mayonnaise under Steady Shear. *Journal of Texture Studies, 14*(4), 431-442. doi: DOI 10.1111/j.1745-4603.1983.tb00360.x

Genovese, D. B., & Rao, M. A. (2005). Components of vane yield stress of structured food dispersions. *Journal of Food Science, 70*(8), E498-E504.

Goodman, C. L., Fawcett, S., & Barringer, S. A. (2002). Flavor, viscosity, and color analyses of hot and cold break tomato juices. *Journal of Food Science, 67*(1), 404-408. doi: DOI 10.1111/j.1365-2621.2002.tb11418.x

Gould, W.A. (1974). *Tomato Production, Processing and Quality Education*: Westfort, connecticut The AVI Publishing.

Gould, W.A. (1992). *Tomato Production, Processing and Technology*: Woodhead Publishing.

Greve, L. C., Mcardle, R. N., Gohlke, J. R., & Labavitch, J. M. (1994). Impact of Heating on Carrot Firmness - Changes in Cell-Wall Components. *Journal of Agricultural and Food Chemistry, 42*(12), 2900-2906. doi: Doi 10.1021/Jf00048a048

Greve, L. C., Shackel, K. A., Ahmadi, H., Mcardle, R. N., Gohlke, J. R., & Labavitch, J. M. (1994). Impact of Heating on Carrot Firmness - Contribution of Cellular Turgor. *Journal of Agricultural and Food Chemistry, 42*(12), 2896-2899. doi: Doi 10.1021/Jf00048a047

Hsu, K. C. (2008). Evaluation of processing qualities of tomato juice induced by thermal and pressure processing. *Lwt-Food Science and Technology, 41*(3), 450-459. doi: DOI 10.1016/j.lwt.2007.03.022

Jackman, R. L., & Stanley, D. W. (1995). Perspectives in the Textural Evaluation of Plant Foods. *Trends in Food Science & Technology, 6*(6), 187-194. doi: Doi 10.1016/S0924-2244(00)89053-6

Lopez-Sanchez, P., Nijsse, J., Blonk, H. C. G., Bialek, L., Schumm, S., & Langton, M. (2011). Effect of mechanical and thermal treatments on the microstructure and rheological properties of carrot, broccoli and tomato dispersions. *Journal of the Science of Food and Agriculture, 91*(2), 207-217. doi: Doi 10.1002/Jsfa.4168

Lopez-Sanchez, P., Rincon, M., Wang, D., Brulhart, S., Stokes, J. R., & Gidley, M. J. (2014). Micromechanics and Poroelasticity of Hydrated Cellulose Networks. *Biomacromolecules, 15*(6), 2274-2284. doi: 10.1021/bm500405h

Massa, A., Gonzalez, C., Maestro, A., Labanda, J., & Ibarz, A. (2010). Rheological Characterization of Peach Purees. *Journal of Texture Studies, 41*(4), 532-548. doi: 10.1111/j.1745-4603.2010.00240.x

Mewis, J., & Schryvers, J. (1996). *International Fine Particle Research Institute Report*.

Moelants, K. R. N., Cardinaels, R., Jolie, R. P., Verrijssen, T. A. J., Van Buggenhout, S., Van Loey, A. M., . . . Hendrickx, M. E. (2014). Rheology of Concentrated Tomato-Derived Suspensions: Effects of Particle Characteristics. *Food and Bioprocess Technology, 7*(1), 248-264. doi: DOI 10.1007/s11947-013-1070-3

Moelants, K. R. N., Cardinaels, R., Van Buggenhout, S., Van Loey, A. M., Moldenaers, P., & Hendrickx, M. E. (2014). A Review on the Relationships between Processing, Food Structure, and Rheological Properties of Plant-Tissue-Based Food Suspensions. *Comprehensive Reviews in Food Science and Food Safety, 13*(3), 241-260. doi: 10.1111/1541-4337.12059

Nelson, P. E., & Hoff, J. E. (1969). Tomato Volatiles - Effect of Variety Processing and Storage Time. *Journal of Food Science, 34*(1), 53-&. doi: DOI 10.1111/j.1365-2621.1969.tb14361.x

Ormerod, A. P., Ralfs, J. D., Jackson, R., Milne, J., & Gidley, M. J. (2004). The influence of tissue porosity on the material properties of model plant tissues. *Journal of Materials Science, 39*(2), 529-538. doi: Doi 10.1023/B:Jmsc.0000011508.02563.93

Rao, M. Anandha. (2007). Flow and Functional Models for Rheological Properties of Fluid Foods *Rheology of Fluid and Semisolid Foods: Principles and Applications* (pp. 27-58). Boston, MA: Springer US.

Rickman, J. C., Barrett, D. M., & Bruhn, C. M. (2007). Nutritional comparison of fresh, frozen and canned fruits and vegetables. Part 1. Vitamins C and B and phenolic compounds. *Journal of the Science of Food and Agriculture, 87*(6), 930-944. doi: 10.1002/jsfa.2825

Sanchez, M. C., Valencia, C., Ciruelos, A., Latorre, A., & Gallegos, C. (2003). Rheological properties of tomato paste: Influence of the addition of tomato slurry. *Journal of Food Science, 68*(2), 551-554. doi: DOI 10.1111/j.1365-2621.2003.tb05710.x

Sankaran, A. K., Nijsse, J., Cardinaels, R., Bialek, L., Shpigelman, A., Hendrickx, M., . . . Van Loey, A. M. (2015). Effect of Enzymes on Serum and Particle Properties of Carrot Cell Suspensions. *Food Biophysics, 10*(4), 428-438. doi: 10.1007/s11483-015-9403-6

Sharma, S. K., LeMaguer, M., Liptay, A., & Poysa, V. (1996). Effect of composition on the rheological properties of tomato thin pulp. *Food Research International, 29*(2), 175-179. doi: Doi 10.1016/0963-9969(96)00010-5

Stokes, J. R., & Frith, W. J. (2008). Rheology of gelling and yielding soft matter systems. *Soft Matter, 4*(6), 1133-1140. doi: 10.1039/b719677f

Takada, N., & Nelson, P. E. (1983). A New Consistency Method for Tomato Products - the Precipitate Weight Ratio. *Journal of Food Science, 48*(5), 1460-1462. doi: DOI 10.1111/j.1365-2621.1983.tb03516.x

Thakur, B. R., Singh, R. K., & Nelson, P. E. (1996). Quality attributes of processed tomato products: A review. *Food Reviews International, 12*(3), 375-401.

Tiback, E., Langton, M., Oliveira, J., & Ahrne, L. (2014). Mathematical modeling of the viscosity of tomato, broccoli and carrot purees under dynamic conditions. *Journal of Food Engineering, 124*, 35-42. doi: 10.1016/j.jfoodeng.2013.09.031

Valencia, C, Sanchez, MC, Ciruelos, A, Latorre, A, Franco, JM, & Gallegos, C. (2002). Linear viscoelasticity of tomato sauce products: influence of previous tomato paste processing. *European Food Research and Technology, 214*(5), 394-399. doi: 10.1007/s00217-002-0501-6

Valencia, C., Sanchez, M. C., Ciruelos, A., Latorre, A., Franco, J. M., & Gallegos, C. (2002). Linear viscoelasticity of tomato sauce products: influence of previous tomato paste processing. *European Food Research and Technology, 214*(5), 394-399. doi: DOI 10.1007/s00217-002-0501-6

Van Buggenhout, S., Sila, D. N., Duvetter, T., Van Loey, A., & Hendrickx, M. (2009). Pectins in Processed Fruits and Vegetables: Part III - Texture Engineering. *Comprehensive Reviews in Food Science and Food Safety, 8*(2), 105-117. doi: 10.1111/j.1541-4337.2009.00071.x

Verlent, I., Hendrickx, M., Rovere, P., Moldenaers, P., & Van Loey, A. (2006). Rheological properties of tomato-based products after thermal and high-pressure treatment. *Journal of Food Science, 71*(3), S243-S248.

Weltmann, R. N. (1943). Breakdown of thixotropic structure as function of time. *Journal of Applied Physics, 14*(7), 343-350. doi: Doi 10.1063/1.1714996

Wu, B. (2011). *Tomato product viscosity is determined by the physical properties of the pulp*. (M.s.), Purdue University. Retrieved from http://login.ezproxy.lib.purdue.edu/login?url=http://gateway.proquest.com/openurl?url_ver=Z39.882004&rft_val_fmt=info:ofi/fmt:kev:mtx:dissertation&res_dat=xri:pqm&rft_dat=xri:pqdiss:1510030

Wu, B. C., Patel, B. K., Chong, H. H., Fei, X., Jones, O. J., Camapanella, O. H., & Reuhs, B. L. (In preparation). *Break-Solubilized Pectin is a Minor Component of Processed Tomato Sera*.

# CHAPTER 8. SUMMARY AND RECOMMENDATIONS

## 8.1 Summary of the Dissertation

This Ph.D. research has identified and determined the effects that influence the rheology of tomato suspensions systems including (1) soluble pectin; (2) particle physical properties; and (3) processing conditions. The rheological behavior of industrially processed tomato suspensions has also been characterized. The main findings are as follows:

1. The soluble pectin in the serum phase has been identified as a limited contribution to the overall viscosity of the tomato suspension. However, it plays an important role on the stabilization of the suspension by promoting the interaction between their particles. Both prepared pectin solutions and isolated sera exhibited Newtonian behavior with a low viscosity. Proton NMR of the dialyzed sera confirmed the presence of pectin in the serum phase. By using a cone-plate geometry for the suspension viscosity measurements, significant wall slip was observed due to phase separation in the suspension. The phenomenon was more noticeable when the pectin content in the sera was low. By using a vane geometry, a sound correlation ($R^2$=0.91) between fundamental measurements of suspension viscosity and the empirical Bostwick consistometer method was established; therefore, the vane geometry was the preferred method to evaluate the rheology of plant-cell-wall-derived suspensions generated in this chapter. It is also recommended as a suitable tool to measure viscosity of suspensions containing deformable particles

2. The particle volume fraction and particle properties displayed predominant roles in determining the rheological properties of the suspensions. Viscosity can be increased by increasing the cell-wall-derived particle concentration. Particles with intact cellular structures exhibited higher water retention and mechanical strength, and formed suspensions with higher

viscosity and viscoelastic properties such as the storage modulus (G'). Suppression of PME activity in some tomato Ohio 8245 cultivars resulted in a closely packed cellular structure and smaller pore size comparted to the tissue of the original wild type tomato (OWT). An 85-90% reduction in PME activity significantly strengthened the microstructures of cell wall particles, and was able to reduce serum separation and therefore improve the rheological properties of the tomato suspensions. In addition, the local Young's modulus distribution of individual particles, investigated by an AFM based approach, was related to results obtained from bulk rheology measurements. It could be concluded that the differences in the rheological properties of the suspensions were originated from the physical properties of the particles.

3. Different processing conditions created particles with various structures and strengths and, thereby, considerably altered the rheology of suspensions including these particles. In the research, the effects of thermal breaking, ultrasound, and high shear were studied in a laboratory processing scale whereas the concentration process to produce tomato paste at an industrial scale was also investigated. Thermal breaking alone didn't change the particle size, but the subsequent ultrasound and high shear treatments dramatically reduced the particle size of suspensions. As visualized by cryo-SEM, ultrasound treated suspensions have more intact cells, resulting in an increase of the strength of the particles, which was evaluated by a compression test. By contrast, high shear treated suspensions consisted of mostly ruptured cells that already have lost structural integrity and turgor pressure. Therefore, the ultrasound treatment led to an increase in viscosity and viscoelasticity whereas the high shear treatment caused a decrease of these rheological properties. The water-soluble pectin (WSP) fraction in the suspensions increased after ultrasound and shear treatments. Therefore, soluble pectin is not the cause for changes in the rheology of

suspensions; however it is an indicator or consequence of the change of particle properties, which is directly responsible for changes in the suspension rheological properties.

During the industrial concentration process, the particle size and particle properties were modified due to the prolonged and intense heating, which resulted in a viscosity loss when diluted back to suspensions with the same soluble solid content. Average particle size and viscoelastic properties of tomato juice were found considerably large, but significantly reduced after a concentration process. The concentration process not only reduced the particle volume but also concentrated their mass into smaller size and therefore negatively altered the particle properties, which can explain the viscosity loss during concentration. The reconstituted juices had a relatively lower volume fraction and elasticity compared to original tomato juice, which led to a lower consistency and viscosity. Furthermore, those particles cannot fully re-expend to the original shape and the concentrated solute was only partially re-solubilized upon dilution, which explains the need to use more paste to achieve the same soluble solids measured as °Brix, in the reconstituted juice as well as its viscosity.

4. The flow behavior of industrially processed hot-break (HB) and cold-break (CB) tomato suspensions was investigated under steady-state and dynamic oscillatory shear conditions. HB particles appeared to have a better water retention structure and higher mechanical strength, which contributes to a considerably higher viscosity and viscoelastic properties than CB. The HB and CB suspensions demonstrated both to have temperature-dependent and time-dependent rheological behaviors. The consistency coefficient ($k$) decreased with increasing temperature, and could be modeled by an Arrhenius-like equation. The difference in temperature dependence is probably caused by the particle structures in the two suspension systems, since the activation energy of the HB sample was higher than that of the CB sample, indicating HB has a more

integral structure which requires more energy to change. The thixotropic behaviors of the HB and CB suspensions were accurately described by the Stretch Exponential equation. The characteristic time ($\lambda_s$) for the HB sample increased with temperature, whereas it showed a decrease for the CB sample. The differences appear to be caused by particle structure and the initial viscosity. Particle interactions have showed great effects on the rheological properties. At low particle concentration (solid % < 1.0%), the HB and CB samples almost had the same apparent viscosity due to a limited contact and similar volume fractions. As particle concentration was increased, the particle-particle contact significantly increased, and the HB sample demonstrated a considerably higher viscosity than the CB sample. The complex modulus ($G^*$) was further modeled by the Adams' equations at a high relative volume, and the results demonstrated that the HB system has larger particle elasticity and stronger particle interaction than the CB system.

## 8.2 Recommendations for the Future Work

### 8.2.1 *In Situ* Visualization of Structural Pectin in Particles

There are several physicochemical techniques available in the literature to characterize pectin structure, such as nuclear magnetic resonance (NMR), gas chromatography-mass spectrometry (GC-MS), and high performance size exclusion chromatography (HPSEC). However, results from these analytical methods greatly depend on the nature of the extracted material, and sometimes extraction itself causes destruction of particles as well as an alteration of the pectin. Therefore, it could not fully illustrate the functionality of pectin in the particles and its changes during processing. In the future work, immunolabelling with monoclonal antibodies such as JIM5, JIM7, LM18, LM19, PAM1 and 2F4 (i.e. plant cell wall monoclonal antibodies)

can be used to visualize pectin within the particles using Fluorescence Microscopy based on the fact that each antibody locates specific pectin structure. *In situ* visualization of the cell wall changes (e.g. pectin modification) will provide an insight into the changes of particle structure due to processing and interactions between particles.

### 8.2.2 Improvement of AFM Measurement

The present research showed Young's modulus distribution differences between particles obtained after the HB and CB treatments at the individual particle level. However, this study only focused on the elastic range of these particles, but more research needs to be done to explore the viscoelastic range with the improvement of AFM techniques. Since the plant cell wall particles are much larger than other biological cells and polymeric particles, cantilevers with large spherical probe (e.g. radius 10 μm) are recommended for use in future research. In addition, the droplet technique was applied in the current study. However, water would be dried out in 2 h, which posed difficulties with the force-mapping procedure. AFM accessories such as the Fluid Cells and the Dish Heater will be great helpful in further studies.

### 8.2.3 Modeling of Particle Interaction

Due to the higher deformable nature of plant cell wall particles, it is hard to accurately measure the volume fraction of suspensions containing these particles. Furthermore, studies on associated particle interactions in this soft, non-colloidal system by classic methods derived for colloidal system would be extremely complicated and not appropriate. A model system, such as non-colloidal (~ 10 μm) spherical agarose micro-gels would be a good alternative. These soft particles are filled with a Newtonian fluid (i.e. water) and can be manufactured with a wide elastic modulus range. Results from this study will yield more information in regards to the effects of particle elasticity and volume fraction on the rheology of suspensions. Further

simulation modeling could couple more parameters including particle volume, particle wall thickness and internal pressure. Lattice-Boltzmann and Finite-Element computational modeling methods could be applied to develop a simulation technique. Studies in this area will give us a better understanding of particle interactions in the suspension systems and their influence on the bulk rheology.

# APPENDIX

1. Supplementary Information for Chapter 3

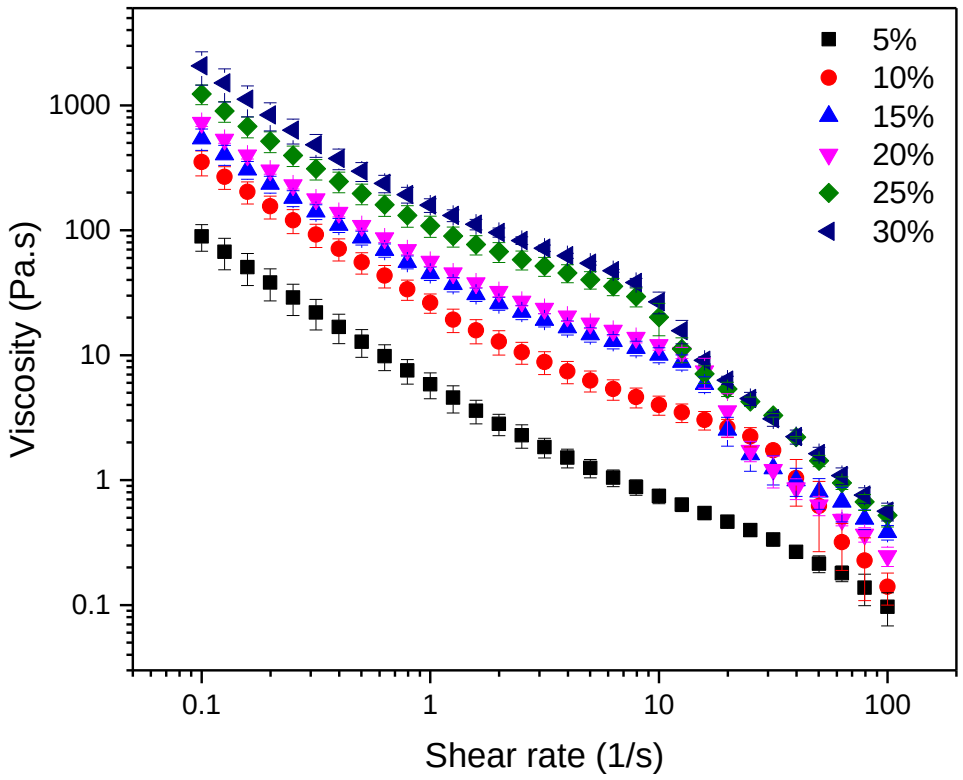


Figure A3.1 Viscosity versus shear rate curves of reconstituted suspensions with different pulp fraction using cone-plate geometry. In these suspensions, the serum phase was reconstituted with deionized distilled water and the pectin concentration of the serum was considered to be 0.

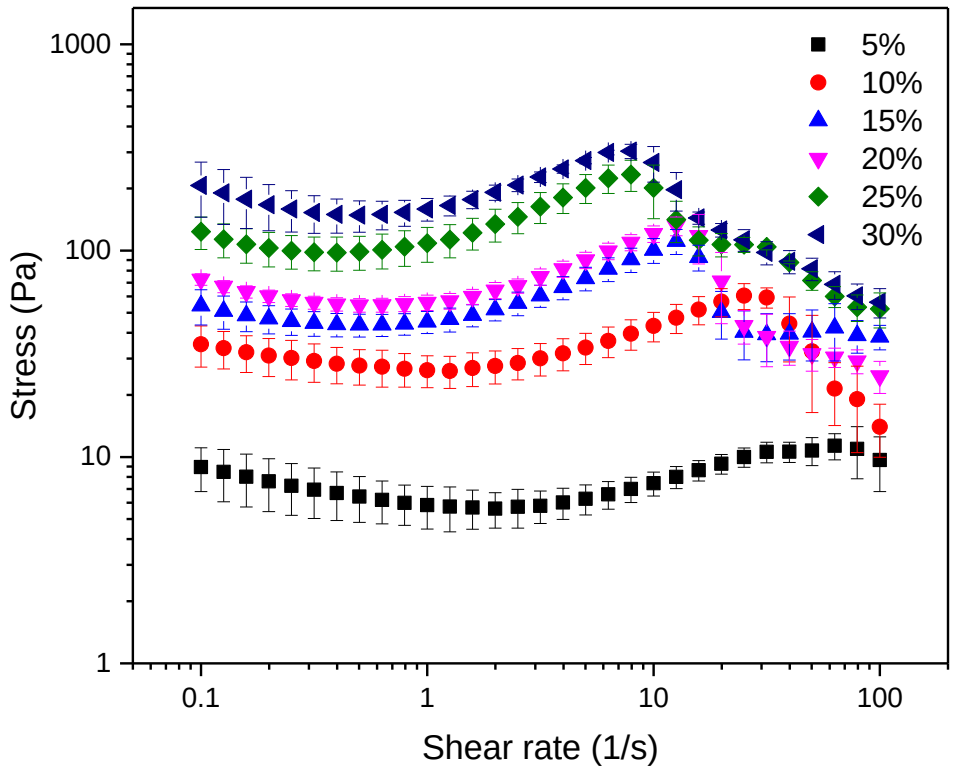


Figure A3.2 Shear stress plot of reconstituted suspensions varied with pulp% as a function of shear rate determined using the cone-plate geometry. In these suspensions, the serum phase was deionized distilled water and the pectin concentration was considered as 0. This plot revealed obvious wall slip when cone-plate was used. The wall slip became more noticeable when the suspensions had higher particle concentrations.

Table A3.1 Consistency coefficient (*k*) (± standard deviation) of reconstituted suspensions with different pulp fraction (pulp %). The vane and cone-plate geometries were used for the measurements and the concentration of pectin in the serum was assumed as 0. For the vane geometry, the range of shear rate used in the fitting was 0.1-100 $s^{-1}$ whereas for the cone-plate geometry a valid range had to be selected from a shear rate 1/s to the shear rate at which wall slip started. Data generated by each geometry was tested by Tukey grouping. Means with the same letter are not significantly different.

| Sample (Pulp %) | Vane Geometry Consistency Coefficient (*k*) ($Pa.s^n$) | Cone-plate Geometry Consistency Coefficient (*k*) ($Pa.s^n$) |
|---|---|---|
| Pulp%_5% | 0.2 ±0.0 f | 4.8 ±1.0 d |
| Pulp%_10% | 2.1 ±0.1 e | 21.6 ±4.5 cd |
| Pulp%_15% | 4.4 ±0.3 d | 40.0 ±4.8 c |
| Pulp%_20% | 8.6 ±0.5 c | 50.2 ±4.2 c |
| Pulp%_25% | 13.7 ±0.2 b | 101.4 ±19.4 b |
| Pulp%_30% | 20.5 ±0.5 a | 151.9 ±17.5 a |

2. Supplementary Information for Chapter 4

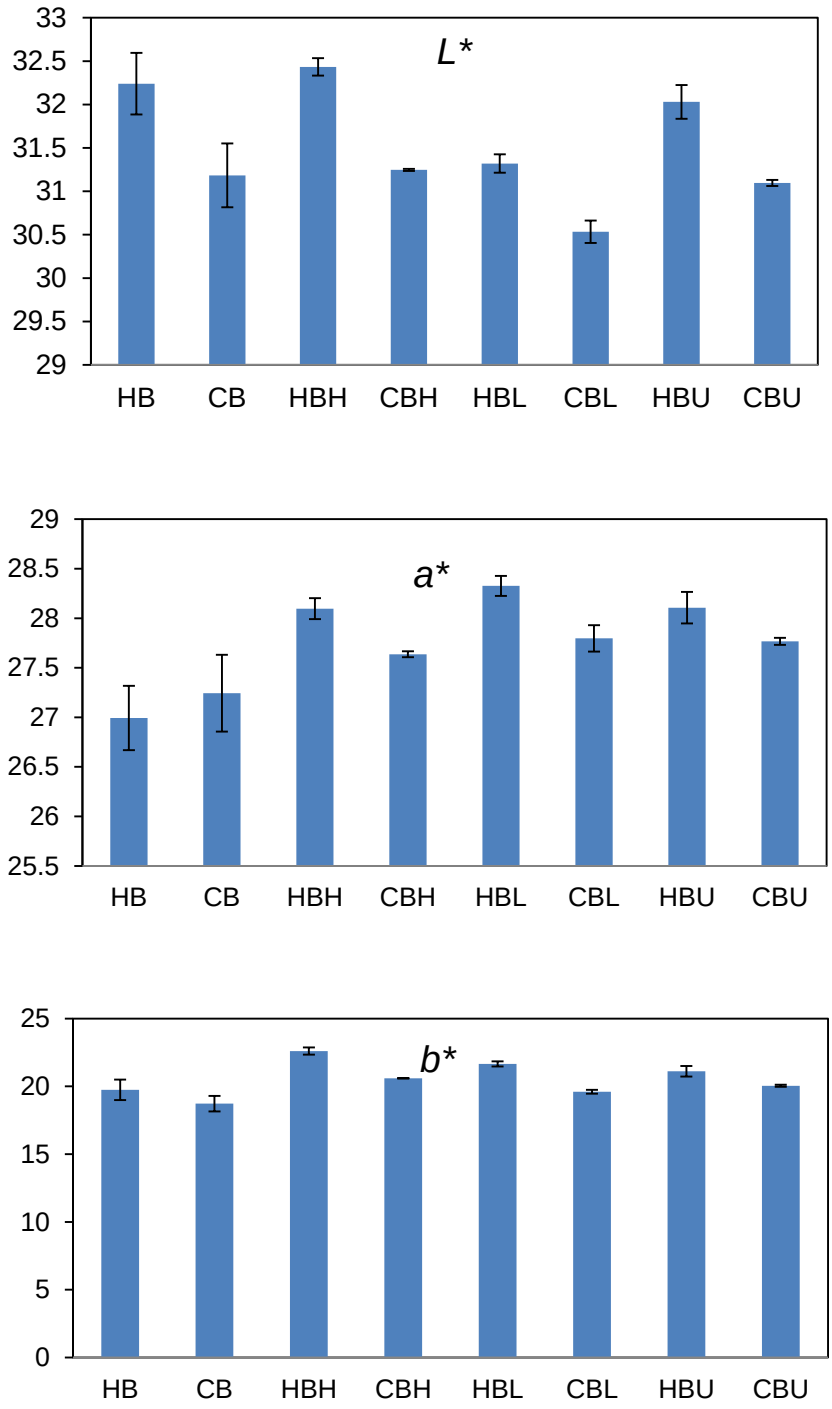


Figure A4.1 Color values ($L^*$, $a^*$, and $b^*$) of tomato suspensions obtained from ultrasound and shear treatments.

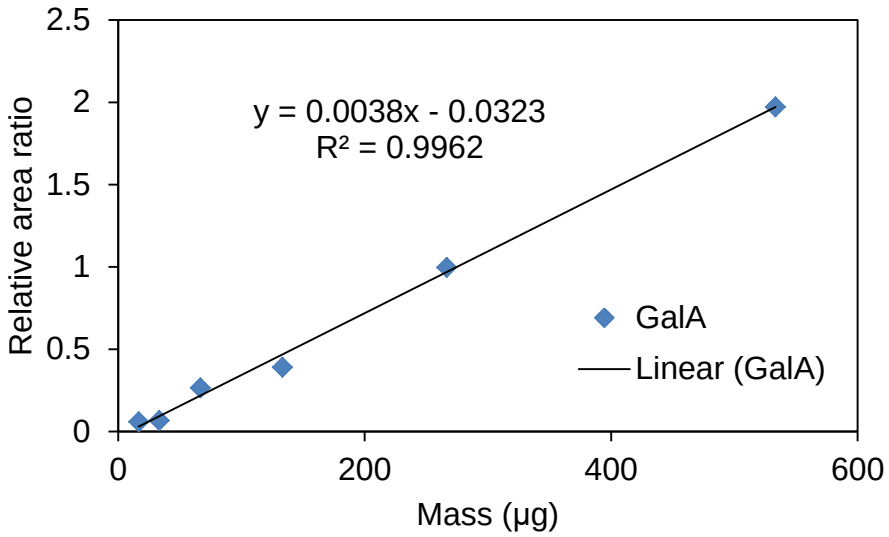


Figure A4.2 Galacturonic acid standard curve ($R^2$=0.9962) built for quantification of pectin content in samples.

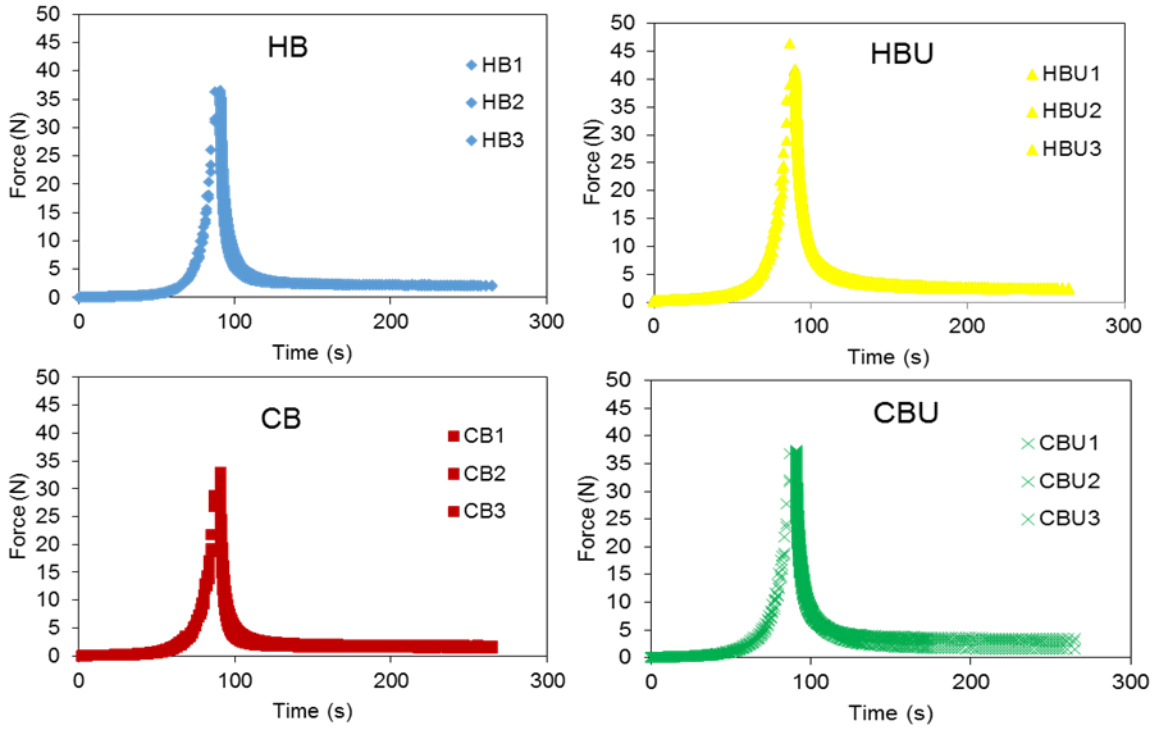


Figure A4.3 Force-time curves for ultrasound treated suspensions (HBU and CBU) compared with original HB and CB samples. Each samples showed unique peak force which indicates the cell wall elasticity.

Table A4.1 Moisture content of tomato suspensions obtained from ultrasound and shear treatments

| Sample | HB | CB | HBU | CBU | HBH | HBL | CBH | CBL |
|---|---|---|---|---|---|---|---|---|
| Moisture (%) | 95.9 ±0.0 | 96.0 ±0.0 | 95.9 ±0.0 | 96.1 ±0.0 | 95.9 ±0.0 | 95.8 ±0.0 | 95.9 ±0.0 | 96.2 ±0.0 |

3. Supplementary Information for Chapter 7

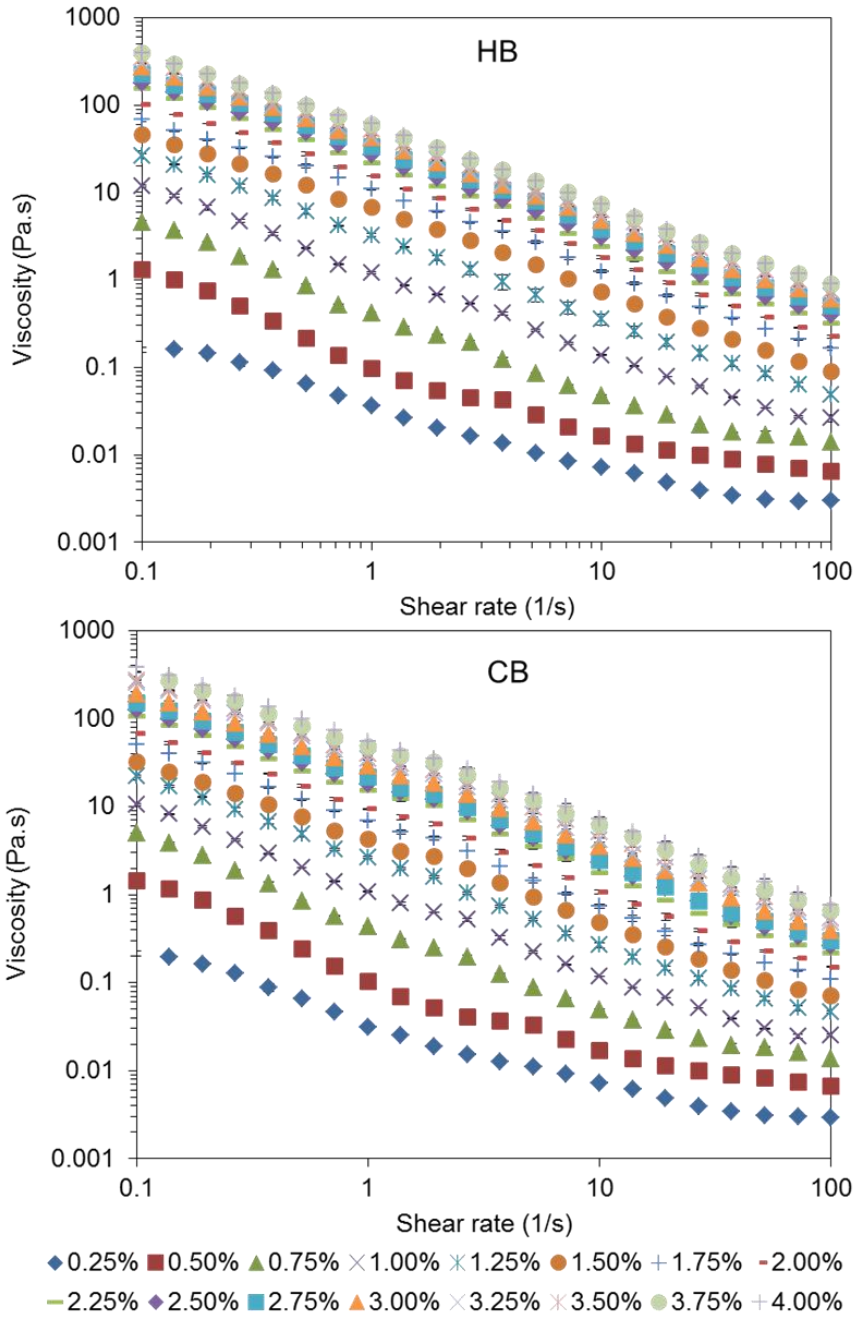


Figure A7.1 Viscosity versus shear rate curves of reconstituted HB and CB products with different solid content from 0.25 to 4.00%.

# VITA

Xing Fei received his B.E. in Food Science and Engineering from Huazhong Agricultural University, China in 2006 and his M.S. in Food Science from Guangdong Ocean University, China in 2009. Then he was working as a research scientist at Fishery Machinery and Instrument Research Institute, Chinese Academy of Fishery Sciences, Shanghai, China. In January 2014, Xing began his Ph.D. studies at the Department of Agriculture and Biological Engineering at Purdue under the guidance of Dr. Osvaldo Campanella. His research focuses on the mechanical properties of plant cell wall particles in relation to the rheological properties of derived foods.